

GEOCHRONOLOGY OF METASEDIMENTARY  
AND IGNEOUS ROCKS IN THE LAMBOO  
PROVINCE, KIMBERLEY REGION:  
REASSESSING COLLISIONAL GEODYNAMIC MODELS

DW Maidment, Y Lu, C Phillips, FJ Korhonen, IOH Fielding,  
MTD Wingate, CL Kirkland, R Murphy, R Tilhac, M Poujol and J Zhao



Government of **Western Australia**  
Department of **Mines, Industry Regulation  
and Safety**

REPORT 215

# GEOCHRONOLOGY OF METASEDIMENTARY AND IGNEOUS ROCKS IN THE LAMBOO PROVINCE, KIMBERLEY REGION: REASSESSING COLLISIONAL GEODYNAMIC MODELS

DW Maidment<sup>1</sup>, Y Lu, C Phillips, FJ Korhonen, IOH Fielding, MTD Wingate, CL Kirkland<sup>2</sup>, R Murphy<sup>3</sup>,  
R Tilhac<sup>3</sup>, M Poujol<sup>4</sup> and J Zhao<sup>5</sup>

1 Newmont Australia, 3 Bellows Street, Welshpool WA 6106, Australia

2 Centre for Exploration Targeting – Curtin Node, School of Earth and Planetary Sciences, Curtin University,  
GPO Box U1987, Perth WA 6845, Australia

3 ARC Centre of Excellence for Core to Crust Fluid Systems (CCFS) and GEMOC, Department of Earth and Planetary  
Sciences, Macquarie University, Sydney NSW 2109, Australia

4 Université de Rennes, CNRS, Géosciences Rennes – UMR 6118, 35000 Rennes, France

5 Radiogenic Isotope Facility, School of Earth Sciences, The University of Queensland, Brisbane QLD 4072, Australia

PERTH 2022



**Geological Survey of  
Western Australia**



**MINISTER FOR MINES AND PETROLEUM**  
**Hon Bill Johnston MLA**

**DIRECTOR GENERAL, DEPARTMENT OF MINES, INDUSTRY REGULATION AND SAFETY**  
**Richard Sellers**

**EXECUTIVE DIRECTOR, GEOLOGICAL SURVEY AND RESOURCE STRATEGY**  
**Jeff Haworth**

#### REFERENCE

**The recommended reference for this publication is:**

Maidment, DW, Lu, Y, Phillips, C, Korhonen, FJ, Fielding, IOH, Wingate, MTD, Kirkland, CL, Murphy, R, Tilhac, R, Poujol, M and Zhao, J 2022, Geochronology of metasedimentary and igneous rocks in the Lamboo Province, Kimberley region: reassessing collisional geodynamic models: Geological Survey of Western Australia, Report 215, 82p.

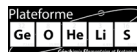
**ISBN** 978-1-74168-964-8

**ISSN** 1834-2280



A catalogue record for this book is available from the National Library of Australia

Grid references in this publication refer to the Geocentric Datum of Australia 1994 (GDA94). Locations mentioned in the text are referenced using Map Grid Australia (MGA) coordinates, Zone 50. All locations are quoted to at least the nearest 100 m.



#### About this publication

U–Pb measurements of Geological Survey of Western Australia (GSWA) samples were conducted using SHRIMP II ion microprobes in the John de Laeter Centre at Curtin University in Perth, Western Australia. These facilities receive financial support from AuScope and the Australian Research Council (ARC). Lu–Hf measurements were conducted using LA-MC-ICPMS at the ARC National Key Centre for Geochemical Evolution and Metallogeny of Continents (GEMOC), via the ARC Centre of Excellence for Core to Crust Fluid Systems (CCFS), based in the Department of Earth and Planetary Sciences at Macquarie University, Australia. Sm–Nd measurements were conducted at the GeOHeLiS analytical platform, based in the Geosciences Department at the University of Rennes, France, and at the Radiogenic Isotope Facility at the University of Queensland. Isotope analyses were funded in part by the Western Australian Government Exploration Incentive Scheme (EIS).

#### Disclaimer

This product uses information from various sources. The Department of Mines, Industry Regulation and Safety (DMIRS) and the State cannot guarantee the accuracy, currency or completeness of the information. Neither the department nor the State of Western Australia nor any employee or agent of the department shall be responsible or liable for any loss, damage or injury arising from the use of or reliance on any information, data or advice (including incomplete, out of date, incorrect, inaccurate or misleading information, data or advice) expressed or implied in, or coming from, this publication or incorporated into it by reference, by any person whatsoever.

#### Published 2022 by the Geological Survey of Western Australia

This Report is published in digital format (PDF) and is available online at <[www.dmirs.wa.gov.au/GSWApublications](http://www.dmirs.wa.gov.au/GSWApublications)>.



© State of Western Australia (Department of Mines, Industry Regulation and Safety) 2022

With the exception of the Western Australian Coat of Arms and other logos, and where otherwise noted, these data are provided under a Creative Commons Attribution 4.0 International Licence. (<https://creativecommons.org/licenses/by/4.0/legalcode>)

#### Further details of geoscience products are available from::

First Floor Counter, Department of Mines, Industry Regulation and Safety  
100 Plain Street, EAST PERTH WESTERN AUSTRALIA 6004  
Telephone: +61 8 9222 3459 Email: [publications@dmirs.wa.gov.au](mailto:publications@dmirs.wa.gov.au)  
[www.dmirs.wa.gov.au/GSWApublications](http://www.dmirs.wa.gov.au/GSWApublications)

**Cover photograph:** Metadolerite dyke intruding metasedimentary gneiss of the Tickalara Metamorphics, Fletcher Creek Rockholes

# Contents

Abstract.....	1
Introduction.....	2
Geology of the Lamboo Province .....	4
Western Zone .....	5
Central Zone .....	5
Eastern Zone .....	7
Mafic-ultramafic layered intrusions (1857–1823 Ma) .....	7
Halls Creek Orogeny (1837–1808 Ma) .....	8
Dougalls Suite .....	8
Sally Downs Supersuite .....	9
Poonta Suite (1804–1788 Ma).....	9
Kimberley Basin (1814–1740 Ma).....	9
Yampi Orogeny (900–800 Ma).....	9
Wunaamin Miliwundi Orogeny (590–500 Ma) .....	10
Alice Springs Orogeny (450–295 Ma) .....	10
Mineralization.....	10
Geodynamic models .....	11
Sampling rationale.....	12
Analytical methods.....	13
U–Pb geochronology .....	13
Lu–Hf isotopes.....	14
Sm–Nd isotopes .....	14
Geochronology results .....	14
Western Zone – Wunaamin Miliwundi Orogen .....	14
GSWA 206102: sandstone, Marboo Formation.....	14
GSWA 212327: pelitic schist, Marboo Formation .....	15
GSWA 212335: metagabbro, Ruins Dolerite .....	15
GSWA 212317: pelitic migmatite, Mount Joseph Migmatite .....	18
GSWA 212315: pelitic migmatite, Mount Joseph Migmatite .....	18
GSWA 212344: pelitic schist, Marboo Formation .....	20
Western Zone – Halls Creek Orogen .....	20
GSWA 215562: metasandstone, Marboo Formation .....	20
GSWA 206154: pelitic migmatite, Marboo Formation .....	20
GSWA 218305: metasiltstone, Marboo Formation .....	24
GSWA 218330: lithic metasandstone, Marboo Formation .....	24
GSWA 206173: psammitic schist, Marboo Formation.....	24
GSWA 206106: pelitic migmatite, Marboo Formation .....	26
GSWA 218310: metasandstone, Marboo Formation .....	26
GSWA 206155: porphyritic dacite, Whitewater Volcanics .....	26
Central Zone .....	28
GSWA 218315: psammitic gneiss, Tickalara Metamorphics .....	28
GSWA 206131: migmatitic pelitic gneiss, Tickalara Metamorphics .....	28
GSWA 218321: pelitic gneiss, Tickalara Metamorphics .....	28
GSWA 218333: psammitic gneiss, Tickalara Metamorphics .....	28
GSWA 206128: pelitic schist, Tickalara Metamorphics.....	30
GSWA 218318: muscovite–chlorite schist, Winnama Formation.....	30
GSWA 216661: lithic sandstone, Milba Formation.....	30
GSWA 226523: biotite–muscovite granodiorite gneiss, Rose Bore Granite.....	34
GSWA 218350: biotite–hornblende metatonalite, Dougalls Tonalite.....	34
GSWA 218313: metamonzogranite, Violet Valley Tonalite .....	35
GSWA 218355: biotite–hornblende metatonalite, Mabel Downs Tonalite .....	36
GSWA 124442: biotite–hornblende syenogranite, Kevins Dam Monzogranite .....	36
Lu–Hf isotope results.....	37
Discussion.....	39
Nature and origin of zircons in metasedimentary rocks .....	39
Western Zone succession .....	41
Marboo Formation (Wunaamin Miliwundi Orogen) .....	41
Hooper Orogeny .....	43
Marboo Formation (Halls Creek Orogen) .....	43
Central Zone succession .....	44
Tickalara Metamorphics.....	44
Milba Formation .....	45
Winnama Formation.....	46
Rose Bore Granite.....	46
Halls Creek Orogeny metamorphism.....	46



Western–Central Zone boundary in the northern Halls Creek Orogen .....	47
Comparison of provenance signatures across the Lamboo Province .....	48
Detrital zircon age spectra .....	49
Lu–Hf isotope constraints on provenance .....	49
Potential stratigraphic correlations .....	51
Potential sediment source regions .....	52
Successions older than c. 1870 Ma .....	52
1870–1835 Ma successions (Detrital P provenance) .....	54
Regional correlations .....	56
Igneous geochemistry and isotope constraints .....	60
c. 1873 Ma Ruins Dolerite .....	60
1867–1849 Ma bimodal magmatic rocks .....	60
1845–1840 Ma bimodal magmatic rocks .....	64
Central Zone an ensialic rift, not an oceanic arc? .....	65
Burial of the Tickalara Metamorphics .....	65
1850–1847 Ma (c. 1838 Ma?) Dougalls Suite .....	66
1837–1808 Ma Sally Downs Supersuite .....	70
Proposed geodynamic evolution of the Lamboo Province .....	70
1912–1904 Ma – intraplate extension .....	71
1904–1870 Ma – intraplate (back-arc?) extension .....	71
1870–1855 Ma – intraplate (back-arc?) extension, c. 1865 Ma Hooper Orogeny .....	71
1855–1840 Ma – Central Zone rift, Savannah Event .....	73
1838–1808 Ma – rift inversion, Halls Creek Orogeny .....	73
1808–1740 Ma – regional extension and subsidence, Kimberley Basin .....	73
Neoproterozoic–Paleozoic deformation – Yampi, Wunaamin Miliwundi, Alice Springs Orogenies .....	73
Geodynamic context of mineral systems .....	73
Conclusions .....	74
References .....	75

## Appendices

*Available with the PDF online as an accompanying digital resource*

1. Lu–Hf isotope data
2. Sm–Nd isotope data
3. Whole-rock geochemical data for mafic rocks

## Figures

1. Location of the Kimberley region .....	2
2. Generalized geology of the Kimberley region .....	3
3. Space–time plot for the Kimberley region .....	4
4. Previous interpretations of the evolution of the Lamboo Province .....	13
5. Location of geochronology samples from the Wunaamin Miliwundi Orogen .....	15
6. Geochronology results for Unit 1 of the Marboo Formation and Ruins Dolerite .....	16
7. Field photographs of geochronology samples, Wunaamin Miliwundi Orogen .....	17
8. Geochronology results for metasedimentary rocks in the Wunaamin Miliwundi Orogen .....	19
9. Field photographs of Marboo Formation sample sites (Wunaamin Miliwundi and Halls Creek Orogens) .....	21
10. Location of geochronology samples in the Halls Creek Orogen .....	22
11. Geochronology results for the Marboo Formation, Halls Creek Orogen .....	23
12. Geochronology results and CL image for the Marboo Formation and Whitewater Volcanics, Halls Creek Orogen .....	25
13. Field photographs of samples from the Western and Central Zones, Halls Creek Orogen .....	27
14. Geochronology results for the Tickalara Metamorphics .....	29
15. Field photographs of samples of the Tickalara Metamorphics .....	31
16. Field photographs of geochronology sample sites, Central Zone .....	32
17. Geochronology results for metasedimentary rocks in the Central Zone .....	33
18. Field photographs of granitic and quartzofeldspathic rocks, Central Zone .....	35
19. CL images and concordia plots for granitic and quartzofeldspathic rocks, Central Zone .....	36
20. Field and sample photographs of granitic rocks, Central Zone .....	37
21. CL images and concordia plots for granitic rocks, Central Zone .....	38
22. Initial $^{176}\text{Hf}/^{177}\text{Hf}$ evolution plot for detrital and igneous zircons, Western and Central Zones .....	39
23. Detrital zircon probability density diagrams for metasedimentary rocks, Western and Central Zones .....	42
24. Locations of geochronology samples, northern Halls Creek Orogen .....	48
25. Representative detrital zircon probability density diagrams for the Lamboo Province .....	50
26. Compilation of detrital zircon dates for Lamboo Province units with Detrital P provenance .....	51
27. Compilation of detrital zircon dates for units in the North Australian Craton underlying Detrital P units .....	52
28. Initial $^{176}\text{Hf}/^{177}\text{Hf}$ evolution plots for detrital zircons from metasedimentary rocks .....	53
29. Initial $^{176}\text{Hf}/^{177}\text{Hf}$ evolution plot for 2000–1800 Ma detrital zircons .....	54
30. Compilation of geochronology of igneous rocks pre-dating the Halls Creek Orogeny .....	55
31. Radiometric images of the Kimberley region .....	57

32.	Compilation of detrital zircon dates for units of the North Australian Craton with the Detrital P signature .....	58
33.	Possible geodynamic setting for the development of the North Australian Craton 1885–1855 Ma .....	59
34.	Bouguer gravity image of the Kimberley region .....	61
35.	Textures of mafic and felsic rocks in the Halls Creek Orogen .....	62
36.	Th/Yb vs Nb/Yb for 1860–1845 Ma mafic extrusive and intrusive rocks, Central Zone .....	63
37.	Distribution of 1870–1855 Ma tectonism and sedimentation in the North Australian Craton .....	64
38.	Time–event chart for the Central Zone, 1865–1815 Ma .....	66
39.	$\epsilon_{\text{Nd}}$ vs $\text{K}_2\text{O}/\text{Na}_2\text{O}$ for granitic rocks of the 1838–1808 Ma Sally Downs Supersuite .....	67
40.	Bouguer gravity image of the Halls Creek Orogen .....	68
41.	Distribution of 1860–1830 Ma felsic and mafic magmatic rocks, Halls Creek Orogen .....	69
42.	Schematic evolution of the Lamboo Province .....	72

## Tables

1.	Ages and igneous associations of intrusive units referred to in this Report .....	6
2.	Summary of isotopic ages obtained for metasedimentary and igneous rocks .....	40



# Geochronology of metasedimentary and igneous rocks in the Lamboo Province, Kimberley region: reassessing collisional geodynamic models

DW Maidment<sup>1</sup>, Y Lu, C Phillips, FJ Korhonen, IOH Fielding, MTD Wingate, CL Kirkland<sup>2</sup>, R Murphy<sup>3</sup>, R Tilhac<sup>3</sup>, M Poujol<sup>4</sup> and J Zhao<sup>5</sup>

## Abstract

U–Pb and Lu–Hf isotope data for detrital zircons from metasedimentary rocks of the 1912–1788 Ma Lamboo Province provide a test of collisional and intraplate geodynamic models for the Paleoproterozoic development of the region. Metasedimentary rocks deposited between c. 1885 and 1870 Ma are dominated by variable proportions of Archean to early Paleoproterozoic detritus, possibly derived from local basement sources, which include a common c. 2500 Ma age component. Conformably overlying turbiditic metasedimentary rocks deposited across the Western, Central and Eastern Zones between c. 1870 and 1840 Ma have remarkably consistent detrital zircon age signatures, with a dominant 1875–1860 Ma age component and a subsidiary c. 2500 Ma age component. These age components have similar Lu–Hf isotope values across all three zones, consistent with a common source for the sedimentary protoliths. The close similarities in provenance suggest that all three zones of the Lamboo Province developed in a continental intraplate setting prior to the 1837–1808 Ma Halls Creek Orogeny, which has previously been considered to represent a collision between an exotic Kimberley Craton and the proto-North Australian Craton. Comparable provenance signatures of coeval metasedimentary rocks across the broader North Australian Craton suggest that assembly of the main craton elements was complete prior to c. 1885 Ma.

Deposition of 1885–1840 Ma metasedimentary protoliths is interpreted to have occurred as a result of prolonged intraplate extension and subsidence, possibly within a back-arc basin related to subduction north of the Lamboo Province. Voluminous felsic and mafic rocks of the 1867–1849 Ma Paperbark Supersuite are interpreted to be a consequence of this extension, which was interrupted in the southwest by the c. 1865 Ma Hooper Orogeny. Granitic rocks of the Paperbark Supersuite dated at 1854–1852 Ma intrude across the boundary between the Western and Central Zones, indicating that these terranes were adjacent at this time. Extension was subsequently focused into the Central Zone, culminating in the 1852–1840 Ma Savannah Event, which was associated with bimodal magmatism and high-T, low-P metamorphism in the lower parts of an inferred intraplate rift. Intraplate deformation during the 1837–1808 Ma Halls Creek Orogeny was partitioned into this rift, resulting in the generation of a range of granitic rocks sourced from differing proportions of juvenile mafic underplate and Archean and Paleoproterozoic crust.

**KEYWORDS:** detrital zircon geochronology, geodynamics, Halls Creek Orogeny, Hooper Orogeny, Kimberley, Lamboo Province, Savannah Event

---

1 Newmont Australia, 3 Bellows Street, Welshpool WA 6106, Australia

2 Centre for Exploration Targeting – Curtin Node, School of Earth and Planetary Sciences, Curtin University, GPO Box U1987, Perth WA 6845, Australia

3 ARC Centre of Excellence for Core to Crust Fluid Systems (CCFS) and GEMOC, Department of Earth and Planetary Sciences, Macquarie University, Sydney NSW 2109, Australia

4 Université de Rennes, CNRS, Géosciences Rennes – UMR 6118, 35000 Rennes, France

5 Radiogenic Isotope Facility, School of Earth Sciences, The University of Queensland, Brisbane QLD 4072, Australia

## Introduction

The Lamboo Province in the Kimberley region of Western Australia consists of a multiply deformed assemblage of Paleoproterozoic metasedimentary and meta-igneous rocks in the northwestern part of the North Australian Craton (Figs 1, 2). Previous studies have established a well-constrained event framework that involves several phases of sedimentation, magmatism, deformation and metamorphism between c. 1912 and 1788 Ma (Fig. 3; Gemuts, 1971; Hancock and Rutland, 1984; Tyler et al., 1995, 1999, 2012; Bodorkos et al., 1999, 2000b; Sheppard et al., 1999b, 2001; Griffin et al., 2000a; Page et al., 2001; Phillips et al., 2016; Mole et al., 2018). The Lamboo Province has been divided into three largely fault-bound tectonostratigraphic terranes: the Western, Central and Eastern Zones (Fig. 2). Differences between the geological histories of the three zones have been interpreted in the context of subduction and collision between an inferred exotic terrane and the proto-North Australian Craton (Tyler et al., 1995; Sheppard et al., 1999b, 2001; Griffin et al., 2000a). This model has been widely accepted in subsequent studies of the province (e.g. Hollis et al., 2015; Occhipinti et al., 2016; Lindsay et al., 2016; Kohanpour et al., 2017, 2018, 2019a; Mole et al., 2018; Stachel et al., 2018), and has in turn been incorporated in geodynamic models for the Proterozoic assembly of Australia (Betts et al., 2002, 2016; Wingate and Evans, 2003; Fraser et al., 2007; Cawood and Korsch, 2008; de Vries et al., 2008; Payne et al., 2009; Huston et al., 2012; Johnson, 2013; Aitken et al., 2018).

Two variants of this collisional model have been proposed, both of which consider the Western Zone to be part of an exotic terrane (the Kimberley Craton) that collided with the Eastern Zone (proto-North Australian Craton) during the 1837–1808 Ma Halls Creek Orogeny (Griffin et al., 2000a). The Central Zone is considered to have developed either as an oceanic arc that accreted to the Western Zone before collision, or an ensialic marginal basin developed on the eastern margin of the Kimberley Craton. Features consistent with this model include differences in the geological histories of the three zones prior to the Halls Creek Orogeny (Tyler et al., 1995), differences in detrital zircon age spectra of some pre-collision metasedimentary rocks (Tyler et al., 1999) and the geochemistry of felsic and mafic rocks in the Central Zone, which include components comparable to those found in Phanerozoic subduction zone settings (Ogasawara, 1988; Sheppard et al., 1999b, 2001; Mole et al., 2018).

Although some aspects of the geology are consistent with subduction and collision, other features are more difficult to place in this setting, or may be explained by other processes. These include the overall bimodal character of magmatic rocks, which have a paucity of intermediate compositions typical of magmatic arcs (Wyborn and Blake, 2000), and detrital zircon age data for the Central and Western Zones, some of which show similarities with units in the Eastern Zone and broader North Australian Craton (Page, 1996a,b; Bodorkos et al., 1999; Tyler et al., 1999; Page and Hoatson, 2000; Mole et al., 2018).

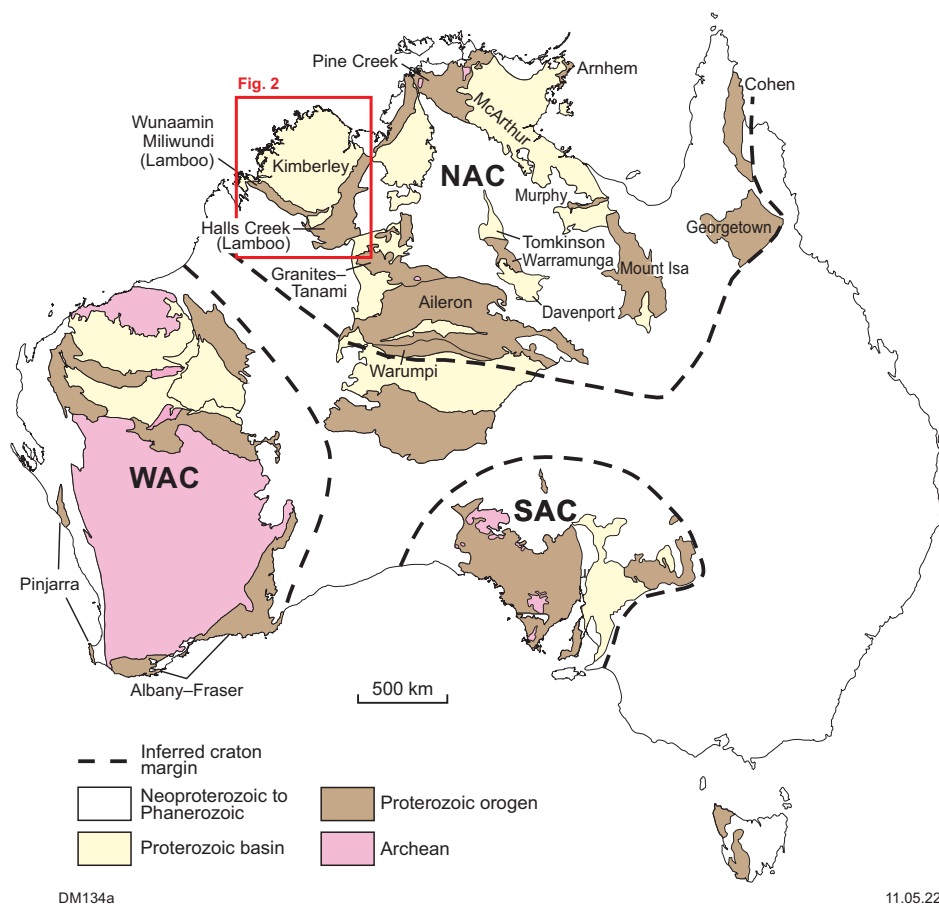


Figure 1. Location of the Kimberley region within the North Australian Craton



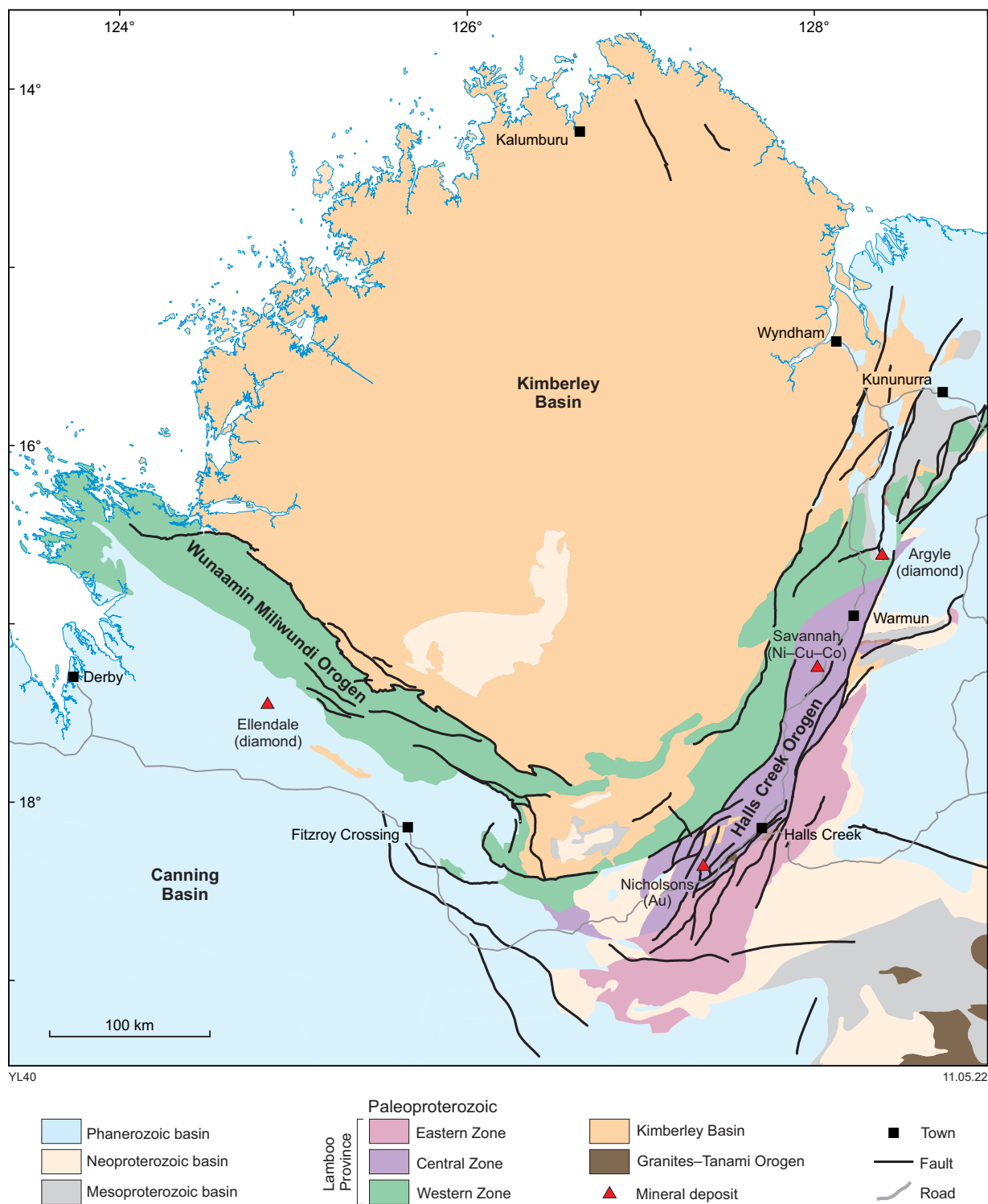


Figure 2. Generalized geology of the Kimberley region, showing the locations of the Western, Central and Eastern Zones of the Lamboo Province

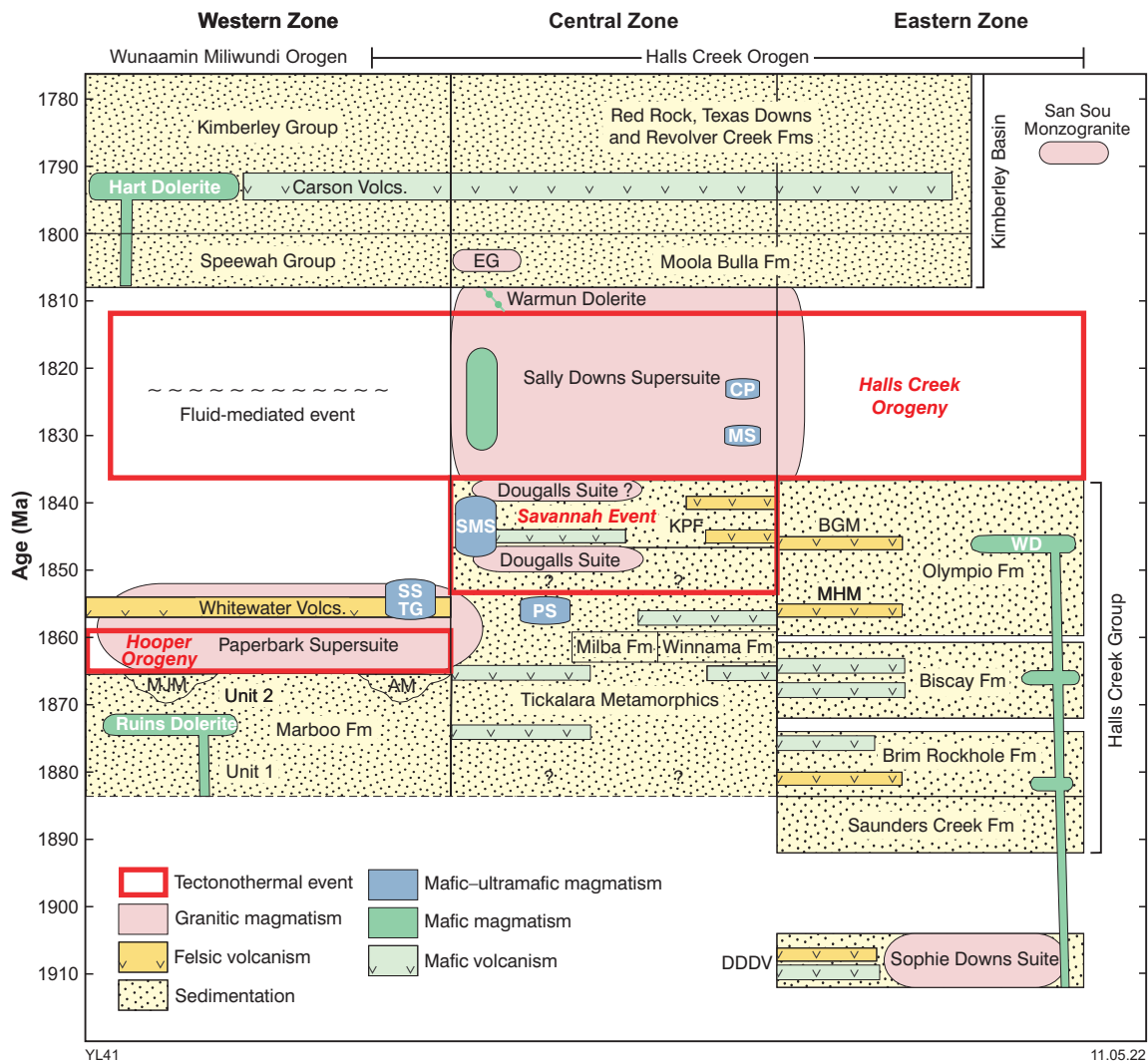


Figure 3. Time-space plot for the Kimberley region. Abbreviations: AM, Amhurst Metamorphics; BGM, Butchers Gully Member; CP, Copernicus pyroxenite; EG, Eastman Granite; DDDV, Ding Dong Downs Volcanics; KPF, Koongie Park Formation; MHM, Maude Headley Member; MJM, Mount Joseph Migmatite; MS, McIntosh Suite; PS, Pantom Suite; SMS, Sally Malay Suite; SS, Springvale Suite; TG, Toby Gabbro; WD, Woodward Dolerite. Note that the representation of mafic volcanic units in the Lamboo Province is schematic and these rocks have not been directly dated

Other aspects include the presence of layered mafic/ultramafic intrusions, which are more commonly associated with intraplate extensional settings (Hoatson, 2000b), a lack of granitic rocks with arc-like compositions prior to c. 1850 Ma, the presence of mafic and felsic igneous rocks in the Halls Creek Orogen that are not diagnostic of subduction – though able to be placed in a post-collisional setting (Sheppard et al., 2001) – and Sm–Nd isotope evidence for significant evolved crustal material in the Central Zone (Sun and Hoatson, 2000; Sheppard et al., 2001), contrasting with the dominantly juvenile signatures expected in oceanic arcs.

In this study, detrital zircons from metasedimentary rocks of the Western and Central Zones of the Lamboo Province were dated to better constrain the age and provenance of successions deposited prior to the Halls Creek Orogeny. Representative Lu–Hf isotope data for detrital zircons were also collected for some samples, which can be used to provide further constraints on interpretations of sediment provenance and stratigraphic correlations (e.g. Howard et al.,

2009). The results are compared with data from the Eastern Zone (Phillips et al., 2016) and the broader region (e.g. Maidment et al., 2020) to assess whether the Western and Central Zones represent exotic terranes or are autochthonous with respect to the proto-North Australian Craton.

## Geology of the Lamboo Province

The 1912–1788 Ma Lamboo Province is exposed in two linear orogens along the structural margins of the overlying 1814–1740 Ma Kimberley Basin (Fig. 2; Tyler et al., 2012). In the east, the Lamboo Province is exposed in the north-northeasterly trending Halls Creek Orogen, whereas, in the west, it is exposed in the west-northwesterly trending Wunaamin Miliwundi Orogen (previously known as the King Leopold Orogen). The nature of basement beneath the Kimberley Basin is not well constrained, but it appears to contain a significant proportion of granitic rock (Gunn and



Meixner, 1998) and it is possible that the Lamboo Province extends beneath most or all of the basin. Basement to the Lamboo Province is not exposed, though Archean basement rocks have been inferred from the Sm–Nd and Lu–Hf isotope characteristics of granitic rocks and xenoliths in kimberlite, the abundance of Archean detrital zircons in overlying sedimentary successions, Re–Os whole-rock and mineral isotope data for lamproite and kimberlite, and the seismic velocity structure of the crust (Hollis et al., 2015, and references therein).

The geological terminology for the province has changed with time, with the term ‘Lamboo Complex’ previously applied to rocks exposed in the Halls Creek Orogen, and ‘Hooper Orogen’ used to refer to the rocks exposed in the Wunaamin Miliwundi Orogen (e.g. Griffin et al., 2000a; Page et al., 2001). This terminology was subsequently modified to the ‘Lamboo and Hooper Provinces’ (Tyler et al., 2012), and current Geological Survey of Western Australia terminology places all these rocks within a single ‘Lamboo Province’ (e.g. Phillips et al., 2016), recognizing that the rocks exposed in the Wunaamin Miliwundi Orogen are likely correlatives of those exposed in the western Halls Creek Orogen. The Lamboo Province is divided into three tectonostratigraphic terranes: the Western, Central and Eastern Zones (Figs 2, 3). This reflects reduction from four domains defined by Hancock and Rutland (1984) to three domains by Griffin and Tyler (1992), and subsequent revision of the boundaries between the zones by Tyler et al. (1995). The Western Zone is exposed in the Wunaamin Miliwundi Orogen and the western part of the Halls Creek Orogen, whereas the Central and Eastern Zones are exposed only in the Halls Creek Orogen. The Lamboo Province extends beneath younger sedimentary cover to the southeast, where it may be transitional with the Granites–Tanami Orogen (Phillips et al., 2016; Iaccheri et al., 2018; Maidment et al., 2020). In many areas, the boundaries between zones coincide with steeply dipping, north-northeasterly trending faults, which disrupted zonal boundaries that originally trended northeast–southwest to east-northeast–south-southwest (Tyler et al., 1995). The present pattern of exposure of the Lamboo Province is a result of exhumation during several Paleoproterozoic to Paleozoic deformational events in the Halls Creek and Wunaamin Miliwundi Orogens.

Numerous individual intrusive bodies and volcanic units within the Lamboo Province have been named, with many, but not all, of these assigned to igneous suites. The igneous associations and ages of units discussed in this report are listed in Table 1, and more complete information about the current nomenclature and description of units is available in the GSWA Explanatory Notes System (ENS), accessible through [GeoVIEW.WA](#). The [Australian Stratigraphic Units Database](#), managed by Geoscience Australia, includes information about obsolete or superseded unit nomenclature.

## Western Zone

The Western Zone consists of siliciclastic metasedimentary rocks of the Marboo Formation, which are intruded by voluminous felsic and mafic rocks of the 1867–1849 Ma Paperbark Supersuite and mafic sills of the Ruins Dolerite (Tyler et al., 1999; Griffin et al., 2000a; Page et al., 2001; Lu et al., 2017a,e–g). These rocks are overlain by felsic

volcanic rocks of the Whitewater Volcanics, which form a younger extrusive component of the Paperbark Supersuite (Griffin et al., 2000a). The Marboo Formation consists of turbiditic feldspathic quartz sandstone, siltstone and mudstone, with minor graphitic schist (Hancock, 1991; Tyler et al., 1999). In the Wunaamin Miliwundi Orogen, the Marboo Formation has informally been divided (Hancock, 1991) into a ~3000 m-thick lower package (Unit 1) and an overlying package up to ~3500 m thick (Unit 2). Unit 1 consists of metamorphosed turbiditic quartz–feldspar wacke and siltstone, with significant thicknesses of laminated metasilstone. A package containing carbonaceous metapelitic schist intruded by the Ruins Dolerite has been assigned to the base of Unit 2, which is overlain by a compositionally and texturally immature package of quartz–feldspar–muscovite±biotite schist with a greater felsic component than Unit 1. U–Pb zircon dating of a sample of Unit 1 yielded a range of detrital ages between c. 2500 and 1903 Ma, whereas dating of a metamorphosed equivalent of Unit 2, the Mount Joseph Migmatite, yielded a youngest detrital age component at  $1872 \pm 9$  Ma (Tyler et al., 1999).

The Marboo Formation and Ruins Dolerite were overprinted by a layer-parallel foliation (local  $S_1$ ) and locally metamorphosed in low- to moderate-pressure (low- to moderate- $P$ ), high-temperature (high- $T$ ) conditions (Korhonen et al., 2022), with  $S_1$  deformed by upright northwesterly trending folds (local  $F_2$ ) (Tyler and Griffin, 1990). The  $D_1$  and  $D_2$  events are collectively referred to as the Hooper Orogeny, which overlapped with the emplacement of the Paperbark Supersuite. Metamorphic zircon rims in the Mount Joseph Migmatite dated at  $1861 \pm 5$  Ma were developed during this tectonism (Tyler et al., 1999), whereas monazite associated with peak metamorphism yields slightly younger ages of c. 1855 Ma (e.g. Fielding et al., 2019c). Although metamorphic grades can locally be relatively high, particularly near granitic rocks, much of the Marboo Formation has not been metamorphosed above greenschist facies.

Felsic volcanic rocks of the 2000–3000 m-thick Whitewater Volcanics unconformably overlie the Marboo Formation and have yielded U–Pb zircon dates of  $1857 \pm 4$  and  $1854 \pm 5$  Ma in the Kimberley region (Griffin et al., 2000a), and  $1849 \pm 6$  Ma for an inferred correlative in the Northern Territory (Worden et al., 2008).

## Central Zone

The boundary between the Central and Western Zones is taken to be a combination of several faults – the Ramsay Range and Springvale Faults and northern part of the Halls Creek Fault – whereas the boundary between the Central Zone and Eastern Zone is taken to be a combination of the Angelo, Halls Creek and Osmond Faults (Tyler et al., 1995).

The oldest rocks exposed in the Central Zone are the Tickalara Metamorphics, a deformed and metamorphosed succession of pelitic and psammitic sedimentary rocks, lesser tholeiitic mafic volcanic rocks, and minor carbonate, calc-silicate rock, chert, graphitic schist, quartzite and banded iron-formation (Dow and Gemuts, 1969; Gemuts, 1971; Tyler et al., 1995). In some areas of lower strain, mafic units within the Tickalara Metamorphics are demonstrably volcanic, preserving relict pillow textures (Blake et al., 2000; Tyler, 2004).

Table 1. Ages and igneous associations of intrusive units referred to in this Report

<i>Supersuite</i>	<i>Suite</i>	<i>Unit</i>	<i>Zone</i>	<i>Dominant composition</i>	<i>Inferred age (Ma)</i>
Sally Downs Supersuite	Poonta Suite	San Sou Monzogranite	Eastern	Felsic	c. 1788
		Warmun Dolerite	Western/Central	Mafic	1829–1814
	Kevins Dam Suite	Mount Christine Granite	Central/Eastern	Felsic	c. 1808
	Mabel Downs Suite	Sally Downs Tonalite	Central	Felsic	c. 1821
	"	Mabel Downs Tonalite	Central	Felsic	1837–1829
	"	McHale Granite	Central	Felsic	c. 1827
	"	Loadstone Monzogranite	Central	Felsic	c. 1827
	"	Emull Gabbro	Central	Mafic	1832–1808
	McIntosh Suite		Central	Mafic–ultramafic	c. 1830
	Sally Malay Suite		Central	Mafic–ultramafic	1848–1839
		Woodward Dolerite	Eastern	Mafic	1904–1846 (c. 1846?)
		Rose Bore Granite	Central	Felsic/ metasedimentary?	1863–1822
		Fletcher Creek Granite	Central	Felsic	c. 1850/1838?
	Dougalls Suite	Dougalls Tonalite	Central	Felsic	1849–1847, 1838?
Paperbark Supersuite	Panton Suite		Central	Mafic–ultramafic	c. 1856
		Whitewater Volcanics	Western	Felsic	1857–1854
	"	Violet Valley Tonalite	Western/Central	Felsic	c. 1852
	"	Kevins Dam Monzogranite	Western/Central	Felsic	c. 1854
	"	Greenvale Porphyry	Western	Felsic	c. 1855
	"	Toby Gabbro	Western	Mafic	c. 1855
	"	Springvale Suite	Western	Mafic	c. 1857
	"	Mount Nyulas Granite	Western	Felsic	c. 1859
	"	Neville Granodiorite	Western	Felsic	c. 1860
	"	Crooked Creek Granite	Western	Felsic	1864–1854
	"	Dinner Creek Tonalite	Western	Felsic	1864–1859
	"	Lennard Granite	Western	Felsic	1864–1862
		Ruins Dolerite	Western	Mafic	c. 1873

Detrital zircon geochronology of the Tickalara Metamorphics yields consistent maximum depositional ages of c. 1865 Ma (Page, 1996a,b; Bodorkos et al., 1999, 2000b; Oliver et al., 1999; Page and Hoatson, 2000; Mole et al., 2018). U–Pb zircon dating of the Rose Bore Granite, which intrudes the Tickalara Metamorphics, yielded a date of  $1863 \pm 3$  Ma, which has been interpreted as a magmatic age and a minimum depositional age for the host unit (Page and Hoatson, 2000). The Tickalara Metamorphics were metamorphosed at up to granulite facies under high-*T*, low-*P* conditions (750–800 °C, 3.5 – 5.0 kbar) (Thornett, 1986; Bodorkos et al., 1999, 2002). U–Pb dating of zircon rims yields dates of  $1843 \pm 4$  Ma (Bodorkos et al., 2000b),  $1847 \pm 3$  Ma (calculated from data of Oliver et al., 1999) and 1846–1837 Ma (Mole et al., 2018). Monazite from leucosome is dated at  $1845 \pm 3$  Ma (Oliver et al., 1999). This metamorphism and associated bimodal mafic magmatism has been termed the ‘Savannah Event’ by Mole et al. (2018) and this informal terminology is followed here.

The Koongie Park Formation is exposed in the southern Central Zone and consists of a  $\geq 2000$  m-thick metamorphosed succession of tholeiitic basalt, A-type felsic volcanic and volcanoclastic rocks, turbiditic sandstone, laminated siltstone and mudstone, chert, carbonate and iron-formation (Griffin and Tyler, 1994; Orth, 1997, 2002). The contact between this unit and the Tickalara Metamorphics is poorly exposed, faulted or intruded by granitic rocks, but U–Pb zircon dates of  $1845 \pm 2$ ,  $1843 \pm 5$  and  $1840 \pm 4$  Ma for felsic volcanic rocks (Page et al., 1994) indicate that the Koongie Park Formation is younger than the Tickalara Metamorphics.

The fault-bound Milba Formation in the southeastern Central Zone consists of greywacke, siltstone and mudstone, lithic and minor quartz sandstone, calcareous rocks and chert, with minor mafic volcanic rocks and sills, metamorphosed at greenschist facies (Blake et al., 2000). The unit is probably  $>1000$  m thick, but estimates are limited by deformation, a lack of marker units and the fact that the upper and lower contacts are not preserved (Blake et al., 1999). The previously undated Milba Formation has been suggested to be a possible lower metamorphic-grade correlative of the Tickalara Metamorphics or a correlative of the Koongie Park Formation (Blake et al., 2000).

The Winnama Formation crops out in the Osmond Range in the eastern Lamboo Province and is considered to be part of the Central Zone, with the contact with the Eastern Zone in this area taken as the east-northeasterly trending Osmond Fault (Tyler et al., 1995). The Winnama Formation consists of greywacke, lithic sandstone, siltstone and mudstone, with intercalated basalt and lesser carbonate that has been metamorphosed at low to medium grade (Tyler et al., 1997a; Blake et al., 2000). The unit has not been previously dated, but a minimum age is provided by the  $1827 \pm 3$  Ma McHale Granite, which intrudes the succession (Page et al., 2001).

## Eastern Zone

The oldest rocks in the Eastern Zone, and the Lamboo Province overall, are bimodal volcanic rocks and A-type granitic rocks of the Sophie Downs Suite, which are exposed in the cores of domal structures (Blake et al., 1999; Phillips et al., 2016). Felsic volcanic rocks of the Ding Dong Downs

Volcanics, which form part of the Sophie Downs Suite, are associated with minor metasedimentary rocks and have been dated at 1912–1904 Ma, overlapping with dates of c. 1912 and 1911 Ma obtained from granitic intrusive equivalents (Phillips et al., 2016).

Metasedimentary and metavolcanic rocks of the 1904–1837 Ma Halls Creek Group unconformably overlie the Sophie Downs Suite and comprise most of the outcropping Eastern Zone (Hancock and Rutland, 1984; Blake et al., 1999; Phillips et al., 2016). The Halls Creek Group is divided into the Saunders Creek, Brim Rockhole, Biscay and Olympio Formations (Fig. 3), which have an estimated combined thickness of 5–8 km (Hancock and Rutland, 1984; Phillips et al., 2016).

The  $\leq 200$  m-thick Saunders Creek Formation forms the base of the Halls Creek Group and consists of sandstone and conglomerate deposited in a fluvial setting. It is conformably overlain by the  $\leq 200$  m-thick Brim Rockhole Formation, which comprises carbonate and siliciclastic metasedimentary rocks, felsic and mafic volcanic rocks and lesser graphitic schist deposited in an interpreted shallow marine setting. A felsic volcanic unit within the Brim Rockhole Formation has been dated at  $1881 \pm 4$  Ma (Blake et al., 1999). The Biscay Formation overlies the Brim Rockhole Formation above a low-angle unconformity and consists of a  $>700$  m thickness of mafic volcanic and volcanoclastic rocks, sandstone, siltstone, carbonate and pelitic schist deposited in a marine setting. The Olympio Formation overlies the Biscay Formation and forms a thick package of turbiditic siliciclastic metasedimentary rocks with two intercalated alkaline felsic volcanic units, the Maude Headley and Butchers Gully Members (Fig. 3). These volcanic rocks have been dated at  $1856 \pm 6$  and  $1846 \pm 4$  Ma (Blake et al., 1999), and a metasedimentary rock from the uppermost part of the formation yielded a maximum depositional age of  $1834 \pm 8$  Ma (GSWA 206184; Wingate et al., 2015), indicating that this unit was deposited over an extended period (Phillips et al., 2016). The thickness of the Olympio Formation is difficult to estimate due to the effects of deformation, but is likely to be at least 4000 m.

The Sophie Downs Suite and Halls Creek Group are intruded by dolerite and gabbro sills of the Woodward Dolerite, which are up to 200 m thick (Griffin and Tyler, 1992; Blake et al., 1999). At least some of these undated sills post-date the c. 1846 Ma Butchers Gully Member, and were folded during the Halls Creek Orogeny (Phillips et al., 2016).

## Mafic–ultramafic layered intrusions (1857–1823 Ma)

Multiple mafic–ultramafic layered intrusions intruded the Western and Central Zones in the Halls Creek Orogen prior to and during the Halls Creek Orogeny (Dow and Gemuts, 1969; Page and Hoatson, 2000; Hoatson, 2000a). The intrusions are localized in the central part of the orogen, range up to 7.8 km thick and have outcropping areas of up to 240 km<sup>2</sup>. The intrusions are broadly coincident with a major regional gravity high that is indicative of a significant volume of mafic rock at depth (Shaw et al., 2000; Lindsay et al., 2016). Smaller, irregularly shaped mafic intrusions have been assigned to the Tickalara Metamorphics (Hoatson, 2000a).

Geochronology and field relationships indicate that the mafic–ultramafic intrusions were emplaced over an extended period (Page and Hoatson, 2000; Hoatson, 2000a; Mole et al., 2018), though most were emplaced before the Halls Creek Orogeny. Three intrusions (Panton, Springvale and Toby) have U–Pb zircon dates of 1857–1854 Ma (Page and Hoatson, 2000; Kemp et al., 2015). Intrusions comprising the Sally Malay Suite have U–Pb zircon dates between c. 1848 and 1839 Ma and a baddeleyite date of  $1846 \pm 5$  Ma (Page and Hoatson, 2000; Mole et al., 2018). The Corridor gabbro has a similar zircon date of c. 1842 Ma (Kemp et al., 2015). An  $1830 \pm 3$  Ma date for zircon rims in the Tickalara Metamorphics adjacent to the McIntosh intrusion has been interpreted to date contact metamorphism associated with its emplacement (Page and Hoatson, 2000). The youngest dated intrusion is an  $1823 \pm 3$  Ma pyroxenite at the Copernicus deposit (Mole et al., 2018).

## Halls Creek Orogeny (1837–1808 Ma)

Deformation of the Halls Creek Orogeny affected the eastern part of the Lamboo Province, where it forms a north-northeasterly trending zone of upright folding and faulting associated with the emplacement of felsic and mafic intrusive rocks of the 1837–1808 Ma Sally Downs Supersuite. The effects of this event have recently been recognized in the Wunaamin Miliwundi Orogen, with the growth of monazite at 1825–1804 Ma attributed to an influx of fluids during deformation within the stability field of andalusite (Fielding et al., 2019d,e; Korhonen et al., 2022).

In the Central Zone, two phases of folding have been associated with the Halls Creek Orogeny. An older generation of open, upright, east–west-trending folds (local  $D_3/F_3$ ) is overprinted by a younger generation of regional-scale, north-northeasterly trending, open to tight folds (local  $D_4/F_4$ ) and associated shear zones (Thornett, 1986; Oliver and Barr, 1997; Bodorkos et al., 2000a). The metamorphic conditions during ductile  $D_3$  deformation are not tightly constrained, but were of lower grade than those of the Savannah Event. Predominantly brittle deformation during  $D_4$  was associated with greenschist facies assemblages, reflecting progressive cooling of the Central Zone during the Halls Creek Orogeny (Bodorkos et al., 2000b).

In the Eastern Zone, the oldest recognized structures are layer-parallel shear zones affecting the Sophie Downs Suite and Halls Creek Group. This shearing is interpreted to reflect extension prior to the Halls Creek Orogeny, with locally developed andalusite-bearing assemblages indicative of moderate-temperature, low-pressure metamorphism (Hancock, 1991; Warren, 1994, 1997; Tyler et al., 1998). Deformation during the Halls Creek Orogeny in this area consists of east-northeasterly to northeasterly trending, open to isoclinal, inclined to upright folds with an axial planar foliation developed under greenschist to locally amphibolite facies conditions (Tyler et al., 1998; Blake et al., 2000).

The age of the Halls Creek Orogeny is largely constrained by overprinting relationships between structures and dated igneous rocks, with a paucity of direct dates for metamorphism. In the Central Zone, the Halls Creek Orogeny post-dates deposition of the 1845–1840 Ma Koongie Park

Formation, providing a maximum age constraint. Dating of the broadly syn-deformational granitic rocks of Mabel Downs Tonalite has yielded dates of  $1837 \pm 6$  Ma for an older phase that is overprinted by  $S_3$ ,  $1832 \pm 3$  Ma for a syn- $D_3$  phase and  $1827 \pm 7$  Ma for a post- $D_3$  felsic vein (Bodorkos et al., 2000a). The  $D_4$  event is younger than  $1827 \pm 7$  Ma, and may be responsible for a foliation developed in an  $1817 \pm 4$  Ma phase of the Mount Christine Granite, which is crosscut by an unfoliated younger intrusion at  $1808 \pm 3$  Ma (Page et al., 2001). In the Eastern Zone,  $D_4$  deformation affects the upper Olympio Formation, which was deposited after  $1834 \pm 8$  Ma (Phillips et al., 2016), consistent with the constraints obtained from the Central Zone.

A suite of northwesterly trending dolerite dykes in the central and southern Halls Creek Orogen crosscuts structures associated with the Halls Creek Orogeny, but does not appear to extend into the Kimberley Basin (Phillips et al., 2018). These undated dykes have been recently renamed as the Warmun Dolerite (formerly the Bow River dykes) and may reflect extension following the Halls Creek Orogeny, possibly related to orogenic collapse, or initiation of the Kimberley Basin.

## Dougalls Suite

The Dougalls Suite in the Central Zone consists of relatively small bodies and dykes of sodic granitic rocks, which are spatially associated with coeval mafic intrusive rocks (Ogasawara, 1988; Sheppard et al., 2001). These rocks contain a high-grade foliation, interpreted as  $S_2$ , which is folded by  $F_3$  and  $F_4$  folds developed during the Halls Creek Orogeny (Bodorkos et al., 1999). This suggests emplacement of the Dougalls Suite prior to, or synchronous with, the Savannah Event ( $D_2$ ). A date of  $1849 \pm 3$  Ma for the Dougalls Tonalite (Page et al., 2001) is consistent with this interpretation. Although re-dating of this sample (Kemp et al., 2015) yielded a date of c. 1838 Ma, which would indicate emplacement near the start of the Halls Creek Orogeny, another sample of Dougalls Tonalite yielded a crystallization age of  $1847 \pm 5$  Ma (GSWA 218350, Lu et al 2020c).

The Dougalls Suite is exposed in the central and northern part of the Central Zone and consists of tonalite, trondhjemite and quartz diorite with high  $\text{Na}_2\text{O}$ ,  $\text{CaO}$  and  $\text{K/Rb}$ , and low  $\text{K}_2\text{O}$ ,  $\text{Rb}$ ,  $\text{LREE}$ ,  $\text{Y}$ ,  $\text{Th}$ ,  $\text{U}$  and  $\text{Rb/Sr}$  (Ogasawara, 1988; Sheppard et al., 2001). It has been divided into two geochemical groups. One group comprises quartz diorite and mafic tonalite (58–67 wt%  $\text{SiO}_2$ ), and has moderate  $\text{Y}$  and  $\text{Yb}$  and weakly fractionated REE patterns, whereas the second group, composed of tonalite and trondhjemite (62–73 wt%  $\text{SiO}_2$ ), has high  $\text{Sr/Y}$  and strongly fractionated REE patterns with positive  $\text{Eu}$  anomalies. This second group has the characteristics of high- $\text{Al}$  TTG (trondhjemite–tonalite–granodiorite) or adakite, consistent with melting of a dominantly mafic source at depths  $\geq 40$  km (Sheppard et al., 2001; Martin et al., 2005; Richards and Kerrich, 2007; Moya, 2009; Castillo, 2012). These characteristics are similar to those of Phanerozoic granitic rocks in active continental margin or oceanic arc settings, and a similar geodynamic setting has been interpreted for the emplacement of these magmas (Sheppard et al., 2001).



## Sally Downs Supersuite

Felsic and mafic intrusive rocks of the 1837–1808 Ma Sally Downs Supersuite were intruded over a broad area of the east Kimberley during the Halls Creek Orogeny. These igneous rocks are largely restricted to the Central Zone, though a few intrusions in the Western and Eastern Zones are also thought to be part of this magmatic event (Sheppard et al., 2001; Page et al., 2001). The Sally Downs Supersuite is subdivided into three geochemical components: the Mabel Downs, Syenite Camp and Kevins Dam Suites, which have field relationships indicating that they were coeval with mafic magmas (Blake et al., 2000; Sheppard et al., 2001). The biotite- and hornblende-bearing Mabel Downs Suite has geochemical similarities to the adakite-like component of the Dougalls Suite, but with slightly higher  $K_2O$ , less pronounced or no positive Eu anomalies and less fractionated REE (Ogasawara, 1988; Sheppard et al., 2001). Samples of the Mabel Downs Suite have been dated at 1837–1821 Ma (Bodorkos et al., 2000a; Page et al., 2001).

The Syenite Camp and Kevins Dam Suites are more felsic than the Mabel Downs Suite and trend towards high  $K_2O$  with increasing  $SiO_2$  – differing from the Mabel Downs Suite, which does not show a similar increase in  $K_2O$  with increasing  $SiO_2$  – and are interpreted to be derived from crust of significantly different bulk composition (Sheppard et al., 2001). The Kevins Dam Suite is the most potassic, having high  $K_2O$ , Rb, Y, Th and  $K_2O/Na_2O$  and low Sr, Sr/Y and K/Rb. This composition is similar to that of the Paperbark Supersuite, and both are interpreted to have been sourced from mid-crustal depths under relatively high geothermal gradients (Griffin et al., 2000a; Sheppard et al., 2001). The Syenite Camp Suite is also relatively potassic, with compositions generally intermediate between those of the Kevins Dam and Mabel Downs Suites. Three samples of the Kevins Dam Suite have yielded U–Pb zircon crystallization ages of 1827–1808 Ma, whereas a single sample of the Syenite Camp Suite yielded an age of  $1817 \pm 4$  Ma (Page et al., 2001).

## Poonta Suite (1804–1788 Ma)

Several small late-stage plutons of biotite monzogranite intrude the southern part of the Central and Eastern Zones. These have not been assigned a formal geochemical grouping, but were informally referred to as the San Sou suite by Page et al. (2001), who obtained U–Pb zircon dates of  $1804 \pm 5$  and  $1788 \pm 6$  Ma for the Eastman Granite and San Sou Monzogranite, respectively. These granitic rocks are now assigned to the newly defined Poonta Suite, which possibly forms an extension of a west-northwesterly trending belt of 1815–1790 Ma granitic rocks in the Granites–Tanami Orogen and Aileron Province of central Australia (Maidment et al., 2020).

## Kimberley Basin (1814–1740 Ma)

The Lamboo Province is unconformably overlain by the Kimberley Basin, which covers much of the Kimberley region (Harms, 1959; Dow et al., 1964; Gellatly et al., 1975; Griffin et al., 1994; Thorne et al., 1999; Phillips, 2019). The basin is up to 7 km thick and consists of fluvial to shallow-marine siliciclastic rocks with lesser mafic volcanic rocks and dolerite sills that comprise the Hart–Carson

Large Igneous Province (Tyler et al., 2006; Phillips et al., 2017; Ramsay et al., 2019). The Kimberley Basin consists of the Speewah and Kimberley Groups, with the Speewah Group now incorporated within the Kimberley Basin rather than being assigned to a distinct basin (Phillips et al., 2017). A unit in the Speewah Group in the lower part of the basin has a maximum depositional age of  $1814 \pm 10$  Ma (Ramsay et al., 2017). This is significantly younger than an  $1835 \pm 3$  Ma age component obtained from an interpreted volcanoclastic rock in the Speewah Group (Page and Sun, 1994; Sheppard et al., 2012), which has previously been used as evidence of initiation as a foreland basin during the Halls Creek Orogeny (Sheppard et al., 2012; Hollis et al., 2014b). The c. 1814 Ma maximum depositional age, however, opens up the possibility that the development of the Kimberley Basin entirely post-dates the Halls Creek Orogeny. Granophyric mafic sills of the Hart Dolerite in the lower Kimberley Basin have U–Pb baddeleyite and zircon dates indicating emplacement at  $1792.6 \pm 1.2$  Ma (Ramsay et al., 2019). A  $1740 \pm 6$  Ma date for an intrusive porphyry in the southwestern part of the basin (GSWA 95406; Wingate et al., 2011) provides a minimum age for sedimentation.

## Yampi Orogeny (900–800 Ma)

West-northwesterly trending shear zones in the Wunaamin Miliwundi Orogen affect the Lamboo Province and Kimberley Basin, but are not considered to have affected  $\leq 720$  Ma sedimentary rocks of the Mount House Sub-basin of the Louisa Basin, which unconformably overlie the Kimberley Basin (Tyler and Griffin, 1990). This deformation, termed the Yampi Orogeny, is inferred to be associated with north-northeast–south-southwest shortening under amphibolite facies conditions in the Wunaamin Miliwundi Orogen, and to be expressed as gentle folds in the Kimberley Basin away from the orogen (Tyler and Griffin, 1990). In the Halls Creek Orogen, long-lived, north-northeasterly trending sinistral strike-slip faults and easterly trending dextral faults post-date deposition of the Kimberley Basin and offset sedimentary rocks as young as Devonian (Dow and Gemuts, 1969; Plumb and Gemuts, 1976; Tyler et al., 1995, 1998; Thorne and Tyler, 1996). A significant component of movement took place after deposition of the Carr Boyd Group, which is imprecisely constrained to 1324–1177 Ma (Thorne and Tyler, 1996; Phillips, 2019), and some of this deformation may have taken place during the Yampi Orogeny.

The age of the Yampi Orogeny is poorly constrained and there is little isotopic evidence of high-grade metamorphism associated with this event in the Wunaamin Miliwundi Orogen (Fielding et al., 2020a). K–Ar biotite dates of  $1475 \pm 12$  and  $999 \pm 9$  Ma from granitic rocks in the Wunaamin Miliwundi Orogen were suggested by Shaw et al. (1992) to indicate a  $\geq 1000$  Ma age for the Yampi Orogeny. Bodorkos and Reddy (2004) obtained  $^{40}Ar/^{39}Ar$  biotite and muscovite dates of 900–800 Ma from the Halls Creek Orogen that they suggested might more accurately reflect the timing of Yampi Orogeny deformation, with pre-1000 Ma dates affected by excess Ar. The  $1009 \pm 16$  Ma Cummins Range carbonatite, which was emplaced near the junction of the Wunaamin Miliwundi and Halls Creek Orogens, records evidence of isotope resetting at c. 900 Ma, which is suggested to reflect thermal reworking during the Yampi

Orogeny (Downes et al., 2016). The inferred age of the Yampi Orogeny is broadly comparable to that of tectonism in the east Pilbara region (Jones, 2011) and Capricorn Orogen (Olierook et al., 2019), and it may represent part of a regional-scale intraplate reworking event.

## Wunaamin Miliwundi Orogeny (590–500 Ma)

In the Wunaamin Miliwundi Orogen, southwesterly directed thrusting and large-scale folding of rocks as young as Neoproterozoic are assigned to the Wunaamin Miliwundi Orogeny, formerly known as the King Leopold Orogeny (Griffin and Myers, 1988; Tyler and Griffin, 1990). This deformation is strongly partitioned into the orogen and involved thrusting of less deformed rocks of the Kimberley Basin southwards over the Lamboo Province along a sole thrust. In the Halls Creek Orogen, some of the strike-slip movement along north-northeasterly trending faults is thought to have taken place during the Wunaamin Miliwundi Orogeny, though the nature of deformation at this time is poorly constrained.

The age of the Wunaamin Miliwundi Orogeny is imprecisely defined by K–Ar dates of  $557 \pm 8$  Ma for biotite and  $532 \pm 3$  Ma for muscovite (Shaw et al., 1992). Isotopic disturbance of monazite in the Cummins Range carbonatite at c. 590 Ma has also been associated with this event (Downes et al., 2016). Whole-rock Rb–Sr dates of  $630 \pm 90$  Ma and c. 580 Ma (Bennett and Gellatly, 1970),  $576 \pm 80$  Ma (Plumb, 1981) and c. 568 Ma (Coats and Preiss, 1980) from the orogen are also likely to reflect the thermal effects of the Wunaamin Miliwundi Orogeny. The c. 511 Ma Milliwindi Dolerite (Hanley and Wingate, 2000; Jourdan et al., 2014) forms a >200 km-long dyke that is considered to crosscut structures assigned to the Wunaamin Miliwundi Orogeny and provides a minimum age for this deformation (Griffin et al., 1993). This dyke forms part of the Kalkarindji Large Igneous Province, which includes basalt of the c. 509 Ma Antrim Plateau Volcanics that unconformably overlies older rocks in the east Kimberley region (Jourdan et al., 2014). An inferred c. 511 Ma minimum age for the Wunaamin Miliwundi Orogeny is, however, complicated by recent 505–501 Ma dates for metamorphic monazite, which are interpreted as the age of amphibolite-grade metamorphism, possibly during crustal thickening (Fielding et al., 2019a–c, 2020a). These results are broadly comparable to in situ Rb–Sr dates for biotite from a crenulated fabric in the Marboo Formation from the northwesternmost extent of the Wunaamin Miliwundi Orogen, which yielded an apparent age of  $497 \pm 15$  Ma, interpreted as the time of cooling below  $\sim 300$  °C following greenschist facies metamorphism (Liebmann et al., 2022). These ages indicate that the Wunaamin Miliwundi Orogeny probably extended to c. 500 Ma.

## Alice Springs Orogeny (450–295 Ma)

The Antrim Plateau Volcanics and Cambrian to Late Devonian sedimentary rocks of the Bonaparte Basin are folded and offset by north-northeasterly trending sinistral strike-slip faults in the northern Halls Creek Orogen. Late Devonian sedimentary basins localized in the east Kimberley are interpreted to have developed as stepover

or transtensional basins related to movement on the Halls Creek Fault system (Mory and Beere, 1985; Mory, 1990; Thorne and Tyler, 1996). This sedimentation and deformation has been associated with the Alice Springs Orogeny, which in central Australia consists of multiple compressional events between c. 450 and 295 Ma (Scrimgeour, 2013). The effects of the Alice Springs Orogeny in the Wunaamin Miliwundi Orogen are less well constrained, but may differ from those in the Halls Creek Orogen, with evidence for both extensional and compressional events during this period in the Canning Basin immediately south of the orogen (Braun et al., 1991; Frogtech Geoscience, 2017).

## Mineralization

The Lamboo Province hosts a range of mineral deposits and occurrences, including magmatic Ni–Cu–Co, diamonds, orogenic gold, volcanogenic massive sulfide (VMS) Cu–Pb–Zn–Ag, and hydrothermal-vein-hosted REE (Sanders, 1999; Hassan, 2000, 2004; Ruddock, 2003; Occhipinti et al., 2017).

Mafic–ultramafic layered intrusions dated at 1857–1823 Ma in the Central Zone host orthomagmatic Ni–Cu–Co mineralization, which has been mined at the Savannah and Copernicus deposits. Platinum-group element (PGE) and chromium occurrences have also been identified in some of these intrusions, in particular the Panton sill (Hoatson, 2000c). Orthomagmatic Ni–Cu–Co mineralization has also been identified in the Ruins Dolerite in the Wunaamin Miliwundi Orogen (Buxton Resources Ltd., 2018).

Multiple small intrusions of lamproite and kimberlite with a range of ages occur across the Kimberley region, intruding the Lamboo Province and overlying sedimentary basins (Hutchison, 2018). The  $1177 \pm 47$  Ma lamproite-hosted Argyle deposit in the northern part of the Halls Creek Orogen was emplaced within Mesoproterozoic sedimentary host rocks of the Carr Boyd Group, which unconformably overlie the Lamboo Province (Pidgeon et al., 1989; Boxer et al., 2017).

Orogenic gold deposits and occurrences are localized near major faults in the Halls Creek Orogen and are largely hosted by the Biscay Formation and lower Olympio Formation in the Eastern Zone (e.g. Mount Bradley deposit) (Sanders, 1999). Orogenic gold mineralization is also present in the Koongie Park Formation in the Central Zone (Nicolsons deposit). Muscovite  $^{40}\text{Ar}/^{39}\text{Ar}$  dating of mineralization-related alteration at the Mount Bradley and Nicolsons deposits yielded dates of c. 1838 and 1826 Ma, respectively, interpreted as ages of mineralization and indicating emplacement during the Halls Creek Orogeny (Kohanpour et al., 2019b).

The Koongie Park Formation in the Central Zone hosts several VMS Cu–Pb–Zn–Ag deposits and occurrences, with possible VMS-style mineralization also occurring in the Brim Rockhole Formation in the Eastern Zone and the Marboo Formation in the Western Zone (Hassan, 2000, 2004).

REE-bearing hydrothermal quartz veins occur at the John Galt prospect in the Halls Creek Orogen, hosted by structurally dismembered correlatives of the Kimberley Basin overlying the Lamboo Province. The mineralization has been dated at  $1619 \pm 9$  Ma (Morin-Ka et al., 2016), an age that does not correspond to any previously identified tectonic events in the orogen.

## Geodynamic models

As a geological event framework for the Kimberley region became established as a result of geological mapping (Dow and Gemuts, 1969; Gemuts, 1971; Gellatly et al., 1974, 1975; Plumb and Gemuts, 1976), various geodynamic models were proposed to explain the tectonic development of the Lamboo Province and broader North Australian Craton. Many early models placed tectonism in an intraplate setting, floored by continental crust (Rutland, 1973; Hancock and Rutland, 1984; Thornett, 1986; Etheridge et al., 1987; Wyborn et al., 1987; Wyborn and Blake, 2000). More recent studies favoured mobility between crustal elements, with tectonism driven by subduction, accretion and collision (Ogasawara, 1988; Tyler et al., 1995, 2012; Sheppard et al., 1999b, 2001; Griffin et al., 2000a; Fraser et al., 2007; Cawood and Korsch, 2008; Huston et al., 2012; Lindsay et al., 2016; Betts et al., 2016; Kohanpour et al., 2017; Occhipinti et al., 2017; Aitken et al., 2018; Mole et al., 2018). An overview of the development of 'fixist' and 'mobilst' models for the Lamboo Province is presented below to provide context for the interpretation presented in this study.

Rutland (1973) considered that much of the Proterozoic tectonism in northern Australia was ensialic in nature. Mafic rocks were considered to be continental tholeiites; and high-*T*, low-*P* metamorphism was interpreted to reflect thinner lithosphere and higher heat flow in the Proterozoic. Widespread zones of tectonism were inferred to have developed inboard of subduction in back-arcs that were considerably broader than those developed in the Phanerozoic. Most orogenic belts were interpreted to be intraplate, possibly focused into strike-slip zones, with the Halls Creek and Wunaamin Miliwundi Orogens considered possible examples of a conjugate system.

Hancock and Rutland (1984) considered that the Halls Creek and Wunaamin Miliwundi Orogens were initiated by intraplate extension that isolated a relatively undeformed continental block that now underlies the Kimberley Basin. Extension resulted in crustal thinning, subsidence and high heat flows in the orogens, which were subsequently reactivated under compression, resulting in underthrusting of continental crust and the generation of granitic magmas. In their model, the Halls Creek Group was considered to have correlatives in the Central and Western Zones, though possibly as diachronous units, and extension was not sufficient to generate oceanic crust. Thornett (1986) similarly considered evidence of high geothermal gradients in the Central Zone to be a result of mantle upwelling associated with intraplate rifting.

An ensialic model involving largely fixed relationships between tectonic domains was proposed by Etheridge et al. (1987) and Wyborn et al. (1987) to explain similarities in the timing and nature of sedimentation, deformation and magmatism across much of Proterozoic Australia. In this model, rift zones developed as a result of small-scale mantle convection cells, with the modified rifts now represented by orogens. In the Lamboo Province, bimodal magmatic rocks of the Sophie Downs Suite and overlying sedimentary rocks of the Saunders Creek Formation were interpreted to be rift-related, and units such as the Biscay and Olympio Formations were interpreted to have been deposited during post-rift thermal sag. Similarities in the compositions and ages of widespread potassic I-type granitic rocks were attributed to delamination and partial

melting of mafic underplates emplaced along these rifts. Much of the deformation in the rift zones was considered to be associated with delamination and partitioned compressional deformation, and was collectively termed the Barramundi Orogeny. The relatively uniform compositions of many granitic rocks in these orogens were noted to be different from those of modern magmatic arcs and consistent with melting under high geothermal gradients, which are less readily developed in zones of collision. High-*T*, low-*P* metamorphism and anticlockwise *P*-*T*-*t* paths typical of these belts were also considered to be a result of delamination and upwelling of the asthenosphere. Other aspects of the geology that were considered incompatible with advancing subduction included: (1) an absence of evidence for oceanic crust; (2) an apparent lack of evidence for significant crustal thickening and uplift in metamorphic *P*-*T* estimates or patterns of sedimentation during and after deformation; and (3) an apparent lack of chemical or temporal polarity.

In contrast, Ogasawara et al. (1988) noted that the compositions of some granitic rocks in the Sally Downs Supersuite differ from those of the potassic I-type granites discussed by Etheridge et al. (1987) and Wyborn et al. (1987), and suggested formation in a subduction setting. A similar conclusion was reached by Sheppard et al. (2001), who noted that some tonalites of the Dougalls Suite are compositionally similar to crustally derived adakites formed in modern subduction settings. Potassic granitic rocks of the Sally Downs Supersuite were interpreted to have been emplaced within a subduction to post-collisional setting.

The geochemistry and isotope compositions of mafic igneous rocks of the Halls Creek Orogen have also been used to constrain possible geodynamic settings. Mafic and felsic igneous rocks of the Eastern Zone are interpreted to have been emplaced in an ensialic setting, with consensus that this domain formed part of the proto-North Australian Craton. Sun et al. (1991) noted that the isotopically primitive Woodward Dolerite has compositions comparable to mid-ocean-ridge basalt (MORB), and was likely generated by high degrees of mantle melting ( $\geq 25\%$ ), with a small component of crustal contamination or previously subducted crustal material. An ensialic setting was favoured by these authors, either an intraplate rift or a back-arc. Mafic volcanic rocks in the 1881–1861 Ma Biscay Formation are interpreted to have been emplaced in an intraplate rift or passive margin setting (Sheppard et al., 1999b; Sun and Hoatson, 2000; Phillips et al., 2016). Alkalic rhyolites of the c. 1856 Ma Maude Headley Member of the Olympio Formation have geochemistry consistent with an intraplate setting (Page and Hancock, 1988; Taylor et al., 1995), whereas mafic and alkalic felsic volcanic rocks of the c. 1846 Ma Butchers Gully Member were also considered by Sun and Hoatson (2000) to be of an intraplate style.

In the Central Zone, tholeiitic metabasalts of the Tickalara Metamorphics have been divided into two groups on the basis of their trace element geochemistry (Sheppard et al., 1999b). A depleted group has been suggested to have been emplaced in either an island arc or back-arc setting, whereas a smaller enriched group was noted to have a broad range of possible settings, with similarities to basalts emplaced in back-arc basins, ensialic marginal basins, passive margins and continental flood basalt provinces (Sheppard et al., 1999b). Sun and Hoatson (2000) considered that the geochemical compositions of isotopically juvenile



>1850 Ma mafic intrusive and extrusive rocks in the Tickalara Metamorphic suite are indicative of a high degree of mantle melting in a low-pressure environment. This was not considered to be diagnostic of a particular tectonic setting, but it was noted that the compositions are inconsistent with a simple oceanic arc.

The geochemistry of 1857–1823 Ma mafic–ultramafic layered intrusions in the Halls Creek Orogen has also been used to constrain geodynamic settings. These tholeiitic intrusions have LREE-enriched patterns and higher abundances of incompatible elements relative to older mafic rocks in the Central Zone, with strong depletion of Nb and enrichment of Th and Ba, and have more evolved Sm–Nd and Hf isotope values than the older mafic rocks (Sun and Hoatson, 2000; Mole et al., 2018; Kohanpour et al., 2019a). The mafic–ultramafic rocks extend across a range of fields in discrimination diagrams, plotting within the compositional field of modern MORB, but also overlapping into arc tholeiite and calc-alkaline basalt fields (Sun and Hoatson, 2000). These geochemical and isotopic characteristics can be explained by crustal contamination or incorporation of a subduction-related component into the mantle source (Sun and Hoatson, 2000; Sproule et al., 2002), with subduction-related enrichment of the lithospheric mantle pre-dating, or synchronous with, tectonism in the Halls Creek Orogen (Sun et al., 1991). Although noting considerable uncertainty regarding the overall geodynamic setting, Sun and Hoatson (2000) considered the geochemistry of the intrusions in the Western and Central Zones to be consistent with intraplate emplacement. In contrast, Mole et al. (2018) suggested that these rocks were emplaced in a back-arc setting on the margin of an exotic Kimberley Craton.

Tyler et al. (1995) raised the possibility that the three zones of the Lamboo Province represent exotic terranes, suggesting that differences in the timing and nature of sedimentation, deformation and magmatism between the zones reflect the evolution of distinct crustal blocks that did not share a common history until collision during the Halls Creek Orogeny. These authors suggested that the Halls Creek Group cannot be correlated across the province in its entirety, because the Marboo Formation is constrained to have been deposited prior to c. 1860 Ma metamorphism, whereas much of the Olympio Formation was deposited after c. 1855 Ma. They also pointed out that deformation and high-grade metamorphism of the Tickalara Metamorphics in the Central Zone took place while the Olympio Formation was being deposited, and this high-grade metamorphic event is not known in the Eastern Zone. Similarly, c. 1860 Ma tectonism is not recognized in the Central and Eastern Zones. Tyler et al. (1995) noted that minor felsic magmatism in the Central and Eastern Zones was broadly coeval with voluminous 1867–1849 Ma felsic magmatism of the Paperbark Supersuite in the Western Zone, but suggested that this coeval magmatism took place in geographically separate terranes. A similar geodynamic model to that of Tyler et al. (1995) was incorporated in a review of the Proterozoic assembly of Australia by Myers et al. (1996).

Griffin et al. (2000a) placed magmatism of the Paperbark Supersuite in a post-collisional setting on the eastern margin of an exotic Kimberley Craton, prior to a second, younger collision with the Eastern Zone. In their models, westward subduction of oceanic crust resulted in the collision of a small continental fragment with the Kimberley Craton prior

to c. 1865 Ma, leading to detachment of the down-going slab and crustal melting as a result of upwelling asthenosphere (Fig. 4). Subduction was interpreted to have then either re-commenced with the same polarity, leading to the development of a basin near the margin of the Kimberley Craton (the Tickalara ensialic marginal basin), or to have flipped polarity, leading to the development of an island arc (the Tickalara oceanic arc) between the Kimberley Craton and the proto-North Australian Craton (Eastern Zone). Continued convergence and subduction either closed the marginal basin or accreted the oceanic arc to the Kimberley Craton by 1850–1845 Ma. Subsequent westward subduction then closed an ocean basin between the combined Western and Central Zones and the Eastern Zone, culminating in continental collision during the Halls Creek Orogeny.

Versions of the geodynamic scenarios proposed by Sheppard et al. (1999b) and Griffin et al. (2000a) have been incorporated in almost all subsequent interpretations of the evolution of the Lamboo Province. The oceanic arc variant has been favoured by many workers (Cawood and Korsch, 2008; Tyler et al., 2012; Hollis et al., 2015; Lindsay et al., 2016; Occhipinti et al., 2016; Betts et al., 2016), whereas more recent studies (Kohanpour et al., 2017, 2018, 2019a; Mole et al., 2018) have favoured the ensialic marginal basin variant on the basis of numerical modelling, geochemistry and isotope data.

A discussion of the geodynamic models for the Halls Creek Orogen by Wyborn and Blake (2000) represents a rare exception to the widely accepted collisional model. These authors considered that intraplate extension followed by compression provided a better explanation of the nature of magmatism, which is strongly bimodal and includes relatively little of the andesitic compositions common to magmatic arcs. Shaw et al. (2000) also favoured an intraplate setting, with extension between the Kimberley Craton and proto-North Australian Craton generating the Paperbark Supersuite, and transpression during the Halls Creek Orogeny resulting in magmatism and deformation in the Halls Creek Orogen.

## Sampling rationale

U–Pb and Lu–Hf isotope analysis of detrital zircons from metasedimentary rocks provides a key test of geodynamic models for the development of the Lamboo Province. In an accretion/collision model, pre-collision metasedimentary units deposited on terranes separated by ocean basins might be expected to show significant differences in age, isotope character and provenance (e.g. the Eocene collision of India and Asia – Najman et al., 2017). In a scenario where the Central Zone represents an oceanic arc separated from both the Western and Eastern Zones, all three terranes are likely to be distinct, and the Central Zone should be dominated by young, isotopically juvenile volcanoclastic detritus. If the Central Zone formed as an ensialic marginal basin prior to a collision, it might be expected to show similarities with the terrane with which it was associated, and to differ from unrelated terranes. Alternatively, in an intraplate scenario where all three zones of the Lamboo Province are para-autochthonous, coeval units pre-dating the Halls Creek Orogeny would be expected to have many features in common.



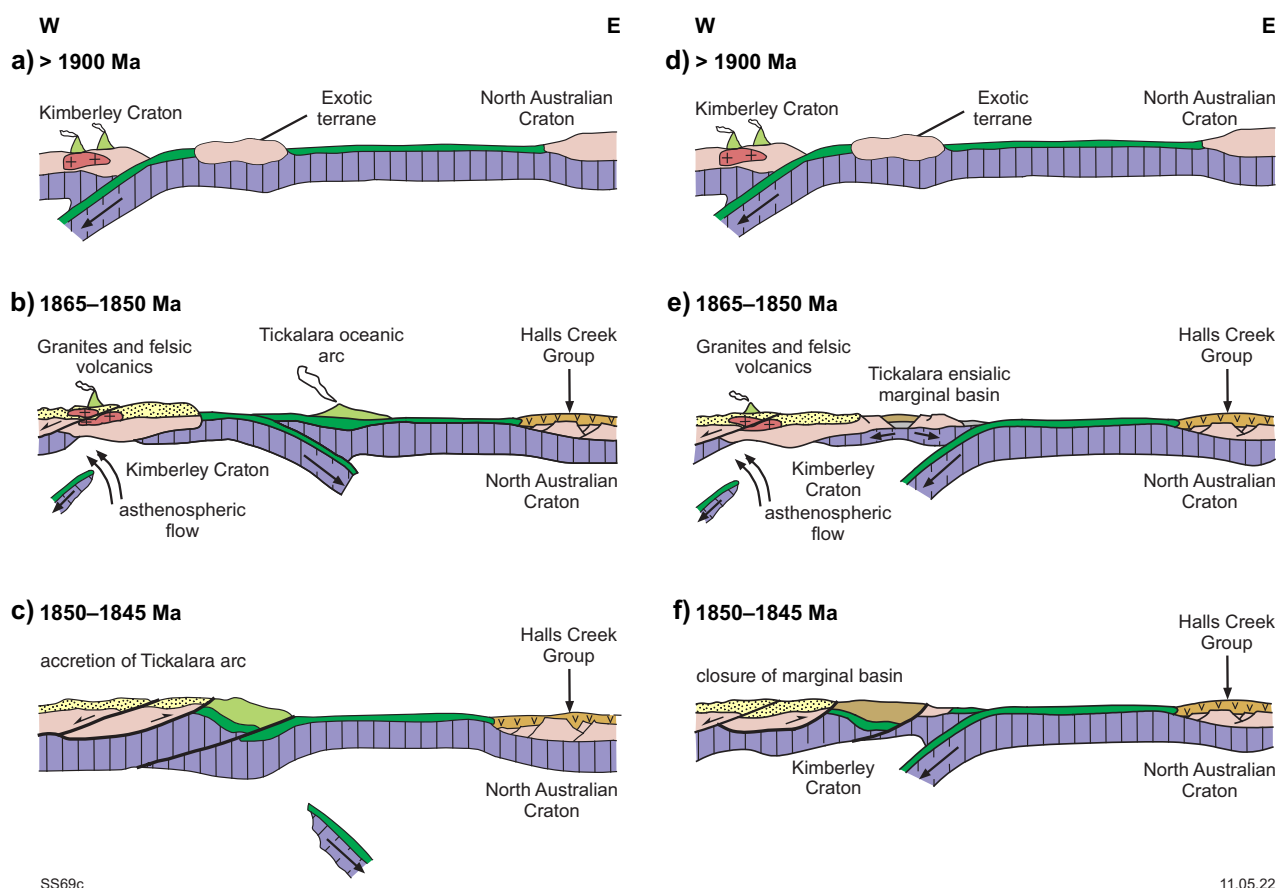


Figure 4. Postulated interpretations of the geodynamic evolution of the Lamboo Province (Griffin et al., 2000a), involving collision between an exotic Kimberley Craton (Western Zone) and the proto-North Australia Craton (Eastern Zone). One variant of this model (a–c) considers the Central Zone to be an oceanic arc that accreted to the Western Zone before collision with the Eastern Zone during the Halls Creek Orogeny. A second variant (d–f) considers the Central Zone to have developed as an ensialic marginal basin on the Western Zone

The metasedimentary succession of the Eastern Zone is relatively well characterized by previous U–Pb and Lu–Hf data for metasedimentary and felsic volcanic rocks (Phillips et al., 2016) and forms a reference section against which units from the Central and Western Zones can be compared. Sampling in this study focused on detrital zircon dating of metasedimentary rocks from the Central Zone (Tickalara Metamorphics, Winnama Formation and Milba Formation) and the Western Zone (Marboo Formation and Mount Joseph Migmatite). Sampling was carried out to cover the range of exposed stratigraphy and to provide a broad spatial coverage. Several relatively closely spaced samples of metasedimentary rocks and one ‘stitching’ granitic rock were collected from the northern part of the Halls Creek Orogen to help constrain the nature of the boundary between the Western and Central Zones, which in this area is not defined by a major fault. In addition, samples of the Ruins Dolerite, Whitewater Volcanics and Rose Bore Granite provide constraints on the ages of sedimentation and magmatism in the Western and Central Zones.

## Analytical methods

### U–Pb geochronology

U–Pb zircon geochronology was conducted using the SHRIMP II ion microprobes at Curtin University. Reflected-light, transmitted-light and cathodoluminescence (CL) images were used to ensure analyses were made on discrete zircon growth phases. Analyses were conducted using a spot size of c. 20 µm diameter and a primary ion beam ( $O_2^-$ ) with an intensity between 2 and 3 nA. U/Pb ratios and element concentrations were determined relative to an appropriate zircon standard and  $^{207}Pb^*/^{206}Pb^*$  ratios ( $Pb^*$  indicates radiogenic Pb) were monitored using the OG1 zircon standard (Stern et al., 2009). Correction for common Pb was made using measured  $^{204}Pb/^{206}Pb$  and contemporaneous isotope compositions (Stacey and Kramers, 1975). Isotopic ages are weighted mean ages unless noted otherwise, and are quoted with 95% uncertainties and the mean square of weighted deviates (MSWD). Detailed sample preparation, analytical procedures and data processing followed the approach described in Lu et al. (2020a).

## Lu–Hf isotopes

Zircon Hf isotope analyses were carried out in situ at GEMOC (Macquarie University) using a New Wave / Merchantek UP-213 laser-ablation microprobe attached to a Nu Plasma MC-ICP-MS system. The Hf analyses were conducted on the same spots as the previous SHRIMP U–Pb analyses, using a beam diameter of 55 microns and a 5 Hz repetition rate, resulting in total Hf signals of  $(1\text{--}6) \times 10^{-11}$  A (depending on conditions and Hf contents). Typical ablation times were 100–120 s, resulting in ablation pits 40–60  $\mu\text{m}$  deep. Helium carrier gas transported the ablated aliquot from the laser-ablation cell via a mixing chamber to the ICP-MS torch.

Interference of  $^{176}\text{Lu}$  on  $^{176}\text{Hf}$  was corrected by measuring the intensity of the interference-free  $^{175}\text{Lu}$  isotope and using  $^{176}\text{Lu}/^{175}\text{Lu} = 0.02669$  (DeBièvre and Taylor, 1993) to calculate  $^{176}\text{Lu}/^{177}\text{Hf}$ . Similarly, the isobaric interference of  $^{176}\text{Yb}$  on  $^{176}\text{Hf}$  was corrected by measuring the interference-free  $^{172}\text{Yb}$  isotope and using  $^{176}\text{Yb}/^{172}\text{Yb}$  to calculate  $^{176}\text{Yb}/^{177}\text{Hf}$ . The appropriate value of  $^{176}\text{Yb}/^{172}\text{Yb}$  was determined by spiking the JMC475 Hf standard with Yb, and determining the value of  $^{176}\text{Yb}/^{172}\text{Yb}$  (0.58669) required to yield the value of  $^{176}\text{Hf}/^{177}\text{Hf}$  obtained on the pure Hf solution. Detailed discussion regarding the overlap corrections for  $^{176}\text{Lu}$  and  $^{176}\text{Yb}$  has been provided by Pearson et al. (2008). Two zircon standards, Mud Tank and Temora, were analysed to evaluate the accuracy of the laser-ablation results. During the entire session, Mud Tank yielded an average  $^{176}\text{Hf}/^{177}\text{Hf}$  of  $0.282503 \pm 0.000035$  (s.d.,  $n = 28$ ) (the recommended value is  $0.282528 \pm 0.000026$ ) and Temora gave an average  $^{176}\text{Hf}/^{177}\text{Hf}$  of  $0.282662 \pm 0.000028$  (s.d.,  $n = 16$ ) (the recommended value is  $0.282686 \pm 0.000034$ ). Analytical procedures were detailed by Griffin et al. (2000b, 2002).

For calculation of  $\epsilon_{\text{Hf}(t)}$  values, this Report has employed the present-day Chondritic Uniform Reservoir (CHUR) values of Bouvier et al. (2008):  $^{176}\text{Lu}/^{177}\text{Hf} = 0.0336$  and  $^{176}\text{Hf}/^{177}\text{Hf} = 0.282785$ . Also used in calculation is the decay constant for  $^{176}\text{Lu}$  of  $1.867 \times 10^{-11} \text{ a}^{-1}$  (Söderlund et al. 2004).

To calculate model ages ( $T_{\text{DM}}$ ) based on a depleted mantle source, the depleted mantle (DM) reservoir is assumed to have developed from an initially chondritic mantle, and is complementary to subsequent crustal extraction. Values employed for present-day DM are  $^{176}\text{Lu}/^{177}\text{Hf} = 0.0384$  and  $^{176}\text{Hf}/^{177}\text{Hf} = 0.28325$  (Griffin et al., 2000b). For each zircon analysis, a two-stage ‘crustal’ model age ( $T_{\text{DM}}^2$ ) has been calculated, on assumption that its parental magma was produced from average continental crust (i.e.  $^{176}\text{Lu}/^{177}\text{Hf} = 0.015$ ) derived from depleted mantle (Griffin et al., 2002). A table of Lu–Hf isotope values reported here is provided in Appendix 1.

## Sm–Nd isotopes

Sm–Nd isotope values were determined on crushed and milled whole-rock samples by isotope dilution at the University of Rennes (France) or by ICP-MS at the University of Queensland. At the University of Rennes, the instrument used was a seven-collector Finnigan MAT-262 mass spectrometer. Samples were spiked with a  $^{149}\text{Sm}$ – $^{150}\text{Nd}$  solution and dissolved in a  $\text{HF}$ – $\text{HNO}_3$  mixture. They were then dried and taken up with concentrated  $\text{HCl}$ . Rare earth elements (REEs) were separated using cationic resin and then Sm and Nd were collected by passing the solution

through an additional set of ion-exchange columns loaded with Ln-spec Eichrom resin. Sm and Nd were loaded with  $\text{HNO}_3$  reagent onto double Re filaments and analysed in static collection mode. In each analytical session, the unknowns were analysed together with the Ames Nd-1 Nd standard. All the analyses of the unknowns have been adjusted to the long-term  $^{143}\text{Nd}/^{144}\text{Nd}$  value of 0.511963 for Ames Nd-1. Mass fractionation was monitored and corrected using the value  $^{146}\text{Nd}/^{144}\text{Nd} = 0.7219$ . Procedural blank analyses yielded values of 50–200 pg for Nd, which are therefore considered to be negligible.

Neodymium isotope analyses were performed using a Nu Plasma multi-collector ICP-MS at the University of Queensland following procedures documented in Wei et al. (2014). Measured  $^{143}\text{Nd}/^{144}\text{Nd}$  ratios were corrected for mass fractionation to  $^{146}\text{Nd}/^{144}\text{Nd} = 0.7219$ . In each analytical session, the unknowns were analysed together with the AMES Nd metal standard (Wei et al., 2014). All the analyses of the unknowns have been adjusted to the long-term  $^{143}\text{Nd}/^{144}\text{Nd}$  value of 0.511966 for AMES Nd metal standard. Total Nd procedural blanks run in the lab typically range from 20 to 100 pg, which is considered negligible compared to the total quantity of Nd in the samples. A table of the new Nd isotope values reported here is provided in Appendix 2.

## Geochronology results

### Western Zone – Wunaamin Miliwundi Orogen

#### GSWA 206102: sandstone, Marboo Formation

Zircons extracted from a previously dated sample of quartz wacke from Unit 1 of the Marboo Formation (GA 87598014; Tyler et al., 1999) were dated to add to the dataset for this generally poorly exposed unit. In this area (Fig. 5), Unit 1 is exposed in the core of the Richenda Anticline, where it is intruded by the  $1858 \pm 5$  Ma Richenda Microgranodiorite (Tyler et al., 1999). The  $1873 \pm 4$  Ma Ruins Dolerite (GSWA 212335, Lu et al., 2017b) intrudes the lowermost part of the overlying Unit 2 about 500 m to the northeast.

Zircons from this sample are anhedral to subhedral, and colourless to brown and opaque. The grains are up to 200  $\mu\text{m}$  long, with aspect ratios up to 5:1, and are variably rounded or broken. In CL images, the grains show near-ubiquitous concentric zoning. Further sample and analytical details are provided in Kirkland et al. (2013). Seventy-seven analyses were obtained from 75 zircons (Fig. 6a,b). Thirteen analyses are >5% discordant and not considered further. The remaining 64 zircons yield  $^{207}\text{Pb}^*/^{206}\text{Pb}^*$  dates of 3236–1942 Ma, with the youngest, relatively imprecise, analysis at  $1942 \pm 88$  Ma ( $1\sigma$ ). The youngest 12 analyses form a weighted mean date of  $1983 \pm 9$  Ma (MSWD = 1.6), which represents a conservative maximum depositional age. Results for this sample are similar to those reported by Tyler et al. (1999), with most analyses indicating latest Neoproterozoic to early Paleoproterozoic ages (2585–1983 Ma), and significant age components at c. 2513, 2454, 2184, 2057 and 1983 Ma.

## GSWA 212327: pelitic schist, Marboo Formation

A sample of foliated pelitic schist was collected ~8 km northwest of the Merlin prospect in the western part of the Wunaamin Miliwundi Orogen (Figs 5, 7a). The stratigraphic position of this sample is not certain, but the presence of the Ruins Dolerite within the succession and the quartz-rich nature of the sampled metasedimentary rock suggest it is part of Unit 1.

The schist consists of 80–82% quartz, 8% chlorite, 5% muscovite, 3% chloritoid, 1% biotite, 1% opaque minerals, and accessory green tourmaline and zircon. Zircons from the sample are colourless to pale brown, anhedral to subhedral, and strongly rounded, with pitted outer surfaces. The crystals are up to 200  $\mu\text{m}$  long and equant to elongate, with aspect ratios up to 4:1. In CL images, most grains have concentric zoning, which is commonly truncated at grain boundaries. Further sample and analytical details are provided in Lu et al. (2017c).

Seventy-seven analyses were obtained from 77 zircons (Fig. 6c,d). Nine analyses are >5% discordant and are not considered further. The remaining 68 zircons yield  $^{207}\text{Pb}^*/^{206}\text{Pb}^*$  dates of 3577–1851 Ma, with the youngest individual analysis at  $1851 \pm 11$  Ma (1 $\sigma$ ) representing a maximum depositional age. A more conservative maximum depositional age of  $1954 \pm 16$  Ma (MSWD = 1.8) can be based on the next five youngest coherent analyses. The data indicate significant age components at c. 2609, 2503, 2468, 2316, 2206, 2108, 2058, 2041, 1995, 1970 and 1933 Ma.

## GSWA 212335: metagabbro, Ruins Dolerite

The Ruins Dolerite was sampled ~1.6 km south-southwest of the Merlin prospect and ~6.0 km southwest of Clara Hill in the northwestern Wunaamin Miliwundi Orogen (Figs 5, 7b–d). A sample was collected from the plagioclase-phyric leucocratic metagabbro phase of a mafic sill, which forms a low northwest-trending ridge surrounded by a plain underlain by metasedimentary rocks of the Marboo Formation.

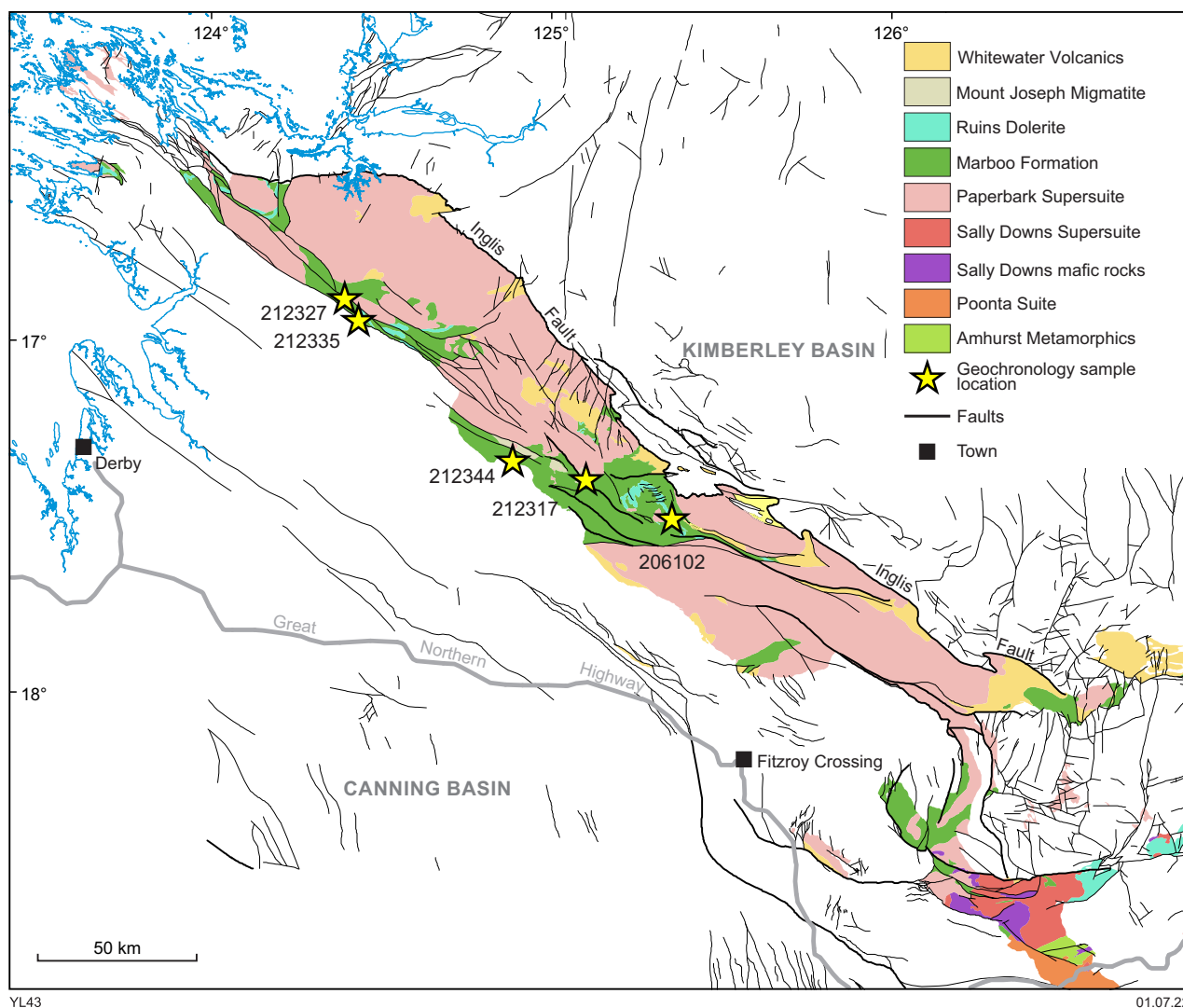


Figure 5. Location of geochronology samples from the Wunaamin Miliwundi Orogen, based on the GSWA 1:500 000-scale interpreted basement geology map of Western Australia (2016)

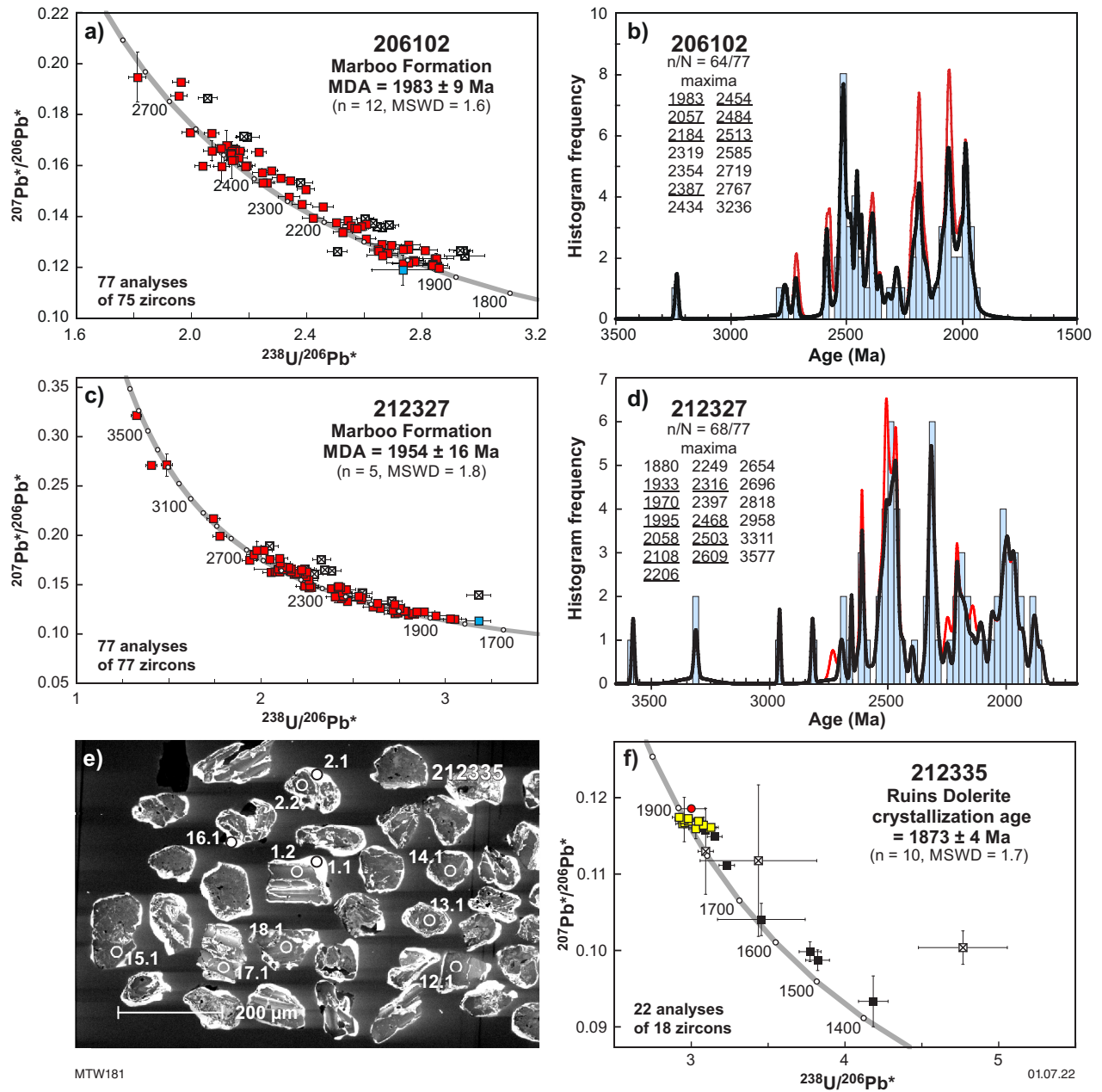


Figure 6. Concordia and probability density diagrams for metasedimentary rocks of the Marboo Formation and CL image and concordia diagram for zircons from metagabbro of the Ruins Dolerite in the Western Zone (Wunaamin Miliwundi Orogen): a) and b) sandstone, Marboo Formation (GSWA 206102); c) and d) pelitic schist, Marboo Formation (GSWA 212327). Concordia diagrams – blue square: analysis of the youngest detrital zircon; red squares: analyses of older detrital zircons; crossed squares: analyses excluded due to discordance or high common Pb; MDA: maximum depositional age. Probability density diagrams – thin red line: all data; thick black line: accepted data; n/N: number of accepted data / total data; underlined maxima values are those based on three or more ages. e) CL image for zircons from metagabbro, Ruins Dolerite (GSWA 212335); f) concordia diagram for zircons from metagabbro, Ruins Dolerite (GSWA 212335) – yellow squares: analyses of magmatic zircons used to calculate the crystallization age; red circle: analyses of xenocrysts; black squares: analyses interpreted to reflect radiogenic-Pb loss; crossed squares: analyses excluded due to discordance >5% or high common Pb





Figure 7

Field photographs of geochronology samples in the Western Zone (Wunaamin Miliwundi Orogen): a) quartz-rich pelitic schist of the Marbo Formation (GSWA 212327); b) deformed plagioclase-phyric gabbro of the Ruins Dolerite (GSWA 212335); c) less-deformed plagioclase-phyric gabbro of the Ruins Dolerite, same locality as GSWA 212317; d) contact between even-grained gabbro and plagioclase-phyric gabbro, Ruins Dolerite, same locality as GSWA 212317; e) cordierite-sillimanite pelitic migmatite, Mount Joseph Migmatite (GSWA 212317) – networks of leucosome formed within east-west-trending foliation have pooled in perpendicular north-south-striking domains; f) xenolith of Mount Joseph Migmatite in the Lennard Granite (MGA 715135E, 8082105N, Zone 51); g) migmatitic pelitic gneiss of the Mount Joseph Migmatite (GSWA 212315)



The sampled leucocratic phase has irregular contacts with more mafic phases of the sill, and contains corroded plagioclase phenocrysts, which may reflect magma mixing. All phases are overprinted by a locally high-strain, subvertical, west-northwesterly striking foliation ( $S_3$ ) containing a moderately southeast-plunging mineral lineation, with asymmetric porphyroblast tails indicating a sinistral sense of movement. The metagabbro has been metamorphosed at amphibolite facies, and consists of a groundmass of fine-grained, bladed amphibole and plagioclase that hosts medium- to coarse-grained relict plagioclase phenocrysts. Further sample and analytical details are provided in Lu et al. (2017b).

About 80 zircons were isolated from about 3 kg of sample. They are up to 150  $\mu\text{m}$  long and equant to slightly elongate, with aspect ratios up to 3:1. The crystals are mainly colourless, transparent to turbid and anhedral to subhedral. In CL images, they are relatively homogeneous in brightness and texture, and exhibit broad planar to concentric zoning, although some show mottled textures (Fig. 6e). All zircons are overgrown by rims of bright zircon that also pervades into fractures.

Twenty-two analyses were obtained from 18 zircons (Fig. 6f). Two analyses are >5% discordant and one is interpreted to represent a mixture of core and rim material. The remaining 19 analyses can be divided into three groups. The first group comprises 10 analyses of zircon cores, which yield a weighted mean  $^{207}\text{Pb}^*/^{206}\text{Pb}^*$  date of  $1873 \pm 4$  Ma (MSWD = 1.7), interpreted as the crystallization age of the gabbro. These analyses are from cores with relatively uniform character in CL images, which show relatively high U (680–2351 ppm) and Th (431–2948 ppm) and yield Th/U ratios of 0.26 – 1.30. This is consistent with a magmatic origin, and differs from what would be expected if the grains were xenocrysts, because zircons from the host Marboo Formation have a much larger range of ages and concentrations of U and Th. Lu–Hf isotope values for these zircons have a very narrow range of radiogenic (primitive) values (see below), also consistent with a magmatic origin. A single analysis of a zircon core yields a date of  $1899 \pm 5$  Ma (1o), and was interpreted as inherited (Lu et al. (2017b). Eight analyses of four zircon cores and four zircon rims yield  $^{207}\text{Pb}^*/^{206}\text{Pb}^*$  dates of 1860–1779 and 1656–1447 Ma, respectively. These dates are interpreted to reflect ancient (Mesoproterozoic?) Pb loss, with the younger dates reflecting Pb loss from low U (44–107 ppm) and relatively low Th/U (0.22 – 0.28) rims that possibly formed after c. 1700 Ma.

### **GSWA 212317: pelitic migmatite, Mount Joseph Migmatite**

The Mount Joseph Migmatite was sampled ~0.8 km southwest of Mount Joseph (Fig. 5). In this area, migmatitic metasedimentary rocks consist of pelitic (biotite–sillimanite) and psammitic melanosome separated by patches of cordierite-rich, in situ leucosome (Fig. 7e). Leucosome networks developed along an east–west-trending foliation are concentrated in steep north–south-striking domains at a high angle to the foliation, consistent with pooling of melt in the orientation of least compressive stress during  $D_2$  folding. The sample collected is a pelitic migmatite consisting of 40% quartz, 25% K-feldspar, 15% cordierite, 10% biotite, 5%

sillimanite and 3% plagioclase, and is interpreted to be a metasedimentary rock metamorphosed at upper amphibolite facies. Further sample and analytical details are provided in Fielding et al. (2020b).

Zircons from the sample are colourless, anhedral to subhedral, and variably rounded. They are up to 300  $\mu\text{m}$  long, with aspect ratios up to 3:1. In CL images, most crystals exhibit concentric zoning and are overgrown by high-U zircon rims. Ninety-five analyses were obtained from 86 zircons (Fig. 8a,b). Seven analyses are >5% discordant, two analyses represent mixtures of core and rim material and one analysis indicates high within-run variation in isotope ratios. The dates obtained from these 10 analyses are not considered further.

Seventy-two analyses of 67 zircon cores are concordant, with U concentrations of 109–3251 ppm and generally moderate Th/U ratios of 0.004 – 0.866 (median 0.366). They yield  $^{207}\text{Pb}^*/^{206}\text{Pb}^*$  dates of 2623–1848 Ma, with a dominant age component at c. 1874 Ma. A weighted mean date of  $1873 \pm 2$  Ma (MSWD = 0.96) for the youngest 45 analyses represents a conservative maximum depositional age for the metasedimentary protolith. Thirteen analyses of 11 zircon rims indicate 822–2147 ppm U and very low Th/U ratios of 0.005 – 0.091 (median 0.012). These yield a weighted mean  $^{207}\text{Pb}^*/^{206}\text{Pb}^*$  date of  $1865 \pm 4$  Ma, which is interpreted as the age of metamorphism and partial melting. This date overlaps with dates of 1867–1862 Ma for the Lennard Granite (Griffin et al., 2000a; Lu et al., 2017f,g), which intrudes the Mount Joseph Migmatite (Fig. 7f).

### **GSWA 212315: pelitic migmatite, Mount Joseph Migmatite**

A sample of the Mount Joseph Migmatite was collected from an area of rocky outcrop on Napier Downs Station, about 8.8 km west-northwest of Mount Joseph and 9.9 km north-northeast of Windjana Gorge (Fig. 5). This sample is a migmatitic pelitic gneiss, consisting of about 47% quartz, 22% plagioclase, 20% biotite, 4% muscovite, 3% K-feldspar, 3% sillimanite, 1% ilmenite, and accessory monazite, zircon, xenotime, apatite and tourmaline. Folded leucosome layers, up to 2 cm thick, are composed of quartz, K-feldspar and plagioclase with minor muscovite and biotite±fibrolite schlieren (Fig. 7g). The sample is interpreted to be a metasedimentary rock metamorphosed at upper amphibolite facies. Further sample and analytical details are provided in Fielding et al. (2020c).

Zircons isolated from this sample are mainly colourless, anhedral to subhedral, and variably rounded. The crystals are up to 250  $\mu\text{m}$  long and elongate, with aspect ratios up to 3:1. In CL images, most zircons exhibit concentric zoning truncated at grain boundaries, which is consistent with sedimentary transport, and are overgrown by high-uranium zircon rims. Eighty-two analyses were obtained from 76 zircons (Fig. 8c,d). Seven analyses are >5% discordant and are not considered further. Fifty-five analyses of 52 zircon cores have moderate Th/U ratios of 0.04 – 1.73 (median 0.44) and yield  $^{207}\text{Pb}^*/^{206}\text{Pb}^*$  dates of 2702–1856 Ma. A conservative estimate of the maximum depositional age can be based on the weighted mean  $^{207}\text{Pb}^*/^{206}\text{Pb}^*$  date of  $1874 \pm 3$  Ma (MSWD = 1.2) for the 35 youngest analyses.

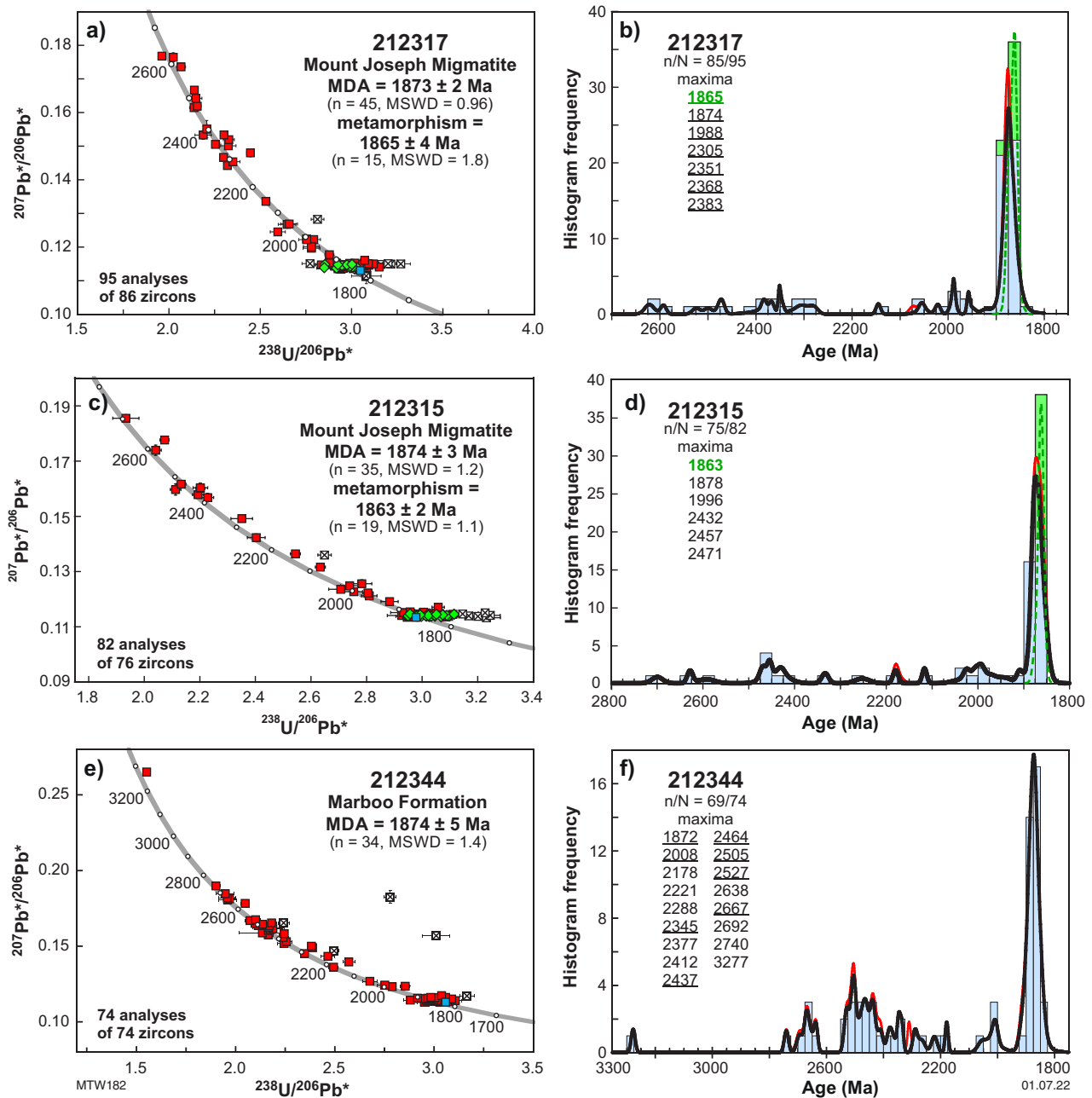


Figure 8. Concordia and probability density diagrams for metasedimentary rocks in the Western Zone (Wunaamin Miliwundi Orogen): a) and b) pelitic migmatite, Mount Joseph Migmatite (GSWA 212317); c) and d) pelitic migmatite, Mount Joseph Migmatite (GSWA 212315); e) and f) pelitic schist, Marboo Formation (GSWA 212344) – green diamonds: analyses of metamorphic zircon rims; green rectangles and dashed line: distribution of  $^{207}\text{Pb}^*/^{207}\text{Pb}^*$  dates obtained from metamorphic zircon rims. Other notes as in Figure 6

Nineteen analyses of 19 zircon rims with very low Th/U ratios of 0.005 to 0.045 (median 0.013) yield a weighted mean  $^{207}\text{Pb}^*/^{206}\text{Pb}^*$  date of  $1863 \pm 2$  Ma (MSWD = 1.1), interpreted as the age of metamorphism and partial melting.

### **GSWA 212344: pelitic schist, Marboo Formation**

A sample of the Marboo Formation was collected in the headwaters of Napier Creek, ~6.4 km northwest of Baralama Spring and ~22.5 km west-northwest of GSWA 212317 (Fig. 5). The sample was taken close to an intrusive contact with the Lennard Granite. No Ruins Dolerite is known from this area, and the radiometric signature of metasedimentary rocks is similar to that of Unit 2 further to the east, with which this sample is tentatively correlated. Pelitic schist in the area sampled contains garnet porphyroblasts, within quartz-rich domains, that preserve sigmoidal muscovite inclusion trails interpreted as  $S_1$  (Fig. 9a,b). Garnet porphyroblasts are large and euhedral in more competent quartzofeldspathic layers and flattened within  $S_2$  in more micaceous layers, and are interpreted to have grown during local  $D_2/M_2$ . Sigmoidal inclusion trails in garnet and asymmetries in surrounding quartz-rich domains are consistent with top-down-to-the-northeast movement on  $S_2$ , which contains a northeast-plunging  $L_2$  lineation defined by leucocratic selvages and sillimanite.

The sampled rock consists of 60% quartz, 30% biotite, 3% garnet, 1% andalusite, and accessory iron–titanium minerals and chlorite. The unit is strongly foliated, with andalusite forming porphyroblasts oriented transcurrent to the foliation. Garnet forms porphyroblasts >5 mm in diameter. Zircons from this sample are colourless to light brown, anhedral to subhedral, and variably rounded. The crystals are up to 200  $\mu\text{m}$  long and equant to elongate, with aspect ratios up to 4:1. In CL images, concentric zoning is ubiquitous, and commonly truncated at grain boundaries. Some grains have pitted exteriors, whereas others have thin, homogeneous dark rims up to several micrometres thick that could not be analysed. Further sample and analytical details are provided in Lu et al. (2016f).

Seventy-four analyses were obtained from 74 zircons (Fig. 8e,f). Five analyses are >5% discordant and are not considered further. The remaining 69 analyses have  $^{207}\text{Pb}^*/^{206}\text{Pb}^*$  dates of 3277–1847 Ma, with a dominant age component at c. 1872 Ma and subsidiary age components at c. 2667, 2527, 2505, 2464, 2437, 2345 and 2008 Ma. A weighted mean date of  $1874 \pm 5$  Ma (MSWD = 1.4) for the youngest 34 analyses represents a conservative maximum depositional age for the metasedimentary protolith, with 1867–1862 Ma dates for the Lennard Granite (Griffin et al., 2000a; Lu et al., 2017f,g) providing a minimum age constraint.

## **Western Zone – Halls Creek Orogen**

### **GSWA 215562: metasandstone, Marboo Formation**

A metasandstone was sampled from a poorly exposed succession of interbedded muscovite–biotite metasiltstone and lesser metasandstone in the southwestern part of the Halls Creek Orogen (Figs 9c, 10). The sample was taken ~1.4 km southeast of Neville Gorge, immediately adjacent to the intrusive contact between the Marboo Formation and the Neville Granodiorite of the Paperbark Supersuite, which has been dated at  $1860 \pm 3$  Ma by a sample taken ~2 km to the northeast (Page et al., 2001).

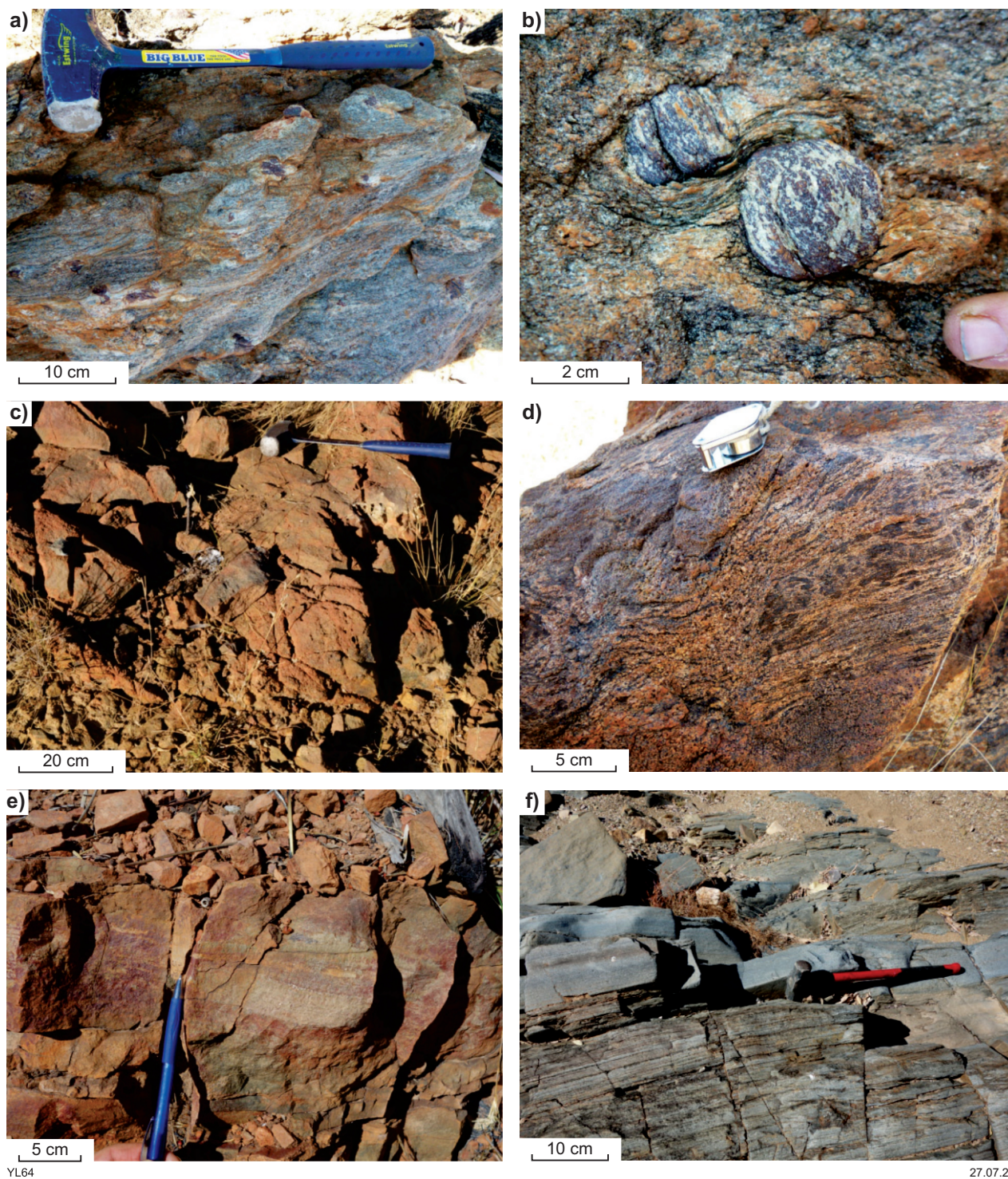
The sample is a fine- to medium-grained metasandstone, consisting of 50% quartz, 30–35% sericitized lithic clasts, 5–7% feldspar, 5–7% chlorite, 4–5% muscovite, and accessory titanite and zircon. Most muscovite and chlorite (after biotite) grains appear to be detrital, but a small proportion form randomly oriented, overprinting, acicular crystals. Zircons from this sample are colourless to light yellow and anhedral to euhedral, with a significant proportion of subhedral to euhedral grains. The crystals are up to 200  $\mu\text{m}$  long and equant to elongate, with aspect ratios up to 5:1. Further sample and analytical details are provided in Lu et al. (2017d).

Eighty-three analyses were obtained from 83 zircons (Fig. 11a,b). A significant number (41) of analyses are >5% discordant and are not considered further. The remaining 42 analyses yield  $^{207}\text{Pb}^*/^{206}\text{Pb}^*$  dates of 3438–1834 Ma, with a dominant age component at c. 1866 Ma and a minor component at c. 2484 Ma. A weighted mean  $^{207}\text{Pb}^*/^{206}\text{Pb}^*$  date of  $1865 \pm 6$  Ma (MSWD = 0.77) for the youngest 28 analyses forms a conservative maximum depositional age for this unit, and a minimum age for deposition is provided by the  $1860 \pm 3$  Ma age of the crosscutting Neville Granodiorite (Page et al., 2001).

### **GSWA 206154: pelitic migmatite, Marboo Formation**

The Marboo Formation was sampled from the central part of the Halls Creek Orogen, ~1.7 km northwest of Paperbark Bore (Fig. 10), where it consists of migmatitic psammitic to pelitic metasedimentary rocks (Fig. 9d). In this area, the Marboo Formation is intruded, and enclosed, by the Paperbark Granite, which has been dated at  $1854 \pm 3$  Ma (Page et al., 2001), and is also intruded by the Springvale mafic–ultramafic intrusion, dated at  $1857 \pm 2$  Ma (Page and Hoatson, 2000). Leucosomes are subparallel to, and also crosscut, a gneissic fabric.





YL64

27.07.20

Figure 9. Field photographs of Marboo Formation geochronology samples in the Western Zone (Wunaamin Miliwundi and Halls Creek Orogens): a) garnet-sillimanite-muscovite-biotite schist with garnet porphyroblasts in the central Wunaamin Miliwundi Orogen (GSWA 212344); b) garnet porphyroblasts in  $S_2$  with sigmoidal muscovite inclusion trails ( $S_1$ ) (GSWA 212344); c) metasandstone outcrop in the southwestern Halls Creek Orogen (GSWA 215562); d) migmatitic psammitic to pelitic metasedimentary rocks in the central part of the Halls Creek Orogen (GSWA 206154); e) metasiltstone from the northwestern part of the Halls Creek Orogen (GSWA 218305); f) interbedded metasandstone and metasiltstone from the northern part of the Halls Creek Orogen (GSWA 218330)



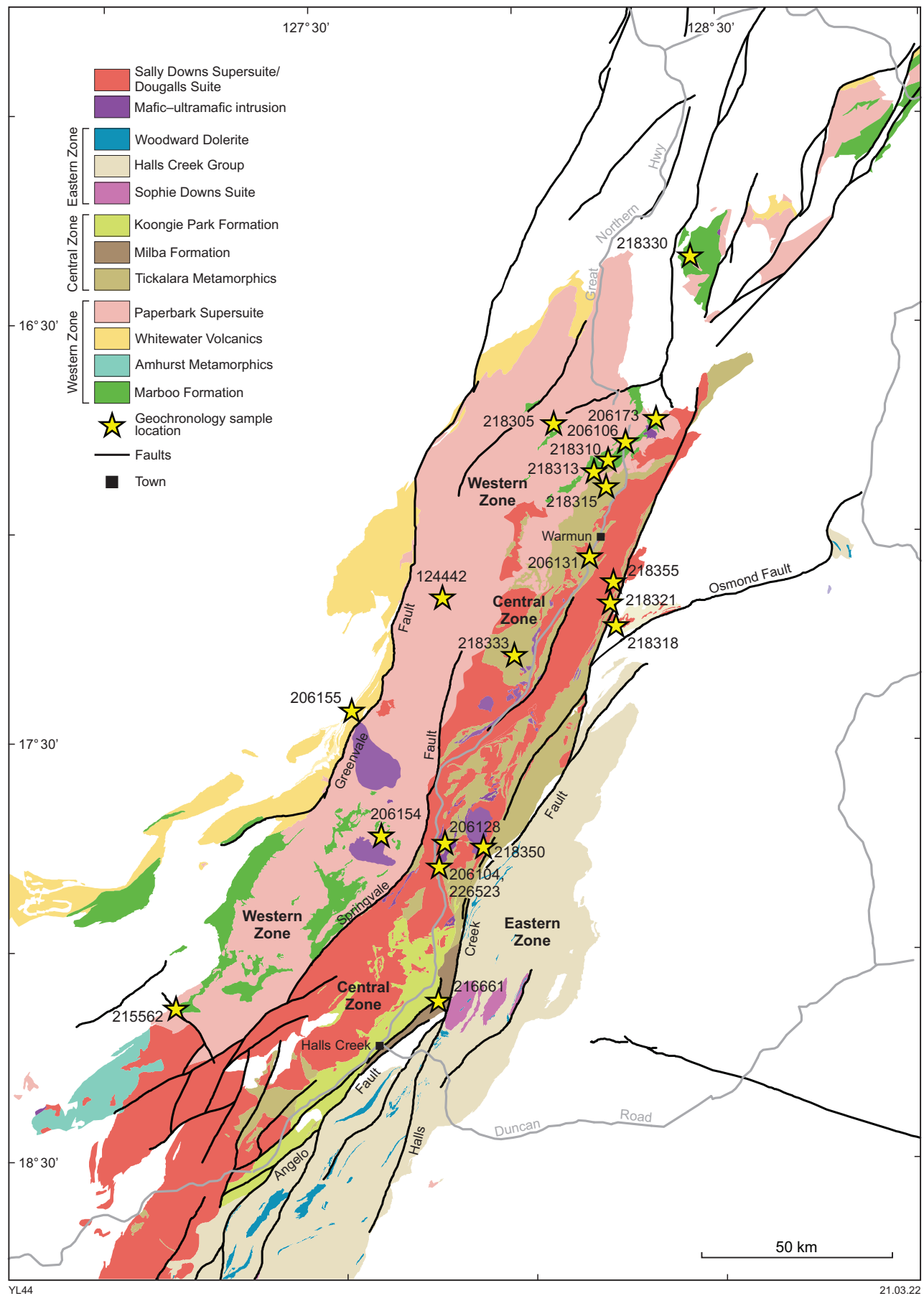


Figure 10. Location of geochronology samples from the Lamboo Province in the Halls Creek Orogen over the GSWA 1:500 000-scale interpreted basement geology map of Western Australia (2016)

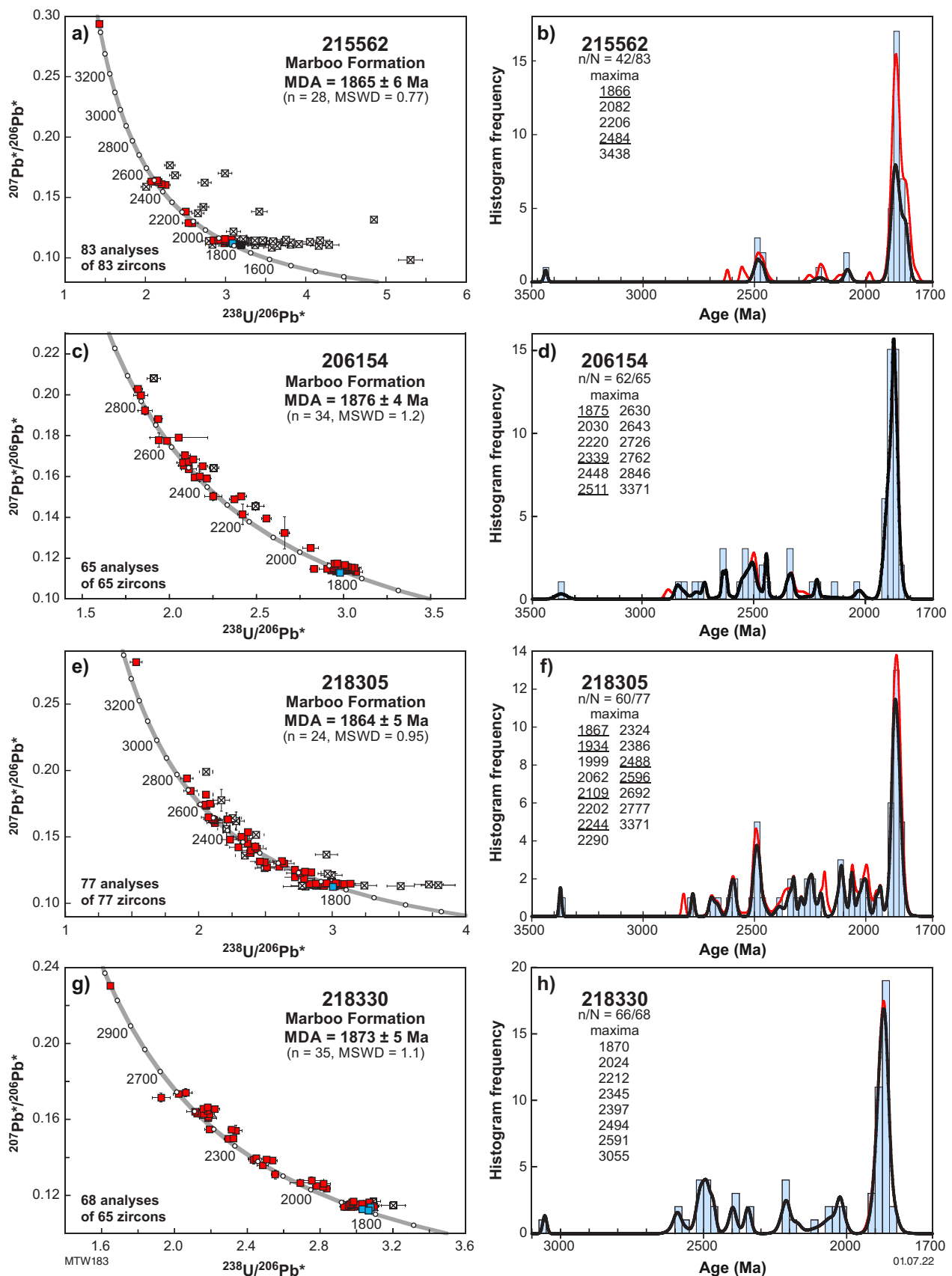


Figure 11. Concordia and probability density diagrams for metasedimentary rocks of the Marboo Formation in the Western Zone (Halls Creek Orogen): a) and b) metasandstone (GSWA 215562); c) and d) pelitic migmatite (GSWA 206154); e) and f) metasilstone (GSWA 218305); g) and h) metalitharenite (GSWA 218330). Diagram notes as in Figure 6

The sample is a medium- to coarse-grained pelitic migmatite, consisting of 50% quartz, 30% microcline, 10% garnet, 4% biotite, 2% cordierite, 2% sillimanite, and accessory opaque oxide minerals, zircon and monazite. Zircons from the sample are mostly colourless to light brown, subhedral to euhedral, and up to 250  $\mu\text{m}$  long. The grains are equant to elongate, with aspect ratios up to 6:1. Some crystals have pitted outer surfaces and, in CL images, many exhibit concentric zoning truncated at grain edges. Some crystals have thin, homogeneous, low-CL-response domains and rims. Further sample and analytical details are provided in Kirkland et al. (2014).

Sixty-five analyses were obtained from 65 zircon cores (Fig. 11c,d). Three analyses are >5% discordant and are not considered further. The remaining 62 analyses yield  $^{207}\text{Pb}^*/^{206}\text{Pb}^*$  dates of 3371–1846 Ma, with a dominant age component at c. 1875 Ma and minor components at c. 2511 and 2339 Ma. A weighted mean  $^{207}\text{Pb}^*/^{206}\text{Pb}^*$  date of  $1876 \pm 4$  Ma (MSWD = 1.2) for the youngest 34 analyses forms a maximum depositional age, with a minimum age provided by the  $1857 \pm 2$  Ma Springvale intrusion. Zircon rims were too thin to be dated.

### **GSWA 218305: metasilstone, Marboo Formation**

A sample of the Marboo Formation was collected from the northwestern Halls Creek Orogen, adjacent to O'Donnell Brook, ~16 km northeast of Bow River homestead (Fig. 10). The Marboo Formation in this area is surrounded and intruded by the undated Crooked Creek Granite of the Paperbark Supersuite. The sample is a thinly bedded metasilstone (Fig. 9e) consisting of 40–50% quartz, 40–50% sericite (largely after feldspar), 5% biotite, and minor chlorite and opaque minerals. The unit contains a weak bedding-parallel foliation.

Zircons from this sample are colourless to dark brown, anhedral to euhedral, and variably rounded. The crystals are up to 200  $\mu\text{m}$  long and equant to elongate, with aspect ratios up to 4:1. In CL images, the zircons display concentric zoning. Further sample and analytical details are provided in Lu et al. (2017h).

Seventy-seven analyses were obtained from 77 zircons (Fig. 11e,f). Seventeen analyses are 5% discordant or indicate high within-run variation of isotope ratios and are not considered further. The remaining 60 analyses yield  $^{207}\text{Pb}^*/^{206}\text{Pb}^*$  dates of 3371–1837 Ma, with a dominant age component at c. 1867 Ma, a subsidiary component at c. 2488 Ma and minor components at c. 2596, 2244, 2019, 1999 and 1934 Ma. A weighted mean  $^{207}\text{Pb}^*/^{206}\text{Pb}^*$  date of  $1864 \pm 5$  Ma (MSWD = 0.95) for the youngest 24 analyses is interpreted as a maximum depositional age for this unit.

### **GSWA 218330: lithic metasandstone, Marboo Formation**

The Marboo Formation was sampled from the northern part of the Halls Creek Orogen, about 15.7 km north-northwest of Mount Chambers and 15 km east-southeast of Cassidys Bore (Fig. 10). The sample was collected from

a ~25 cm-thick massive layer of meta-litharenite within a greenschist facies succession of interlayered sandstone and siltstone containing a layer-parallel foliation (Fig. 9f). The sample consists of about 65–70% lithic fragments, 20% quartz, 10% feldspar, 5% matrix, and accessory tourmaline, opaque minerals, detrital mica and zircon.

Zircons from this sample are colourless to dark brown, anhedral to subhedral, and variably rounded. The grains are up to 350  $\mu\text{m}$  long and equant to elongate, with aspect ratios up to 4:1. In CL images, concentric zoning is ubiquitous. Further sample and analytical details are provided in Lu et al. (2018c).

Sixty-eight analyses were collected from 65 zircons (Fig. 11g,h). Two analyses are >5% discordant and not considered further. The remaining 66 analyses yield  $^{207}\text{Pb}^*/^{206}\text{Pb}^*$  dates of 3055–1833 Ma, with a dominant age component at c. 1870 Ma. The youngest 35 analyses yield a weighted mean  $^{207}\text{Pb}^*/^{206}\text{Pb}^*$  date of  $1873 \pm 5$  Ma (MSWD = 1.1). This date is interpreted as a maximum depositional age for this part of the Marboo Formation.

### **GSWA 206173: psammitic schist, Marboo Formation**

A sample of the Marboo Formation from the northern part of the Halls Creek Orogen was collected from a small quarry on the north side of Lissadell Road, ~8.1 km east of Mount Nyulasy (Fig. 10). In this area, the Marboo Formation consists of metasandstone and metasilstone with abundant quartz veins and is intruded by the Dinner Creek Tonalite of the Paperbark Supersuite. Farther to the west, the Marboo Formation and Dinner Creek Tonalite are intruded by the Mount Nyulasy Granite, which has been dated at  $1859 \pm 3$  Ma (Page et al., 2001). The sample is a psammitic schist, consisting of 50% feldspar, 30% quartz, 15% chlorite and 3% iron–titanium oxide minerals.

Zircons from this sample are colourless to dark brown, subhedral to euhedral, and variably rounded. The crystals are up to 350  $\mu\text{m}$  long and equant to elongate, with aspect ratios up to 4:1. In CL images, most crystals exhibit concentric zoning. Further sample and analytical details are provided by Lu et al. (2016e), who suggested this unit was part of the Tickalara Metamorphics on the basis of the youngest age component. Although this remains a possibility, this sample is assigned here to the Marboo Formation, in line with previous mapping of the area (Sheppard et al., 1999a) – see discussion below.

Fifty-two analyses were obtained from 52 zircons (Fig. 12a,b). Five analyses are >5% discordant and not considered further. The remaining 47 analyses yield  $^{207}\text{Pb}^*/^{206}\text{Pb}^*$  dates of 3330–1844 Ma, with a dominant age component at c. 1868 Ma and a minor component at c. 2522 Ma. The youngest 14 analyses in the dominant age group yield a weighted mean  $^{207}\text{Pb}^*/^{206}\text{Pb}^*$  date of  $1857 \pm 4$  Ma (MSWD = 0.83), which defines a maximum depositional age. This date is indistinguishable from that of the c. 1859 Ma Mount Nyulasy Granite, and constrains deposition to close to the age of the youngest detrital zircon component.

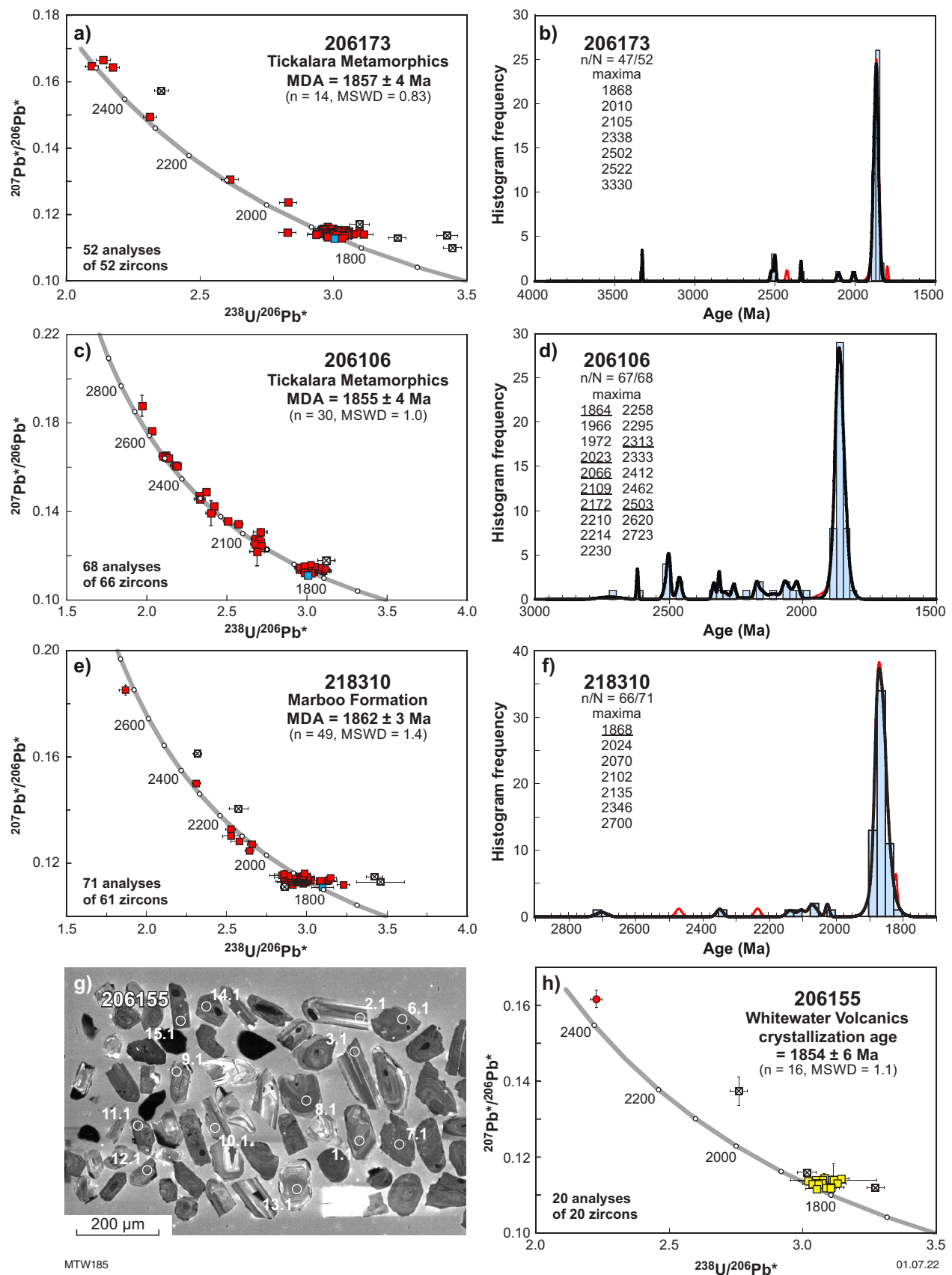


Figure 12. Concordia and probability density diagrams and CL image for metasedimentary rocks of the Marboo Formation and Whitewater Volcanics in the Western Zone (Halls Creek Orogen): a) and b) psammitic schist, Marboo Formation (GSWA 206173); c) and d) pelitic migmatite, Marboo Formation (GSWA 206106); e) and f) metasandstone, Marboo Formation (GSWA 218310); g) cathodoluminescence image of zircons from porphyritic dacite, Whitewater Volcanics (GSWA 206155); h) porphyritic dacite, Whitewater Volcanics (GSWA 206155). Diagram notes as in Figure 6



## GSWA 206106: pelitic migmatite, Marboo Formation

The Marboo Formation was sampled in the north of the Halls Creek Orogen, where the Great Northern Highway crosses Bow River, ~1.6 km southwest of Sugar Bag Yard (Fig. 10). In this area, the Marboo Formation consists of variably strained migmatite with abundant cordierite-bearing leucosome (Fig. 13a,b). The metasedimentary rocks are intruded by the Dinner Creek Tonalite of the Paperbark Supersuite and the Violet Valley Tonalite, dated at  $1852 \pm 3$  Ma (GSWA 218313, Lu et al., 2020b).

The sample is a pelitic migmatite, consisting of 40% quartz, 25% muscovite, 20% plagioclase and 12% biotite, with accessory iron–titanium oxide minerals, chlorite and apatite. Zircons from this sample are pale pink to dark brown, subhedral to euhedral, and variably rounded. The crystals are up to 250  $\mu\text{m}$  long and equant to elongate, with aspect ratios up to 4:1. In CL images, most crystals exhibit faded concentric and convoluted zoning, and some have pitted outer surfaces and truncations of zoning at grain boundaries. Many crystals have euhedral shapes and a few have very thin, dark, structureless rims that could not be analysed. Further sample and analytical details are provided in Lu et al. (2016a).

Sixty-eight analyses were obtained from 66 zircons (Fig. 12c,d). One analysis is >5% discordant and is not considered further. The remaining 67 analyses yield  $^{207}\text{Pb}^*/^{206}\text{Pb}^*$  dates of 2723–1820 Ma, with a dominant age component at c. 1864 Ma and subsidiary components at c. 2503, 2313, 2172, 2109, 2066 and 2023 Ma. A weighted mean  $^{207}\text{Pb}^*/^{206}\text{Pb}^*$  date of  $1855 \pm 4$  Ma (MSWD = 1.0) for the youngest 30 analyses represents a conservative maximum depositional age for this unit. This result is similar to the c. 1852 Ma age of the Violet Valley Tonalite, indicating deposition took place close to 1855 Ma.

## GSWA 218310: metasandstone, Marboo Formation

Metasedimentary rocks assigned to the Marboo Formation were sampled ~2 km north of the contact between the Western and Central Zones in the north of the Halls Creek Orogen, ~2.4 km south-southwest of Sydney Harbour Yard and 1.4 km east of Bow River (Fig. 10). In this area, interlayered psammitic and lesser pelitic units of amphibolite facies contain granitic veins up to 2 cm thick that are tightly folded and attenuated (Fig. 13c). These veins are of similar appearance to the  $1859 \pm 3$  Ma Mount Nyulasy Granite (Page et al., 2001), which intrudes the Marboo Formation ~300 m to the northwest, and may be related to this intrusion.

The dated sample was collected from a relatively homogeneous psammitic unit lacking felsic veins. It consists of 45–50% quartz, 20–25% feldspar, 15–20% biotite, 10% muscovite, and accessory apatite and zircon. Zircons from this sample are colourless to dark brown, anhedral to subhedral, and variably rounded. The grains are up to 350  $\mu\text{m}$  long and equant to elongate, with aspect ratios up to 5:1. In CL images, concentric zoning is ubiquitous, with some grains

showing truncation of zoning at grain boundaries, consistent with sedimentary transport. Further sample and analytical details are provided in Lu et al. (2018a).

Seventy-one analyses were obtained from 61 zircons (Fig. 12e,f). Five analyses are >5% discordant and not considered further. The remaining 66 analyses yield  $^{207}\text{Pb}^*/^{206}\text{Pb}^*$  dates of 2700–1814 Ma, with a dominant age component at c. 1868 Ma. A weighted mean  $^{207}\text{Pb}^*/^{206}\text{Pb}^*$  date of  $1862 \pm 3$  Ma (MSWD = 1.4) for the youngest 49 analyses represents a maximum depositional age for this unit, with the  $1859 \pm 3$  Ma date for the intruding Mount Nyulasy Granite (Page et al., 2001) providing a minimum age for deposition.

## GSWA 206155: porphyritic dacite, Whitewater Volcanics

A dacitic volcanic rock from the western Halls Creek Orogen was sampled on the western side of the Springvale – Bedford Downs track, 4.7 km south of Idamere Yard (Fig. 10). The volcanic unit is overlain by sandstone of the O'Donnell Formation in the lower Kimberley Basin, and also has a faulted lower contact with the O'Donnell Formation. The unit was previously thought to represent a volcanic horizon within the Speewah Group (Dow and Gemuts, 1967; Tyler et al., 1998), but the crystallization age obtained for this sample suggests that it is part of the Whitewater Volcanics of the Lamboo Province, structurally emplaced within the O'Donnell Formation.

The sample is a fine-grained, dark grey porphyritic dacite (Fig. 13d), consisting of ~60% feldspar aggregates, 20% plagioclase phenocrysts, 15% cryptocrystalline matrix, and accessory chlorite, iron–titanium oxide minerals, titanite and apatite. Zircons from the sample are colourless, subhedral to anhedral and some are rounded. In CL images, the zircons have a relatively uniform appearance and concentric zoning is ubiquitous. Further sample and analytical details are provided in Lu et al. (2016d).

Twenty analyses were collected from 20 zircons (Fig. 12g,h). Two analyses are >5% discordant and one analysis is interpreted as a mixture of core and rim material; these three analyses are not considered further. One analysis of a zircon core yields a  $^{207}\text{Pb}^*/^{206}\text{Pb}^*$  date of c. 2473 Ma and is interpreted to reflect inheritance. The remaining sixteen analyses yield a weighted mean  $^{207}\text{Pb}^*/^{206}\text{Pb}^*$  date of  $1854 \pm 6$  Ma (MSWD = 1.1), interpreted to date the magmatic crystallization of the dacite. Although it is possible that all the zircons are xenocrysts – given that subhedral to euhedral detrital zircons of this age occur in metasedimentary rocks of the Lamboo Province – this is considered to be unlikely due to the lack of pitted outer surfaces typical in detrital zircons, the relatively uniform U and Th compositions of the zircons and the high  $\text{SiO}_2$  (67 wt%) and high Zr (332 ppm) concentrations of this sample, indicating zircon saturation. The c. 1854 Ma date is comparable to the c. 1857 to 1849 Ma ages obtained for the Whitewater Volcanics elsewhere in the Lamboo Province, and the dated sample has a comparable geochemical composition (Griffin et al., 2000a; GSWA WACHEM database).





Figure 13. Field photographs of geochronology samples from the Western and Central Zones in the Halls Creek Orogen: a) and b) variably deformed biotite-muscovite pelitic migmatite of the Marboo Formation in the northern Halls Creek Orogen (GSWA 206106); c) pelitic migmatite of the Marboo Formation in the northern Halls Creek Orogen, with thin leucosomes and deformed granitic veins (GSWA 218310); d) porphyritic dacite of the Whitewater Volcanics in the western Halls Creek Orogen (GSWA 206155); e) psammitic gneiss of the Tickalara Metamorphics, with domains of layer-parallel, biotite-rich leucosome (GSWA 218315); f) garnet-cordierite-biotite-sillimanite diatexite of the Tickalara Metamorphics, ~5 km south-southwest of Warmun (GSWA 206131)



## Central Zone

### GSWA 218315: psammitic gneiss, Tickalara Metamorphics

A sample of the Tickalara Metamorphics was collected from the northern Halls Creek Orogen, 6.0 km southeast of Bow River homestead and 4.1 km north-northwest of Stock Route Bore (Fig. 10). The sample is a medium-grained psammitic gneiss with compositional layering defined by quartz- or biotite-rich layers and contains layer-parallel, coarse-grained, biotite-rich leucosomes (Fig. 13e). The Tickalara Metamorphics are intruded by the  $1852 \pm 3$  Ma Violet Valley Tonalite 800 m to the northwest (GSWA 218313, Lu et al., 2020b).

The sample consists of 40–45% quartz, 35–40% plagioclase, 10% biotite, 5% muscovite, 3% sericite, 1% epidote, 1% opaque minerals, and accessory zircon. Zircons from the sample are up to 400  $\mu\text{m}$  long and equant to elongate, with aspect ratios up to 4:1. In CL images, concentric zoning is ubiquitous and some zircons have thin, dark rims. Further sample and analytical details are provided in Lu et al. (2017i).

Eighty-seven analyses were obtained from 84 zircons (Fig. 14a,b). The thin rims present on some zircons could not be analysed. The zircons yield  $^{207}\text{Pb}^*/^{206}\text{Pb}^*$  dates of 3409–1835 Ma, with a dominant age component at c. 1868 Ma. A weighted mean  $^{207}\text{Pb}^*/^{206}\text{Pb}^*$  date of  $1865 \pm 2$  Ma (MSWD = 1.0) for the youngest 63 analyses represents a maximum depositional age for the sedimentary protolith.

### GSWA 206131: migmatitic pelitic gneiss, Tickalara Metamorphics

The Tickalara Metamorphics were sampled from an outcrop on the western side of the Great Northern Highway, 4.9 km west-southwest of Warmun community and 3.7 km north of Six Mile Bore (Fig. 10). The sample is a garnet–biotite–sillimanite–andalusite diatexite containing layer-parallel and crosscutting garnet-bearing leucosomes (Fig. 13f).

The pelitic gneiss consists of about 30% quartz, 25% biotite, 20% microcline, 15% sillimanite, 5% plagioclase, 2% garnet, and accessory epidote, iron–titanium oxide minerals and andalusite. Zircons from the sample are pale to dark brown, subhedral to euhedral, and variably rounded. The crystals are up to 400  $\mu\text{m}$  long and equant to elongate, with aspect ratios up to 4:1. In CL images, most grains are concentrically zoned and many contain domains or rims of homogeneous high-U zircon. Further sample and analytical details are provided in Lu et al. (2016c).

Twenty-eight analyses were obtained from 28 zircons (Fig. 14c,d), with the thin, high-U domains and rims unable to be analysed. The zircons yield  $^{207}\text{Pb}^*/^{206}\text{Pb}^*$  dates of 2447–1834 Ma, with a dominant age component at c. 1868 Ma. The youngest 25 analyses yield a weighted mean  $^{207}\text{Pb}^*/^{206}\text{Pb}^*$  date of  $1864 \pm 4$  Ma (MSWD = 1.6), which represents a maximum depositional age for the sedimentary protolith.

### GSWA 218321: pelitic gneiss, Tickalara Metamorphics

A sample of the Tickalara Metamorphics was collected from the eastern part of the Central Zone on the western side of a north-trending track, 5.9 km west of Mount Parker and 0.9 km north of Winnama Yard (Fig. 10). The succession comprises interlayered siliciclastic metasedimentary rocks and amphibolite, with lesser calc-silicate rock and marble (Fig. 15a,b). The succession is overprinted by a steeply dipping, north–south-trending, layer-parallel foliation that forms an elongated zone of high strain adjacent to the Halls Creek Fault, ~350 m to the east. A sample was taken from a shear-bound block of garnet-bearing pelitic to psammitic gneiss, to determine the age of the sedimentary protolith and to provide an age for the high-grade metamorphism.

The sampled gneiss consists of about 40–45% quartz, 25–30% plagioclase, 15–20% garnet, 10–12% biotite, 5% opaque minerals, and accessory zircon. Garnet-rich leucosomes form elongated, layer-parallel domains a few centimetres in size. Zircons from the sample are mainly colourless, anhedral to subhedral, and variably rounded. The crystals are up to 300  $\mu\text{m}$  long and equant to elongate, with aspect ratios up to 5:1. In CL images, most grains consist of oscillatory-zoned cores overgrown by homogeneous rims. Further sample and analytical details are provided in Lu et al. (2017j).

Ninety-five analyses were obtained from 64 zircons (Fig. 14e,f). Twenty-nine analyses are >5% discordant or indicate high within-run variation of isotope ratios, and are not considered further. Thirty-seven analyses of zircon cores yield  $^{207}\text{Pb}^*/^{206}\text{Pb}^*$  dates of 1999–1797 Ma, with a dominant age component at c. 1903 Ma. The youngest core analysis is imprecise ( $1797 \pm 46$  Ma, 1 $\sigma$ ) and a weighted mean  $^{207}\text{Pb}^*/^{206}\text{Pb}^*$  date of  $1879 \pm 15$  Ma (MSWD = 1.0) for the 11 youngest analyses is interpreted as a more conservative maximum depositional age. Twenty-nine analyses of zircon rims indicate low to moderate U contents of 65–265 ppm and low Th/U of 0.01 – 0.31 (median 0.05). The rims yield a weighted mean  $^{207}\text{Pb}^*/^{206}\text{Pb}^*$  date of  $1820 \pm 9$  Ma (MSWD = 1.6), which is interpreted as the age of high-grade metamorphism. Monazite inclusions in garnet porphyroblasts and within the quartz–plagioclase–biotite matrix of this sample yield an identical age of  $1820 \pm 8$  Ma (GSWA 218321, Fielding et al., 2022).

### GSWA 218333: psammitic gneiss, Tickalara Metamorphics

Metasedimentary gneiss of the Tickalara Metamorphics was sampled from Fletcher Creek, ~7.3 km southeast of Nine Mile Bore, 6.4 km west of Two Mile Bore and ~6.3 km north-northwest of the Savannah Ni–Cu–Co mine (Fig. 10). In this area, the succession consists of migmatitic psammitic to pelitic gneiss and layer-parallel units of mafic gneiss metamorphosed at upper amphibolite to granulite facies (Fig. 15c–e; Oliver and Barr, 1997). An older generation of stromatic, layer-parallel leucosomes has previously been dated at 1850–1840 Ma in this area, and gabbroic dykes to 2 m thick intruding syn- to post-peak

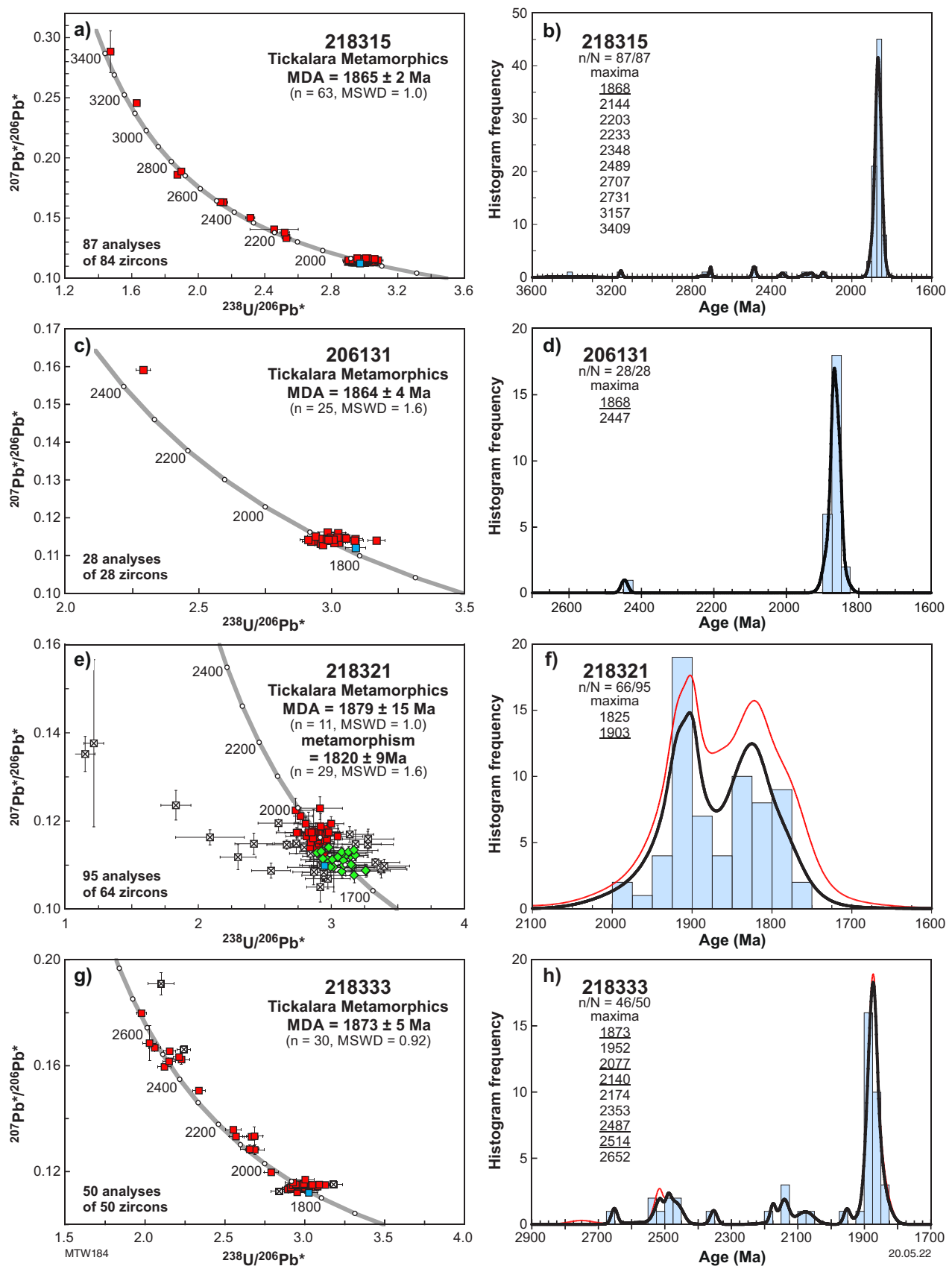


Figure 14. Concordia and probability density diagrams for metasedimentary rocks of the Tickalara Metamorphics in the Central Zone: a) and b) psammitic gneiss (GSWA 218315); c) and d) migmatitic pelitic gneiss (GSWA 206131); e) and f) pelitic gneiss (GSWA 218321); g) and h) psammitic gneiss (GSWA 218333). Green diamonds indicate analyses of metamorphic zircon rims. Other notes as in Figure 6



metamorphism produced leucosomes in country rocks along their margins dated at 1845–1830 Ma (Fig. 15f; Oliver et al., 1999). These ages are similar to 1848–1838 Ma dates for mafic–ultramafic intrusive rocks intruding the Tickalara Metamorphics in the Savannah Ni–Cu–Co mine area (Mole et al., 2018).

A sample of psammitic to psammopelitic gneiss lacking significant leucosome was collected from a ~40 cm-thick layer within an interlayered succession of pelitic and psammitic gneiss (Fig. 15c). The sample is fine-grained, and consists of about 40% quartz, 20–23% K-feldspar, 15–20% cordierite, 7% biotite, 5% garnet, 5% plagioclase, 2% sillimanite, 1% opaque mineral, and accessory apatite and zircon. Zircons from this sample are up to 350  $\mu\text{m}$  long and equant to elongate, with aspect ratios up to 4:1. In CL images, most grains exhibit concentric zoning, which is truncated at grain boundaries in some grains. Some zircons have very thin, irregularly developed dark rims that were too narrow to analyse. Further sample and analytical details are provided in Lu et al. (2018d).

Fifty analyses were obtained from 50 zircons (Fig. 14g,h). Four analyses are >5% discordant and are not considered further. The remaining 46 analyses yield  $^{207}\text{Pb}^*/^{206}\text{Pb}^*$  dates of 2652–1833 Ma, with a dominant age component at c. 1873 Ma. A weighted mean  $^{207}\text{Pb}^*/^{206}\text{Pb}^*$  date of  $1873 \pm 5$  Ma (MSWD = 0.92) for the youngest 30 analyses is interpreted as a maximum depositional age for the sedimentary protolith. Minimum depositional ages of 1850–1845 Ma are provided by the oldest dates for leucosome and mafic intrusive rocks.

### **GSWA 206128: pelitic schist, Tickalara Metamorphics**

A sample of the Tickalara Metamorphics was collected from the central Halls Creek Orogen, 4.8 km northeast of Rose Bore and 11.7 km west of Alice Downs homestead (Fig. 10). The Panton layered mafic–ultramafic intrusion, which intrudes the Tickalara Metamorphics 200 m to the southeast, is dated at  $1856 \pm 2$  Ma (Page and Hoatson, 2000). The sample consists of psammitic to pelitic biotite–muscovite schist with rare andalusite and a crenulated schistosity (Fig. 16a).

The sample consists of about 60% quartz, 20% biotite, 15% muscovite, and accessory iron oxide minerals and epidote. Muscovite post-dates and replaces biotite and is commonly oriented at a high angle to the foliation. Zircons from the sample are colourless to dark brown, subhedral to euhedral, and variably rounded. The crystals are up to 200  $\mu\text{m}$  long and equant to elongate, with aspect ratios up to 4:1. In CL images, concentric zoning is ubiquitous. Further sample and analytical details are provided in Lu et al. (2016b).

Sixty-three analyses were obtained from 63 zircons (Fig. 17a,b). Seven analyses are >5% discordant and are not considered further. The remaining 56 analyses yield  $^{207}\text{Pb}^*/^{206}\text{Pb}^*$  dates of 2764–1836 Ma, with a dominant age component at 1875–1860 Ma. The 36 youngest analyses yield a weighted mean  $^{207}\text{Pb}^*/^{206}\text{Pb}^*$  date of  $1867 \pm 4$  Ma (MSWD = 2.0), which represents a maximum depositional age for the sedimentary protolith. A minimum age is provided by the  $1856 \pm 2$  Ma Panton intrusion (Page and Hoatson, 2000).

### **GSWA 218318: muscovite–chlorite schist, Winnama Formation**

The Winnama Formation was sampled from the eastern part of the Halls Creek Orogen, 8.1 km southwest of Mount Parker and 5.0 km south of Winnama Yard (Fig. 10). The unit consists of muscovite–chlorite psammitic and pelitic schist, which is layered on a millimetre- to centimetre-scale, and interlayered with hornblende amphibolite about 50 m to the northwest. The schist contains a strong layer-parallel foliation, which is crosscut by granitic dykes 15–20 cm thick (Fig. 16b) that are in turn overprinted by two generations of folding. The Winnama Formation is intruded by the  $1827 \pm 3$  Ma McHale Granite (Page et al., 2001) approximately 1 km to the east.

The sample consists of about 65% quartz, 15–18% feldspar, 12% muscovite, 5% chlorite (probably retrogressed biotite), and accessory tourmaline, hematite and zircon. Zircons from this sample are colourless to dark brown and opaque, and range from subhedral to anhedral. The grains are up to 350  $\mu\text{m}$  long and equant to elongate, with aspect ratios up to 6:1. In CL images, concentric zoning is ubiquitous and many grains are dominated by high-uranium, metamict domains. Further sample and analytical details are provided in Lu et al. (2018b).

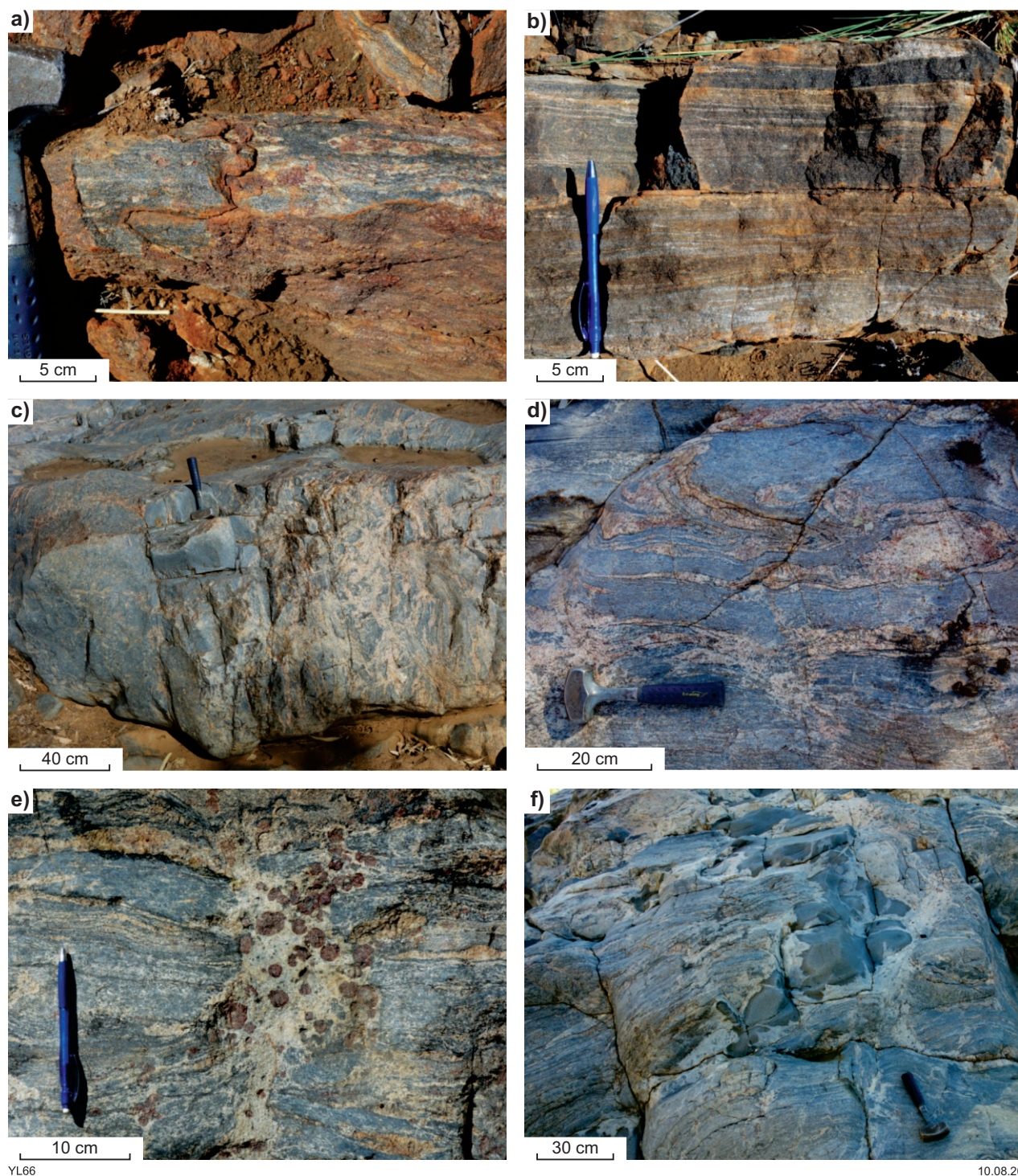
Eighty-one analyses were obtained from 80 zircons (Fig. 17c,d). Fifty analyses are >5% discordant, forming a discordia with an imprecise lower intercept at 550–500 Ma. This age is comparable to that of the c. 511 Ma Kalkarindji Large Igneous Province, which had an eruptive centre in the east Kimberley region (Jourdan et al., 2014), and the age possibly reflects hydrothermal fluid flow in basement rocks during associated magmatic events (cf. Maidment et al., 2020). The remaining 31 analyses yield  $^{207}\text{Pb}^*/^{206}\text{Pb}^*$  dates of 2471–1802 Ma, with a dominant age component at c. 1869 Ma. A single analysis at c. 1802 Ma has comparable U, Th and Th/U to other analyses and is interpreted to reflect ancient loss of radiogenic lead. A weighted mean  $^{207}\text{Pb}^*/^{206}\text{Pb}^*$  date of  $1870 \pm 6$  Ma (MSWD = 1.2) for the next youngest 26 analyses represents a maximum depositional age for the sample.

### **GSWA 216661: lithic sandstone, Milba Formation**

The Milba Formation was sampled on the eastern side of a track, 9.1 km west-northwest of The Brim Rockhole and 7.8 km north of Sophie Downs homestead (Fig. 10). The sampled unit is a poorly sorted, medium- to coarse-grained lithic sandstone, with no sedimentary structures preserved (Fig. 16c). Rounded lithic clasts comprise up to 10% and consist of quartz arenite, siltstone and rare chert. The sandstone contains a poorly developed foliation that wraps around quartz granules.

The sample consists of about 40–45% quartz, 20–25% lithic grains, 20% matrix (fine-grained clay and feldspar), 15% feldspar, and accessory opaque minerals, muscovite, tourmaline and zircon. Zircons from this sample are pale brown to dark brown, anhedral to subhedral, and variably rounded. The crystals are up to 300  $\mu\text{m}$  long and equant to elongate, with aspect ratios up to 7:1. In CL images, concentric zoning is ubiquitous. Further sample and analytical details are provided in Lu et al. (2018e).





YL66

10.08.20

Figure 15. Field photographs of geochronology samples of the Tickalara Metamorphics in the Central Zone: a) garnet-biotite psammitic gneiss adjacent to the Halls Creek Fault (GSWA 218321); b) interlayered metasedimentary rock and amphibolite near the GSWA 218321 sample site, containing a pervasive north-south-trending foliation subparallel to the Halls Creek Fault; c) layer of psammitic gneiss sampled for geochronology (GSWA 218333) within more migmatitic pelitic gneiss; d) folded garnet-bearing leucosome and psammitic gneiss, adjacent to GSWA 218333 sample site; e) discordant garnet-rich leucosome domain in psammitic gneiss, Fletcher Creek Rockholes (MGA 393890E, 8086700N); f) leucosome mantle associated with intrusion of mafic dyke into  $S_1$ -bearing metasedimentary gneiss, cross-cutting stromatic leucosomes, Fletcher Creek Rockholes (MGA 393905E, 8086695N)



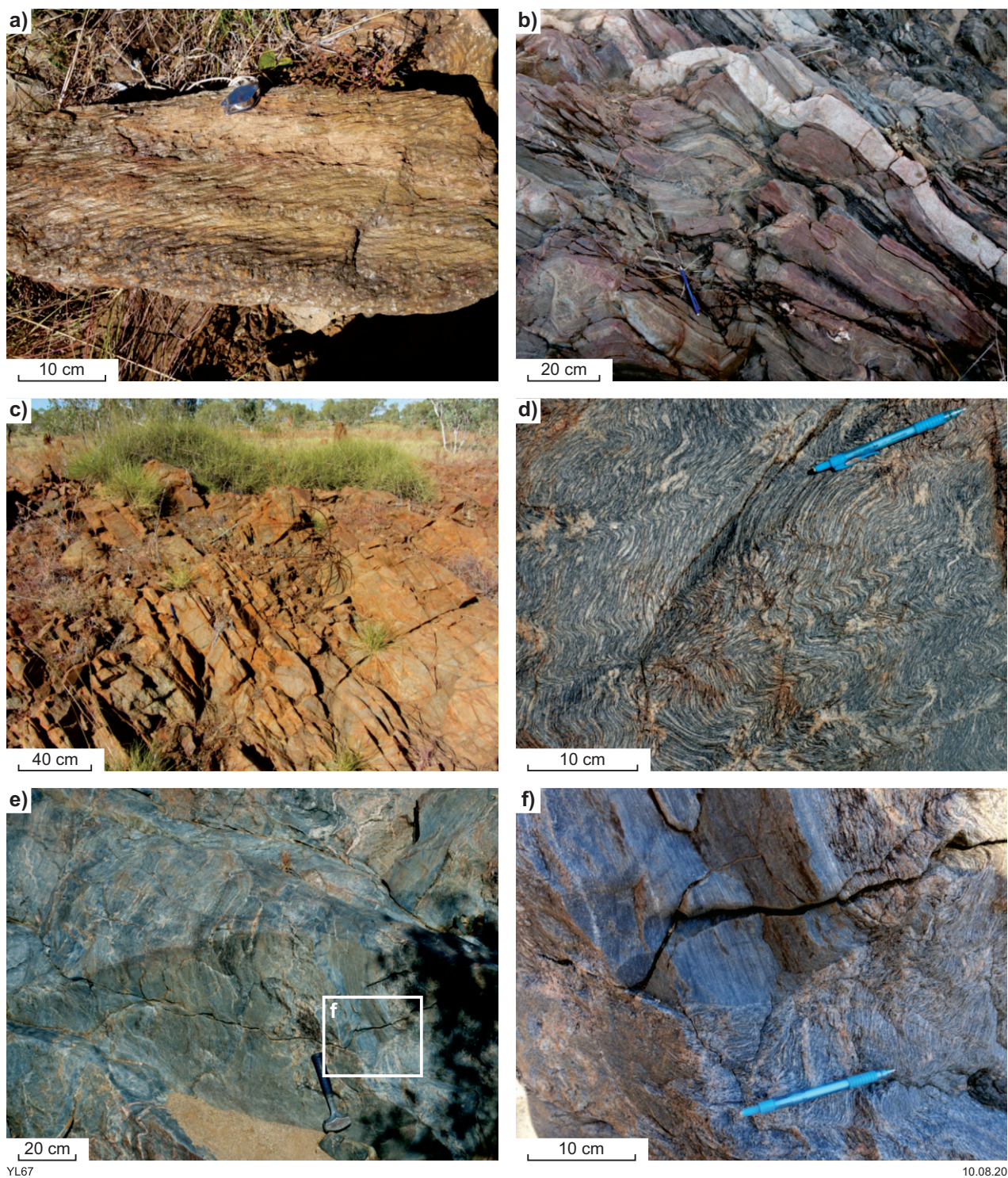


Figure 16. Field photographs of geochronology sample sites from the Central Zone: a) andalusite-muscovite schist of the Tickalara Metamorphics, showing a crenulation cleavage oblique to  $S_0/S_1$ , near the Pantom mafic-ultramafic intrusion in the central Halls Creek Orogen (GSWA 206128); b) foliated psammitic biotite-muscovite schist of the Winnama Formation intruded by a granitic dyke of the Sally Downs Supersuite and folded by deformation associated with the Halls Creek Orogeny (GSWA 218318); c) metasandstone of the Milba Formation in the southeastern Central Zone (GSWA 216661); d) homogeneous quartzofeldspathic gneiss of the Rose Bore Granite (MGA 375104E, 8031664N); e) heterogeneous, layered Rose Bore Granite (MGA 374996E, 8031668N); f) detail of termination of competent metasedimentary unit within homogeneous quartzofeldspathic gneiss shown in e)

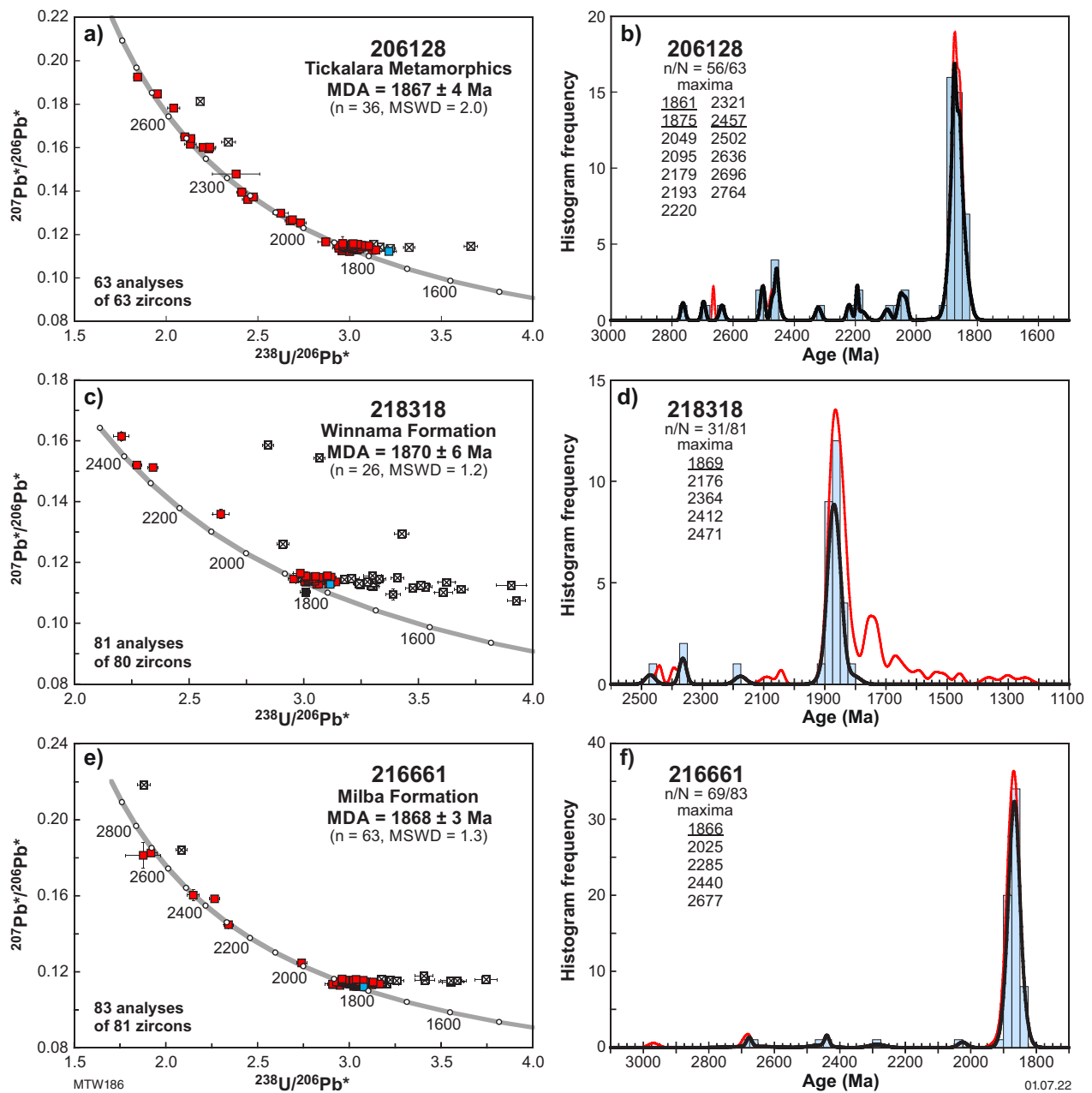


Figure 17. Concordia and probability density diagrams for metasedimentary rocks in the Central Zone: a) and b) pelitic schist, Tickalara Metamorphics (GSWA 206128); c) and d) muscovite–chlorite schist, Winnama Formation (GSWA 218318); e) and f) lithic sandstone, Milba Formation (GSWA 216661). Diagram notes as in Figure 6



Eighty-three analyses were obtained from 81 zircons (Fig. 17e,f). Fourteen analyses are >5% discordant and are not considered further. The remaining 69 analyses yield  $^{207}\text{Pb}^*/^{206}\text{Pb}^*$  dates of 2677–1834 Ma, with a dominant age component at c. 1866 Ma. A weighted mean  $^{207}\text{Pb}^*/^{206}\text{Pb}^*$  date of  $1868 \pm 3$  Ma (MSWD = 1.3) for the youngest 63 analyses represents a maximum depositional age for the sandstone.

### **GSWA 226523: biotite–muscovite granodiorite gneiss, Rose Bore Granite**

A previous c. 1863 Ma date for the Rose Bore Granite, interpreted as an igneous crystallization age by Page and Hoatson (2000), is indistinguishable from the dominant detrital zircon age component in the Tickalara Metamorphics, raising the possibility that this date reflects inheritance from host rocks. Two samples were collected from outcrops in the bed of the Pantan River, about 2.6 km southeast of Rose Bore (Fig. 10), to further test the age of the Rose Bore Granite. In this area, quartzofeldspathic gneiss of the Rose Bore Granite forms a sheet-like body within quartz–biotite–muscovite–feldspar±sillimanite±andalusite schist and gneiss of the Tickalara Metamorphics. The Pantan mafic–ultramafic layered intrusion immediately to the northwest does not contain the strong foliation that is present in the Rose Bore Granite and Tickalara Metamorphics and is considered to have intruded these units, resulting in migmatization of the host rocks in the contact metamorphic aureole (Hoatson, 2000a; Page and Hoatson, 2000). The Rose Bore Granite comprises domains of homogeneous, foliated micaceous migmatitic gneiss (Fig. 16d) and more heterogeneous domains that include layered quartz- and mica-rich units that appear to have been derived from sedimentary protoliths (Figs 16e,f, 18a).

In an attempt to date metamorphism of the unit, sample GSWA 206104 was taken from a domain of quartzofeldspathic gneiss containing a relatively high proportion of leucosome, but no zircon was recovered. However, the present sample of homogeneous quartzofeldspathic gneiss with a smaller amount of leucosome, collected ~70 m to the west, yielded sufficient zircons for dating. This sample contains a pervasive gneissic foliation defined by micas and flattened leucocratic mineral aggregates, and is deformed by small-scale, upright, north-northwesterly trending folds (Fig. 18b). Irregular small patches of leucosome overprint the pervasive foliation and locally pool in fold hinges. The folds and leucosomes are crosscut by thin, pegmatitic quartz–tourmaline veins in places.

The sample is a biotite–muscovite granodiorite gneiss consisting of about 35% quartz, 35% plagioclase, 15% K-feldspar, 10% biotite, 5% muscovite, and accessory magnetite and zircon. Quartz is anhedral, up to 1.5 mm in size and partly occurs in aggregates, elongate quartz lenses or augen up to 8 mm long. Plagioclase is anhedral, equant to elongate and up to 2 mm in size. K-feldspar is mainly anhedral, microperthitic and up to 1.5 mm in size, with patches showing microcline twinning. Subhedral laths of brown biotite up to 1.7 mm long form semi-continuous folia. Muscovite forms subhedral laths, in part with cleavage parallel to that in adjacent biotite, but also with cleavage orthogonal to the foliation. Bladed magnetite is up to 0.3 mm long and mainly parallel to cleavage within micas.

The relatively small number of zircons (33) isolated from the sample are colourless to dark brown, and mainly anhedral. The crystals are up to 200  $\mu\text{m}$  long and equant to elongate, with aspect ratios up to 4:1. In CL images, concentric zoning is ubiquitous (Fig. 19a). Further sample and analytical details are provided in Lu et al. (2020d).

Twenty-seven analyses were obtained from 27 zircons (Fig. 19b). One analysis is >5% discordant and the remaining 26 analyses can be divided into two groups based on their  $^{207}\text{Pb}^*/^{206}\text{Pb}^*$  ratios. Thirteen analyses (132–738 ppm U, 29–360 ppm Th and Th/U = 0.13 – 0.82) yield a weighted mean  $^{207}\text{Pb}^*/^{206}\text{Pb}^*$  date of  $1822 \pm 5$  Ma (MSWD = 1.4). The other thirteen analyses yield  $^{207}\text{Pb}^*/^{206}\text{Pb}^*$  dates of 2088–1847 Ma. Eleven of these analyses (74–882 ppm U, 37–604 ppm Th and Th/U = 0.26 – 1.1) yield a weighted mean  $^{207}\text{Pb}^*/^{206}\text{Pb}^*$  date of  $1863 \pm 5$  Ma (MSWD = 0.94), which is indistinguishable from the  $1863 \pm 3$  Ma age component obtained by Page and Hoatson (2000) for the Rose Bore Granite and the  $1867 \pm 4$  Ma dominant detrital age component in the Tickalara Metamorphics 5.9 km to the north-northeast (GSWA 206128, Lu et al., 2016b). Although it is possible that the c. 1863 Ma date defines an igneous crystallization age, the low abundance of zircons in the Rose Bore Granite and their irregular shapes raise the possibility that the zircons have a xenocrystic origin. The  $1822 \pm 5$  Ma date is younger than the inferred minimum age for this unit based on the c. 1856 Ma age of the Pantan intrusion (Page and Hoatson, 2000) and might reflect metamorphism during the Halls Creek Orogeny. The range of possible interpretations for this sample is discussed in more detail below.

### **GSWA 218350: biotite–hornblende metatonalite, Dougalls Tonalite**

Tonalite of the Dougalls Suite is exposed in the eastern part of the Central Zone, where it forms a  $15 \times 1.5$  km domain of complex sills and dykes within the Tickalara Metamorphics. These granitic rocks were previously termed the Dead Finish Tonalite (Tyler et al., 1997a) but are now assigned to the Dougalls Tonalite. A sample was collected 1.9 km west of Alice Downs homestead (Fig. 10), where tonalite forms a network of irregular thin dykes within amphibolite. In some places, the tonalite dykes are sharply defined and include angular mafic xenoliths (Fig. 18c). In other outcrops, contacts between tonalite and amphibolite are irregular, with rounded mafic xenoliths in the tonalite and textures suggestive of magma mingling (Fig. 18d). A variably developed high-grade metamorphic foliation overprints the tonalite and amphibolite.

The sample is a foliated, recrystallized, fine- to medium-grained biotite–hornblende metatonalite, consisting of about 45–50% plagioclase, 35–40% quartz, 7–8% biotite, 4–5% amphibole (probably actinolitic hornblende), 1% secondary epidote, 1% magnetite, and accessory zircon. The sampled rock has 298 ppm Zr and zircons from this sample are colourless to pale brown, and subhedral to euhedral. The crystals are up to 350  $\mu\text{m}$  long and equant to elongate, with aspect ratios up to 4:1. Acicular inclusions are abundant. In CL images, concentric zoning is ubiquitous and some zircons appear to contain older cores (Fig. 19c). Irregular domains of convoluted zoning cut the concentric zoning in places. Further sample and analytical details are provided in Lu et al. (2020c).

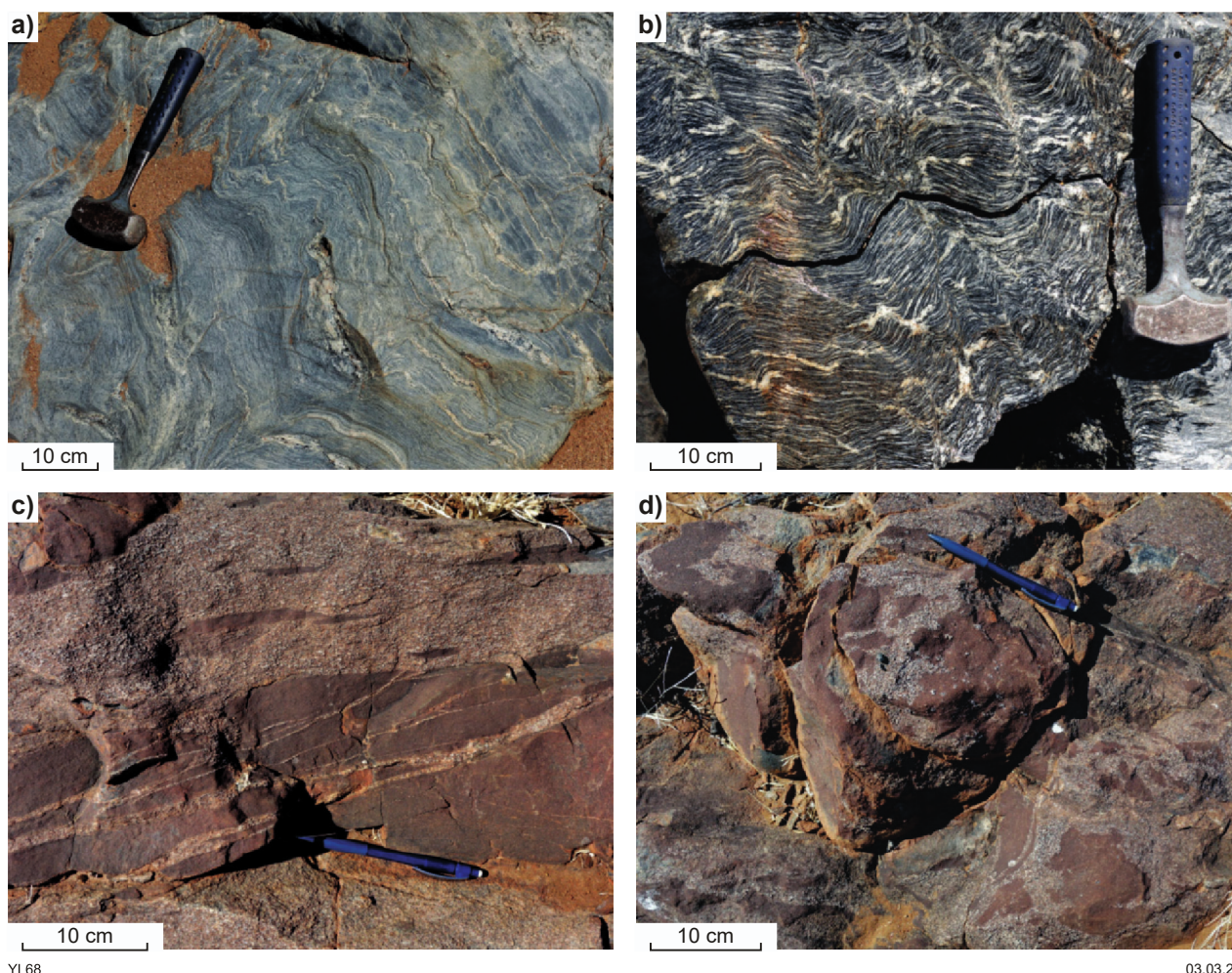


Figure 18. Field photographs of quartzofeldspathic rocks in the Central Zone: a) layered migmatitic gneiss within the Rose Bore Granite (MGA 374990E, 3031673N); b) block sampled for geochronology, Rose Bore Granite (GSWA 226523); c) granitic dyke of Dougalls Tonalite in the Tickalara Metamorphics, containing angular mafic xenoliths derived from wall rocks (GSWA 218350); d) irregular mafic xenoliths within the Dougalls Tonalite near c) (MGA 385650E, 3035810N), showing apparent magma-mingling textures

Eighteen analyses were obtained from 17 zircons (Fig. 19d). The analyses are concordant to moderately discordant and form a single group with a weighted mean  $^{207}\text{Pb}^*/^{206}\text{Pb}^*$  date of  $1847 \pm 5$  Ma (MSWD = 0.95), interpreted as the crystallization age of the tonalite.

### GSWA 218313: metamonzogranite, Violet Valley Tonalite

The Violet Valley Tonalite forms a northeasterly trending igneous complex ~50 km long and 1.5 to 7.0 km wide, consisting of several phases of biotite granodiorite, monzonite and tonalite (Dow and Gemuts, 1969; Sheppard et al., 1999a). It intrudes across the boundary between the Western and Central Zones and was previously assigned to the Kevins Dam Suite of the Sally Downs Supersuite. The Violet Valley Tonalite was sampled from a bouldery outcrop 1.2 km east-northeast of Bow River homestead, where it intrudes migmatitic metasedimentary rocks of the Tickalara Metamorphics (Figs 10, 20a,b). In this area, the monzogranite contains rounded mafic and metasedimentary enclaves up to ~50 cm in size, which are widespread but not abundant.

The sample is a medium-grained, equigranular biotite metamonzogranite, consisting of about 35% plagioclase, 20–25% K-feldspar, 15–20% quartz, 15–20% biotite, 5% mineral grains replaced by fine micas, 1% secondary epidote, and accessory allanite, magnetite, zircon and rutile. The metamonzogranite has undergone weak deformation and minor recrystallization at moderate grade, indicated by the presence of flame perthite, strained biotite and recrystallized quartz. Zircons from this sample are pale brown to dark brown, mainly euhedral and show ubiquitous concentric zoning (Fig. 21a). Further sample and analytical details are provided in Lu et al. (2020b).

Twenty-three analyses were collected from 23 zircons (Fig. 21b), which form a concordant to slightly discordant group that yields a weighted mean  $^{207}\text{Pb}^*/^{206}\text{Pb}^*$  date of  $1852 \pm 3$  Ma (MSWD = 0.93). This date is interpreted as the magmatic crystallization age of the monzogranite and indicates that it is too old to be part of the 1837–1808 Ma Sally Downs Supersuite. Although the c. 1852 Ma age is similar to 1850–1847 Ma dates obtained for the Dougalls Tonalite and Fletcher Creek Granite (Page et al., 2001; GSWA 218350, Lu et al., 2020c), the Violet Valley Tonalite is more compositionally similar to granitic rocks of the Paperbark



Supersuite (Sheppard et al., 2001), the youngest components of which are dated at c. 1852 Ma (Griffin et al., 2000a). The Violet Valley Tonalite is thus here interpreted to be a possible younger component of the Paperbark Supersuite.

### GSWA 218355: biotite–hornblende metatonalite, Mabel Downs Tonalite

A sample of deformed metatonalite was collected from a prominent outcrop (Fig. 20c) west of a north-northeast-trending track on Mabel Downs Station, about 3.7 km north-northeast of Winnama Yard and 5.5 km west-northwest of Mount Parker (Fig. 10). The sampled unit forms a narrow, strike-extensive sheet >7 km long and ~150 m wide within the Tickalara Metamorphics within a north-northeast-trending, high-strain zone ~300 m west of the Halls Creek Fault.

The sample is a strongly foliated, partially recrystallized, medium-grained biotite–hornblende metatonalite consisting of about 45% plagioclase, 35% quartz, 8–10% biotite, 5% hornblende, 2–3% K-feldspar and 1% magnetite, with accessory myrmekite, allanite, apatite and zircon. The steeply west-northwesterly dipping foliation in this sample is defined by elongate lenses and grains of quartz and by biotite±hornblende folia, indicating deformation in amphibolite facies conditions. Zircons from this sample are colourless to pale brown, subhedral to euhedral, up to 400 µm long and have aspect ratios up to 8:1. In CL images, concentric zoning is ubiquitous and some crystals appear to

contain older cores (Fig. 21c). Further sample and analytical details are provided in Lu et al. (2020f).

Twenty-three analyses were obtained from 20 zircons (Fig. 21d). Twenty-two analyses of 19 zircons are concordant to slightly discordant and yield a weighted mean  $^{207}\text{Pb}^*/^{206}\text{Pb}^*$  date of  $1829 \pm 3$  Ma (MSWD = 0.63), which is interpreted as the magmatic crystallization age of the tonalite. One analysis of a zircon core yielded a  $^{207}\text{Pb}^*/^{206}\text{Pb}^*$  date of c. 1886 Ma, which is interpreted as the age of an inherited zircon. The metatonalite was previously assigned to the Corkwood Tonalite of the Dougalls Suite (Tyler et al., 1997b) but its c. 1829 Ma age suggests that it is a component of the 1832–1827 Ma Mabel Downs Tonalite (Bordorkos et al., 2000a), which is exposed as a much larger, sub-parallel igneous complex ~1 km to the west.

### GSWA 124442: biotite–hornblende syenogranite, Kevins Dam Monzogranite

A sample of syenogranite was collected from the western part of the 55 x 15 km Kevins Dam Monzogranite, about 7.5 km east-southeast of Turkey Nest Dam and 15.7 km northeast of Foal Creek Yard (Fig. 10). The western margin of the Kevins Dam Monzogranite has a chilled contact against the c. 1855 Ma Greenvale Porphyry of the Paperbark Supersuite (Griffin et al., 2000a), whereas its eastern margin is in contact with the Tickalara Metamorphics and granitic rocks of the Sally Downs Supersuite.

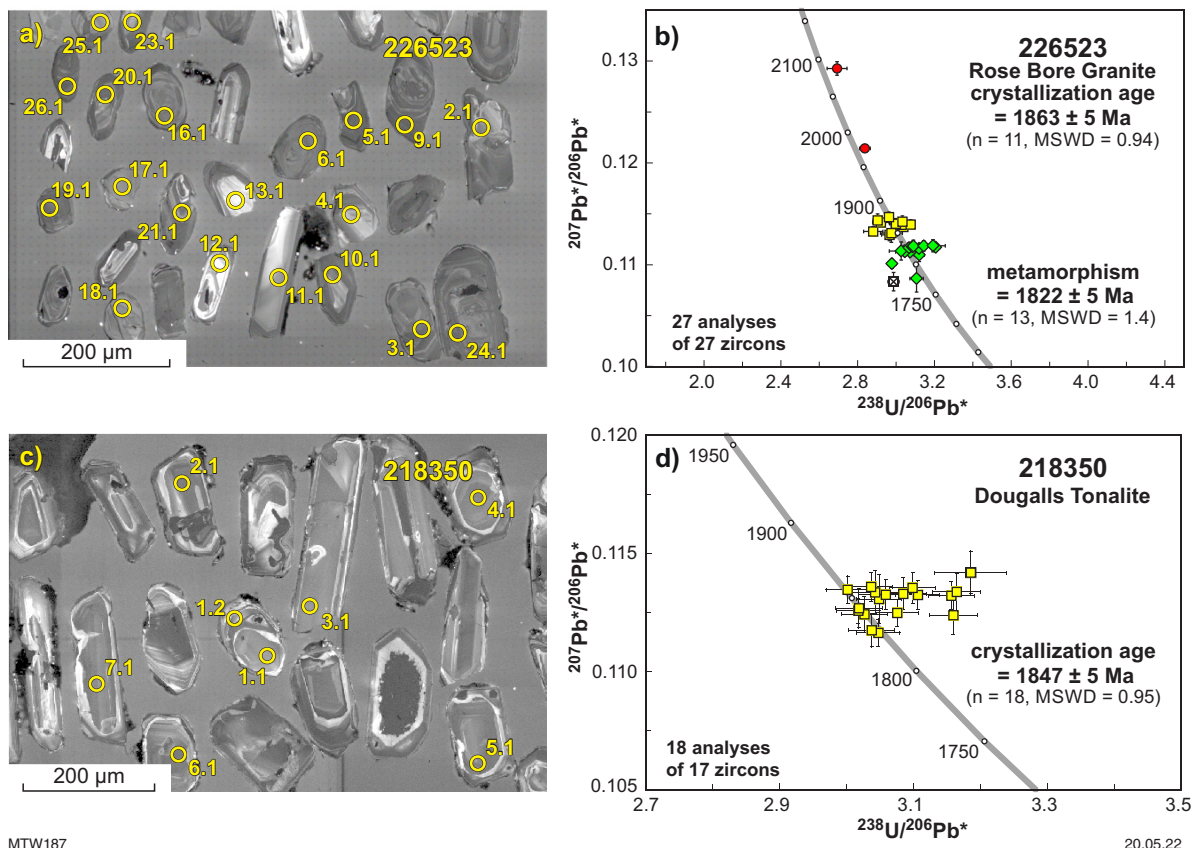


Figure 19. CL images and concordia diagrams for quartzofeldspathic rocks in the Central Zone: a) CL image of zircons from the Rose Bore Granite (GSWA 226523); b) concordia diagram for the Rose Bore Granite (GSWA 226523); c) CL image of zircons from the Dougalls Tonalite (GSWA 218350); d) concordia diagram for the Dougalls Tonalite (GSWA 218350). Green diamonds: analyses of metamorphic zircon rims; other notes as in Figure 6



Figure 20. Field and sample photographs of granitic rocks in the Central Zone: a) outcrop of the Violet Valley Tonalite at geochronology sample site GSWA 218313, with mafic xenoliths in lower right; b) sampled boulder of the Violet Valley Tonalite (GSWA 218313); c) sample site of Mabel Downs Tonalite (GSWA 218355); d) hand specimen of Kevins Dam Monzogranite (GSWA 124442)

The unit sampled is a medium- to coarse-grained biotite–hornblende syenogranite (Fig. 20d), consisting of about 45–50% K-feldspar, 35–38% quartz, 12% plagioclase, 3% biotite, 2% hornblende, and accessory magnetite, allanite and zircon. Apart from strained quartz, the sample is undeformed, and the secondary mineralogy is consistent with lower greenschist facies metamorphic conditions. Zircons from this sample are pale brown to dark brown, mainly euhedral, up to 300  $\mu\text{m}$  long and have aspect ratios up to 6:1. In CL images, concentric zoning is ubiquitous (Fig. 21e). Further sample and analytical details are provided in Lu et al. (2020e).

Twenty-two analyses were obtained from 22 zircons (Fig. 21f). The analyses are concordant to slightly discordant and form a single group with a weighted mean  $^{207}\text{Pb}^*/^{206}\text{Pb}^*$  date of  $1854 \pm 5$  Ma (MSWD = 0.71), which is interpreted as the magmatic crystallization age of the syenogranite. This age is significantly older than granitic rocks of the Sally Downs Supersuite and the syenogranite is thus interpreted to be a component of the Paperbark Supersuite, rather than the Sally Downs Supersuite as previously thought (Sheppard et al., 2001).

## Lu–Hf isotope results

Lu–Hf isotope data were collected for representative zircons from seven samples of the Marboo Formation (GSWA 206102, 212344, 215562, 206154, 218305, 206173 and 206106), four samples of the Tickalara Metamorphics (GSWA 218315, 206131, 218321 and 206128) and one sample of the Ruins Dolerite (GSWA 212335). The data for these samples are plotted in Figure 22 and listed in Appendix 1.

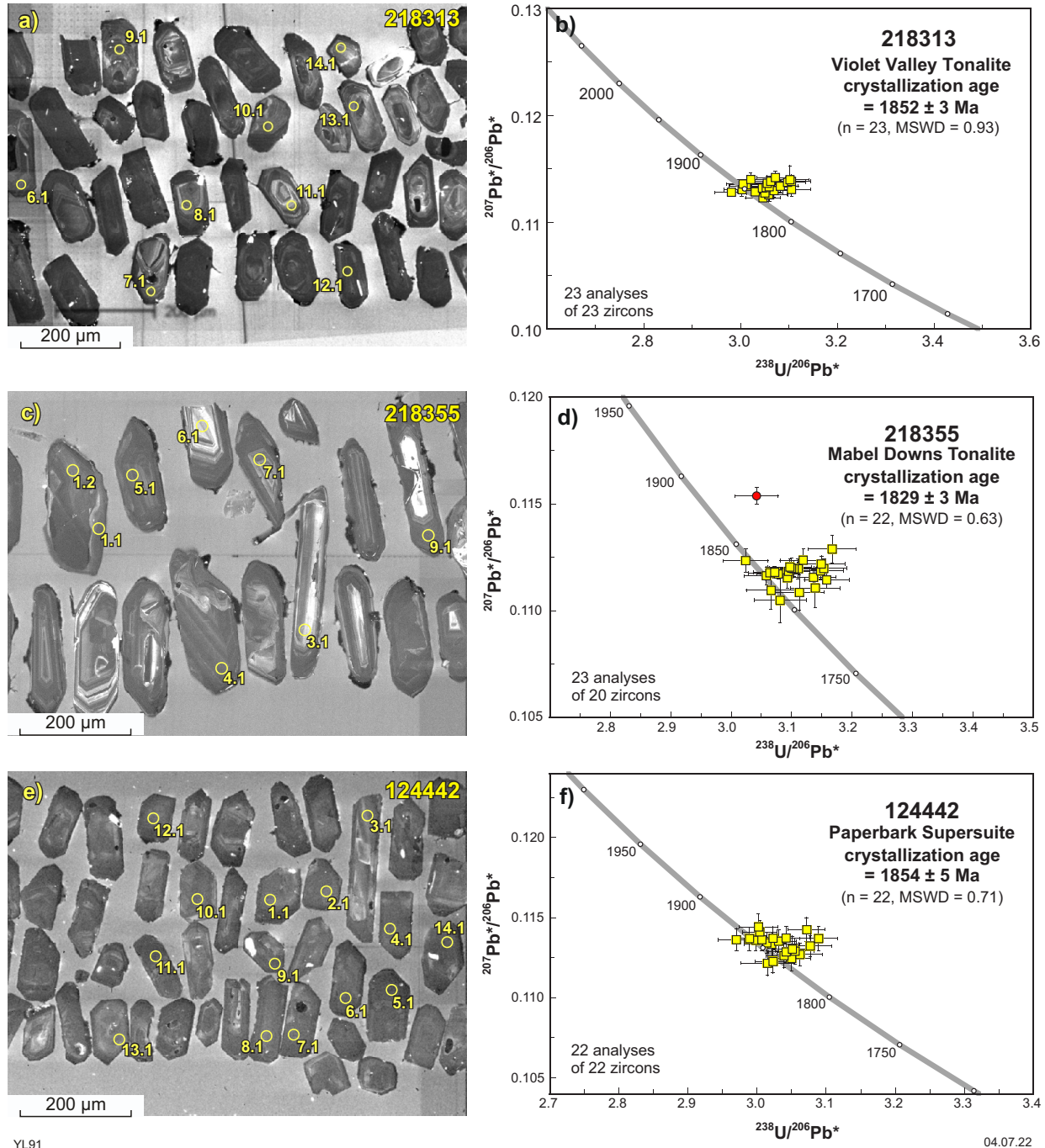
The oldest detrital zircons, at 3.45 – 3.15 Ga, in the Marboo Formation and Tickalara Metamorphics have initial  $^{176}\text{Hf}/^{177}\text{Hf}$  values mostly close to CHUR and yielded  $T_{\text{DM}}^2$  of c. 3.7 Ga, suggesting reworking of a c. 3.7 Ga juvenile source. One analysis at c. 3.3 Ga yielded a much older  $T_{\text{DM}}^2$  of 4.16 Ga, possibly indicating derivation from Hadean crust. Detrital zircons between c. 2.8 and 2.6 Ga show overlap between the Marboo Formation and Tickalara Metamorphics, mostly at or below CHUR, though some more juvenile values are present. Detrital zircons at c. 2.5 Ga show a large range of  $^{176}\text{Hf}/^{177}\text{Hf}$  values from 0.2810 to 0.2815 and  $T_{\text{DM}}^2$  of 3.7 – 2.5 Ga, indicating their derivation from a juvenile



2.5 Ga component and an evolved 3.7 Ga component. The 3.7 Ga component is similar to  $T_{DM}^2$  for the 3.45 – 3.15 Ga zircons, suggesting reworking of the same 3.7 Ga crust at 3.45 – 3.15 and 2.5 Ga. Detrital zircons dated at 2.4 – 2.0 Ga in both the Marboo Formation and Tickalara Metamorphics yielded  $T_{DM}^2$  between c. 3.7 and c. 2.5 Ga, indicating mainly reworking of 3.7 – 2.5 Ga sources with limited juvenile magmatic input between 2.4 and 2.0 Ga.

Detrital zircons dated at 1915–1900 Ma from a sample of the Tickalara Metamorphics (GSWA 218321, Lu et al., 2017))

show a relatively restricted range of ratios at supra-CHUR values. The dominant 1875–1860 Ma zircons present in many samples have a large variation of  $^{176}\text{Hf}/^{177}\text{Hf}$  values from 0.2813 to 0.2818, suggesting their derivation from reworking of >2.5 Ga crust with some juvenile input at c. 1.85 Ga. Analyses of c. 1820 Ma metamorphic zircon rims in GSWA 281321 show a narrow range of Hf isotope values close to CHUR. The values are comparable to those of the 1915–1900 Ma detrital age component in this rock, suggesting closed-system behavior of the Lu–Hf isotope system during metamorphic zircon growth.



YL91

04.07.22

Figure 21. CL images and concordia diagrams for granitic rocks in the Central Zone: a) CL image of zircons from the Violet Valley Tonalite (GSWA 218313); b) concordia diagram for the Violet Valley Tonalite (GSWA 218313); c) CL image of zircons from the Mabel Downs Tonalite (GSWA 218355); d) concordia diagram for the Mabel Downs Tonalite (GSWA 218355); e) CL image of zircons from the Kevins Dam Monzogranite (GSWA 124442); f) concordia diagram for the Kevins Dam Monzogranite (GSWA 124442). Diagram notes as in Figure 6

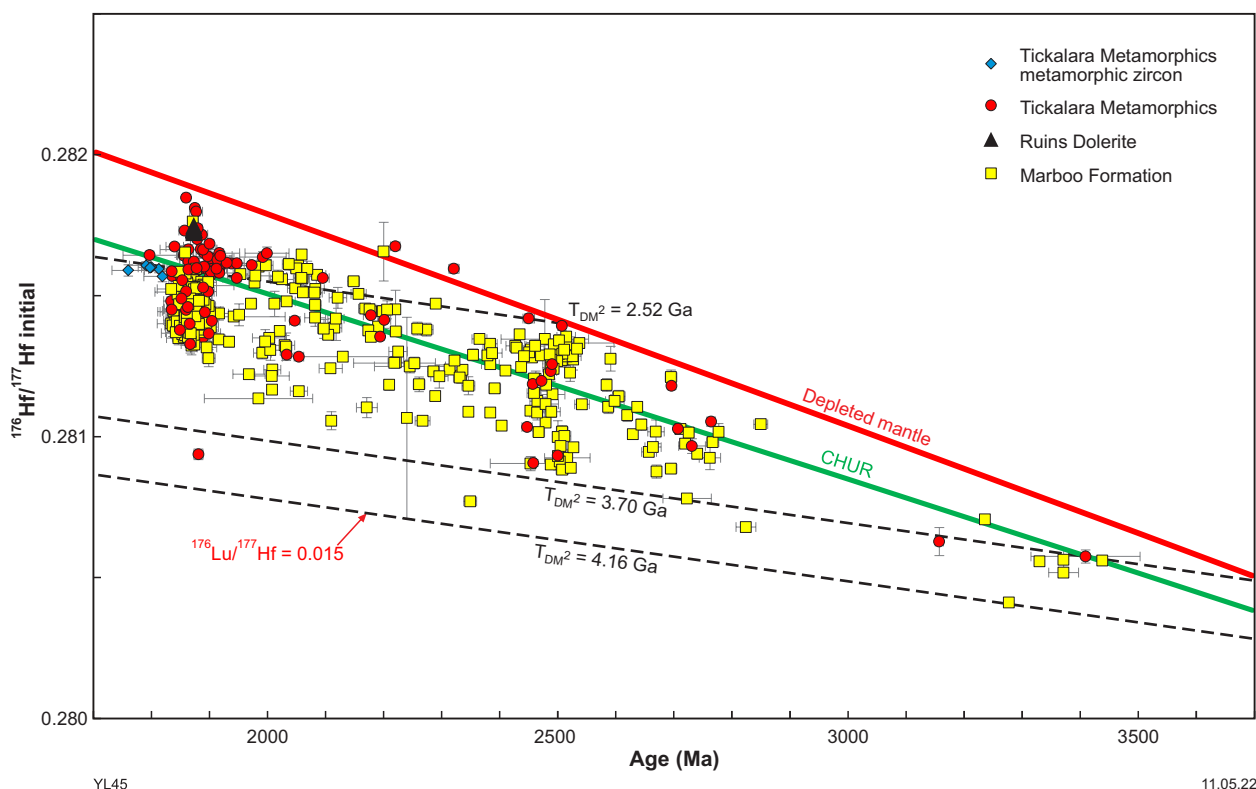


Figure 22. Initial  $^{176}\text{Hf}/^{177}\text{Hf}$  evolution plot for detrital and igneous zircons from the Western and Central Zones. Western Zone: Marboo Formation (GSWA 206102, 206106, 206154, 206173, 212344, 215562 and 218305) and Ruins Dolerite (GSWA 212335); Central Zone: Tickalara Metamorphics (GSWA 206128, 206131, 218315 and 218321). Abbreviation: CHUR, chondritic uniform reservoir. Dashed lines show the evolution of average continental crust extracted from depleted mantle at c. 4.16 Ga, 3.70 Ga and 2.52 Ga, respectively. Error bars are at 1 sigma

## Discussion

### Nature and origin of zircons in metasedimentary rocks

The interpretation of the origin of zircons in metasedimentary units of the Lamboo Province is a fundamental consideration in any discussion of sediment provenance or the relationships between terranes of the province. A key question is whether units dominated by zircons with dates close to the inferred depositional age of their sedimentary protoliths might have been derived from erosion of slightly older bedrock sources (i.e. are epiclastic) or are a result of coeval volcanism, either proximal or distal (e.g. Barham et al., 2019). For example, a regionally extensive zircon age component could conceivably have occurred as a result of ashfall across exotic terranes separated by small ocean basins (e.g. Yang et al., 2021), whereas epiclastic zircons could reflect either a linked depositional system or unrelated basins with different source regions of comparable age. In any interpretation, further constraints are required to provide more robust interpretations, including detrital zircon age spectra, zircon Lu–Hf isotope data, lithofacies distributions and the ages and patterns of magmatism and metamorphism.

Bodorkos et al. (2000b) first noted the rapidity of zircon cycling in the Tickalara Metamorphics, demonstrating metamorphism of zircon in metasedimentary rocks

c. 20 million years after crystallization of their primary igneous source. The results of the present study, coupled with previous work (Phillips et al., 2016), show that other metasedimentary rocks within the Lamboo Province also have dominant zircon age components close to their inferred depositional age, including examples in the upper Marboo Formation in the Western Zone, the Milba and Winnama Formations in the Central Zone and the Biscay and Olympio Formations in the Eastern Zone. Some samples of Marboo Formation in the northern Halls Creek Orogen (GSWA 206173, 206106 and 218310) appear to have very small gaps between the ages of their youngest zircon age components and the dates of igneous rocks intruding the units, with these maximum and minimum age constraints being indistinguishable within the limits of analytical uncertainty (Table 2). This may be indicative of a coeval volcanic component in these samples, although uncertainties associated with individual dates and the possibility of unresolved Pb loss in detrital zircon populations make it difficult to determine the timing of events with a high degree of precision. Most units, however, have a larger gap between their maximum and minimum age constraints, typically in the order of 5–20 million years.

Bodorkos et al. (2000b) interpreted a distal plutonic source for zircon in the Tickalara Metamorphics, noting the lack of zircons with needle-like, dendritic or skeletal morphology that would be indicative of rapid crystallization in a volcanic rock.

Table 2. Summary of isotopic ages obtained for metasedimentary and igneous rocks

<i>GSWA Sample ID</i>	<i>Latitude (°S)</i>	<i>Longitude (°E)</i>	<i>Lithology</i>	<i>Unit</i>	<i>Orogen</i>	<i>Zone</i>	<i>Isotopic age (Ma)</i>	<i>n</i>	<i>MSWD</i>	<i>Interpretation</i>	<i>Reference</i>	<i>Metasedimentary unit minimum age (Ma)</i>	<i>Minimum age reference</i>
206102	17.48564	125.36031	Sandstone	Marboo Formation	WMO	Western	1983 ± 9	12	1.6	MDA	Kirkland et al., 2013	1873 ± 4 (Ruins Dolerite)	This study
212327	16.88302	124.41036	Pelitic schist	Marboo Formation	WMO	Western	1954 ± 16	5	1.8	MDA	Lu et al., 2017c	1873 ± 4 (Ruins Dolerite)	This study
212335	16.94822	124.46265	Metagabbro	Ruins Dolerite	WMO	Western	1873 ± 4	10	1.7	IGN	Lu et al., 2017b		
212317	17.37022	125.09621	Pelitic migmatite	Mount Joseph Migmatite	WMO	Western	1873 ± 2	45	1.0	MDA	Fielding et al., 2020b	1864 ± 4, 1862 ± 5 (Lennard Granite)	Griffin et al. (2000a)
"	"	"	"	"	"	"	1865 ± 4	15	1.8	MET	"		
212315	17.33630	125.02440	Pelitic migmatite	Mount Joseph Migmatite	WMO	Western	1874 ± 3	35	1.2	MDA	Fielding et al., 2020c	1864 ± 4, 1862 ± 5 (Lennard Granite)	Griffin et al. (2000a)
"	"	"	"	"	"	"	1863 ± 2	19	1.1	MET	"		
212344	17.32405	124.88947	Pelitic schist	Marboo Formation	WMO	Western	1874 ± 5	34	1.4	MDA	Lu et al., 2016f	1864 ± 4, 1862 ± 5 (Lennard Granite)	Griffin et al. (2000a)
215562	18.13719	127.15405	Metasandstone	Marboo Formation	HCO	Western	1865 ± 6	28	0.8	MDA	Lu et al., 2017d	1860 ± 3 (Neville Granodiorite)	Page et al. (2001)
206154	17.73243	127.67611	Pelitic migmatite	Marboo Formation	HCO	Western	1876 ± 4	34	1.2	MDA	Kirkland et al., 2014	1857 ± 2 (Springvale intrusion)	Page and Hoatson (2000)
218305	16.74972	128.10459	Metasiltstone	Marboo Formation	HCO	Western	1864 ± 5	24	1.0	MDA	Lu et al., 2017h	1859 ± 3 (Mt Myulasy Granite)	Page et al. (2001)
218330	16.35370	128.44129	Lithic metasandstone	Marboo Formation	HCO	Western	1873 ± 5	35	1.1	MDA	Lu et al., 2018c	1859 ± 3 (Mt Myulasy Granite)	Page et al. (2001)
206173	16.74612	128.35510	Psammitic schist	Marboo Formation	HCO	Western	1857 ± 4	14	0.8	MDA	Lu et al., 2016e	1859 ± 3 (Mt Myulasy Granite)	Page et al. (2001)
206106	16.79521	128.28158	Pelitic migmatite	Marboo Formation	HCO	Western	1855 ± 4	30	1.0	MDA	Lu et al., 2016a	1859 ± 3 (Mt Myulasy Granite)	Page et al. (2001)
218310	16.83588	128.23624	Metasandstone	Marboo Formation	HCO	Western	1862 ± 3	49	1.4	MDA	Lu et al., 2018a	1859 ± 3 (Mt Myulasy Granite)	Page et al. (2001)
206155	17.43880	127.60084	Porphyritic dacite	Whitewater Volcanics	HCO	Western	1854 ± 6	16	1.1	IGN	Lu et al., 2016d		
218315	16.89999	128.23137	Psammitic gneiss	Ticklara Metamorphics	HCO	Central	1865 ± 2	63	1.0	MDA	Lu et al., 2017i	1852 ± 3 (Violet Valley Tonalite)	This study
206131	17.06988	128.19176	Migmatitic pelitic gneiss	Ticklara Metamorphics	HCO	Central	1864 ± 4	25	1.6	MDA	Lu et al., 2016c	1852 ± 2 (pegmatitic leucosome)	Page and Sun (1994)
218321	17.17865	128.24684	Pelitic gneiss	Ticklara Metamorphics	HCO	Central	1879 ± 15	11	1.0	MDA	Lu et al., 2017j	1829 ± 3 (Mabel Downs Tonalite)	This study
"	"	"	"	"	"	"	1820 ± 9	29	1.6	MET	Lu et al., 2017j		
218333	17.30156	128.00149	Psammitic gneiss	Ticklara Metamorphics	HCO	Central	1873 ± 5	30	0.9	MDA	Lu et al., 2018d	1854 ± 5 (Kevins Dam Monzogranite)	This study
206128	17.74701	127.83027	Pelitic schist	Ticklara Metamorphics	HCO	Central	1867 ± 4	36	2.0	MDA	Lu et al., 2016b	1856 ± 2 (Panton intrusion)	Page and Hoatson (2000)
218318	17.23145	128.25398	Muscovite–chlorite schist	Winnama Formation	HCO	Central	1870 ± 6	26	1.2	MDA	Lu et al., 2018b	1827 ± 3 (McHale Granite)	Page et al. (2001)
216661	18.12361	127.80831	Lithic sandstone	Milba Formation	HCO	Central	1868 ± 3	63	1.3	MDA	Lu et al., 2018e	1837–1808 Sally Downs Supersuite	No date within unit
226523	17.79890	127.81990	Biotite–muscovite granodiorite gneiss	Rose Bore Granite	HCO	Central	1863 ± 5	11	0.9	INH	Lu et al., 2020d	1856 ± 2 (Panton intrusion)	Page and Hoatson (2000)
"	"	"	"	"	"	"	1822 ± 5	13	1.4	MET	Lu et al., 2020d		
218350	17.76200	127.92140	Biotite–hornblende metatonalite	Dougalls Tonalite	HCO	Central	1847 ± 5	18	1.0	IGN	Lu et al., 2020c		
218313	16.86760	128.19710	Metamonzogranite	Violet Valley Tonalite	HCO	Western/ Central	1852 ± 3	23	0.9	IGN	Lu et al., 2020b		
124442	17.16610	127.81500	Biotite–hornblende syenogranite	Kevins Dam Monzogranite	HCO	Western/ Central	1854 ± 5	22	0.7	IGN	Lu et al., 2020e		
218355	17.15420	128.25700	Biotite–hornblende metatonalite	Mabel Downs Tonalite	HCO	Central	1829 ± 3	22	0.6	IGN	Lu et al., 2020f		

**NOTES:** Age uncertainties are at 95% confidence level  
Abbreviations: MDA, maximum depositional age; n, number of analyses in calculation of mean age; IGN, igneous crystallization age;  
MET, age of high-grade metamorphism; MSWD, mean square of weighted deviates; INH, age of inheritance; HCO, Halls Creek Orogen; WMO, Wunaamin Miliwundi Orogen  
Metasedimentary unit minimum age derived from ages of the nearest intrusive rocks or metamorphism of unit



Considering a potential 5–10 km depth of emplacement of a source pluton (cf. the Yerrington Batholith in Nevada, parts of which were emplaced at paleodepths of 3–6 km; Dilles, 1987; Carter et al., 2021), Bodorkos et al. (2000b) calculated a relatively rapid exhumation rate in the order of ~1 mm/year. This is comparable to rates of exhumation experienced in the Himalaya during Cenozoic collision, with typical calculated values there in the order of 0.25 – 4.0 mm/year (e.g. Adlakha et al., 2013; Huyghe et al., 2020). It is also possible that zircon was derived from erosion of felsic volcanic rocks at a higher crustal level, which would require significantly less exhumation in the source region. Although needle-like and skeletal zircons can occur in some felsic volcanic rocks, more equant, oscillatory-zoned zircons can also be dominant (e.g. the Whitewater Volcanics), which may reflect zircon crystallization in a sub-volcanic magma chamber prior to eruption. Abrasion during sediment transport has the potential to selectively remove or modify needle-like volcanic zircons and thus the relatively equant, oscillatory-zoned zircon in metasedimentary rocks of the Lamboo Province could plausibly have been derived as detrital grains from plutonic or volcanic sources.

None of the metasedimentary rocks dated in this study or in previous studies (e.g. Tyler et al., 1999; Bodorkos et al., 2000b; Phillips et al., 2016) appear to contain a major coeval felsic volcanic component and no 1875–1865 Ma felsic volcanic rocks have been identified in the Lamboo Province that would indicate the area was a major volcanic centre that provided a local source for the dominant age component observed in many samples. Although many of the sampled units are compositionally relatively immature, all the metasedimentary units are quartz-rich and show subsidiary components of small, rounded lithic clasts in less metamorphosed and deformed samples taken from them (e.g. the Marboo and Olympio Formations). In these units, the lithic clasts comprise differing proportions of quartz arenite, siltstone, felsic volcanic, chert and granitic rock, with detrital K-feldspar, muscovite, tourmaline, zircon, rutile, chlorite after biotite and minor plagioclase in addition to the dominant subangular to subrounded quartz component (Hancock, 1991; Tyler et al., 1999; Phillips et al., 2016). These lithic clast populations indicate source areas comprising a mix of compositionally mature sedimentary rocks and intrusive and extrusive felsic igneous rocks, with the relatively feldspar-rich composition of the matrix suggesting that felsic igneous rocks were a major component. Most of the metasedimentary rocks in the Lamboo Province are interpreted to have been deposited as turbidites on a continental shelf or slope (e.g. Tyler et al., 2012; Phillips et al., 2016) and, for the most part, lack the abrupt and complex changes in lithofacies and thickness that might be expected if they were deposited proximal to, or within, an active volcanic centre. Similarly, the detrital zircon age signatures of the packages younger than c. 1870 Ma (discussed in more detail below) are remarkably homogeneous and lack the variability seen in successions interpreted to include a component of distal ashfall (e.g. Barham et al., 2016). The consistency of both the lithofacies and the detrital zircon age spectra can be explained by homogenization of detritus during sedimentary transport, with deposition taking place at a distance from an eroded source region. For these reasons,

the zircons in the metasedimentary rocks of the Lamboo Province are interpreted to be dominantly epiclastic rather than volcanic in nature.

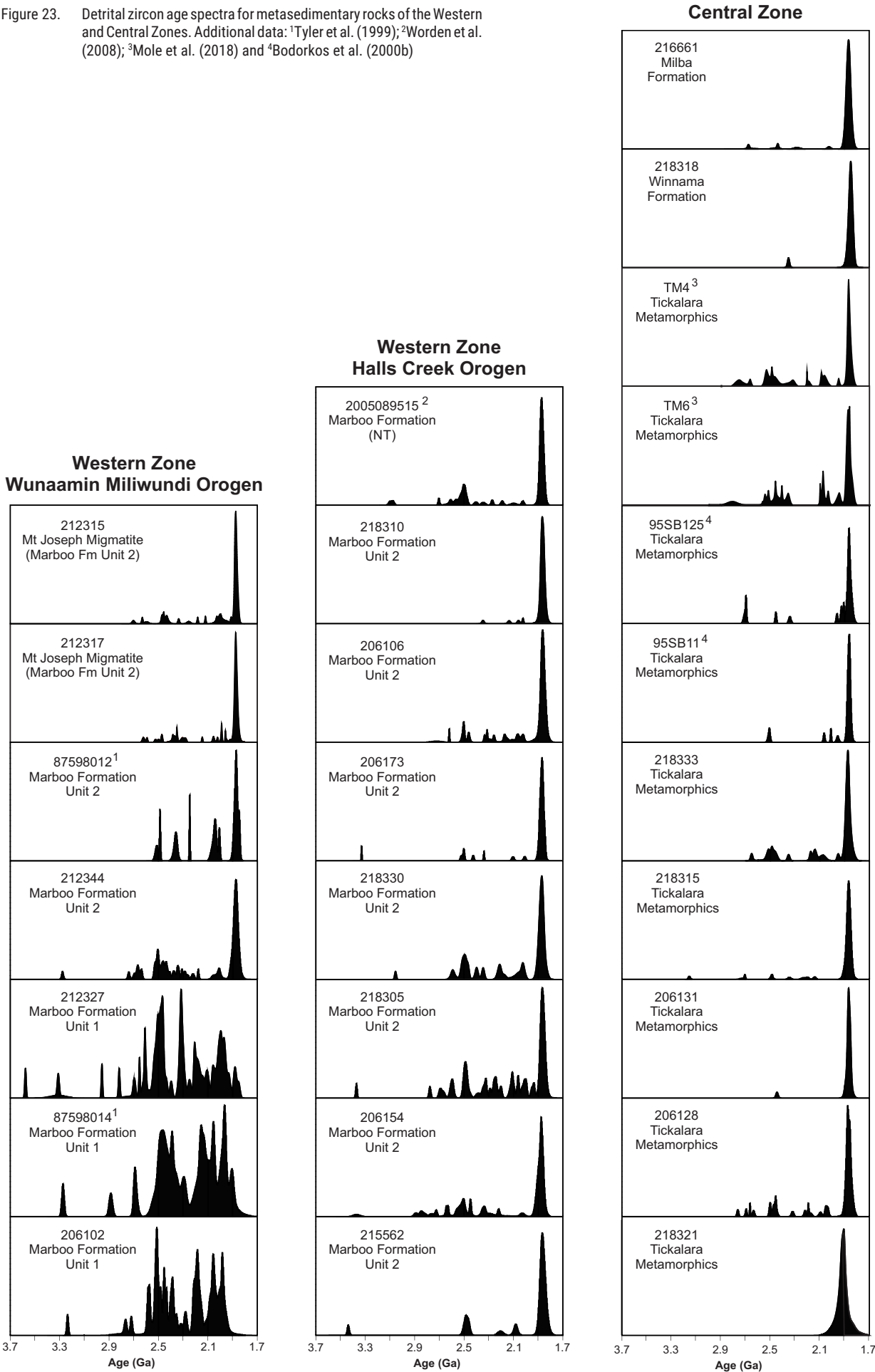
As noted above, a subsidiary coeval volcanic component is a possibility for some units in the Lamboo Province, given the local presence of felsic volcanic units in parts of these successions (e.g. the Olympio Formation in the Eastern Zone, which contains felsic volcanic units dated at c. 1856 and 1846 Ma; Phillips et al., 2016). However, lithological and petrographic data suggest that volcanic components are typically not dominant, and most volcanic units are younger than the dominant zircon age components in the host siliciclastic succession. For example, two samples of siliciclastic rocks from the Butchers Gully Member of the Olympio Formation yielded dominant zircon age components at c. 1868 Ma, defining a maximum depositional age (Phillips et al., 2016). A felsic volcanic rock from the same sample site as one of the metasedimentary rocks yielded a much younger magmatic age of c. 1848 Ma, and a felsic volcanic unit lower in the succession is dated at c. 1856 Ma (Phillips et al., 2016). As discussed in more detail below, the uppermost parts of the Marboo and Olympio Formations appear to be an exception to this pattern, containing an additional younger detrital zircon age component that is of similar age to local felsic volcanism. The bulk of the metasedimentary successions, however, appear to be dominated by detrital zircons derived from an older source rock.

## Western Zone succession

### Marboo Formation (Wunaamin Miliwundi Orogen)

Dating of the Marboo Formation in the Wunaamin Miliwundi Orogen reveals significant differences in provenance between the lower and upper parts of the formation. A previously dated sample from the upper part of Unit 1 in the core of the Richenda Anticline (GA 87598014) yielded detrital zircon ages  $\leq 5\%$  discordant between c. 3273 and 1903 Ma, with no dominant age components (Tyler et al., 1999). Additional dating of zircons from the same sample (GSWA 206102, Kirkland et al., 2013) yielded similar results, with detrital zircon ages between c. 3236 and 1942 Ma, and a conservative maximum depositional age of  $1983 \pm 9$  Ma, defined by 12 analyses (Fig. 23). A similar detrital zircon age spectrum was obtained from a second sample interpreted to be part of Unit 1 (GSWA 212327, Lu et al., 2017c), which yielded ages between c. 3577 and  $1851 \pm 11$  Ma ( $1\sigma$ ). Although the youngest individual analysis could be taken as a maximum depositional age, it is an isolated result and may not be reliable, and is also younger than the  $1873 \pm 4$  Ma Ruins Dolerite which intrudes this unit (GSWA 212335, Lu et al., 2017b). A more conservative maximum depositional age of  $1954 \pm 16$  Ma for this sample is provided by a concordia age for the next five youngest analyses. The limited data thus indicate deposition of Unit 1 between  $1903 \pm 26$  Ma ( $2\sigma$ ) and  $1873 \pm 4$  Ma, and potentially closer to the younger end of this range given the conformable relationship between Units 1 and 2.

Figure 23. Detrital zircon age spectra for metasedimentary rocks of the Western and Central Zones. Additional data: <sup>1</sup>Tyler et al. (1999); <sup>2</sup>Worden et al. (2008); <sup>3</sup>Mole et al. (2018) and <sup>4</sup>Bodorkos et al. (2000b)



The two samples of Unit 2 have detrital age spectra distinct from those of Unit 1 (Fig. 23). A sample of pelitic schist (GSWA 212344, Lu et al., 2016f) is dominated by an  $1874 \pm 5$  Ma age component – which forms a maximum depositional age – and contains a smaller proportion of Neoproterozoic to early Paleoproterozoic ages than Unit 1, with an age component at c. 2505 Ma. The Mount Joseph Migmatite forms a relatively restricted domain of high-grade metamorphic rocks reflecting partial melting of Unit 2 under high-*T*, low- to moderate-*P* conditions (675–750 °C and 2.9 – 7.2 kbar) (Korhonen et al., 2022). Analyses of zircon cores from GSWA 212317, interpreted as detrital grains, yield a maximum depositional age of  $1873 \pm 2$  Ma (Fielding et al., 2020b). High-U, low-Th/U zircon rims yield a date of  $1865 \pm 4$  Ma, interpreted as the age of partial melting and metamorphism. This result is similar to that obtained from another sample of the Mount Joseph Migmatite (GSWA 212315, Fielding et al., 2020c), which yielded a maximum depositional age of  $1874 \pm 3$  Ma and an interpreted metamorphic age of  $1863 \pm 2$  Ma, as well as that from another sample dated by Tyler et al. (1999), which yielded a maximum depositional age of  $1872 \pm 9$  Ma and a metamorphic age of  $1861 \pm 5$  Ma. These data constrain the deposition of this part of Unit 2 to approximately 1873–1865 Ma, with the limits of analytical uncertainty possibly allowing for a slightly wider age range.

The areally extensive Lennard Granite intrudes the Mount Joseph Migmatite (Fig. 7f) and has been dated at 1867–1862 Ma, with the nearest dated samples of granite – 18–25 km distant from the Mount Joseph Migmatite – yielding dates of  $1864 \pm 4$  and  $1862 \pm 5$  Ma (Griffin et al., 2000a; Lu et al., 2017f,g). This intrusion forms part of the voluminous granitic magmatism of the 1867–1849 Ma Paperbark Supersuite, which appears to have been a significant contributor to the locally high heat flows associated with metamorphism and partial melting (Tyler et al., 1999). The intrusions of granitic rocks of the Paperbark Supersuite provide minimum age constraints on the deposition of their host rocks, and may date the termination of Marboo Formation deposition in the Wunaamin Miliwundi Orogen. However, it is possible that sedimentation continued during early granite emplacement, so a more definitive minimum age for Unit 2 in the Wunaamin Miliwundi Orogen is provided by an  $1854 \pm 5$  Ma date for the Whitewater Volcanics, which unconformably overlie the Marboo Formation (Griffin et al., 2000a).

## Hooper Orogeny

The development of a low- to medium-grade layer-parallel foliation (*S*<sub>1</sub>) and upright folding under medium- to high-grade metamorphic conditions (*F*<sub>2</sub>) have both been assigned to the Hooper Orogeny (Griffin et al., 1993). This has been suggested to possibly reflect transpressional overprinting (*D*<sub>2</sub>/*M*<sub>2</sub>) of an extensional regime associated with deposition of the Marboo Formation (*D*<sub>1</sub>/*M*<sub>1</sub>) (Tyler and Griffin, 1990; Griffin et al., 1993) or a collision between the Kimberley Craton and another exotic terrane to the east (Griffin et al., 2000a; Tyler et al., 2012).

The available geochronological constraints indicate that deposition of the upper Marboo Formation and tectonism of the Hooper Orogeny took place within a relatively short period of time, with individual events difficult to resolve within the limits of analytical uncertainty. Maximum

depositional ages for Unit 2 are  $1872 \pm 9$  Ma (Tyler et al., 1999),  $1873 \pm 2$  Ma (GSWA 212317),  $1874 \pm 3$  Ma (GSWA 212315) and  $1874 \pm 5$  Ma (GSWA 212344), whereas ages for *M*<sub>2</sub> leucosome crystallization are  $1865 \pm 4$  Ma (GSWA 212317),  $1863 \pm 2$  Ma (GSWA 212315) and  $1861 \pm 5$  Ma (Tyler et al., 1999). This constrains development of the layer-parallel *S*<sub>1</sub> foliation to shortly after deposition of the host rock, and potentially coeval with continued deposition of the stratigraphically uppermost parts of the Marboo Formation, consistent with formation in the extensional setting proposed by Tyler and Griffin (1990). The oldest leucosomes in the Mount Joseph Migmatite are sub-parallel to *S*<sub>1</sub>, possibly reflecting a higher temperature progression of *D*<sub>1</sub>/*M*<sub>1</sub> extension, but most leucosome pooled in domains parallel to upright *F*<sub>2</sub> axial planes or crosscuts *F*<sub>2</sub> folds (Griffin et al., 1993). This is potentially a result of crustal shortening overprinting the high-*T* extensional domain, causing structural thickening and burial to depths of 10–21 km (2.9 – 7.2 kbar) (Tyler et al., 1999; Korhonen et al., 2022), though the folding does not necessarily require a compressional driver. If *D*<sub>1</sub>/*M*<sub>1</sub> was related to extension and *D*<sub>2</sub>/*M*<sub>2</sub> was a compressional event, the Hooper Orogeny may be better defined to be associated with *D*<sub>2</sub> only, though more work is required to better understand the structural evolution during this period.

The crystallization ages of granitic rocks of the Paperbark Supersuite overlap with the age of *D*<sub>2</sub>/*M*<sub>2</sub>, and possibly also *D*<sub>1</sub>/*M*<sub>1</sub>. One possibility is that emplacement of the Paperbark Supersuite during both extension and compression is a consequence of the high geothermal gradient established during *D*<sub>1</sub>/*M*<sub>1</sub> extension, with partial melting of still-hot mid-crustal rocks during *D*<sub>2</sub> shortening resulting in continued felsic and mafic magmatism between c. 1867 and 1854 Ma. Younger components of the Paperbark Supersuite crosscut *F*<sub>2</sub> folds and *M*<sub>2</sub> leucosomes (Tyler and Griffin, 1990; Fig. 7f) as well as their extrusive equivalents, the Whitewater Volcanics, dated at c. 1854 Ma in this area (Griffin et al., 2000a). U–Pb dates of c. 1855 Ma for monazite associated with amphibolite-grade metamorphism in the Mount Joseph Migmatite (GSWA 212305, Fielding et al., 2019d; GSWA 95521, preliminary data) indicate that this younger magmatism was also associated with locally high geothermal gradients. The Whitewater Volcanics unconformably overlie rocks of the Marboo Formation deformed during *D*<sub>2</sub>, and are themselves folded by structures assigned to this event (Hancock and Rutland, 1984; Tyler and Griffin, 1990). This would indicate a prolonged or multi-phase compressional event but, if the folding of the Whitewater Volcanics is related to a younger event (e.g. the Halls Creek Orogeny, the effects of which have recently been recognized in the Wunaamin Miliwundi Orogen; Fielding et al., 2019d,e; Korhonen et al., 2022), compression might have been relatively short-lived at c. 1865 Ma.

## Marboo Formation (Halls Creek Orogen)

The Marboo Formation in the Halls Creek Orogen, comprising the easternmost part of the Western Zone, has not been subdivided in regional mapping (Griffin and Tyler, 1994; Tyler et al., 1997a; Sheppard et al., 1997b; Thorne et al., 1998; Phillips et al., 2018). Griffin et al. (1998) and Sheppard et al. (1999a) suggested that the Marboo Formation in the southern and northern parts of the orogen is consistent with the upper part of the unit, and the generally compositionally immature nature of the unit along the orogen suggests that



most exposures, if not all, are Unit 2. The Ruins Dolerite is not known in the Halls Creek Orogen, which might also indicate that only the upper Marboo Formation is exposed, but it is also possible that this mafic magmatism was restricted to the Wunaamin Miliwundi Orogen. As in the Wunaamin Miliwundi Orogen, the Marboo Formation in the Halls Creek Orogen is extensively intruded by voluminous granitic rocks of the Paperbark Supersuite, in some areas forming relatively small inliers enclosed by granite. A domain of dominantly mafic intrusive rocks in the central-west part of the orogen is broadly comagmatic with granitic rocks of the Paperbark Supersuite (Sheppard et al., 1997c), with one granitic intrusion in this area dated at  $1854 \pm 3$  Ma (Page et al., 2001). The Marboo Formation locally experienced high- $T$ , low- $P$  metamorphism (e.g. the Amhurst Metamorphics in the southwest), which is thought to be broadly coeval with Paperbark Supersuite magmatism (Griffin et al., 1998), but there are currently no direct dating constraints.

Seven samples of the Marboo Formation were dated over ~250 km of strike length of the western Halls Creek Orogen (Fig. 10) and range in metamorphic grade from lower greenschist to amphibolite facies. Relatively high-grade metasedimentary rocks in the northern part of the orogen (GSWA 206106, 218310) are similar in character to nearby metasedimentary rocks of the Tickalara Metamorphics and their stratigraphic affiliation is less certain, but they are considered to be part of the Marboo Formation, consistent with the mapping of Sheppard et al. (1997b).

All the samples assigned to the Marboo Formation in the Halls Creek Orogen have similar detrital zircon age spectra, containing a dominant age component between c. 1875 and 1860 Ma and a smaller proportion of older Paleoproterozoic to Neoproterozoic ages, including a significant c. 2.5 Ga age component (Fig. 23). A sample assigned to the Marboo Formation from the interpreted northeasterly extension of the Western Zone in the Northern Territory also yielded a similar age spectrum and a maximum depositional age of c. 1871 Ma (Worden et al., 2008). Although the overall spectra are similar, there are subtle differences between samples. Maximum depositional ages derived from the youngest coherent group of at least three analyses in a sample incorporate most (but not all) of the dates that comprise the dominant age component, with some of the older analyses dispersed beyond that expected from a single age component. Maximum depositional ages calculated in this manner yield dates of  $1876 \pm 4$ ,  $1874 \pm 5$ ,  $1865 \pm 6$ ,  $1864 \pm 5$ ,  $1862 \pm 3$ ,  $1857 \pm 4$  and  $1855 \pm 4$  Ma (Table 2). The range of ages is less pronounced when considering only the dominant age components determined for each sample, which range between c. 1875 and 1864 Ma. The additional younger age components of c. 1857 and 1855 Ma, in samples GSWA 206173 and 206106, could reflect a local coeval volcanic or volcanoclastic component derived from the 1857–1854 Ma Whitewater Volcanics, superimposed on a 'background' c. 1865 Ma detrital zircon age component. A minimum age constraint provided by the  $1859 \pm 3$  Ma Mount Nyulasy Granite (Page et al., 2001), which intrudes the Marboo Formation in the northern Halls Creek Orogen, indicates that deposition of the upper parts of the Marboo Formation was essentially coeval with eruption of the Whitewater Volcanics. The lack of exposed contacts between the Marboo Formation and Whitewater Volcanics in this part of the province allows for the possibility that the contact between the two units in this area was more conformable than in the Wunaamin Miliwundi Orogen.

The available age constraints thus suggest that the Marboo Formation was deposited over a significant period of time, with the oldest components deposited close to c. 1875 Ma and the youngest close to c. 1855 Ma. The samples with the oldest maximum depositional ages of c. 1876 and 1873 Ma (GSWA 206154 and 218330) contain a higher proportion of 2850–1900 Ma ages than samples with maximum deposition ages of c. 1865 Ma and younger. Although the significance of this is difficult to assess due to the relatively low numbers of analyses and the potential for sampling bias, the slightly higher proportion of these ages could reflect deposition during the transition between the Unit 1 and upper Unit 2 provenance signatures.

The 1865–1855 Ma maximum depositional ages obtained for several samples of the Marboo Formation in the Halls Creek Orogen opens up the possibility that sedimentation in this area continued for longer than that in the Wunaamin Miliwundi Orogen. If the c. 1865 and 1861 Ma ages for leucosome in the Mount Joseph Migmatite (Unit 2) provide an approximate younger age limit for the Marboo Formation in the Wunaamin Miliwundi Orogen, the 1865–1855 Ma maximum depositional ages from the Halls Creek Orogen suggest the eastern part of the Western Zone did not experience the same degree of uplift and exhumation as the Wunaamin Miliwundi Orogen during the D<sub>2</sub> Hooper Orogeny. This may indicate that extension continued for longer in the Halls Creek Orogen, and may also account for the voluminous bimodal intrusive components of the Paperbark Supersuite exposed in this area, including 1857–1855 Ma mafic–ultramafic intrusive complexes (Page and Hoatson, 2000). The presence of the Whitewater Volcanics unconformably overlying folded Ruins Dolerite and Marboo Formation in the Wunaamin Miliwundi Orogen (Tyler et al., 1999) suggests significant exhumation and erosion took place during the Hooper Orogeny, prior to regional subsidence being re-established by 1857–1854 Ma, when the Whitewater Volcanics were deposited across the Western Zone (Griffin et al., 2000a). It is also possible that sedimentation switched from the Wunaamin Miliwundi Orogen to the Halls Creek Orogen at the time of the Hooper Orogeny, although maximum depositional ages of c. 1876 and 1874 Ma for two samples of the Marboo Formation in the Halls Creek Orogen mean that this is not required and pre-Hooper Orogeny deposition of the Marboo Formation is considered likely to have extended across the whole of the Western Zone.

## Central Zone succession

### Tickalara Metamorphics

Five samples of metasedimentary rocks from the Tickalara Metamorphics were collected over a distance of ~100 km in the central and northern parts of the orogen (Fig. 10). The samples are all of relatively high metamorphic grade, ranging from schist to gneiss and migmatite. Despite the high-grade metamorphism and the development of partial melt in some samples, only one sample had well-developed zircon overgrowths that could be used to date metamorphism, and most analyses are interpreted to be of detrital grains.

Four of the samples have remarkably similar detrital zircon age spectra, with dominant youngest age components of 1875–1865 Ma and a subsidiary age component at c. 2.5 Ga (Fig. 23). This signature is similar to spectra previously

obtained for other samples of the Tickalara Metamorphics (Page, 1996a,b; Bodorkos et al., 1999, 2000b; Oliver et al., 1999; Page and Hoatson, 2000; Mole et al., 2018) and is similar to those from Unit 2 of the Marboo Formation. Maximum depositional ages of  $1879 \pm 15$ ,  $1873 \pm 5$ ,  $1867 \pm 4$ ,  $1865 \pm 2$  and  $1864 \pm 4$  Ma for samples discussed in this Report are also comparable to those previously obtained from the Marboo Formation.

The detrital zircon age spectrum of sample GSWA 218321 (Lu et al., 2017j) is distinct from those obtained from other samples of the Tickalara Metamorphics, being dominated by an age component at c. 1903 Ma (Fig. 23). It is also significantly different from those obtained from other metasedimentary rocks of the Lamboo Province, though similar age components are present in the Brim Rockhole Formation and Butchers Gully Member of the Olympio Formation in the Eastern Zone (Phillips et al., 2016) and Unit 1 of the Marboo Formation. The only known rocks in the region which might have provided a source of sediment for the c. 1903 Ma age component are felsic igneous of the 1912–1904 Ma Sophie Downs Suite, which underlies the Halls Creek Group in the Eastern Zone (Phillips et al., 2016). Lu–Hf isotope data for the detrital zircons have a tight range of values that are comparable to those obtained from the Sophie Downs Suite by Phillips et al. (2016). The presence in this sample of a smaller component of zircons younger than the c. 1903 Ma age component suggests that the dominant age component does not reflect syn-sedimentary volcanism, but was epiclastic in nature, with the  $1879 \pm 15$  Ma weighted mean date for the youngest 11 analyses representing an imprecise maximum depositional age. It is thus possible that the large c. 1903 Ma age component in sample GSWA 218321 indicates deposition in a local depocentre predominantly deriving sediment from the Eastern Zone, or that correlatives of the Sophie Downs Suite were present elsewhere in the province. Either scenario implies proximity between the Central and Eastern Zones at the time of deposition.

It is possible that sample GSWA 218321 represents an older component of the Tickalara Metamorphics, perhaps comparable to the stratigraphic position of the c. 1881 Ma Brim Rockhole Formation of the Halls Creek Group, or Unit 1 of the Marboo Formation. This would be consistent with the presence in the dated succession of marble, calc-silicate rock and interlayered mafic rocks, which are also components of the Brim Rockhole Formation (Phillips et al., 2016). A recessive graphitic unit in the Tickalara Metamorphics, identified ~15 km along strike to the south-southwest, has been shown by airborne electromagnetic data to extend further to the south-southwest over a strike length of at least 20 km (Sayona Mining, 2015). It is possible that this graphitic unit also extends north-northeast to near the location of sample GSWA 218321, given the continuity of magnetic trends between the two areas. The presence of graphitic schist would also be consistent with a correlation with the Brim Rockhole Formation, which contains a graphitic metasedimentary unit near its base (Phillips et al., 2016). If graphitic units represent a distinctive component of the postulated older package within the Tickalara Metamorphics, then it raises the possibility that other graphitic units within the Central Zone might also be part of this package. This could include an undated domain of Tickalara Metamorphics in the central Halls Creek Orogen that hosts a series of

graphite prospects near the McIntosh intrusion (Hexagon Resources, 2019).

Minimum depositional ages for parts of the Tickalara Metamorphics are provided by the Panton mafic–ultramafic intrusion, dated at  $1856 \pm 2$  Ma, and the Sally Malay mafic–ultramafic complex, dated at 1848–1838 Ma (Page and Hoatson, 2000; Mole et al., 2018). Minimum depositional ages are also provided by 1847–1837 Ma dates for metamorphic zircon and monazite growth in the Tickalara Metamorphics during the Savannah Event (Oliver et al., 1999; Bodorkos et al., 2000b; Mole et al., 2018). Bimodal volcanic rocks of the Koongie Park Formation were erupted in the Central Zone at 1845–1840 Ma (Page et al., 1994), coeval with the extensional Savannah Event. The relationship between the Tickalara Metamorphics and Koongie Park Formation is not well understood because contacts between the two are typically faulted or intruded by igneous rocks. However, if there was no major deformation between c. 1865 and 1845 Ma, it is possible that the Koongie Park Formation conformably overlies the Tickalara Metamorphics, with sedimentation continuing between c. 1865 and 1840 Ma. If sedimentation was not disrupted during this period, deposition of the Tickalara Metamorphics would have extended younger than the c. 1865 Ma depositional age typically inferred for the unit, an interpretation based in large part on a c. 1863 Ma date for the Rose Bore Granite, here interpreted to reflect inheritance or the maximum depositional age of a metasedimentary unit (see below). If deposition did extend younger than c. 1865 Ma, it is possible that some mafic volcanic rocks in the Tickalara Metamorphics are extrusive equivalents of the oldest mafic rocks intruding the Tickalara Metamorphics, such as the Panton intrusion and Norton metagabbro. This would indicate that dates for these intrusive rocks provide minimum age constraints only for their immediate host rocks and may not constrain the age of the unit as a whole. However, the lack of maximum depositional ages younger than c. 1865 Ma for the Tickalara Metamorphics means that the age of the youngest part of the succession remains an open question and a depositional hiatus between the Tickalara Metamorphics and Koongie Park Formation remains a possibility. If sample GSWA 218321 is interpreted to represent an older part of the succession, the depositional age range for the Tickalara Metamorphics is thus constrained to between c. 1879 and 1856 Ma, with many of the dated units deposited after c. 1865 Ma and a possibility that sedimentation continued to c. 1840 Ma.

## Milba Formation

The greenschist to lower amphibolite facies Milba Formation forms a narrow ( $\leq 3$  km wide), fault-bound belt in the southeastern Central Zone and consists of turbiditic metasedimentary rocks and mafic volcanic rocks, with minor chert, iron-formation and calcareous units. The detrital zircon age spectrum obtained from this unit (GSWA 216661, Lu et al., 2018e) is comparable to that of the Tickalara Metamorphics along strike to the north, with a dominant  $1868 \pm 3$  Ma age component that defines a maximum depositional age, and a few older dates to c. 2677 Ma (Fig. 23). The absence of a significant 1845–1840 Ma age component and the dominantly siliciclastic composition of the Milba Formation suggests that it is more likely to be a lower metamorphic-grade correlative of the Tickalara

Metamorphics than a correlative of the Koongie Park Formation, which contains abundant 1845–1840 Ma felsic volcanic and volcanoclastic rocks. This interpretation is supported by a progressive drop in the metamorphic grade of the Tickalara Metamorphics southwards towards the Milba Formation, as well as an apparent continuity of the lithological package across a minor fault that is taken as the boundary between the two units (Tyler et al., 1997a).

## Winnama Formation

The detrital zircon age spectrum for biotite–muscovite schist from the Winnama Formation contains a dominant age component at c. 1869 Ma with a small number of dates between c. 2471 and 2176 Ma, and has a maximum depositional age of  $1870 \pm 6$  Ma (GSWA 218318, Lu et al., 2018b). The similarity between the detrital zircon age spectra of the Winnama Formation and Tickalara Metamorphics, as well their lithological similarity, suggests the two units are broadly correlative. A minimum age for the unit is provided by an  $1827 \pm 3$  Ma date for the McHale Granite (Page et al., 2001).

The small inlier east of the Halls Creek Fault containing the Winnama Formation is considered to be part of the Central Zone (Tyler et al., 1995). The boundary between the Central and Western Zones in this area is the east-northeasterly trending Osmond Fault, which is truncated by younger movement on the north-northeasterly trending Halls Creek Fault (Fig. 10). The Angelo Fault forming the southern boundary of the Milba Formation is thought to be an extension of the Osmond Fault, offset by ~90 km of strike-slip movement (Tyler et al., 1995). Reconstruction of this offset places the Milba and Winnama Formations adjacent to each other, consistent with a broad correlation of these units, and differences in their metamorphic grade may reflect the substantial vertical component of movement on the Halls Creek Fault (Hancock and Rutland, 1984).

## Rose Bore Granite

An  $1863 \pm 3$  Ma date for the Rose Bore Granite (GSWA 113439; Page and Hoatson, 2000) has previously been interpreted as a magmatic crystallization age and a minimum age for deposition of the Tickalara Metamorphics. This date can be recalculated as  $1865 \pm 3$  Ma ( $n = 19$ , MSWD = 1.4), by excluding one analysis with discordance >5%, one analysis that overlapped a zircon crack and one distinctly younger analysis that may reflect Pb loss. An indistinguishable  $1863 \pm 4$  Ma age component was obtained from GSWA 226523 (Lu et al., 2020d). However, the dominance of c. 1865 Ma detrital zircons in the Tickalara Metamorphics, coupled with the low abundance and irregular shapes of zircons recovered from the Rose Bore Granite, raises questions about the geological significance of this age component.

It is notable that relatively few zircons have been recovered from three multi-kilogram samples of the Rose Bore Granite, despite relatively high whole-rock Zr contents: 53 zircons from GSWA 113439 with 229 ppm Zr (Page and Hoatson, 2000); 33 zircons from GSWA 226523 with 225 ppm Zr; and no zircons from GSWA 206104 with 240 ppm Zr. Although it is possible that Zr is present in minerals other than zircon, no other Zr-rich minerals have been observed in thin section.

Zircons comprising the c. 1863 Ma age component in GSWA 226523 consist of rounded to subhedral grains with uranium contents of 132–889 ppm and Th/U of 0.13 – 0.82. Zircons comprising the c. 1822 Ma age component in that sample include grains that are similar in appearance and composition to those of the c. 1863 Ma age component (74–882 ppm U, Th/U = 0.26 – 0.89), although some have diffuse, darker CL rims (Fig. 19a). Two zircons from the c. 1822 Ma age component are subhedral to euhedral and more elongate, with uranium concentrations of 139 and 297 ppm and Th/U values of 0.29 and 1.10. Page and Hoatson (2000) suggested that the irregular zircon shapes are due to resorption of igneous zircon during metamorphism. Although this is a possibility, the fact that the c. 1863 Ma age component is indistinguishable from the dominant detrital zircon age component in the surrounding rocks suggests that a detrital origin is perhaps more likely.

The geological significance of the  $1822 \pm 5$  Ma age component in sample GSWA 226523 is uncertain, but the  $1856 \pm 2$  Ma age of the Panton intrusion that cuts the Rose Bore Granite suggests that the c. 1822 Ma age component may reflect isotopic resetting of detrital grains during metamorphism (see section below) or new zircon growth (e.g. the more elongate, euhedral zircons). The c. 1822 Ma age is similar to ages for emplacement of granitic rocks of the Sally Downs Supersuite, including an  $1824 \pm 4$  Ma muscovite–tourmaline pegmatite dyke in the Panton intrusion (Page and Hoatson, 2000), and high-grade metamorphism that was locally developed during the Halls Creek Orogeny (e.g.  $1820 \pm 9$  Ma, GSWA 218321, Lu et al., 2017j). The pegmatite in the Panton intrusion is mineralogically comparable to pegmatitic quartz–tourmaline veins cutting the folded foliation in the Rose Bore Granite, providing further support for the interpretation that the c. 1822 Ma age component reflects overprinting tectonism.

Although the Rose Bore Granite is widely considered to have a granitic protolith, another possibility is that the gneiss is a metasedimentary unit within the Tickalara Metamorphics. This would be consistent with the compositional layering seen at some locations (Figs 16e,f, 18a) and the presence of both biotite and muscovite, which occur in metasedimentary rocks of the Tickalara Metamorphics but are together uncommon in granitic rocks of the Lamboo Province. If this is the case, the protolith of the sampled homogeneous migmatite may have been a pelitic rock, and the paucity of recovered zircons may be a function of their fine grain size. Although a definitive interpretation is not possible, the c. 1863 Ma age component does not appear to provide a robust age constraint for an igneous rock or a minimum age constraint for the Tickalara Metamorphics.

## Halls Creek Orogeny metamorphism

A sample of the Tickalara Metamorphics from a high-strain zone adjacent to the Halls Creek Fault yielded a weighted mean  $^{207}\text{Pb}^*/^{206}\text{Pb}^*$  date of  $1820 \pm 9$  Ma for zircon rims having low to moderate U and low Th/U (GSWA 218321, Lu et al., 2017j). This date is interpreted as the age of high-grade metamorphism during the Halls Creek Orogeny, and is consistent with a c. 1820 Ma date for monazite in garnet porphyroblasts and matrix in this sample (Fielding et al., 2022). Additional support for high-grade metamorphism and deformation at c. 1820 Ma in the eastern Central Zone is provided by the  $1829 \pm 3$  Ma age obtained from metatonalite



~3 km along strike to the north-northeast (GSWA 218355, Lu et al., 2020f), which provides a maximum age constraint for the overprinting amphibolite-facies foliation.

The metamorphism dated at c. 1820 Ma in sample GSWA 218321 is significantly younger than 1845–1840 Ma dates for the Savannah Event obtained from the Tickalara Metamorphics elsewhere, and there is no evidence for this older metamorphic event in the zircon or monazite data. Samples of the Tickalara Metamorphics that record Savannah Event metamorphism in metamorphic zircon and monazite (Oliver et al., 1999; Bodorkos et al., 2000b; Mole et al., 2018) have a close spatial association with coeval mafic to ultramafic intrusions of the Sally Malay Suite, whereas zircons in those samples more distal from these intrusions have only thin zircon rims that could not be dated (e.g. GSWA 218333) or lack metamorphic zircon overgrowths. Although bulk rock composition is a control on the development of metamorphic zircon and monazite, the spatial patterns suggest that the highest temperatures and most abundant partial melting during the Savannah Event were associated with local advective heat input from mafic–ultramafic intrusions (e.g. Fig. 15f) (Thornett, 1986), with somewhat lower temperature conditions experienced elsewhere.

The relatively imprecise  $1820 \pm 9$  Ma date for metamorphism overlaps age constraints for both the  $D_3$  and  $D_4$  events that comprise the Halls Creek Orogeny (Bodorkos et al., 2000a; Page et al., 2001), but the high metamorphic grade of the dated sample suggests that the zircon rims might date  $D_3/M_3$ , which took place under higher grade metamorphic conditions than  $D_4/M_4$  (Bodorkos et al., 1999). An  $1827 \pm 7$  Ma date for an undeformed felsic vein ~40 km to the south-southwest was interpreted by Bodorkos et al. (2000a) to provide a minimum age for  $D_3$ . Although this date is older than that obtained for metamorphic zircon and monazite in GSWA 218321, the relatively large analytical uncertainties associated with the dates for metamorphism allow for the possibility of a high-grade  $D_3/M_3$  event between c. 1829 and 1820 Ma. There are still comparatively few data to constrain the metamorphic and structural evolution during the Halls Creek Orogeny and further work is needed to better resolve this history.

## Western–Central Zone boundary in the northern Halls Creek Orogen

Several samples dated in this study straddle the boundary between the Western and Central Zones in the northern part of the Halls Creek Orogen (Fig. 24). This area is potentially more instructive about the relationship between the Western and Central Zones than the better studied central part of the orogen, where the boundary is more strongly reworked by deformation during the Halls Creek Orogeny and younger events. In the northern part of the orogen, there is no major structure between the two zones, with metasedimentary rocks of moderate metamorphic grade forming an apparently transitional zone between greenschist-facies rocks of the Marboo Formation and amphibolite-facies, migmatitic rocks of the Tickalara Metamorphics. The Marboo Formation in this area consists of metasilstone northwest of the boundary (GSWA 218305), relatively low-grade metasedimentary schist closer to the

contact (GSWA 206173) and psammitic schist, gneiss and migmatite in the transition zone (GSWA 206106 and 218310). A discrete east–west-trending fault is mapped as separating gneiss assigned to the Marboo Formation (GSWA 218310) from gneiss assigned to the Tickalara Metamorphics (GSWA 218315) (Sheppard et al., 1997b). The differences between the metasedimentary rocks on either side of this fault are subtle, with a generally higher proportion of leucosome in the Tickalara Metamorphics to the south. This difference could reflect a slight difference in exposed crustal level across the fault or differences in bulk composition.

As noted above, the maximum depositional ages of some of the samples in this transitional zone that were assigned to the Marboo Formation are relatively young (c. 1857 and 1855 Ma) and one possibility is that these rocks are in fact part of the Tickalara Metamorphics. If these rocks were to be assigned to the Tickalara Metamorphics, the zone boundary would be constrained to be farther west, within an area of granitic rocks of the Paperbark Supersuite that contains no major faults that would delineate a major structural boundary. If these rocks are assigned to the Marboo Formation, as favoured here and in agreement with the mapping of Sheppard et al. (1999a), the boundary between the Western and Central Zones in this area would be a relatively minor fault within metasedimentary rocks of similar age, lithology, detrital zircon age signatures and metamorphic grade.

The lack of evidence for a major terrane boundary between the Western and Central Zones in this area is further highlighted by the Violet Valley Tonalite, which intrudes both the Marboo Formation and Tickalara Metamorphics, cutting across the inferred zone boundary and representing a ‘stitching’ intrusion (Sheppard et al., 2001) (Fig. 24). The Violet Valley Tonalite had previously been assigned to the Kevins Dam Suite of the 1837–1808 Ma Sally Downs Supersuite, but its  $1852 \pm 3$  Ma age (GSWA 218313, Lu et al., 2020b) indicates that it is older than the Sally Downs Supersuite and may instead be a younger component of the Paperbark Supersuite, which shares compositional similarities with the Kevins Dam Suite (Sheppard et al., 2001). The  $1854 \pm 5$  Ma age obtained for the Kevins Dam Monzogranite (GSWA 124442, Lu et al., 2020e) forms a similar stitching constraint. This  $>300$  km<sup>2</sup> intrusion cuts across the Springvale Fault that separates the Western and Eastern Zones in the central part of the orogen, displaying a chilled margin against the c. 1855 Ma Greenvale Porphyry to the west and an intrusive contact with the Tickalara Metamorphics to the east (Sheppard et al., 1997b).

The dates for the Violet Valley Tonalite and Kevins Dam Monzogranite represent the first instance of felsic Paperbark Supersuite magmatism identified within the Central Zone, and suggest that the Western and Central Zones were adjacent prior to c. 1854 Ma. A similar age constraint on the relationship between the Western and Central Zones at this time may be provided by the large Springvale and Toby mafic–ultramafic intrusions in the Western Zone, dated at  $1857 \pm 2$  and  $1855 \pm 2$  Ma, respectively (Page and Hoatson, 2000). The ages of these intrusions are indistinguishable from the  $1856 \pm 2$  Ma Panton intrusion in the Central Zone, consistent with a single magmatic event intruding across the zone boundary at c. 1856 Ma.

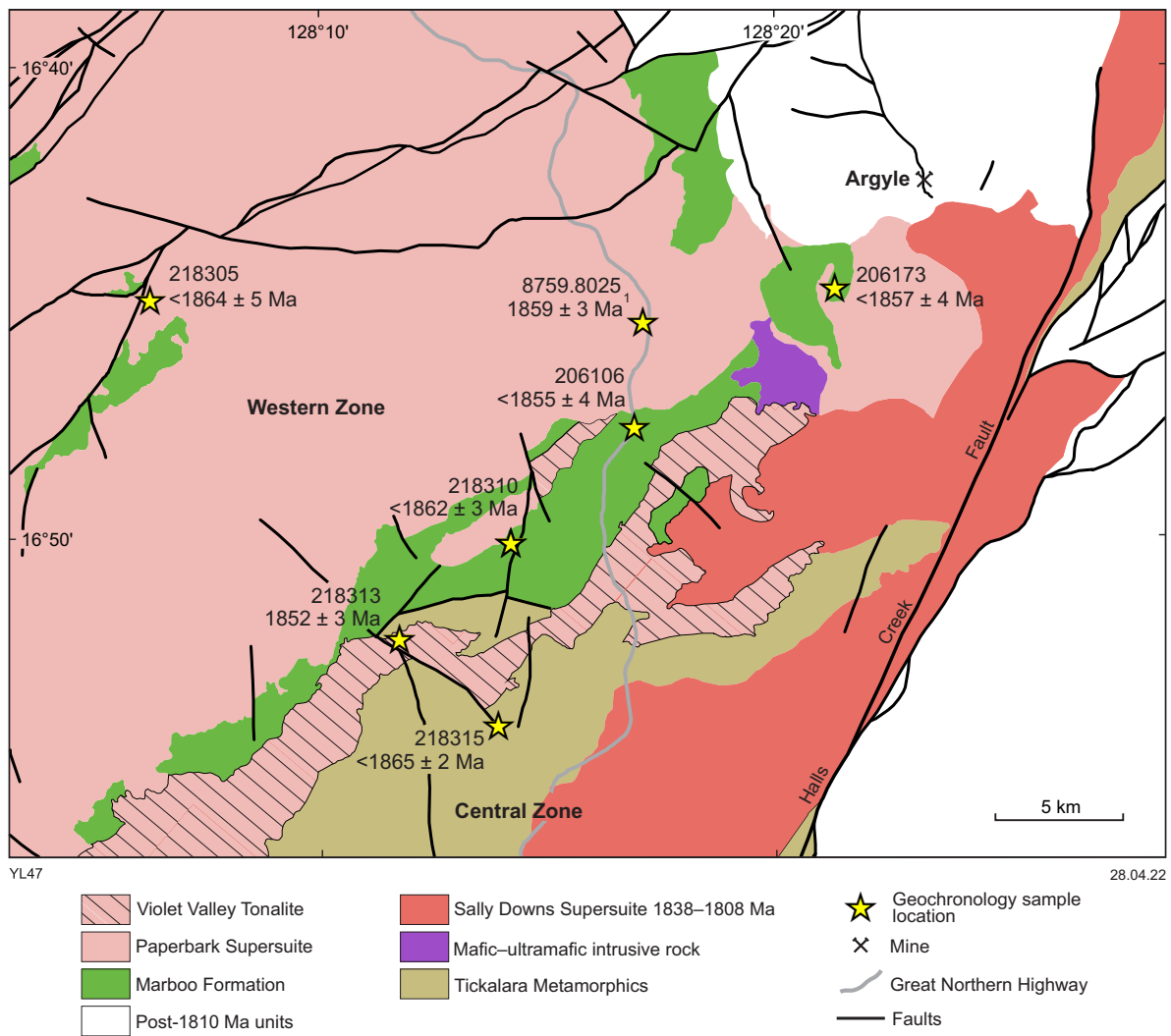


Figure 24. Locations of geochronology samples in the Western and Central Zones, northern Halls Creek Orogen. The boundary between the two zones is indistinct in this area, and possibly gradational. 'Page et al. (2000)

The youngest maximum depositional ages for the Marboo Formation are c. 1857 and 1855 Ma and, as discussed above, it is possible that parts of the upper Tickalara Metamorphics were also deposited at about this time. Given the presence of 'stitching' intrusions between the Western and Central Zones at 1856–1852 Ma, it is possible that the upper Marboo Formation and upper Tickalara Metamorphics formed part of a linked depositional system, and were not deposited on separate terranes juxtaposed by accretion after 1850–1845 Ma (e.g. Griffin et al., 2000a). The lack of a major boundary in this area is consistent with either a marginal basin setting for the Tickalara Metamorphics on the eastern margin of an exotic Kimberley Craton (e.g. Griffin et al., 2000a; Kohanpour et al., 2017) or deposition in an entirely intraplate setting involving no subduction between the Western and Central Zones.

## Comparison of provenance signatures across the Lamboo Province

The provenance of the metasedimentary units of the Lamboo Province forms a key constraint for geodynamic models, with sedimentary rocks deposited on terranes separated by ocean basins likely to show significant differences in age, facies and provenance, and units deposited adjacent to each other in an intraplate setting likely to have many similarities. The provenance of the Lamboo Province successions is here largely evaluated using zircon ages from the metasedimentary units, which are interpreted to be largely epiclastic in nature, with Lu–Hf isotope data from these zircons providing further constraints on sediment sources.

## Detrital zircon age spectra

A summary of representative detrital zircon age spectra for all three zones of the Lamboo Province is presented in Figure 25. A key feature of this plot is the close similarity between detrital zircon age spectra across the province after about 1870–1865 Ma, which show a dominant 1875–1860 Ma age component and a minor c. 2.5 Ga age component. Older metasedimentary units in each zone have significantly different age spectra to the younger units, lacking a significant 1875–1860 Ma age component and having a larger proportion of Archean to early Paleoproterozoic age components. The timing of the change in provenance is not precisely constrained but it appears to have taken place at a similar time across the province. This transition may be related to events in distal source regions, with little evidence for a significant local deformational event separating the successions displaying different provenance signatures. The transition between Unit 1 and Unit 2 of the Marboo Formation in the Western Zone is apparently conformable, though typically intruded by sills of the Ruins Dolerite (Hancock, 1991). A low-angle unconformity is locally present between the Brim Rockhole Formation and Biscay Formation in the Eastern Zone, but this is interpreted to be a result of a depositional hiatus during basin development rather than deformation (Phillips et al., 2016).

The relatively uniform detrital zircon age signatures, dominated by Paleoproterozoic ages, in the upper part of the succession are referred to here as the 'Detrital P' provenance signature for convenience (cf. Maidment et al., 2020). Detrital zircon age spectra of data for all Detrital P units in each zone are shown in Figure 26, highlighting the close similarities across the province.

A compilation of detrital zircon ages for samples of units underlying rocks with the Detrital P signature (Fig. 27) shows differences between the Western and Eastern Zones. The samples from both zones contain a significant age component at c. 2.5 Ga, but the Western Zone samples contain a large proportion of 2.5 – 1.9 Ga ages that are generally not present in the Eastern Zone, and the Eastern Zone samples contain a significant component of 3.6 – 3.3 Ga ages. This suggests that the two domains were sourcing sediment from different areas prior to c. 1870 Ma. A common c. 2.5 Ga age component allows for the possibility that they had at least one source area in common, but this age component may not be diagnostic of a particular source region. The presence of a minor c. 1910 Ma age component in Unit 1 of the Marboo Formation is similar to that in a sample of the Brim Rockhole Formation (Phillips et al., 2016) and the dominant age component in Tickalara Metamorphics sample GSWA 218321 (Lu et al., 2017j). Magmatic rocks of this age are uncommon in northern Australia, and are only known from the 1912–1904 Ma Sophie Downs Suite in the Eastern Zone. The commonality of this age component suggests that the three zones may not have been distant from each other at this time (1885–1875 Ma), although the similarities in age alone are insufficient to demonstrate whether they were adjacent.

The transition to the Detrital P signature in the Eastern Zone post-dates 1881 ± 4 Ma volcanism in the Brim Rockhole Formation and pre-dates the 1856 ± 6 Ma Maude Headley Member of the Olympio Formation (Phillips et al., 2016).

Given that the intervening Biscay Formation also displays the Detrital P signature, the switch to the Detrital P signature may be closer to c. 1881 Ma than c. 1856 Ma. This is broadly consistent with the transition in provenance in the Western Zone, where Unit 1 of the Marboo Formation is intruded by the c. 1873 Ma Ruins Dolerite, and most of Unit 2 apparently post-dates this magmatism.

## Lu–Hf isotope constraints on provenance

Zircon Lu–Hf data for detrital zircons of the Lamboo Province are plotted in Fig. 28a, incorporating previously published data for the Halls Creek Group (Phillips et al., 2016) and the Tickalara Metamorphics (Iaccheri et al., 2018). The key feature of this dataset is the comparable ranges of Hf isotope values for age components in each zone, although some age components are more strongly represented in some zones than others (e.g. 3.6 – 3.3 Ga zircons in the Eastern Zone). This similarity of isotope compositions is pronounced for samples with the Detrital P provenance (Figs 28b, 29), with the dominant 1870–1855 Ma detrital zircon age component having a limited range of Hf isotope values in all three zones, consistent with derivation from similar sources. Samples of this age component from the Western Zone have fewer analyses of the most juvenile isotope values, but the total range is comparable. The isotope values are consistent with reworking of ≥2.5 Ga crust to form felsic igneous rocks in the source region, with a contribution from contemporary mantle-derived juvenile material. Limited oxygen isotope data for this age component from samples of the Tickalara Metamorphics and Olympio Formation are also similar, with a relatively wide range of elevated  $\delta^{18}\text{O}$  values and a smaller component of mantle-like  $\delta^{18}\text{O}$  (Iaccheri et al., 2018; Mole et al., 2018).

There are limited Lu–Hf isotope data for units in the Western and Central Zones that lack the Detrital P signature, which are represented by only a single sample in each domain (Fig. 28c). As noted above, the older metasedimentary rocks in the Western and Eastern Zones have differences in the relative proportions of early Paleoproterozoic to Archean detrital age components, in particular at 3.6 – 3.3 and 2.5 – 1.9 Ga. Both the Western and Eastern Zones include significant c. 2.5 Ga age components but the sample of Unit 1 of the Marboo Formation (GSWA 206102) has significantly more radiogenic values on average for this age component than the Eastern Zone. This may indicate derivation from a different source area or heterogeneity within a source region. The sample of Tickalara Metamorphics in the Central Zone (GSWA 218321) is dominated by a c. 1903 Ma age component, which forms only a minor component of samples analysed in the Western and Central Zones. The Hf isotope values for this age component overlap with those of similar-age zircons in the Eastern Zone, though the samples from the Eastern Zone also include zircons with more evolved values. The Hf values of the c. 1903 Ma age component in the Tickalara Metamorphics sample are comparable to the range of Hf isotope values obtained by Phillips et al. (2016) from samples of the Sophie Downs Suite in the Eastern Zone, consistent with local derivation of this distinctive age component.



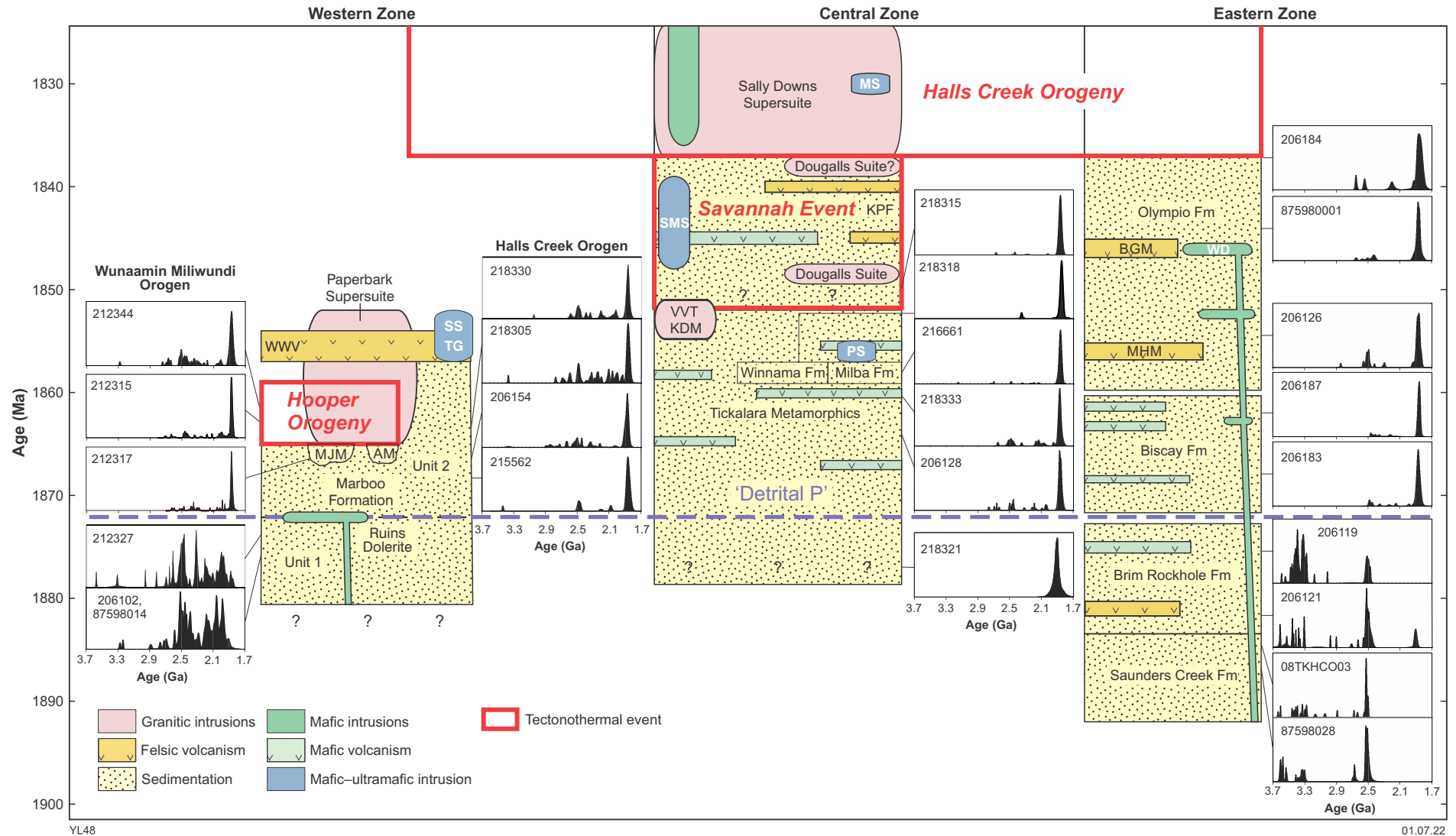


Figure 25. Representative detrital zircon probability density diagrams for the Lamboo Province – based on data from this study, Tyler et al. (1999) and Phillips et al. (2016). Blue dashed line shows position of major change in sediment provenance. Abbreviations: AM, Amhurst Metamorphics; BGM, Butchers Gully Member; KDM, Kevins Dam Monzogranite; KPF, Koongie Park Formation; MHM, Maude Headley Member; MJM, Mount Joseph Migmatite; MS, McIntosh Suite; PS, Pantou Suite; SMS, Sally Malay Suite; SS, Springvale Suite; TG, Toby Gabbro; VVT, Violet Valley Tonalite; WD, Woodward Dolerite; WWV, Whitewater Volcanics. Note that the representation of mafic volcanic units in the Lamboo Province is schematic and the relative stratigraphic positions of samples of the Tickalara Metamorphics and the Winnama and Milba Formations are not known

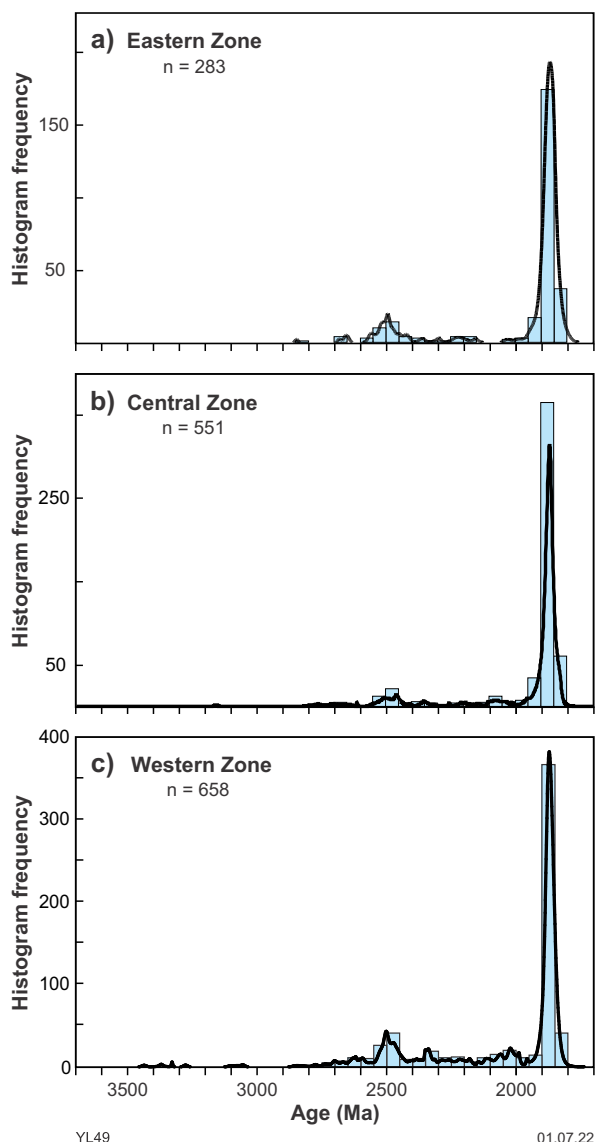


Figure 26. Compilation of  $\leq 5\%$  discordant detrital zircon dates for metasedimentary units of the Lamboo Province that are dominated by a c. 1865 Ma age component, with a subsidiary c. 2.5 Ga component, i.e. the Detrital P signature: a) Eastern Zone (Phillips et al., 2016); b) Central Zone (this study; Page, 1996a,b; Bodorkos et al., 2000b; Mole et al., 2018); and c) Western Zone (this study; Tyler et al., 1999)

Although there are currently few data for the older sedimentary units in the Western and Central Zones, differences in the relative proportions of age components and Lu–Hf isotope values suggest that the 1885–1870 Ma successions had different sediment sources. In isolation, this could be taken as evidence of exotic terranes, but the fact that these units are essentially conformable with overlying units displaying the Detrital P signature suggests that the differences might instead reflect sediment derivation from heterogeneous local sources during the early stages of basin formation on Archean to early Paleoproterozoic basement (cf. Iaccheri et al., 2018). In this scenario, the differences between the Western and Eastern Zones might reflect the presence of a fundamental basement structure between these domains

that juxtaposed different terranes prior to Paleoproterozoic basin formation. In an alternative scenario in which the Western Zone remained separate from the Eastern Zone until c. 1820 Ma (e.g. Griffin et al., 2000a), the youngest age component in metasedimentary rocks with the Detrital P signature could be derived from either unrelated, contemporaneous volcanism on disparate terranes displaying similar Lu–Hf isotope signatures or widespread ashfall across ocean basins from volcanic centres in the Western Zone. For the reasons previously outlined, these latter interpretations are considered to be much less likely, but cannot be ruled out entirely.

### Potential stratigraphic correlations

The similarities in the ages, provenance, lithofacies and stacking patterns of metasedimentary rocks in the Lamboo Province suggest that the three zones were proximal to each other during deposition and that some units may thus correlate across zone boundaries, in a manner similar to that envisaged by early workers (e.g. Hancock and Rutland, 1984). The presence of magmatic events of comparable age across the province may also indicate relative proximity, despite some differences that may reflect spatial variations in tectonism (Figs 25, 30).

The upper part of Unit 1 and the lowermost part of Unit 2 of the Marboo Formation may be age correlatives of the lower Tickalara Metamorphics in the Central Zone and the Brim Rockhole Formation in the Eastern Zone. These units are characterized by relatively quartz-rich siliciclastic rocks that include laminated units of chert, graphitic shale or carbonate, indicating periods of low sediment influx. The Brim Rockhole Formation consists of mafic and felsic volcanic rocks, including an  $1881 \pm 4$  Ma felsic volcanic near the base of the unit (Phillips et al., 2016), and the inferred correlative position in the Tickalara Metamorphics also includes a mafic component. Volcanic rocks of this age have not been recognized near the Unit 1 – Unit 2 position in the Western Zone, though it is possible that the  $1873 \pm 4$  Ma Ruins Dolerite (GSWA 212335, Lu et al., 2017b) could be related to this mafic magmatism.

The upper Marboo Formation (middle to upper Unit 2) consists of compositionally immature turbiditic sedimentary rocks with no volcanic intervals until eruption of the overlying 1857–1852 Ma Whitewater Volcanics. The age constraints on this package suggest correlation with similar metasedimentary rocks in the Tickalara Metamorphics (including the Milba and Winnama Formations) and the Biscay and lower to middle Olympio Formations. The upper Marboo Formation does not contain mafic volcanic rocks, which are present in the inferred correlatives in the Central and Eastern Zones, but in the western Halls Creek Orogen the Marboo Formation is intruded by mafic components of the Paperbark Supersuite, which are of comparable age. Alkaline felsic volcanic rocks of the c. 1856 Ma Maude Headley Member of the lower Olympio Formation in the Eastern Zone are indistinguishable in age to potassic felsic volcanic rocks of the Whitewater Volcanics in the Western Zone. No felsic volcanic rocks of this age have been identified in the Central Zone.

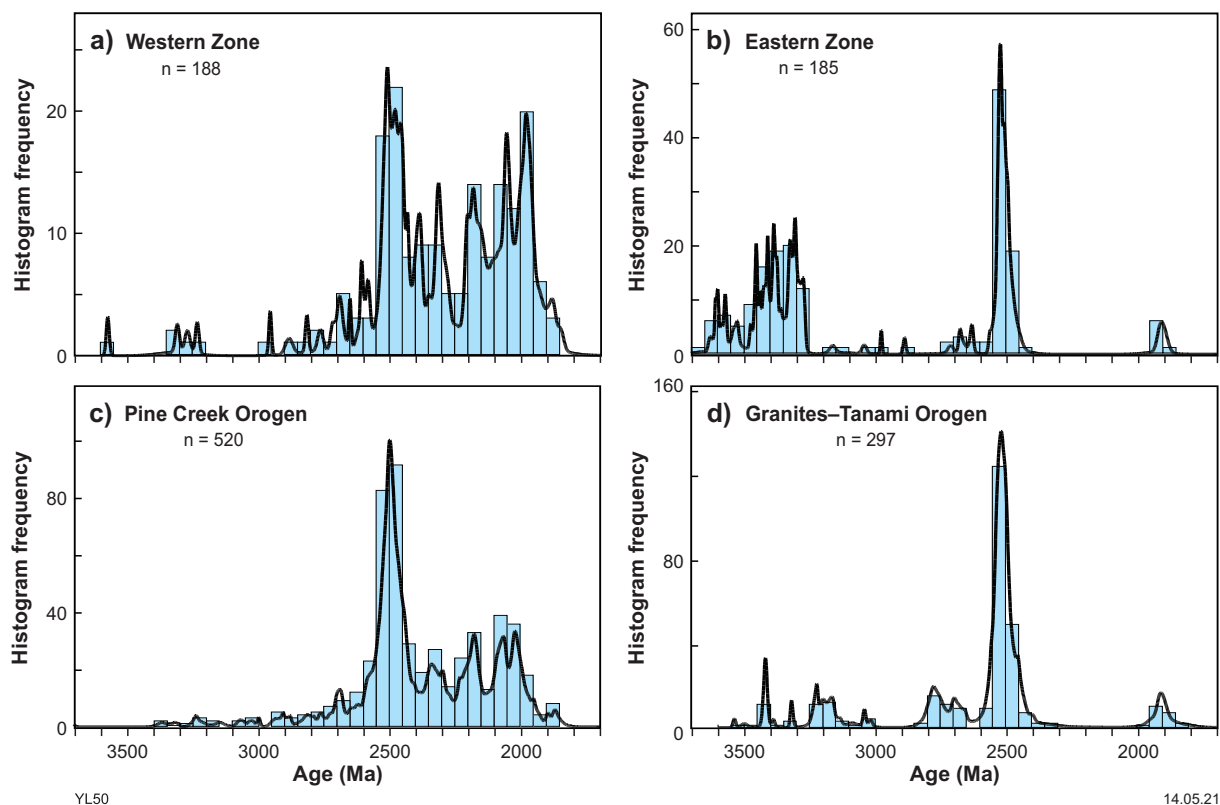


Figure 27. Compilation of  $\leq 5\%$  discordant detrital zircon dates for metasedimentary units underlying rocks with the Detrital P signature: a) Western Zone, Lamboo Province (this study; Tyler et al., 1999); b) Eastern Zone, Lamboo Province (Phillips et al., 2016); c) Pine Creek Orogen (Worden et al., 2006a, 2008; Hollis et al., 2010; Carson et al., 2011; Kositsin et al., 2013b); and d) the Granites-Tanami Orogen (Cross and Crispe, 2007; Worden et al., 2008; Maidment et al., 2020)

Deposition in the Central Zone continued for longer than it did in the Western Zone, with the youngest unit consisting of 1845–1840 Ma bimodal volcanic-dominated rocks of the Koongie Park Formation. Deposition also continued in the Eastern Zone during this period, but differs from that of the Central Zone in that it was dominated by siliciclastic sedimentary rocks of the Olympio Formation, with a minor interval of alkaline felsic volcanic rocks at c. 1845 Ma, comparable in age to the Koongie Park Formation. If the Central and Eastern Zones were proximal at this time, it is thus possible that the Koongie Park Formation is a lateral correlative of the upper parts of the Olympio Formation. Detrital zircon data from a sample of the uppermost Olympio Formation (GSWA 206184, Wingate et al., 2015) contain a youngest age component at  $1834 \pm 8$  Ma in addition to a c. 1871 Ma age component. The c. 1834 Ma age component has slightly more juvenile Lu–Hf values than 1875–1860 Ma zircons comprising the dominant age component of the Detrital P signature (Fig. 29). The source of this younger age component is unclear as there are no known volcanic rocks of this age exposed in the Eastern Zone. It could reflect exposure of a younger igneous domain in a more distal source region or a syn-depositional volcanic component derived from an unknown felsic volcanic unit in the Eastern Zone. Another possibility is that this age component was sourced from felsic igneous rocks of the 1837–1808 Ma Sally Downs Supersuite in the Central Zone during deformation associated with the Halls Creek

Orogeny (Phillips et al., 2016). In any case, the top of the Olympio Formation does not appear to have correlatives in the Central or Western Zones and represents a phase of early syn-orogenic sedimentation that ultimately ceased as progressive deformation affected the Eastern Zone.

## Potential sediment source regions

### Successions older than c. 1870 Ma

In the Western Zone, the broad range of detrital zircon ages in Unit 1 of the Marboo Formation indicates that its source region(s) contained igneous rocks of differing ages and/or sedimentary rocks derived from heterogeneous sources. As discussed previously, the minor c. 1910 Ma age component in Unit 1 (Tyler et al., 1999) is comparable to the 1912–1904 Ma age of the Sophie Downs Suite in the Eastern Zone, which could indicate connectivity with the Eastern Zone. The sources of older detrital age components (predominantly 2.55 – 1.95 Ga) are difficult to assess due to a lack of exposed early Paleoproterozoic source rocks in the region and broader North Australian Craton. Basement rocks to the Western Zone are inferred to comprise Archean to early Paleoproterozoic crust (Hollis et al., 2015), which might have provided local sediment sources, but there is insufficient information to make any conclusions.



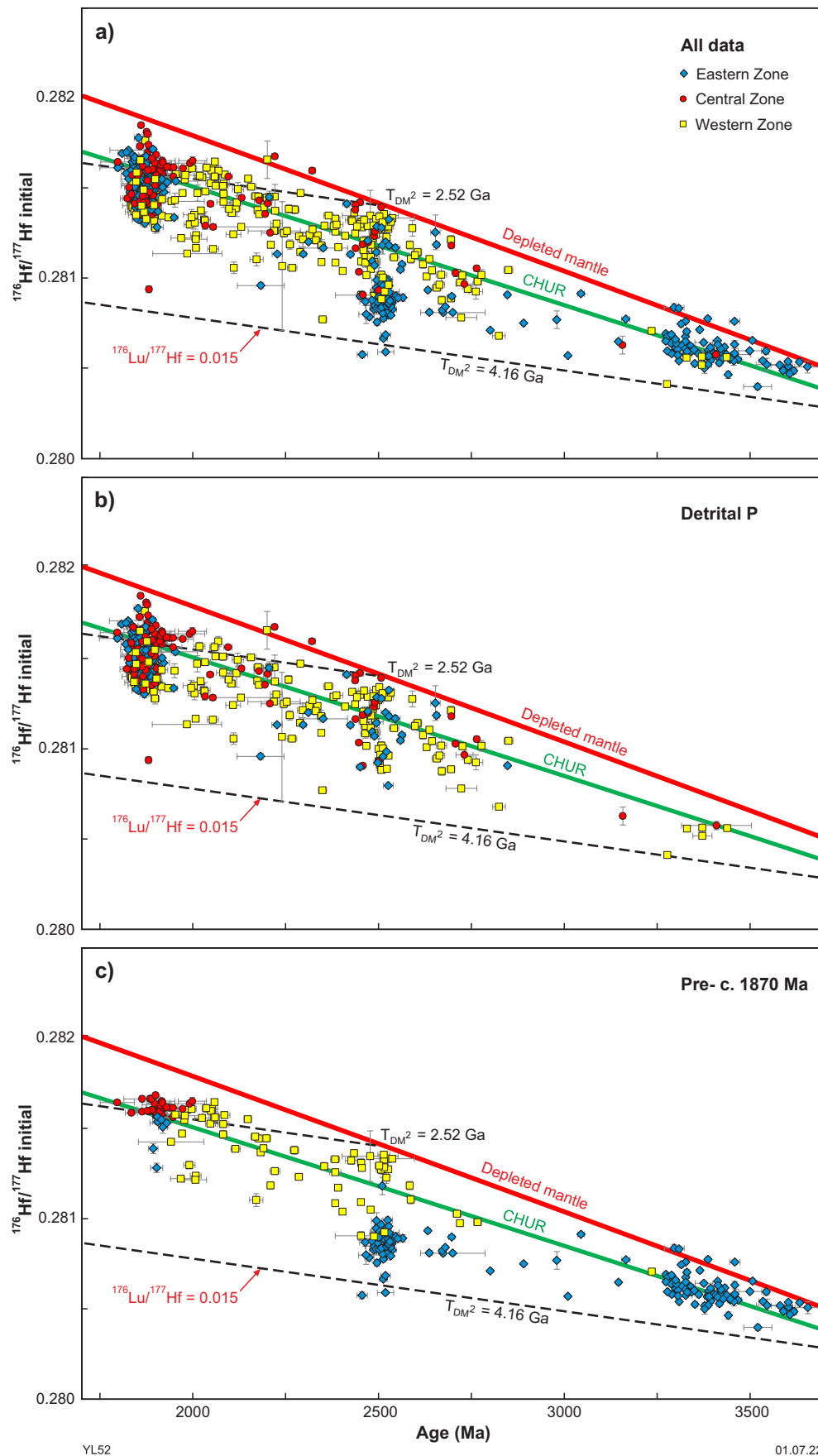


Figure 28. Initial  $^{176}\text{Hf}/^{177}\text{Hf}$  evolution plots for detrital zircons from metasedimentary rocks of the Lamboo Province dated by SHRIMP: a) all data; b) samples with Detrital P provenance; c) samples of older units underlying those with the Detrital P signature. Data sources: the Western and Central Zones, this study, with two samples from the Central Zone sourced from Iaccheri et al. (2018); and Eastern Zone, Phillips et al. (2016). Error bars are at 1 sigma

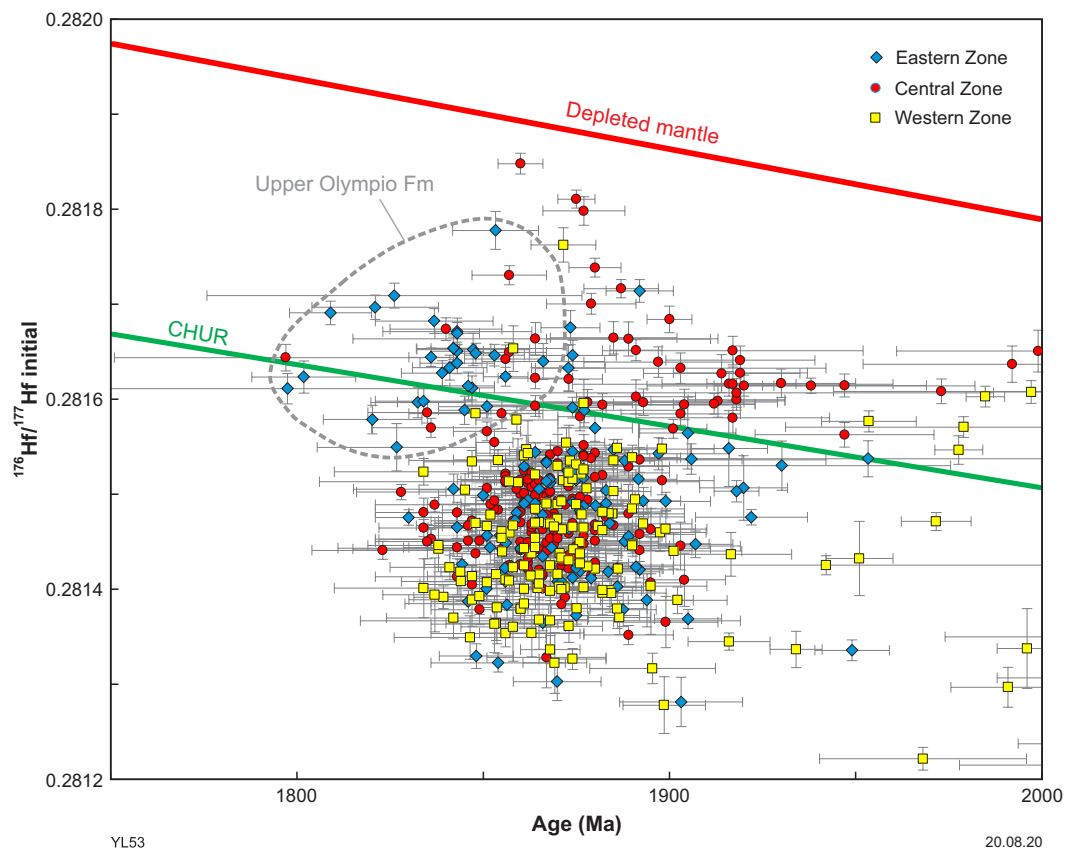


Figure 29. Initial  $^{176}\text{Hf}/^{177}\text{Hf}$  evolution plot for detrital zircons comprising the dominant c. 1865 Ma age component in the Detrital P provenance, showing the close similarity of isotope compositions across all three zones of the Lamboo Province. A slightly less evolved age component at 1845–1840 Ma from the upper Olympio Formation might be derived from volcanism in the Central Zone. Error bars are at 1 sigma

Samples from the Eastern Zone contain a significant c. 2.5 Ga detrital zircon age component, which is similar to the ages of granitic rocks exposed in small basement inliers in the Pine Creek and Granites–Tanami Orogens, representing the only Archean rocks known in the North Australian Craton (Page et al., 1995; Hollis et al., 2009a; Ahmad et al., 2013; Kositcin et al., 2013a). In the Pine Creek Orogen, felsic basement rocks have relatively radiogenic Lu–Hf isotopes (Hollis et al., 2014a), comparable to those of the c. 2.5 Ga age component in the sample of Unit 1. Lu–Hf isotope values for the Billabong Complex basement inlier in the Granites–Tanami Orogen are intermediate between the juvenile values obtained from Unit 1 and the evolved values obtained from this age component in the lower Halls Creek Group (Whelan et al., 2014). The paucity of outcropping basement rocks and isotope data makes it difficult to draw firm conclusions, but there were apparently suitable sediment sources within the North Australian Craton for the c. 2.5 Ga age component.

Because there are no rocks older than c. 2.67 Ga known in the North Australian Craton, the primary source(s) of detrital zircons >2.5 Ga in the Eastern Zone is difficult to assess. Sedimentary rocks deposited at c. 2.02 Ga in the Pine Creek Orogen (Ahmad and Hollis, 2013) are a potential source of reworked Archean detrital zircons. Two samples of these metasedimentary rocks contain a dominant c. 2.5 Ga detrital zircon age component and zircons as old as c. 3.6 Ga (Cross et al., 2005a), but their sources are unknown

and the potential for primary sources of Neoproterozoic to Paleoproterozoic zircon remains unconstrained.

Although the Paleoproterozoic to Archean basement to the North Australian Craton is largely obscured by younger rocks, it is possible that the 3.6 – 2.0 Ga detrital zircons in the lowermost units of the Lamboo Province were derived from local basement sources during basin formation. If this is the case, the ages and isotope compositions of these zircons may provide an indirect window into the nature and ages of these basement rocks.

### 1870–1835 Ma successions (Detrital P provenance)

The dominant 1875–1860 Ma age component in the Detrital P provenance is interpreted to reflect the erosion of a domain containing felsic volcanic or granitic rocks that were emplaced shortly before they were exhumed, eroded and transported as sediment into the Lamboo Province (cf. Bodorkos et al., 2000b). A relatively high proportion of zircons from this age component have euhedral shapes, which indicates that these crystals did not experience a prolonged period of transportation and abrasion. However, the proximity of this source is difficult to estimate, because subaqueous transport of sediment does not typically result in rapid abrasion of detrital grains (Garzanti, 2017) and euhedral crystal shapes may thus only be indicative of first-

cycle erosion. Coeval volcanism may locally have contributed zircons (e.g. in parts of the Olympio Formation and in the uppermost Marboo Formation in the Halls Creek Orogen) but the paucity of felsic volcanism of suitable age in the Lamboo Province and the lack of a clear proximal volcanoclastic component in the metasedimentary rocks suggests that most zircons are epiclastic and derived from sources external to the Lamboo Province. Although the Paperbark Supersuite is of similar age to the main age component of the Detrital P signature, there is no evidence of volcanic centres in the Western Zone associated with 1870–1860 Ma intrusive rocks, though the possibility of unexposed centres cannot be ruled out.

The relatively uniform subsidiary c. 2.5 Ga age component in the Detrital P provenance suggests that rocks of this

age were present in smaller amounts in the source region or that the source region included sedimentary units containing detritus of this age. Zircons dated at c. 2.5 Ga in the Detrital P units are typically considerably more rounded than 1875–1855 Ma zircons, or present as rounded cores mantled by 1875–1855 Ma zircon (Mole et al., 2018), suggesting a reworked sedimentary source and/or inheritance in felsic igneous rocks derived from deeper c. 2.5 Ga sources.

Hancock (1991) recorded limited paleoflow data from the Marboo Formation (probably Unit 2) in the far southwestern part of the Halls Creek Orogen, which indicated south- and southwest-dipping paleoslopes (two outcrops in the Sandy Creek area) and a south-dipping paleoslope in the Little Gold River area obtained from a larger number of measurements.

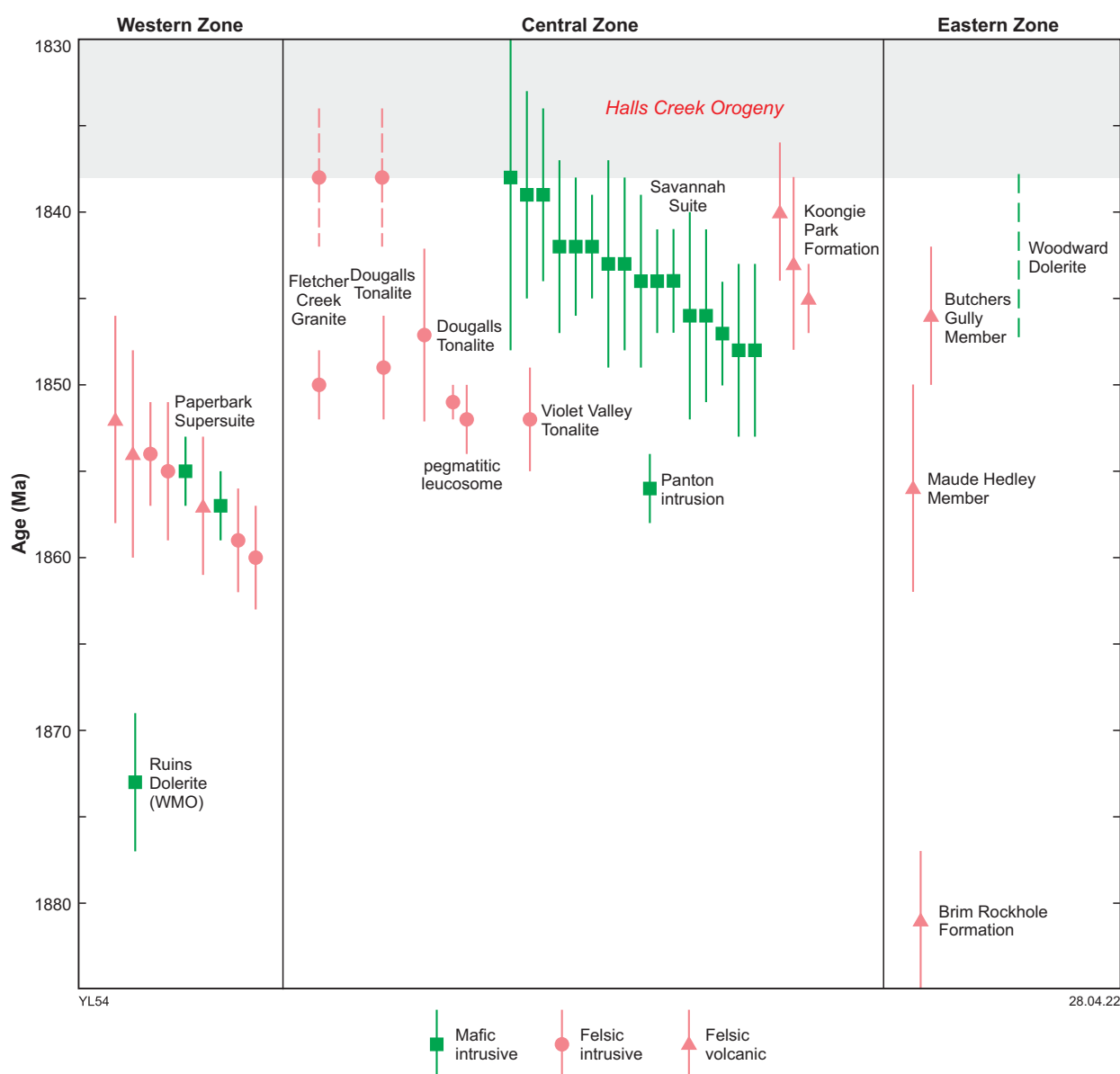


Figure 30. Compilation of isotopic ages for igneous rocks in the Halls Creek Orogen that pre-date the Halls Creek Orogeny, excluding the 1912–1904 Ma Sophie Downs Suite in the Eastern Zone. The Ruins Dolerite in the Wunaamin Miliwundi Orogen (WMO) is included for reference. Data from Griffin et al. (2000a), Page and Hoatson (2000), Page et al. (2001), Kemp et al. (2015), Phillips et al. (2016), Mole et al. (2018) and GSWA samples discussed in this Report. Note that Kemp et al. (2015) obtained younger ages from the same samples of the Fletcher Creek Granite and Dougalls Tonalite dated by Page et al. (2001)



Broadly comparable paleoflow directions have been obtained from limited indicators in the Olympio Formation (north-northeast–south-southwest axis) in the Eastern Zone (Hancock and Rutland, 1984; Hancock, 1991). Together, the limited paleocurrent data are consistent with a source broadly to the north of the Lamboo Province.

Local granitic sources of comparable age to the 1875–1860 Ma detrital components in the upper Marboo Formation include the voluminous and widespread 1867–1849 Ma Paperbark Supersuite, which potentially extends beneath the Kimberley Basin. Radiometric geophysical data indicate that Detrital P units have relatively high K, Th and U contents, reflecting their compositional immaturity (Fig. 31). Where the generally more-weathered metasedimentary rocks are well exposed, their radiometric signature is comparable to that of granitic and volcanic rocks of the Paperbark Supersuite, consistent with derivation from source rocks of similar composition. This character differs somewhat from that of Unit 1 of the Marboo Formation, which typically has a slightly lower intensity in radiometric images, reflecting a lower feldspar content.

Although some uplift and exhumation of the Paperbark Supersuite took place during the Hooper Orogeny ( $D_2$ ), the Marboo Formation is intruded by the Paperbark Supersuite and overprinted by  $D_2$ , which makes it difficult to invoke the Paperbark Supersuite in the Lamboo Province as a sediment source. A similar argument applies to metasedimentary successions in the western and central parts of the Pine Creek Orogen to the northeast, which have similar detrital zircon signatures to the Marboo Formation, and also host granitic rocks of similar age and character to the Paperbark Supersuite (Worden et al., 2008; Ahmad and Hollis, 2013). These areas were not uplifted before c. 1855 Ma, but are instead thought to have been predominantly zones of extension and sedimentation during deposition of the Detrital P units (Carson et al., 2008; Ahmad and Hollis, 2013). This suggests that the Detrital P detritus was not locally derived, which is consistent with the relatively uniform turbiditic character of the metasedimentary rocks and their homogeneous detrital zircon spectra. Although a more distal uplifted source is implied, the felsic source rocks may have formed part of the regional-scale magmatism of this age that included the Paperbark Supersuite.

There are only limited Hf data for granitic rocks of the Paperbark Supersuite and correlatives in the Pine Creek Orogen to help assess the potential of this broader magmatic belt as a sediment source. Samples of igneous zircons from four Paperbark Supersuite granitic rocks in the western Wunaamin Miliwundi Orogen have a narrow range of Hf isotope values comparable to those obtained from the Detrital P provenance signature (GSWA geochronology database). One sample of the Nimbuwah Complex in the eastern Pine Creek Orogen (Iaccheri et al., 2018) has a narrow range of Hf isotope values that overlaps with the more evolved compositions in the main Detrital P age component. Although there are insufficient data to draw firm conclusions, the Lu–Hf data allow for the possibility that the dominant age component of the Detrital P provenance signature was derived from areas where Paperbark Supersuite correlatives were exposed at the time of sedimentation.

Although the lack of significant uplift in the Lamboo Province and western Pine Creek Orogen between c. 1870

and 1840 Ma appears to preclude these areas as major sources of the Detrital P provenance, the eastern Pine Creek Orogen and Arnhem Province further east do appear to have the potential to be sediment sources (Maidment et al., 2020). In the Nimbuwah Domain of the eastern Pine Creek Orogen, relatively high-pressure metamorphism during the c. 1865 Ma Nimbuwah Event was broadly coeval with the emplacement of granitic rocks of the Nimbuwah Complex (Hollis et al., 2009b; Ahmad and Hollis, 2013). This event coincided with a hiatus in sedimentation and was presumably associated with significant uplift as a result of crustal thickening. Sedimentation in the Arnhem Province stopped by c. 1880 Ma, when the area was deformed at moderate to high pressure. It then underwent a clockwise decompression path and cooling over the following 30 Ma, accompanied by the intrusion of granitic rocks between c. 1880 and 1860 Ma (Kositcin et al., 2015, 2018; Reno et al., 2017; Whelan et al., 2017). The ages of orogenic events and granitic magmatism in the northeastern part of the North Australian Craton are consistent with this area being a source of the dominant age component in the Detrital P provenance, with small exposures of c. 2.5 Ga basement rocks in the Pine Creek Orogen potentially representing the source of the subsidiary age component. This area may have formed part of a larger orogen that extended further to the west, beyond the current margins of the North Australian Craton, forming a broad zone of uplift that shed material southwards across the craton (Maidment et al., 2020). Iaccheri and Bagas (2020) noted that several domains external to the North Australian Craton have Neoproterozoic and early Paleoproterozoic age components with zircon Hf isotope values that are consistent with detrital zircons identified in the Lamboo Province. These include the West Dharwar Craton, Aravalli – Lesser Himalaya region, Cathaysia Block and Madagascar, and it is possible that some of these formed part of the postulated orogen shedding detritus across what is now northern Australia.

## Regional correlations

The changes of provenance in 1885–1830 Ma metasedimentary rocks in the Lamboo Province are comparable to those of metasedimentary rocks of similar age elsewhere in the North Australian Craton, suggesting a related geodynamic evolution and providing a minimum age for assembly of the underlying basement domains (Fig. 32; Maidment et al., 2020, and references therein). Where exposed in the Granites–Tanami and Pine Creek Orogens, Paleoproterozoic metasedimentary packages overlying Neoproterozoic basement are dominated by Archean to early Paleoproterozoic detrital zircons. Thick, compositionally immature, turbiditic successions overlying these units are widespread across the proto-craton between c. 1870 and 1840 Ma, including the Pine Creek and Granites–Tanami Orogens and the Aileron, Warramunga and Murphy Provinces. These turbiditic successions are dominated by 1870–1855 Ma detrital zircons with a minor c. 2.5 Ga age component (Maidment et al., 2020), comparable to turbiditic rocks with the Detrital P signature in the Lamboo Province. The similarities in lithostratigraphy and provenance are particularly evident in the Tanami Group of the Granites–Tanami Orogen, which may be a correlative of the Halls Creek Group (Cross and Crispe, 2007; Crispe et al., 2007; Phillips et al., 2016; Maidment et al., 2020).

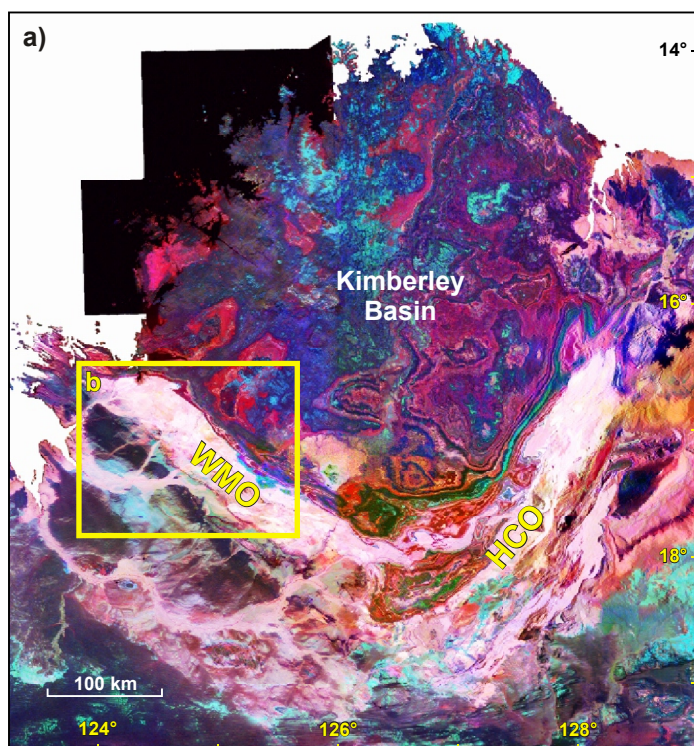
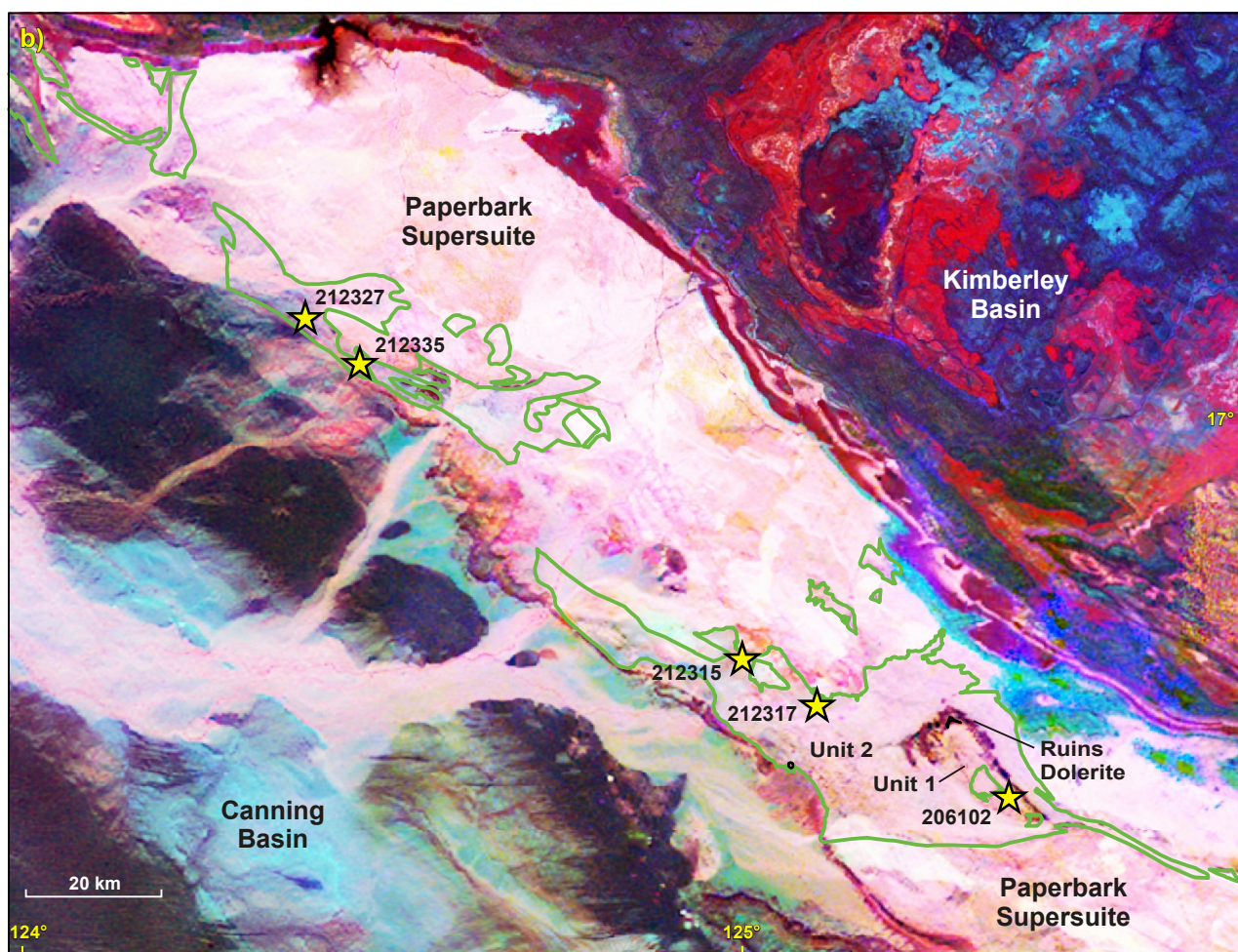


Figure 31. Radiometric images of the Kimberley region: a) regional ternary radiometric image, showing the high contents of K, U and Th (red, green, blue) for the Paperbark Supersuite and metasedimentary rocks of the Lamboo Province (Brett, 2018) – HCO, Halls Creek Orogen; WMO, Wunaamin Miliwundi Orogen; b) ternary radiometric image of the Wunaamin Miliwundi Orogen. The older metasedimentary units in the succession have a less intense signature, reflecting their lower feldspar contents



YL55

22.02.22



Marboo Formation



Geochronology sample location



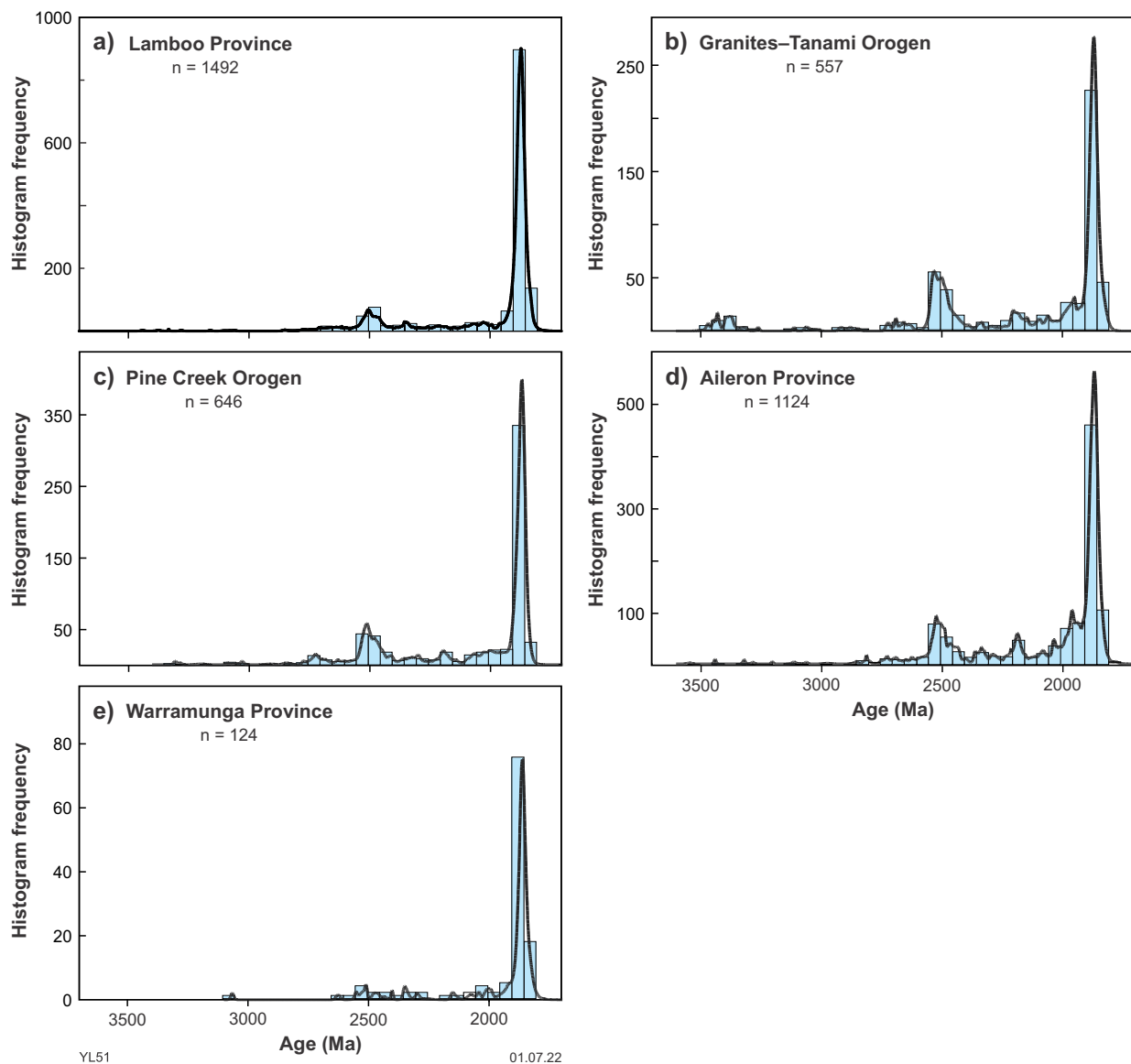


Figure 32. Compiled detrital zircon age spectra for 1880–1840 Ma metasedimentary units of the North Australian Craton with the Detrital P signature (c. 1865 Ma dominant age component, with a subsidiary c. 2.5 Ga component): a) Lamboo Province (this study; Page, 1996a,b; Tyler et al., 1999; Bodorkos et al., 2000b; Worden et al., 2008; Phillips et al., 2016; Mole et al., 2018); b) Granites–Tanami Orogen (Smith, 2001; Cross and Crispe, 2007; Worden et al., 2008; Bagas et al., 2009; Maidment et al., 2020); c) Pine Creek Orogen (Worden et al., 2006a,b, 2008; Hollis et al., 2010; Carson, 2013); d) Aileron Province (Smith, 2001; Worden et al., 2004, 2008; Cross et al., 2005b; Claoué-Long et al., 2008; Carson et al., 2009, 2011; Hollis et al., 2013; Bodorkos et al., 2013); and e) Warramunga Province (Compston, 1995; Maidment et al., 2013b). Data used are analyses with discordance <5%

The widespread occurrence of immature turbiditic metasedimentary rocks deposited between c. 1870 and 1840 Ma across the North Australian Craton supports the interpretation that the Detrital P signature is not related to syn-sedimentary volcanism in the Western Zone of the Lamboo Province, but is instead related to uplift and erosion of a more distal source region. As in the Lamboo Province, the Detrital P successions across the rest of the North Australian Craton are dominantly siliciclastic in nature, with discrete intervals of 1863–1861 Ma felsic volcanic rocks present in the Pine Creek Orogen (Ahmad and Hollis, 2013) and rare c. 1860 Ma felsic volcanic rocks occurring in the central part of the craton (e.g. Donnellan, 2013).

The metasedimentary successions with the Detrital P signature are relatively thick, implying the presence of a

major zone of uplift feeding a large volume of sediment into a continental-scale basin system. Although deformation makes original thicknesses difficult to determine, estimates include: ~3.5 km for Unit 2 of the Marboo Formation (Hancock, 1991; Tyler et al., 1999); >4 km for the Biscay and Olympio Formations (Phillips et al., 2016); 4–5 km for the Killi Killi Formation in the Granites–Tanami Orogen (Crispe et al., 2007; Bagas et al., 2014); ~3 km for the Burrell Creek Formation in the Pine Creek Orogen (Ahmad and Hollis, 2013); and ~3 km for the Warramunga Formation in the Tennant Creek Region (Donnellan, 2013).

The locus of magmatism and high-*T*, low-*P* metamorphism around the northern and northwestern margins of the proto-North Australian Craton at 1870–1850 Ma suggests that a plate margin driver for basin formation and magmatism



within the craton may have been situated north of the currently preserved margin (Maidment et al., 2020). One possibility is that basin development occurred within a broad back-arc setting related to south-directed subduction (Fig. 33). In this setting, deformation and uplift forming a source for Detrital P sediment in the northeast of the craton might have been a result of processes such as accretion of an exotic terrane or subduction of more buoyant crust.

As in the Lamboo Province, metasedimentary rocks underlying Detrital P successions elsewhere in the North Australian Craton show considerable variability in the relative proportions of age components, though some components

are relatively consistent. Combined detrital zircon ages for samples in the Lamboo Province, Pine Creek Orogen and Granites–Tanami Orogen are shown in Figure 27. The age spectra of samples from the Western Zone and Pine Creek Orogen are similar, and differ from those of the Eastern Zone and Granites–Tanami Orogen. As noted above, this difference is not considered to indicate an exotic relationship between the two domains, because metasedimentary rocks with the uniform Detrital P provenance overlie these successions with near-conformity, and there is no evidence for a major orogenic event between these two packages that might indicate a collision. The differences might thus indicate different drainage configurations in the two domains or, if sediment was more locally sourced, changes in the underlying basement geology.

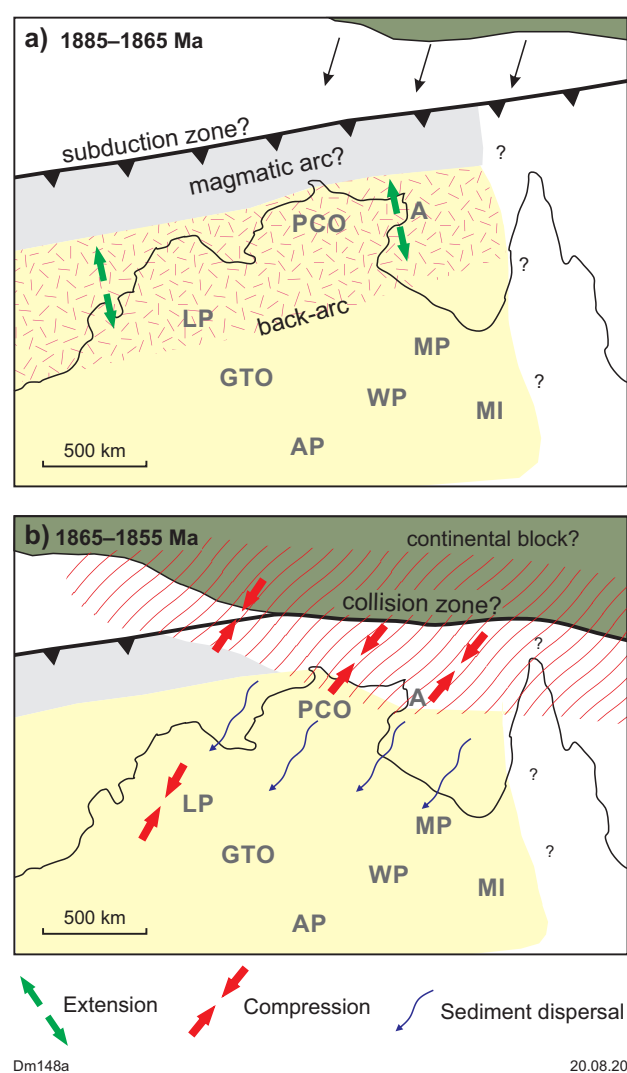


Figure 33. Possible geodynamic evolution of the North Australian Craton between c. 1885 and 1855 Ma (from Maidment et al., 2020): a) widespread extension associated with felsic and mafic magmatism took place along the northern margins of the craton, inboard of a subduction zone that was situated to the north of the currently preserved margin; b) a collisional or accretional event at about 1865–1855 Ma, recorded in the northeastern margin of the craton, resulted in uplift and erosion of crust dominated by 1870–1855 Ma granitic rocks and lesser c. 2.5 Ga crust, providing a source for sedimentary rocks that extended southwards over much of the craton. Abbreviations: A, Aileron Province; AP, Aileron Province; GTO, Granites–Tanami Orogen; LP, Lamboo Province; MI, Mount Isa region; MP, Murphy Province; PCO, Pine Creek Orogen; WP, Warumpi Province

Further context for the Lamboo Province may be provided by 1912–1865 Ma mafic volcanic and metasedimentary rocks in the Granites–Tanami Orogen, 200–300 km southeast of the Lamboo Province. Schmid et al. (2021) reported on the geochemistry of basaltic rocks from the lower Tanami Group, which they noted as being typical of tholeiitic back-arc basalts. This interpretation is consistent with both Bagas et al. (2008) and Li et al. (2013), who described c. 1864 Ma mafic rocks in the Tanami Group with compositions consistent with enriched back-arc basalts. Schmid et al. (2021) dated fine-grained, euhedral zircons from a volcanoclastic unit intercalated with basalt, which yielded a unimodal c. 1912 Ma age component, interpreted as the age of volcanism. These authors suggested that geochemical aspects of interflow metasedimentary rocks, including REE patterns, a lack of Eu anomalies and HFSE ratios, are indicative of a proximal arc to back-arc setting. However, the geochemical features of the volcanoclastic units, which include a wide range in Nb/Yb at constant Th/Yb (and hence varying Th/Nb), clearly also reflect non-igneous processes and may not provide a robust constraint on either an oceanic setting or the presence of a proximal arc. Mixing of mafic-derived and continental detritus is another possible mechanism to produce these signatures. The compositions of the mafic igneous rocks thus appear to represent the most robust constraint and they are consistent with a distal back-arc basin, given the nature of other metasedimentary rocks in the succession and the evidence for Neoproterozoic basement in the Granites–Tanami Orogen (Goleby et al., 2009; Whelan et al., 2014).

The fine-grained (~50 µm), euhedral c. 1912 Ma zircons identified in the mafic volcanoclastic unit by Schmid et al. (2021) conceivably reflect a distal volcanic contribution from Sophie Downs Suite volcanism in the Lamboo Province, deposited into an area that probably contained little local coeval igneous zircon, given the predominantly mafic composition of the volcanic units. Two other dated samples of metasedimentary rocks from a basalt-rich succession in the lower Tanami Group have a more felsic siliciclastic composition and also contain a population of euhedral 1913–1905 Ma zircons as the youngest dated age component, in addition to a range of Archean zircons (Cross and Crispe, 2007). It is possible the younger zircons also reflect a distal volcanic component, although a detrital origin cannot be ruled out. In either case, the available constraints suggest that the Granites–Tanami Orogen was relatively proximal to the Lamboo Province, with both areas at this time potentially developing in an extensional continental setting (e.g. Phillips et al., 2016).

## Igneous geochemistry and isotope constraints

The geochemical and isotope compositions of igneous rocks in the Lamboo Province reflect the geodynamic evolution of the region, and have been used to infer a broad range of geodynamic settings, including post-collisional, intraplate rift, passive margin, back-arc/marginal basin and oceanic arc (e.g. Wyborn et al., 1987; Sheppard et al., 1999b; Wyborn and Blake, 2000; Griffin et al., 2000a; Tyler et al., 2012; Occhipinti et al., 2016; Phillips et al., 2016; Mole et al., 2018; Kohanpour et al., 2019a). The detrital zircon data presented in this study suggest that it is possible there are no exotic terranes within the province, which would imply that magmatism was produced in an intraplate setting, though potentially influenced by external, or older, periods of subduction. The distribution and character of magmatism in the Lamboo Province varied considerably with time and the different magmatic events are re-examined below in light of the intraplate setting favoured in this study.

### c. 1873 Ma Ruins Dolerite

The Ruins Dolerite has not previously been the subject of detailed study, though the recent identification of magmatic Ni–Cu mineralization in ultramafic components at the Merlin prospect has made this unit a focus for mineral exploration (Buxton Resources, 2018). There are presently few samples with a full suite of trace element data that would allow for a robust assessment of this unit. Two whole-rock analyses for the unit dated in this study are presented in Appendix 3. The available data indicate a tholeiitic basaltic composition with a significant ‘crustal’ component, but there are insufficient data to determine whether this reflects a subduction component in the mantle source or crustal contamination. The Lu–Hf data for the dated sample (GSWA 212335, Lu et al., 2017b) (Fig. 22) indicate a uniform isotope composition between depleted mantle and CHUR, consistent with limited incorporation of an evolved crustal component. The emplacement of the Ruins Dolerite into an actively subsiding basin is consistent with a broadly extensional setting, but further work is required to better constrain the magmatic evolution of this magmatism.

### 1867–1849 Ma bimodal magmatic rocks

The presence of voluminous felsic and mafic igneous rocks of the 1867–1849 Ma Paperbark Supersuite distinguishes the Western Zone from the rest of the province, though mafic and felsic igneous rocks of this age are also present in the Central and Eastern Zones. These magmatic rocks may extend beneath the Kimberley Basin, contributing to lobate gravity lows evident in geophysical images (Gunn and Meixner, 1998; Fig. 34). The geochemistry and Sm–Nd isotope characteristics of these rocks have been documented by Griffin et al. (2000a). Granitic and felsic volcanic rocks are I-types characterized by high K<sub>2</sub>O, Rb, Y, Th and K<sub>2</sub>O/Na<sub>2</sub>O, and low Sr, Sr/Y and K/Rb. They have elevated contents of large-ion lithophile elements (LILE) relative to high field strength elements and non-cumulate rocks have negative Eu anomalies. Whole-rock Sm–Nd isotope data indicate relatively evolved compositions, intermediate between values expected for Neoproterozoic crust and coeval depleted mantle. Lu–Hf isotope data for zircons of the Paperbark Supersuite provide similar constraints, with

$\epsilon_{\text{Hf}(t)}$  values between –6.4 and –0.8 (GSWA 95416, 95449, 95459 and 95464, from GSWA, 2022). Silica contents for the supersuite as a whole are distinctly bimodal, with limited intermediate compositions a result of hybridization of coeval mafic and felsic magmas. Mafic components of the supersuite are continental tholeiites, and geochemical trends indicate the mafic and felsic rocks have different magmatic lineages. Sheppard et al. (1997a), Wyborn (1998) and Griffin et al. (2000a) noted the compositions of the granitic rocks of the Paperbark Supersuite differ from those in Phanerozoic continental arc settings, and are consistent with moderate-*P* (8–10 kbar), high-*T* melting of calc-alkaline, presumably Archean, crust interpreted to be caused by emplacement of the mafic component.

Griffin et al. (2000a) suggested that magmatism could have been triggered by lithospheric delamination related to a pre-1870 Ma collision of a currently unexposed terrane with the eastern margin of an exotic Kimberley Craton. In contrast, Etheridge et al. (1987), Wyborn et al. (1987) and Budd et al. (2001) suggested an intraplate extensional origin for the Paperbark Supersuite, associated with either mafic underplating or delamination of an underplate. The constraints provided by detrital zircon geochronology favour an intraplate model, though it is difficult to assess whether underplating or delamination might have been the main driver. Although transient compression of the Hooper Orogeny interrupting more prolonged extension has the potential to have driven a delamination event, emplacement of the Paperbark Supersuite began prior to compression, and the Hooper Orogeny may not have been a major event outside the Wunaamin Miliwundi Orogen. An intraplate setting for the Paperbark Supersuite related to regional extension and mafic underplating is thus tentatively favoured here. If bimodal magmatism of the Paperbark Supersuite marks a domain of significant crustal extension, its eastern margin was relatively sharply defined, with a rapid decrease of this magmatism eastwards into the Central Zone. One possibility is that this rapid transition was influenced by the postulated basement domain boundary between the Western and Eastern Zones, although this is speculative.

Tholeiitic mafic magmatic rocks of similar age to the Paperbark Supersuite occur in the Central Zone, and include the 1856 ± 2 Ma Panton mafic–ultramafic intrusion (Page and Hoatson, 2000) and mafic volcanic rocks in the Tickalara Metamorphics (Fig. 35a,b). Tholeiitic basalts of similar age were also emplaced in the Biscay Formation in the Eastern Zone (Fig. 35c), prior to eruption of 1856 ± 6 Ma alkaline felsic volcanic rocks in the Olympio Formation, which are interpreted to have been emplaced in a continental extensional setting (Phillips et al., 2016).

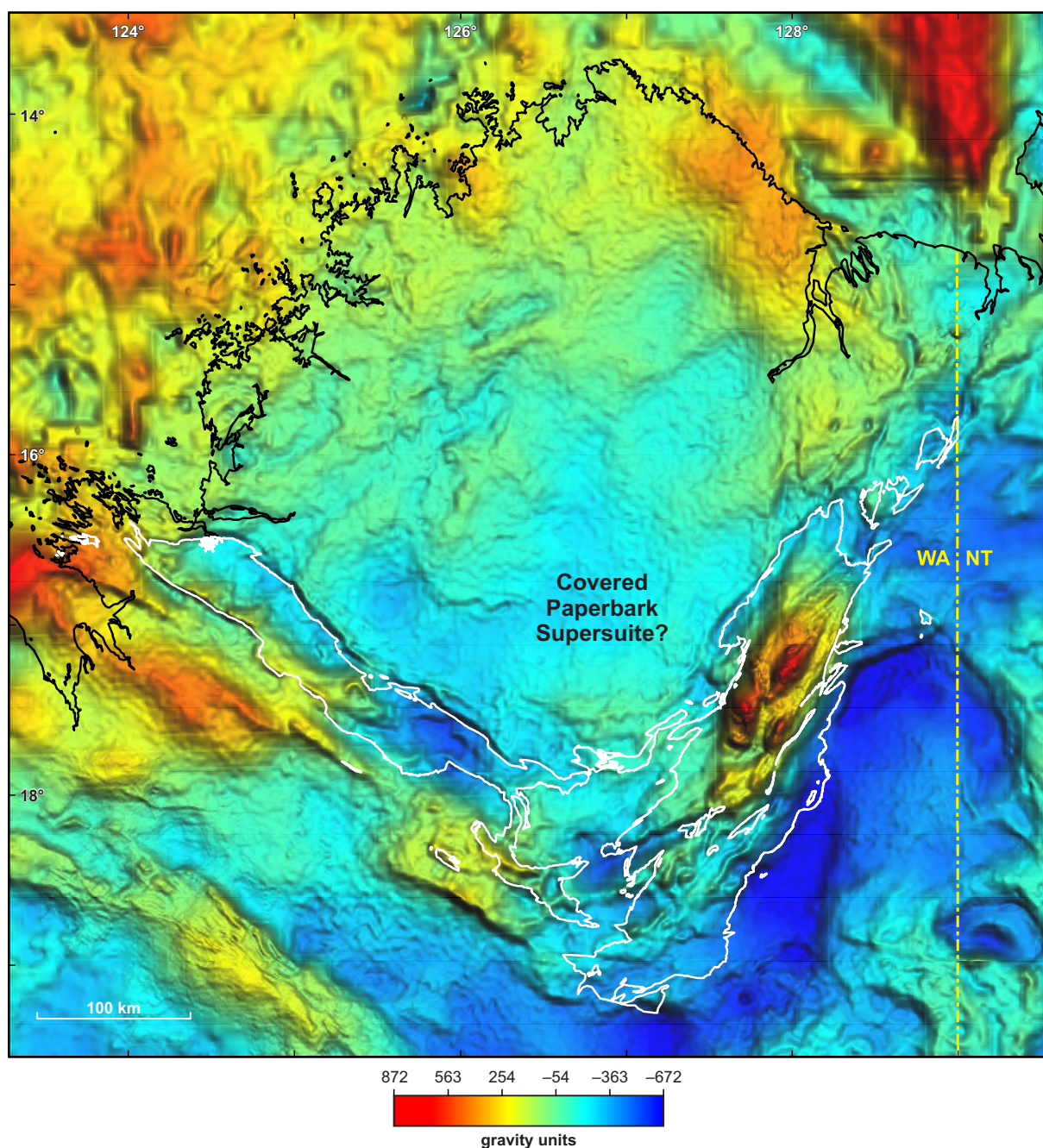
The geochemistry of mafic rocks in the Tickalara Metamorphics has previously been taken as a key line of evidence for plate convergence leading up to the Halls Creek Orogeny (Sheppard et al., 1999b). These authors noted some components have compositions similar to variably depleted tholeiites from oceanic arcs or back-arc basins, whereas others have compositions consistent with E-MORB basalts from oceanic back-arc basins or ensialic marginal basins. A detailed assessment of the geochemistry of these rocks is beyond the scope of this study, but it is worth noting that the ‘crustal’ component of these rocks interpreted to indicate subduction can be incorporated in different ways (Sun and Hoatson, 2000; Kohanpour et al., 2019a). These include subduction enrichment of a mantle source, either during



associated plate convergence or inherited from an older phase of subduction, and crustal contamination of mantle-derived magma during intraplate extension, which may or may not be driven by plate convergence.

Figure 36 plots whole-rock geochemical data for 1881–1846 Ma mafic volcanic rocks and sills of the Central and Eastern Zones on a Nb/Yb vs Th/Yb diagram, which allows discrimination between crustal contamination that took place during emplacement and crustal contamination of a mantle source by subduction (Pearce, 2008). These data include samples collected as part of this study, as well as previously analysed material from the GSWA archive

that was re-analysed to provide a comparable suite of trace elements and analytical methodology (Appendix 3). Although there is potential for some Th mobility in the samples that have experienced the highest grades of metamorphism, the effects are likely to be minor (Alessio et al., 2018) and the analyses are considered to be indicative of primary compositions. Mafic extrusive and intrusive associations form trends that extend between the MORB–OIB array and the modern arc array (i.e. variable Th/Nb). This is consistent with crustal contamination of mantle-derived mafic rocks, and inconsistent with purely arc-related magmatism, which would form a trend of constant Th/Nb along the arc array.

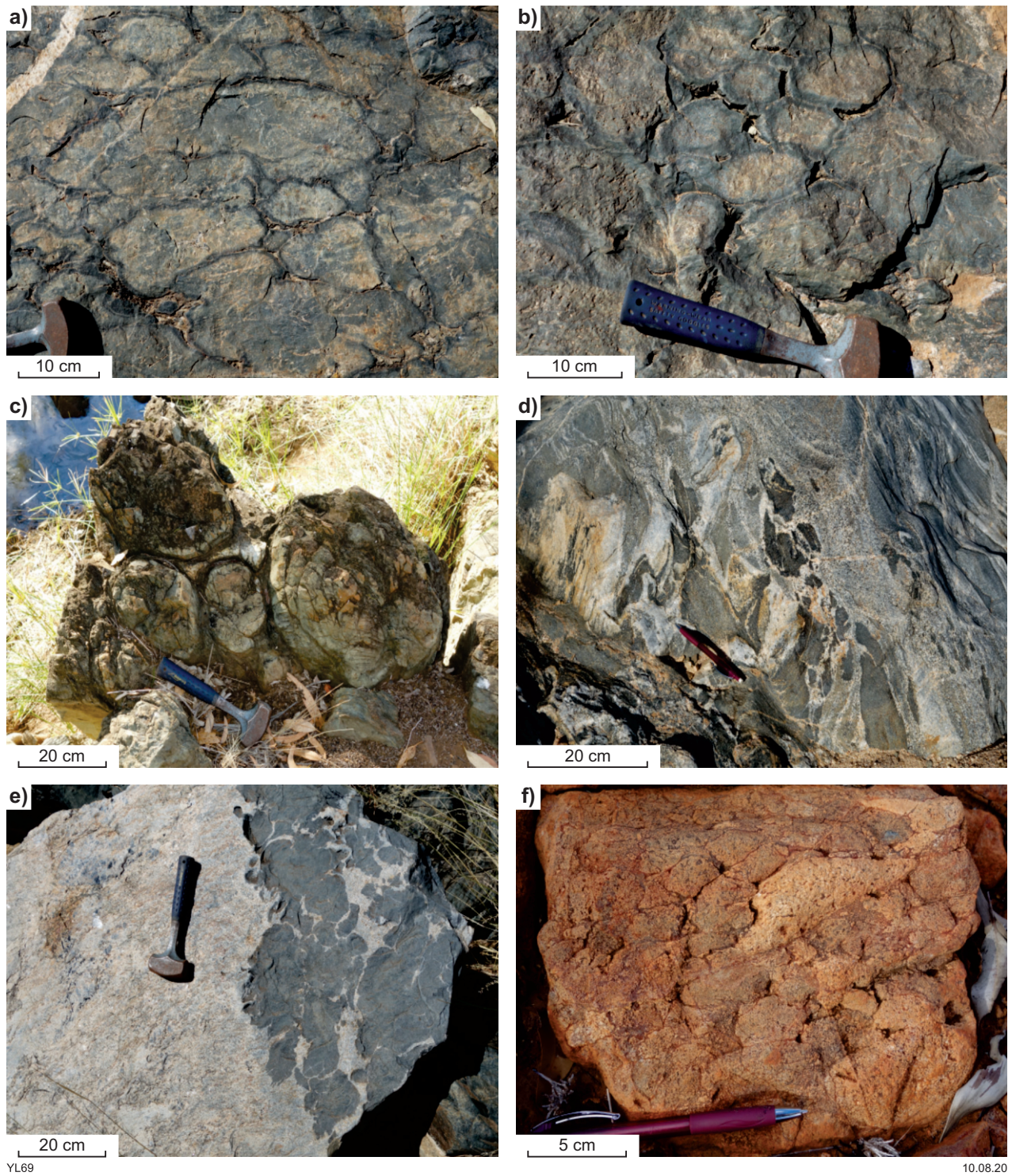


YL56

11.05.22

Figure 34. Bouguer gravity image of the Kimberley region, with the outcropping Lamboo Province outlined in white. Image courtesy of John Brett (GSWA) and uses data sourced from Wynne (2016) and Brett (2019). Lobate gravity lows within the area of the Kimberley Basin may in part be caused by felsic igneous rocks of the Paperbark Supersuite beneath cover





YL69

10.08.20

Figure 35. Textures of mafic and felsic rocks in the Halls Creek Orogen: a) and b) deformed amygdaloidal pillow basalt in amphibolite-facies Tickalara Metamorphics, 600 m east of White Rock Bore, Central Zone (MGA 393666E, 8054116N); c) pillow basalt in the Biscay Formation, Eastern Zone (MGA 357605E, 7962293N); d) magma-mingling textures in the c. 1821 Ma Sally Downs Tonalite (Page et al., 2001), Central Zone (MGA 387041E, 8063141N), consistent with injection of mafic magma into partly molten granitic rock, with associated sheath melting; e) mingled mafic and felsic rocks hosted by the Tickalara Metamorphics, 600 m east of White Rock Well (MGA 393682E, 8054115N); f) interpreted mingling of felsic 'pillows' in gabbro at contact between the Loadstone Monzogranite and Emull Gabbro, 6 km west of Lamboo homestead (MGA 319468E, 7959273N)

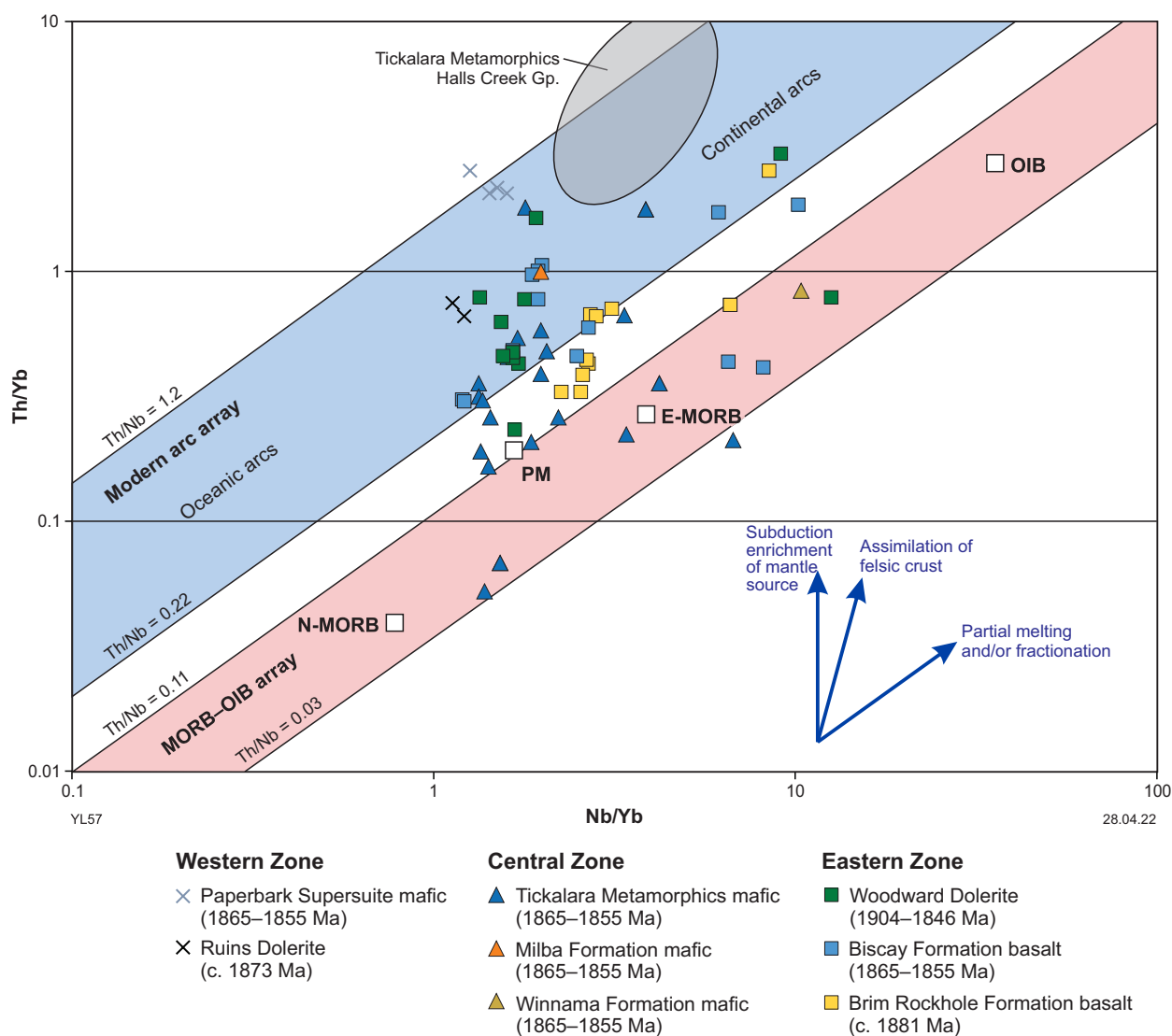


Figure 36. Plot of Th/Yb vs Nb/Yb (Pearce, 2008) for 1881–1846 Ma mafic extrusive and intrusive rocks of the Lamboo Province. Abbreviations: E-MORB, enriched mid-ocean ridge basalt; N-MORB, normal mid-ocean ridge basalt; OIB, ocean island basalt; PM, primitive mantle. The data trend between the MORB–OIB array and the modern arc array, consistent with crustal contamination of an intraplate mantle melt, rather than arc magmatism

There is some apparent heterogeneity evident in the mantle sources but there is no clear distinction between the Central and Eastern Zones. Most mafic rocks in the Tickalara Metamorphics, Biscay Formation and Woodward Dolerite have near-N-MORB primitive compositions, with a smaller population of the Tickalara Metamorphics and Biscay Formation showing a steep trend away from a more enriched mantle composition. It is possible that there is a minor subduction-related component to the mantle source of these magmas, but the constraints provided by the provenance of metasedimentary rocks in the Lamboo Province suggest that any such component was either related to subduction external to the province (e.g. Fig. 33) or reflects older (Archean?) subduction. Sm–Nd isotope data for metabasalt and amphibolite in the Tickalara Metamorphics yield  $T_{DM}^2$  model ages of 2.36 – 2.06 Ga (Appendix 2; Sheppard et al., 2001), consistent with a component of Archean to Paleoproterozoic crustal material. In the intraplate model favoured here, this would dominantly reflect contamination by older continental crust in the Central Zone, rather than a subducted component.

Similar considerations apply to observations that the compositions and stable isotopes of mineral inclusions in c. 1580 Ma diamonds from the Argyle mine imply enrichment of Paleoproterozoic–Neoproterozoic mantle, either by subduction or long-term addition to the lithosphere by asthenospheric sources (Stachel et al., 2018). The mantle enrichment has been inferred to be related to subduction immediately prior to the Halls Creek Orogeny on the basis of previous geodynamic models (Stachel et al., 2018; Jaques et al., 2018). However, if the terranes of the Lamboo Province are para-autochthonous, mantle enrichment could not be related to closure of oceanic basins between the Western and Eastern Zones and other mechanisms must be invoked. In this context, it may be significant that the mantle source of the mafic rocks of the Kalkarindji Large Igneous Province – which includes the Antrim Plateau Volcanics in the east Kimberley – is inferred to have been derived from a mantle source with c. 2.5 Ga subduction enrichment on the basis of Pb isotopes (Ware et al., 2019).



The 1860–1855 Ma mafic and felsic magmatic rocks in the Central and Eastern Zones are thus considered to have been emplaced in a similar intraplate extensional setting to the more voluminous Paperbark Supersuite in the Western Zone, though possibly in domains with a lower degree of extension and crustal attenuation. Granitic rocks in the Pine Creek Orogen with similar ages, compositions and isotope signatures to those in the Western Zone (Fig. 37; Hancock and Rutland, 1984; Carson et al., 2008; Ahmad and Hollis, 2013) may also have formed in a similar setting. A back-arc related to subduction north of the proto-North Australian Craton is one possible setting for magmatism and widespread sedimentation at this time (Maidment et al., 2020), though any interpretation of the broader geodynamic setting is necessarily speculative.

### 1845–1840 Ma bimodal magmatic rocks

In the Central Zone, 1845–1840 Ma magmatic rocks include mafic–ultramafic intrusions in the Savannah Ni–Cu–Co mine area dated at c. 1842 Ma (Page and Hoatson, 2000; Mole et al., 2018) and bimodal volcanic and intrusive rocks within the 1845–1840 Ma Koongie Park Formation (Page et al., 1994). In the Eastern Zone, alkaline felsic

volcanic rocks in the Butchers Gully Member in the Olympio Formation were emplaced at c. 1846 Ma (Phillips et al., 2016). Widespread mafic sills of the Woodward Dolerite in the Eastern Zone have not been dated, but they intrude units as young as the lower Olympio Formation and were deformed during the Halls Creek Orogeny, allowing for the possibility of emplacement during this period. No magmatic rocks of this age are known in the Western Zone.

Mafic and felsic volcanic rocks in the  $\geq 2000$  m-thick Koongie Park Formation are interbedded with turbiditic sandstone, laminated siltstone and mudstone, and include thin chert horizons, carbonate and iron-formation (Griffin et al., 1998). The lower part of the unit is mafic-dominated and the upper part is felsic-dominated. The mafic rocks have MORB-like geochemistry (Griffin et al., 1998) and felsic rocks have geochemical characteristics of A-type magmas (Orth, 2002). This is consistent with an extensional setting for magmatism, which is also compatible with coeval high- $T$ , low- $P$  metamorphism and intrusion of mafic–ultramafic magmas in the underlying Tickalara Metamorphics during the Savannah Event. The lack of structures developed in the Koongie Park Formation during this event (local  $D_2$  of Tyler et al., 1995) may be a factor of its shallower crustal depth.

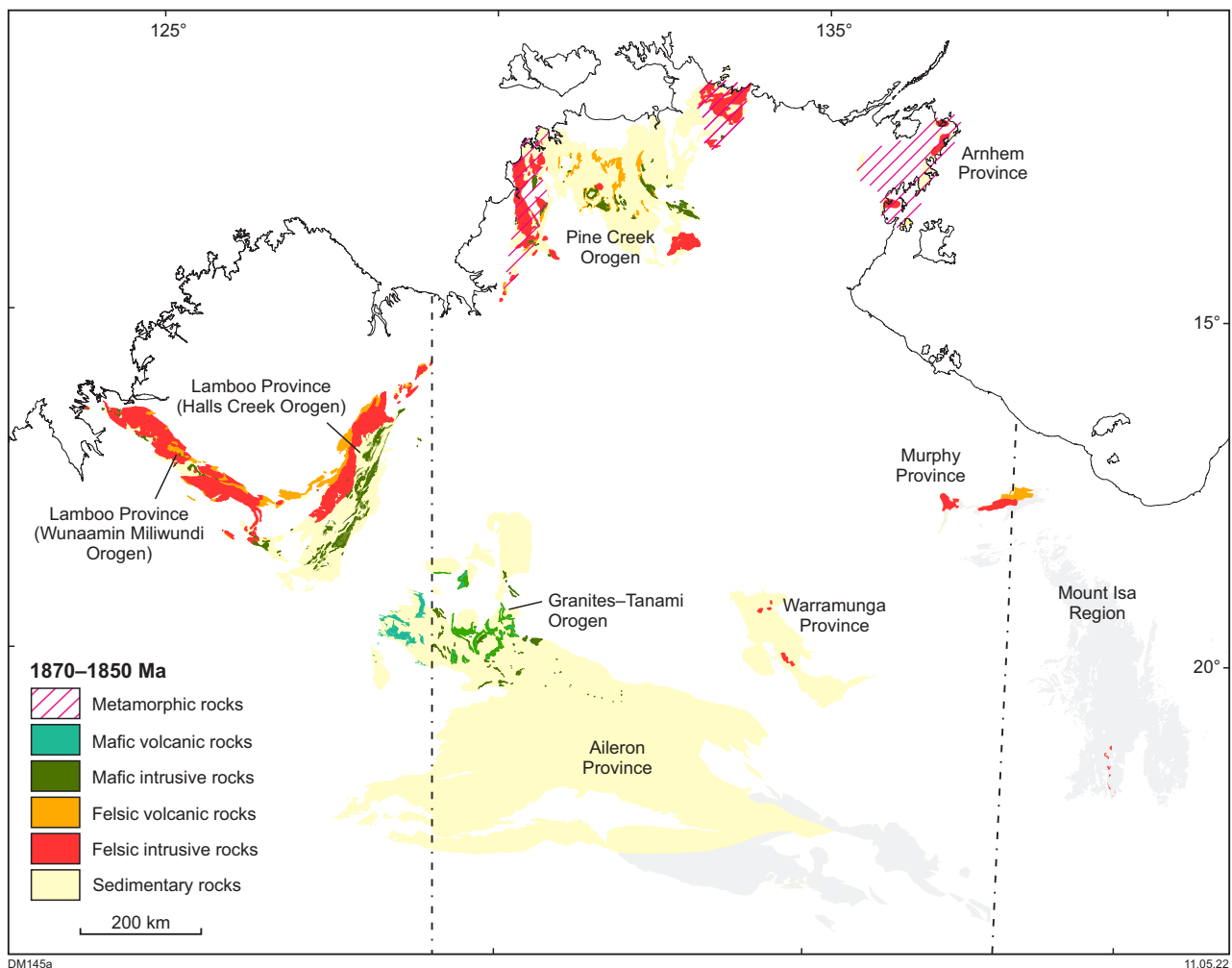


Figure 37. Distribution of 1870–1855 Ma magmatism, metamorphism and sedimentation in the North Australian Craton. A locus of tectonism around the northern margins of the currently preserved craton may have been related to a plate margin further to the north



Postulated geodynamic settings for this extension include a continental rift, back-arc, rifted island arc or extended continental margin (Griffin et al., 1998; Orth, 2002; Tyler et al., 2012; Mole et al., 2018). The constraints provided by the provenance of units deposited prior to the Koongie Park Formation suggest that a rifted oceanic arc setting is unlikely and, if the Central Zone developed in a back-arc setting, the magmatic arc was not located within the Lamboo Province. The constraints are consistent with continental rifting and this is consistent with Sm–Nd data (Appendix 2) for felsic volcanic rocks of the Koongie Park Formation, which indicate a significant component of evolved older crust (GSWA 108577:  $T_{DM^2} = 3.6$  Ga; GSWA 108668:  $T_{DM^2} = 2.9$  Ga). The Cu–Pb–Zn–Ag metal assemblage of VMS deposits within the Koongie Park Formation is also suggestive of the involvement of continental crust (Franklin et al., 2005). The alkaline felsic magmatism in the Eastern Zone at this time, and possibly also the Woodward Dolerite, may reflect a lower degree of extension during deposition of the Olympio Formation, with the Eastern Zone perhaps representing a less attenuated rift shoulder.

Barnes et al. (2021) examined geochemical data for mafic–ultramafic intrusions in the Halls Creek Orogen, many of which represent the 1848–1839 Ma Sally Malay Suite in the Central Zone. On a plot of Nb/Yb vs Th/Yb, the data fall across the area of overlap between continental arc and continental flood basalt fields, with a wide scatter of data that was noted to demonstrate the limitations of inferring tectonic setting from geochemistry alone. The authors suggested that various lines of evidence pointed towards either a back-arc setting or major asthenospheric upwelling due to processes such as post-collision slab break-off, with no clear evidence for an arc in the geochemical data.

### Central Zone an ensialic rift, not an oceanic arc?

Although an oceanic arc model for the Central Zone was only one of the possible settings suggested by Sheppard et al. (1999b) and Griffin et al. (2000a), this interpretation has been adopted in many subsequent geodynamic models (Cawood and Korsch, 2008; Tyler et al., 2012; Hollis et al., 2015; Lindsay et al., 2016; Occhipinti et al., 2016; Betts et al., 2016). As discussed above, detrital zircon geochronology suggests that the Central Zone was not an island arc separated from the Western and Eastern Zones by ocean basins, and there are other aspects of the geology that are also difficult to reconcile with an oceanic arc setting. Although the Tickalara Metamorphics contain a felsic component, they are predominantly siliciclastic rather than volcanoclastic in nature, similar to coeval units in the Western and Eastern Zones, and intercalated with mafic volcanic rocks having compositions similar to those of continental rifts. Mafic–ultramafic intrusions emplaced within the Central Zone at 1857–1830 Ma have Sm–Nd isotope signatures that indicate these rocks incorporate a significant component of evolved crustal material (Sun and Hoatson, 2000; Kohanpour et al., 2019a). The moderately evolved Sm–Nd isotope signatures for A-type felsic volcanic rocks in the Koongie Park Formation are also consistent with a significant evolved crustal component. This is consistent with ensialic rifting during the 1865–1840 Ma development of the Central Zone, though a component of evolved crustal material derived from subduction is typically also present in oceanic arc magmas (Murphy, 2007).

More recently, an ensialic extensional marginal basin setting for the Central Zone was favoured by Kohanpour et al. (2017), on the basis of numeric modelling. Mole et al. (2018) also considered the Central Zone to be an ensialic rift, developed in a back-arc inboard of a subduction zone between the Central and Eastern Zones. In their study, mantle-like oxygen isotope values and trace element geochemistry of c. 1842 Ma mafic–ultramafic rocks were interpreted as evidence that the crustal component in these rocks was subduction-related. A back-arc setting for the Lamboo Province inboard of a subduction zone to the north at this time is also consistent with these isotope and geochemical constraints, as is a continental rift developed over previously subduction-modified lithosphere. A more distal back-arc or continental rift setting for the mafic–ultramafic intrusions in the Halls Creek Orogen is consistent with the relatively low volatile contents of these rocks, which contrast with the relatively high H<sub>2</sub>O and Cl/F contents of subduction-related magmas (Boudreau and Hoatson, 2004).

### Burial of the Tickalara Metamorphics

Metamorphism of the Tickalara Metamorphics at pressures of approximately 3.5 – 5 kbar (10–15 km depth) (Thornett, 1986; Bodorkos et al., 1999, 2002) indicates significant burial between c. 1865 and 1845 Ma in what is here interpreted as a dominantly extensional setting. Although it is possible that there was a transient compressional event separating deposition of the Tickalara Metamorphics and the Koongie Park Formation sometime between c. 1865 and 1850 Ma, there is only limited evidence for crustal shortening during this period (Fig. 38). The oldest recognized structure in the Tickalara Metamorphics is a high-grade, layer-parallel  $S_1$  foliation lacking associated folding, which may have developed during extension (Thornett, 1986). West of the Savannah mine, this foliation is refolded by small-scale to mesoscale recumbent folds ( $F_2$ ) with axial surfaces and  $S_2$  sub-parallel to  $S_1$ , which are in turn refolded by two generations of larger scale upright folds associated with the Halls Creek Orogeny (Thornett, 1986). The  $S_1$  and  $S_2$  foliations developed during prograde metamorphism, with peak metamorphism during the Savannah Event developing syn- to post- $D_2$  (Bodorkos et al., 1999). Although the recumbent  $F_2$  folds could reflect a compressional event prior to the Savannah Event, such as the c. 1865 Ma Hooper Orogeny, recumbent folds can also develop in high-grade terrains during extension (Harris et al., 2002) and might thus instead reflect progressive  $D_1$ – $D_2$  extension during a prolonged Savannah Event. An extended Savannah Event is consistent with a spread of 1850–1840 Ma dates for stromatic, layer-parallel  $M_1$ – $M_2$  leucosomes, which were overprinted by leucosomes developed along the margins of c. 1842 Ma Savannah mafic–ultramafic intrusions (Fig. 15d,e,f; Oliver et al., 1999). Similarly, U–Pb zircon dates of  $1851 \pm 1$  Ma and  $1852 \pm 2$  Ma for pegmatitic leucosome in the Tickalara Metamorphics (Page and Hancock, 1988; Page and Sun, 1994) may also date an early stage of the Savannah Event.

Larger scale recumbent folds assigned to a local  $D_2$  were identified about 25 km to the southeast by Hancock and Rutland (1984). However, it is possible that these folds formed during the first deformational stage of the Halls Creek Orogeny, perhaps comparable to  $F_3$  folds mapped by Bodorkos et al. (1999) in a nearby area.

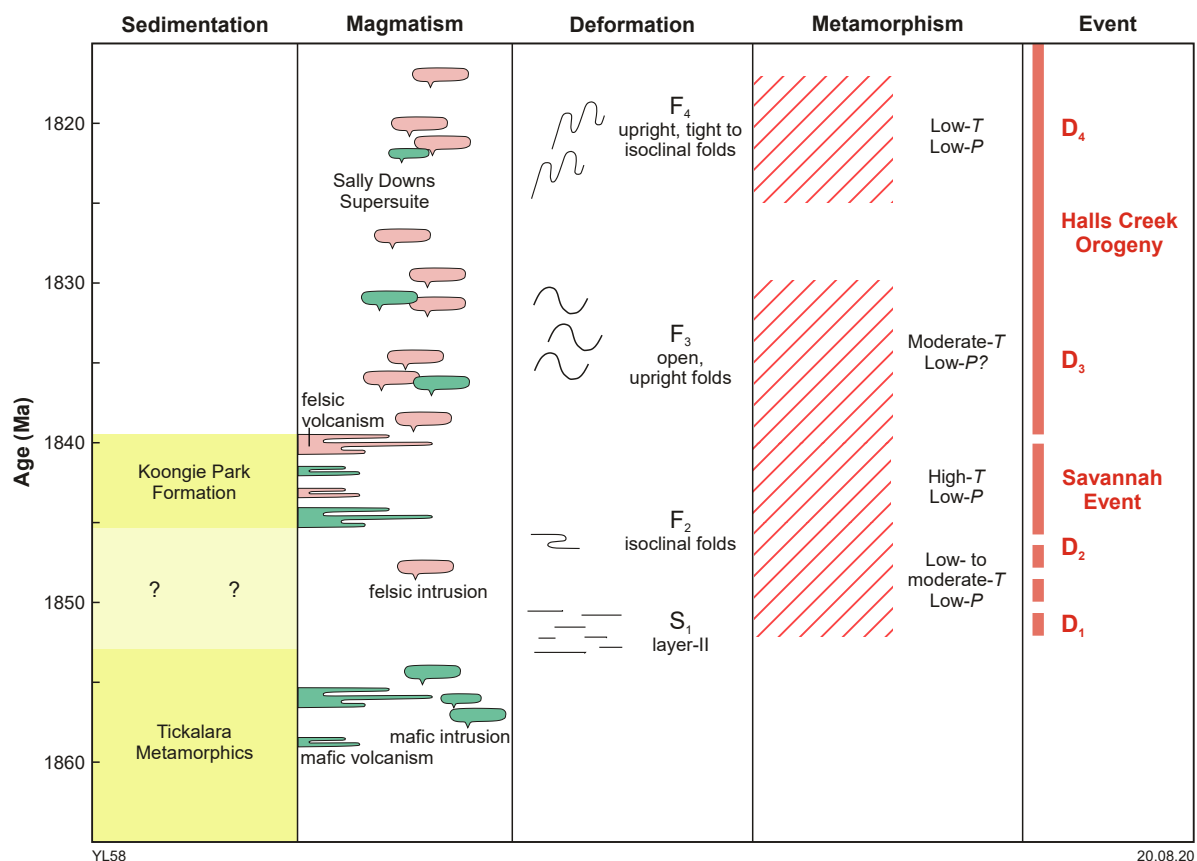


Figure 38. Time–event chart for the Central Zone between 1865 and 1815 Ma

The garnet-bearing, leucocratic Fletcher Creek Granite has previously been used to constrain the timing of tectonism in the Central Zone. It crosscuts  $S_1$ , contains a strong high-grade foliation interpreted as  $S_2$  and is associated with a contact metamorphic aureole overprinted by  $M_2$  metamorphism (Bodorkos et al., 1999; Page et al., 2001). An  $1850 \pm 2$  Ma date for the granite (Page et al., 2001) has been taken as a maximum age for  $D_2$ , but re-dating of the same zircon mount yielded an interpreted igneous age of c. 1838 Ma (Kemp et al., 2015). If the older date represents the crystallization age, it indicates intrusion immediately prior to, or during, the early stages of the Savannah Event and may indicate an extensional origin for  $F_2$  folds. If, however, the Fletcher Creek Granite was emplaced at c. 1838 Ma (near the end of the Savannah Event or in the early stages of the Halls Creek Orogeny), the relative timing of the granite in the broader structural framework would require re-evaluation. Further work is needed to resolve this issue.

In the proposed extensional setting, burial of the Tickalara Metamorphics prior to Savannah Event metamorphism at 1852–1840 Ma could conceivably be a result of sediment loading within a deep sub-basin. The 10–15 km burial depths implied by  $M_2$  metamorphic assemblages in the Tickalara Metamorphics, though significant, are not unrealistic for a rift basin, and a similar mechanism has been proposed as a mechanism for deep burial of Paleozoic supracrustal rocks in the Irindina Province of central Australia (Maidment et al., 2013a; Tucker et al., 2015). Although the burial mechanism remains an open question, one implication of a burial metamorphism scenario is that the original stratigraphic

thickness of the Tickalara Metamorphics would have been much greater than correlative units in the Western and Eastern Zones. A thick succession comprising the Tickalara Metamorphics and Koongie Park Formation may account for the apparent paucity of rocks older than c. 1865 Ma exposed in the Central Zone, despite significant exhumation during subsequent orogenic events.

### 1850–1847 Ma (c. 1838 Ma?) Dougalls Suite

The observation that the Dougalls Suite and Sally Downs Supersuite contain granitic rocks with compositions comparable to those in Phanerozoic magmatic arcs has formed a key line of evidence supporting the interpretation of subduction between the terranes of the Lamboo Province (Ogasawara, 1988; Sheppard et al., 2001). However, the geochemistry of these rocks is not necessarily diagnostic of a particular geodynamic setting and the constraints provided by detrital zircon geochronology suggest that intraplate processes should be considered when assessing their petrogenesis.

Sheppard et al. (2001) identified two compositional subsets of the Dougalls Suite. One group consists of sodic tonalite and trondhjemite with compositions similar to Archean high-Al tonalite–trondhjemite–granodiorite (TTG) suites and Phanerozoic crustal-derived adakites in plate margin settings (Sheppard et al., 2001). The sodic composition, high Sr/Y, low Y, strongly fractionated REE patterns and lack of a negative Eu anomaly in these rocks are consistent

with derivation from partial melting of mafic rocks under conditions where garnet is stable and plagioclase is unstable. Sheppard et al. (2001) suggested that these conditions may have been present at depths  $\geq 40$  km, which would imply unusually thickened crust at the time of emplacement. Alternatively, garnet-present partial melting of mafic rocks could have occurred at shallower depths under more hydrous conditions, which also suppress plagioclase crystallization (Richards, 2011). The second scenario may be more likely for the Central Zone prior to the Halls Creek Orogeny, when the crust is not likely to have been significantly thickened, although mafic underplating may have occurred (Sheppard et al., 2001). The metamorphism of hydrous first-generation sediments in the lower part of the inferred Central Zone rift may have provided a source of fluids that would facilitate partial melting during emplacement of both the Dougalls Suite and Sally Downs Supersuite.

A second, more mafic, component of the Dougalls Suite consists of quartz diorite and mafic tonalite, which has moderate Y and Yb and weakly fractionated REE patterns, consistent with melting of a mafic-dominated source with limited coexisting garnet, possibly at moderate crustal depths (Sheppard et al., 2001).

The limited geochronological data for the Dougalls Suite includes a date of  $1849 \pm 3$  Ma for a sodic, high-Sr/Y component of the Dougalls Tonalite, which is indistinguishable from an  $1850 \pm 2$  Ma date for the garnet-bearing, low-Sr/Y Fletcher Creek Granite (Page et al., 2001). As noted above, re-dating of the zircon mount for the Fletcher Creek Granite yielded a much younger date of c. 1838 Ma, interpreted as an igneous crystallization age (Kemp et al., 2015) and these authors also obtained an indistinguishable c. 1838 Ma date from re-analysis of the Dougalls Tonalite sample. However, the isotope data obtained from the re-analysis of these samples have not been published, making it difficult to assess the validity and significance of these dates. The  $1847 \pm 5$  Ma age for a separate sample of Dougalls Tonalite (GSWA 218350, Lu et al., 2020c) is comparable to the date obtained by Page et al. (2001) but further work may be needed to better constrain the timing of Dougalls Suite magmatism. Metatonalite in the eastern part of the Central Zone previously assigned to the Dougalls Suite (GSWA 218355, Lu et al., 2020f) has a composition that meets the criteria of adakite (Richards and Kerrich, 2007). However, its  $1829 \pm 3$  Ma age indicates that adakitic compositions were also produced after emplacement of the Dougalls Suite as part of the Mabel Downs Suite, which shows compositional overlap with the Dougalls Suite (Sheppard et al., 2001). Thus, two scenarios can be considered: (1) emplacement of the Dougalls Suite immediately prior to, or in the early stages of, the 1852–1840 Ma Savannah Event; and (2) emplacement immediately prior to, or during, the early stages of the 1837–1808 Ma Halls Creek Orogeny.

In the first scenario, sources of 1850–1847 Ma granitic rocks could include lower crustal equivalents of mafic and ultramafic rocks emplaced in the Central Zone between 1865 and 1855 Ma. A dominant component of young mantle-derived material in the source is consistent with the relatively juvenile Sm–Nd and Lu–Hf isotopes and mantle-like oxygen isotopes of the Dougalls Suite (Fig. 39; Sheppard et al., 2001; Kemp et al., 2015), though a smaller component of older crust is also indicated by these data.

In the second scenario, sodic, high-Sr/Y granitic rocks produced at c. 1838 Ma could be sourced from mafic and ultramafic underplate emplaced during 1852–1840 Ma Savannah Event extension as well as those underplates intruded between c. 1865 and 1855 Ma. Granitic magmatism at this time could conceivably have been triggered by the onset of the Halls Creek Orogeny, leading to the partial melting of juvenile, hot mafic underplate in the Central Zone during the early stages of structurally induced crustal thickening. Delamination of a mafic underplate induced by compression is another possible driver for adakitic magmatism (Martin et al., 2005; Moyen, 2009).

A relatively large volume of mafic material in the Central Zone is evident in gravity data, which shows a major positive gravity anomaly in the north-central part of the Halls Creek Orogen (Fig. 40). Some of these mafic rocks are exposed at the surface, but modeling of geophysical data suggests that a significant amount of mafic material is present in the middle to lower crust (Lindsay et al., 2016). The segment of the orogen with the highest gravity values coincides with the segment containing the Dougalls Suite (Fig. 41), which may reflect a relationship between these rocks and older rift-related mafic magmatism.

In an inverted rift scenario, deformation associated with the Halls Creek Orogeny would have been strongly partitioned into the Central Zone, which would have been relatively weak as a result of crustal thinning, magmatism and first-cycle, high-T metamorphism of fertile hydrous sediment during the Savannah Event. Similar partitioning of plate margin strain into a weak intraplate rift has also been invoked for the Paleozoic Alice Springs Orogeny in central Australia (Maidment et al., 2006; Silva et al., 2018).

The relatively high geothermal gradients established in the Central Zone at c. 1845 Ma might also explain the apparent lack of a major topographic high associated with crustal thickening during the Halls Creek Orogeny. Outliers of the Kimberley Basin and correlatives unconformably overlie Lamboo Province rocks that were affected by the Halls Creek Orogeny (Sheppard et al., 1999a, Phillips et al., 2017).

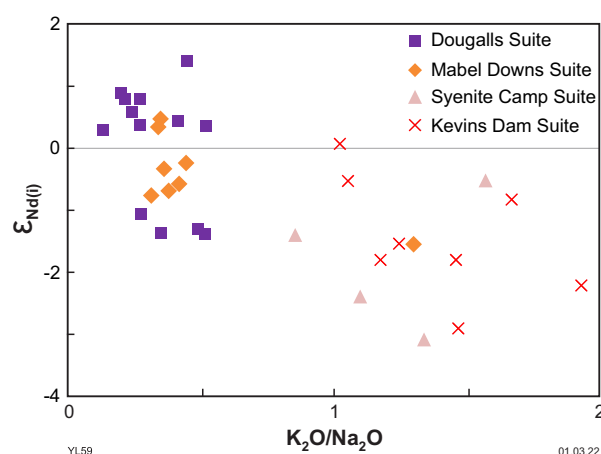
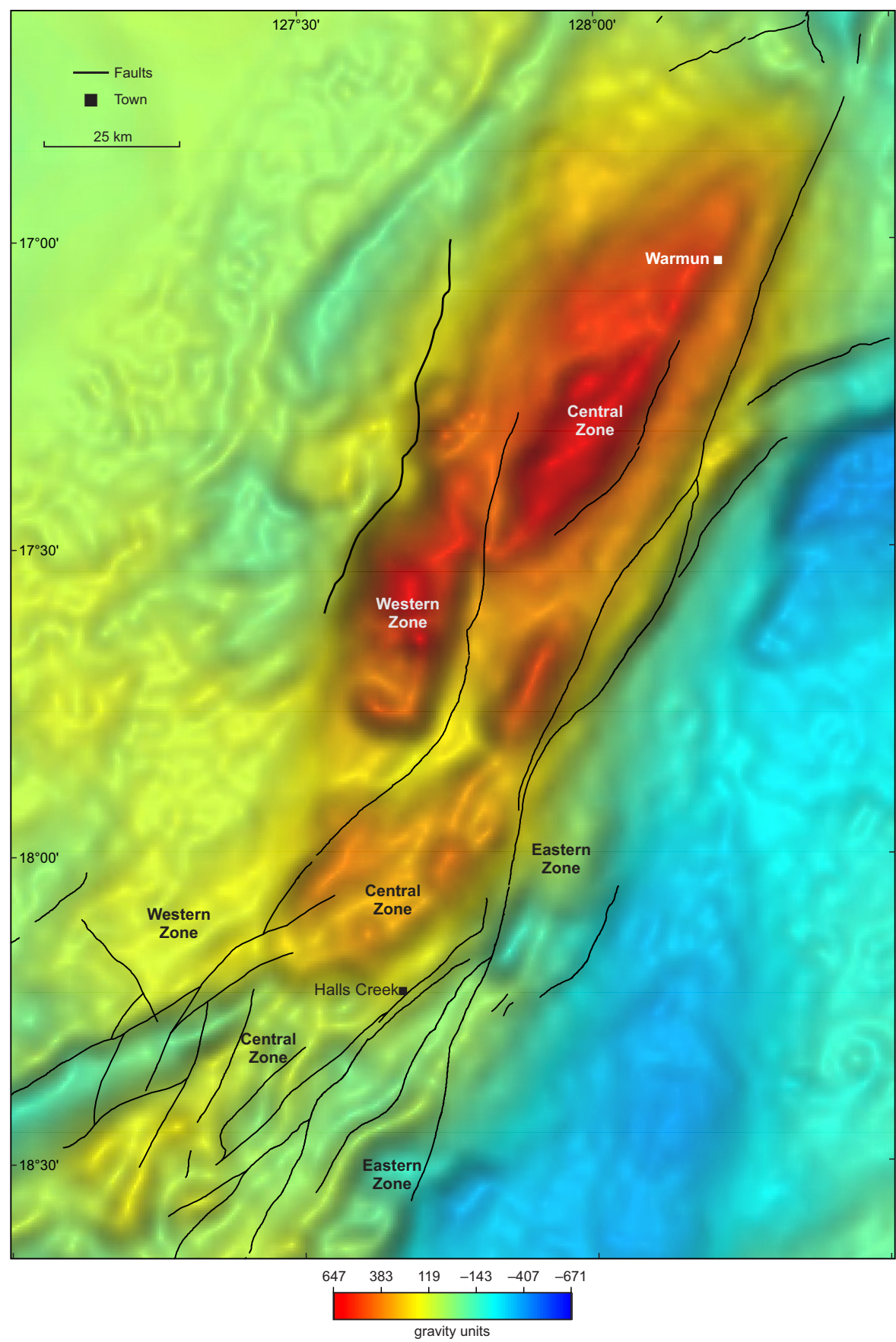


Figure 39. Whole-rock Sm–Nd isotope data for granitic rocks of the 1838–1808 Ma Sally Downs Supersuite, plotting  $\epsilon_{Nd(t)}$  values against  $K_2O/Na_2O$ . Data from GSWA WACHEM database (Appendix 2) and Sheppard et al. (2001). Sodic granitic rocks interpreted to have been derived from rift-related mafic underplate show more juvenile isotope compositions than potassic granitic rocks derived from sources with a larger evolved crustal component





YL60 11.05.22

Figure 40. Bouguer gravity image of the Halls Creek Orogen (Brett, 2019). The major regional-scale gravity high in the central and northern parts of the Central Zone is consistent with a high proportion of mafic material in both the upper crust and at depth. Mafic volcanic rocks in the Eastern Zone are associated with a smaller gravity high, and do not appear to be underlain by similar volumes of mafic material. This possibly reflects development of an intraplate rift that was focused in the Central Zone

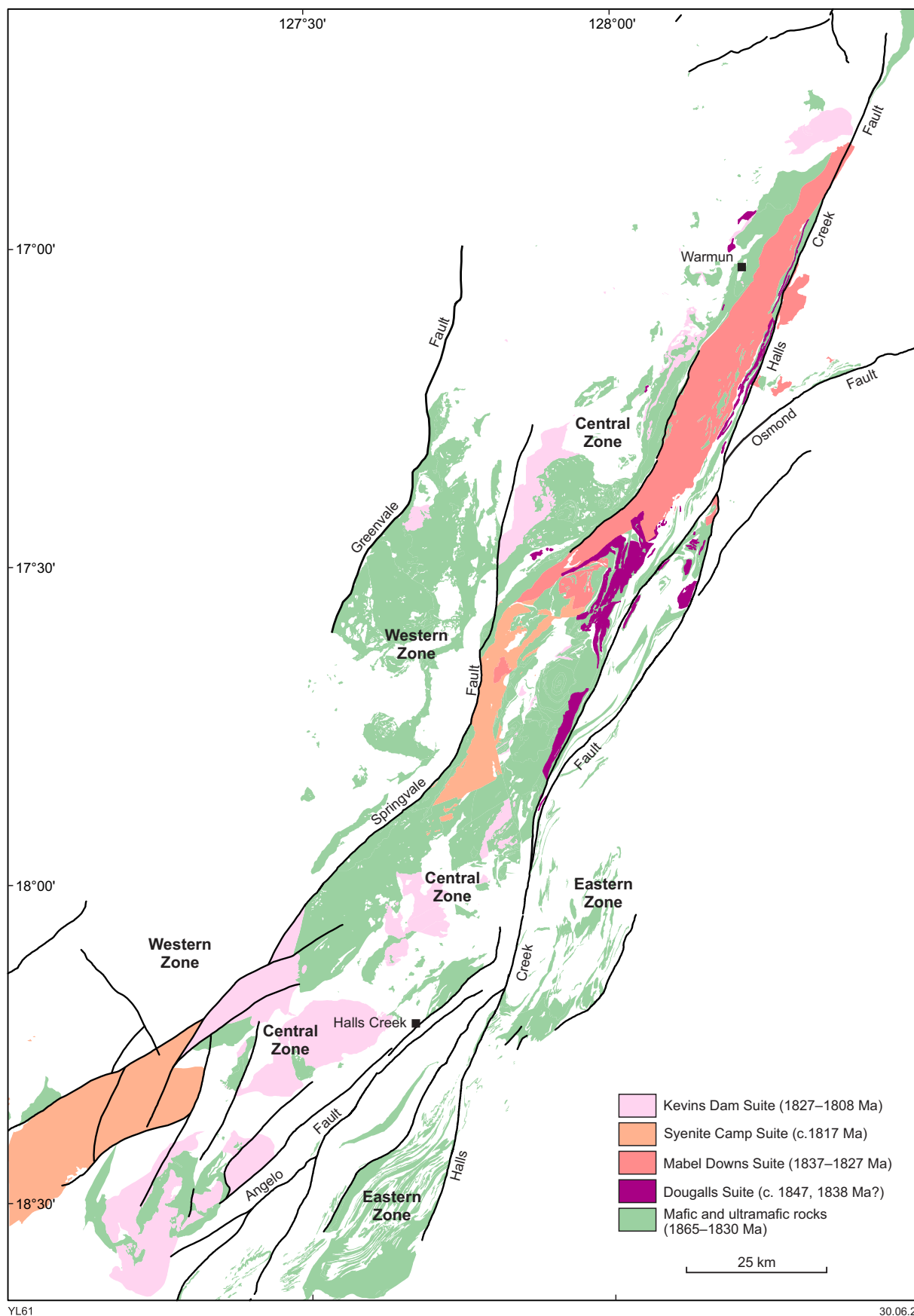


Figure 41. Distribution of 1860–1830 Ma felsic and mafic magmatic rocks in the Halls Creek Orogen, excluding granitic rocks assigned to the Paperbark Supersuite. Sodic, high-Sr/Y granitic rocks of the Dougalls and Mabel Downs Suites developed in a section of the orogen that contained abundant pre- to syn-deformational mafic rocks that are interpreted to have been emplaced in a rift setting. Crustal shortening of this area during the Halls Creek Orogeny possibly resulted in the generation of the sodic granitic rocks by deep melting of mafic-dominated lower crust

The similarities between the lithofacies of the Kimberley Basin sedimentary rocks across the orogen suggest it was not a major topographic high during their deposition, which commenced between c. 1814 and 1795 Ma, shortly after the Halls Creek Orogeny.  $^{40}\text{Ar}/^{39}\text{Ar}$  dating of hornblende, biotite and muscovite in the Central Zone indicates a slow time-averaged cooling rate in the 100 Ma following the Halls Creek Orogeny, implying only a moderate degree of uplift and exhumation as a consequence of orogenesis (Bodorkos and Reddy, 2004). Local topographic influences on sedimentation patterns are inferred for the fluvial to shallow-marine Speewah Group at the base of the Kimberley Basin (Phillips et al., 2017). However, any residual basement topography appears to have been infilled before deposition of flat, sheet-like shallow-marine packages of the Kimberley Group. The lack of substantial crustal thickening, exhumation and uplift during the Halls Creek Orogeny is perhaps unexpected if the orogeny was a result of a continent–continent collision, but is consistent with compressional overprinting of a relatively hot, weak and thinned rift zone, which would be less capable of sustaining significant uplift.

### 1837–1808 Ma Sally Downs Supersuite

Compressional reworking of a juvenile rift has the potential to generate both the adakitic components of the Dougalls Suite and the range of sodic to potassic granitic rocks of the 1837 Ma Sally Downs Supersuite. Sodic, high-Sr/Y tonalites and quartz diorites of the 1832–1827 Ma Mabel Downs Suite share compositional similarities with the Dougalls Suite, but on average have slightly less HREE depletion, slightly higher  $\text{K}_2\text{O}/\text{Na}_2\text{O}$  and less felsic compositions (Ogasawara, 1988; Sheppard et al., 2001). Modelling of Sm–Nd isotope compositions is consistent with a dominant mafic and minor metasedimentary source for the Mabel Downs Suite (Sheppard et al., 2001).

The Syenite Camp and Kevins Dam Suites differ from the Mabel Downs Suite in that they trend towards more potassic compositions with increasing  $\text{SiO}_2$  and were derived from a different source (Sheppard et al., 2001). The Syenite Camp Suite consists of biotite±hornblende granodiorite, tonalite and monzogranite with variable  $\text{K}_2\text{O}/\text{Na}_2\text{O}$  and low to high Sr/Y. The Kevins Dam Suite consists of high-K biotite monzogranite and syenogranite with low Sr/Y. Limited REE fractionation and the presence of negative Eu anomalies in both of these suites are consistent with a paucity of garnet in the source and fractionation of plagioclase. The more potassic compositions are consistent with a lower proportion of mafic rocks in the source, consistent with more evolved Sm–Nd isotope compositions for the Syenite Camp and Kevins Dam Suites (Fig. 39). Dating of the Syenite Camp and Kevins Dam Suites yields ages between 1821 and 1808 Ma (Page et al., 2001), indicating emplacement after the Mabel Downs Suite, in the latter stages of the Halls Creek Orogeny.

Sheppard et al. (2001) noted that the subduction-like components of the Sally Downs Supersuite and Dougalls Suite were coeval with mafic rocks having an intraplate geochemical signature, raising the possibility that the granitic compositions reflect inheritance from an older source rather than contemporaneous subduction. Although these authors favoured a plate margin setting on the basis of differences between the Lamboo Province terranes, the intraplate setting implied by detrital zircon geochronology

suggests that granitic compositions may largely reflect source inheritance and are thus not necessarily diagnostic of geodynamic setting. The nature of the isotopically evolved component of the middle to lower crustal source is not well-constrained, but regionally it is inferred to include a component of Neoproterozoic crust on the basis of isotope and seismic data (Hollis et al., 2015), perhaps comparable to exposures of Neoproterozoic basement in the Tanami Orogen (Whelan et al., 2014).

The transition from partial melting of mafic-dominated crust with the presence of garnet to partial melting of more felsic and isotopically evolved crust lacking garnet during the Halls Creek Orogeny may reflect changes in the thermal structure of the orogen during crustal reworking. Initial partial melting of still-hot, mafic-dominated lower and middle crust during the early stages of the Halls Creek Orogeny would be capable of producing the relatively small-volume adakitic melts of the Dougalls Suite and sodic granitic rocks of the Mabel Downs Suite. As the rift was progressively inverted and deformed, elevated temperatures may have affected higher crustal levels, resulting in more voluminous partial melting of intermediate to felsic crust to produce the potassic granitic rocks of the Kevins Dam and Syenite Camp Suites. In this model, the c. 1837 Ma ages of the oldest granitic rocks in this magmatic event would provide an approximate age for the start of compression associated with the Halls Creek Orogeny.

An inverted rift scenario may also account for the overall bimodal nature of magmatic rocks in the Central Zone, which include only a relatively small component of the intermediate granitic rocks typical of many magmatic arcs (Wyborn and Blake, 2000). Granitic rocks of the Dougalls Suite and Sally Downs Supersuite show an intimate association with mafic igneous rocks, with magma-mingling textures (Figs 18d, 35d–f) indicating that the felsic and mafic magmas were coeval (Blake and Hoatson, 1993; Sheppard, 1996). This coeval bimodal magmatism may reflect a rapid transition between extension and compression, with mafic magmas generated as a result of extension continuing to be emplaced during compressional reworking of the rift.

### Proposed geodynamic evolution of the Lamboo Province

A possible geodynamic evolution of the Lamboo Province is outlined below, incorporating the results of this study and the geological event framework established in previous studies. The development of the province is here interpreted to have taken place within an intraplate setting, in large part on the basis of the constraints provided by detrital zircon dating, but also considering constraints provided by ‘stitching’ intrusions and igneous geochemistry. The interpretation that the dated zircons from the metasedimentary rocks are mostly epiclastic rather than volcanic in nature is a key aspect of this model, with a volcanic interpretation potentially allowing for greater separation between terranes. Differences between the three zones are here considered to reflect spatial variations in tectonism rather than to be evidence of exotic terranes. This interpretation is consistent with a lack of features typically associated with subduction and collision, such as ophiolite slivers, high-*P*–low-*T* metamorphism, abundant intermediate magmas, an accretionary wedge or foreland basin, low-angle thrust



faults, or significant topographic uplift. The model presented here has similarities with aspects of the intraplate models proposed by Hancock and Rutland (1984), Wyborn et al. (1987), Etheridge et al. (1987), Wyborn and Blake (2000) and Shaw et al. (2000), though there are significant differences.

The evolution of the Eastern Zone differs significantly from that of the Central and Western Zones, in that it experienced near-continuous sedimentation during periods of voluminous bimodal magmatism, metamorphism and deformation in the Central and Western Zones (Griffin et al., 2000a). It is possible that this different response was influenced by discontinuities in the underlying Archean basement, which may also be reflected in the differences between the provenance signatures of the older units in the Western Zone / Pine Creek Orogen compared with units of similar age in the Eastern Zone / Granites–Tanami Orogen. A basement discontinuity between the Western and Eastern Zones may have acted as a long-lived influence on younger tectonism, with the Halls Creek Orogen having remained a focus of deformation over an extended period of time. Following the Halls Creek Orogeny, the Halls Creek Orogen marks a change in the character of a belt of 1815–1790 Ma magmatic rocks that extends between the Kimberley region and the southeastern Aileron Province (Maidment et al., 2020). Dominantly mafic rocks of the c. 1793 Ma Hart–Carson Large Igneous Province were emplaced to the northwest of the Halls Creek Orogen and dominantly felsic igneous rocks emplaced to the southeast between c. 1815 and 1790 Ma. Mantle-derived ultramafic intrusive rocks of the c. 1177 Ma Argyle lamproite and the c. 1006 Ma Cummins Range carbonatite are situated near the inferred basement discontinuity, and the east Kimberley is also considered to have formed an eruptive centre for the Cambrian Antrim Plateau Volcanics, the greatest thicknesses of which are preserved immediately east of the Halls Creek Orogen (Glass and Phillips, 2006; Glass et al., 2013). It is also possible that basement influenced the strongly partitioned transpressional reworking of the Halls Creek Orogen during the Paleozoic, although the north-northeasterly trending faults active at this time are oblique to the original northeasterly trend of the Central–Eastern Zone boundary. Geophysics-based models of the present-day character of the lower crust and lithosphere show some differences between these inferred domains (Gunn and Meixner, 1998; Shaw et al., 2000; Aitken et al., 2013; Spratt et al., 2014; Lindsay et al., 2016; Kennett et al., 2018). However, the nature of any difference is difficult to assess due to the lack of basement exposure and the effects of younger tectonism.

The event history outlined below considers the evolution of the province to be the result of extended periods of intraplate extension, sedimentation and magmatism that were punctuated by compressional events (the Hooper and Halls Creek Orogenies). Although the interpretation of the broader geodynamic setting is necessarily speculative, the intraplate setting implied by detrital zircon dating suggests that tectonic drivers were external to the province rather than related to subduction between the constituent crustal elements.

The model presented here thus implies that the assembly of most of the basement elements of the proto-North Australian Craton was complete before c. 1885 Ma, when the large basin system comprising units with the Detrital P signature and their conformably underlying successions was initiated (Maidment et al., 2020). The lack of exposure

of Archean rocks in the North Australian Craton makes it difficult to assess if basement elements developed in proximity to each other or were assembled as a result of subduction and collision. However, geophysical data across the boundary between the Granites–Tanami Orogen and Aileron Province suggest that there was relative motion between some of these basement blocks prior to c. 1885 Ma. In this area, reflection seismic data show two differing basement domains separated by a major structure that has been interpreted to reflect suturing prior to deposition of the Tanami Group (Goleby et al., 2009).

## 1912–1904 Ma – intraplate extension

In the Eastern Zone, bimodal magmatic rocks of the Sophie Downs Suite (Fig. 42a), which include A-type felsic rocks and intercalated volcanoclastic and siliciclastic metasedimentary rocks, represent the oldest known extensional phase (Ogasawara, 1988; Phillips et al., 2016). Although an unconformity separates these rocks from the overlying Halls Creek Group, there is no evidence of a major deformational event at this time (Hancock and Rutland, 1984) and this surface may represent a nonconformity or tilting of the older units during extension. Magmatism may have been localized in the Lamboo Province, because igneous rocks of this age are not known in the Granites–Tanami or Pine Creek Orogens, where Neoarchean basement rocks are exposed.

## 1904–1865 Ma – intraplate (back-arc?) extension

Subsidence and deposition of units dominated by Archean to early Paleoproterozoic detritus (Fig. 42b) are interpreted to reflect regional extension, possibly in a back-arc related to south-directed subduction north of the proto-North Australian Craton, though the broader geodynamic setting remains poorly understood. Sediments may have been largely locally sourced, with variations in detrital zircon spectra reflecting heterogeneous basement geology. Mafic intrusive rocks were emplaced in the Western Zone (Ruins Dolerite) and Central Zone (lower Tickalara Metamorphics), whereas bimodal volcanic rocks were emplaced in the Eastern Zone (Brim Rockhole Formation). Relatively low rates of sedimentation resulted in a significant component of laminated, fine-grained siliciclastic rocks and chemical sedimentary rocks. Sedimentation of similar character and Archean-dominated provenance is regionally widespread, suggesting extension and subsidence was not restricted to the Lamboo Province.

## 1865–1855 Ma – intraplate (back-arc?) extension, c. 1865 Ma Hooper Orogeny

Extension, sedimentation and magmatism in the Lamboo Province were interrupted in the west by transient compressional deformation of the c. 1865 Ma Hooper Orogeny (Fig. 42c). The effects of this deformation were not significant in the east and it may have been related to plate margin interactions to the north or northwest of the Lamboo Province. Emplacement of granitic and mafic rocks of the Paperbark Supersuite in the Western Zone was a consequence of high geothermal gradients established during extension, but magmatism continued during crustal shortening in the Wunaamin Miliwundi Orogen.

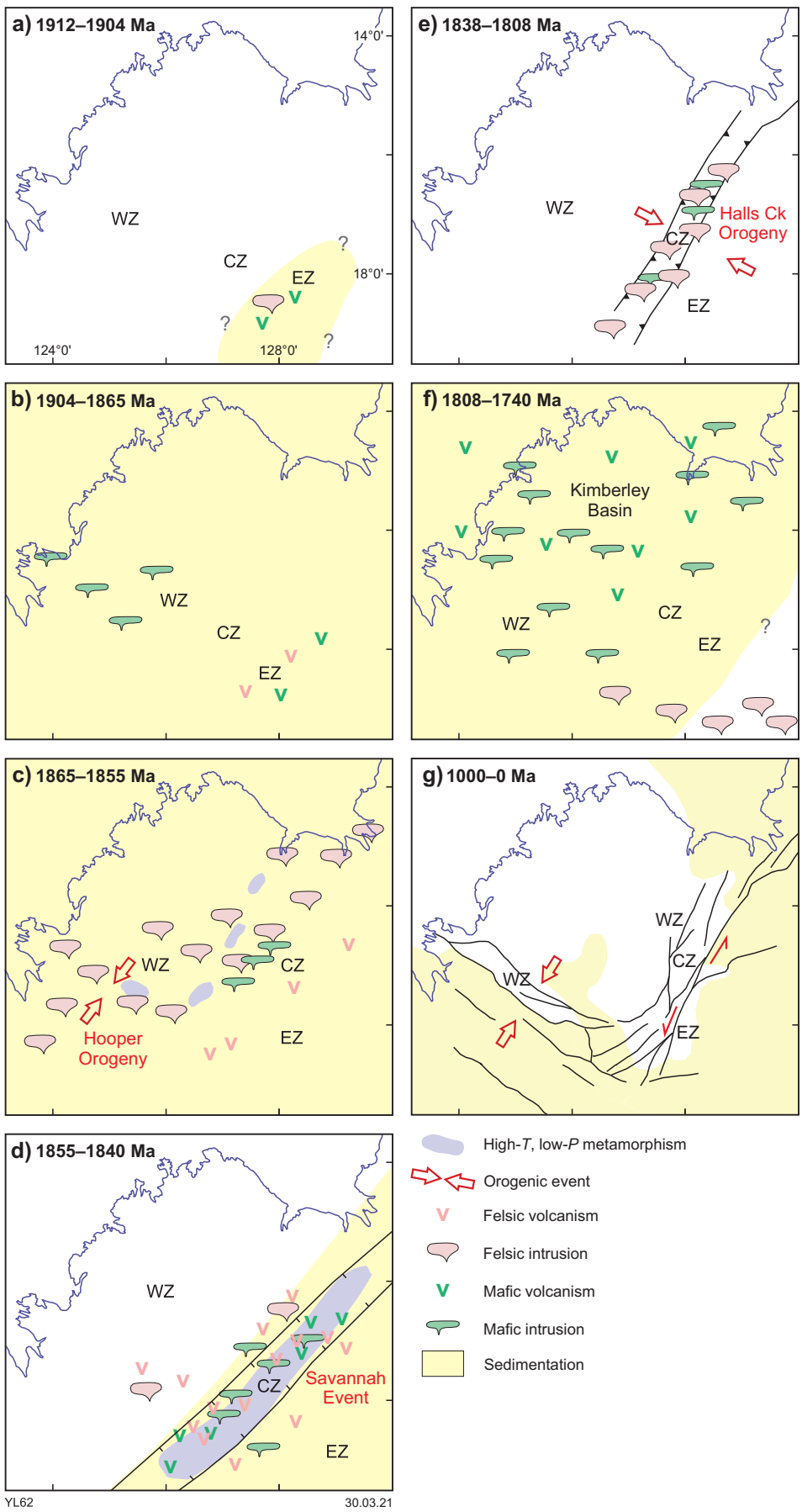


Figure 42. Schematic evolution of the Lamboo Province: a) intraplate extension, bimodal magmatism of the Sophie Downs Suite; b) subsidence (back-arc?), deposition of Marboo Formation Unit 1, Saunders Creek Formation, Brim Rockhole Formation and older Tickalara Metamorphics; c) onset Detrital P provenance sedimentation (Marboo Formation Unit 2, Tickalara Metamorphics, Biscay Formation), bimodal magmatism in Western Zone, mafic magmatism in Central and Eastern Zones, transient compressional event in Western Zone at c. 1860 Ma; d) extension partitioned into Central Zone rift, deposition of Tickalara Metamorphics, Koongie Park Formation and Olympio Formation, mafic magmatism in Western Zone, bimodal magmatism and high-T, low-P metamorphism in Central Zone, alkaline felsic volcanism in Eastern Zone; e) compression partitioned into Central Zone during Halls Creek Orogeny, emplacement of Dougalls Suite and Sally Downs Supersuite; f) regional subsidence and deposition of Kimberley Basin; g) multiple orogenic events  $\leq 1000$  Ma (Yampi, Wunaamin Miliwundi and Alice Springs Orogenies), exhumation of Lamboo Province. Abbreviations: WZ, Western Zone; CZ, Central Zone; EZ, Eastern Zone

Paperbark Supersuite granites locally extended into the Central Zone, and may delineate a domain of greater crustal thinning or delamination of a mafic underplate. Large, extension-related mafic–ultramafic intrusions were emplaced in the Western and Central Zones, and mafic volcanic rocks were erupted in the Central and Eastern Zones. Lesser alkaline felsic volcanic rocks in the Eastern Zone may indicate lower degrees of extension in this part of the province.

Compositionally immature turbiditic sedimentary rocks with the Detrital P provenance were deposited across the province (Marboo Formation Unit 2, Tickalara Metamorphics and Biscay Formation). These sediments may have been sourced from an orogen north of the Lamboo Province, a part of which may be preserved in the eastern Pine Creek Orogen and Arnhem Province in the northeastern North Australian Craton. Thick turbiditic successions with Detrital P provenance signatures were deposited over most of the proto-North Australian Craton, implying the presence of a major uplifted hinterland. One potential scenario involves collisional reworking of a magmatic belt to the north and northwest of the currently preserved craton margins.

### **1855–1840 Ma – Central Zone rift, Savannah Event**

The locus of extension shifted and was partitioned into the Central Zone, culminating in the emplacement of layered mafic–ultramafic intrusions, bimodal volcanism (in the Koongie Park Formation) and high-*T*, low-*P* metamorphism at deeper crustal levels during the 1852–1840 Ma Savannah Event (Fig. 42d). The partitioning of extension was possibly due to the crust in the Western Zone becoming stronger following metamorphism, dehydration and generation of the voluminous magmatic rocks of the Paperbark Supersuite. Deposition of turbiditic sedimentary rocks with Detrital P provenance continued in the Central and Eastern Zones (Tickalara Metamorphics and Olympio Formations). In the Eastern Zone, alkaline felsic volcanic rocks emplaced at c. 1846 Ma and mafic sills of the Woodward Dolerite may be related to Central Zone rifting. Felsic volcanic rocks of the 1857–1854 Ma Whitewater Volcanics form the youngest supracrustal rocks in the Western Zone, which did not apparently experience significant subsidence during this period. The trend of the inferred rift is considered to have been broadly northeast–southwest and it may have extended into an area south of the Wunaamin Miliwundi Orogen now covered by the Canning Basin (Frogtech Geoscience, 2017).

### **1838–1808 Ma – rift inversion, Halls Creek Orogeny**

Deformation during the intraplate Halls Creek Orogeny was partitioned into the Central Zone rift (Fig. 42e), which would have formed a rheologically weak domain due to the thermal effects of extension. The onset of deformation is interpreted to coincide with the emplacement of granitic rocks at c. 1837 Ma and to have ceased between c. 1817 and 1808 Ma (Page et al., 2001). The Halls Creek Orogeny may have been the result of a terrane accretion event or subduction of buoyant crust to the northwest of the Lamboo Province, but there are few constraints on possible drivers.

Deformation was regional in extent, affecting the Wunaamin Miliwundi Orogen and areas as far east as the Granites–Tanami Orogen, where this deformation is known as the Tanami Orogeny (Crispe et al., 2007; Huston et al., 2007). The presence of two phases of folding with differing orientations indicates the orogeny was a complex, multi-phase event.

Sedimentation in the Lamboo Province ceased during the Halls Creek Orogeny, but uplift and exhumation appears to have been limited. Granitic and mafic rocks of the Sally Downs Supersuite were emplaced in the Central Zone, localized by the high geothermal gradient inherited from extension. Sodic granitic rocks of adakitic composition are interpreted to have been derived from deep partial melting of a still-hot mafic–ultramafic underplate emplaced during rifting, either by structural thickening or delamination. Potassic granitic rocks were sourced from shallower crustal depths later in the orogenic cycle, incorporating a larger proportion of intermediate-composition Archean crust.

### **1808–1740 Ma – regional extension and subsidence, Kimberley Basin**

Fluvial to shallow-marine sedimentary rocks of the lower Kimberley Basin were deposited across the Halls Creek Orogen after c. 1814 Ma (Fig. 42f), before emplacement of the c. 1793 Ma Hart–Carson LIP. Basin formation may reflect a re-establishment of the extensional regime that existed prior to the Halls Creek Orogeny, but the regional distribution of tectonism at this time suggests a different driver, possibly related to the southern plate margin of the proto-North Australian Craton (Maidment et al., 2020).

### **Neoproterozoic–Paleozoic deformation – Yampi, Wunaamin Miliwundi, Alice Springs Orogenies**

After 1800 Ma, several deformational events at relatively low metamorphic grades caused exhumation of the Lamboo Province in the Halls Creek and Wunaamin Miliwundi Orogens (Fig. 42g). The number, timing and nature of structural events is not well understood, but most exhumation in the Wunaamin Miliwundi Orogen appears to be related to the 590–500 Ma Wunaamin Miliwundi Orogeny, whereas significant strike-slip deformation in the Halls Creek Orogen during the 450–295 Ma Alice Springs Orogeny resulted in uplift and syn-orogenic sedimentation adjacent to the orogen. The near-orthogonal trends of Lamboo Province exposures in the Wunaamin Miliwundi and Halls Creek Orogens are due in part to these younger deformational events and the obscuring effects of sedimentary basins (though likely influenced by older basement structures) and are not considered to represent a Paleoproterozoic orocline (cf. Betts et al., 2016).

### **Geodynamic context of mineral systems**

The intraplate setting proposed here for the development of the Lamboo Province provides a significantly different context for mineral systems than models involving subduction and collision. If the Lamboo Province developed



well inboard of a plate margin, there would be limited potential for magmatic arc porphyry- and related epithermal-style deposits, though significant uplift and exhumation in the Central Zone would reduce their preservation potential in any case (Occhipinti et al., 2016). The Mount Angelo Cu (Zn–Mo–Ag–Au) prospect in the Central Zone consists of a zone of disseminated mineralization associated with silicic, sericitic and chloritic alteration in the Angelo Microgranite and has been interpreted as a possible porphyry-Cu-style deposit (Sanders, 1999; Hassan, 2000). However, it is not certain that this is a typical arc-related porphyry-style deposit. The Angelo Microgranite has comparable chemistry to the A-type felsic volcanic rocks of the Koongie Park Formation that it intrudes and is considered to be a shallow-level intrusive equivalent of these rocks (Sheppard et al., 1995; Orth, 2002). If mineralization is related to the microgranite, it may represent an intrusion-related style associated with Savannah Event rifting, rather than a porphyry Cu system.

Occurrences of Cu–Pb–Zn–Ag volcanogenic massive sulfide (VMS) mineralization in the Central and Eastern Zones coincide with periods of extension, crustal thinning and felsic and mafic volcanism. The largest deposits are located within the rift-related Koongie Park Formation of the Central Zone, whereas Zn–Cu–Pb–Ag–Au mineralization at the Little Mount Isa, Twin Hills and Ilmars Zn–Cu–Au prospects is hosted by the Brim Rockhole Formation, which is interpreted to have been deposited during an older phase of extension. An association between mineralization and felsic volcanic rocks may be indicative of periods of greater crustal attenuation and heat flow, producing felsic crustal melts and shallow-level hydrothermal systems. Fewer VMS occurrences are known in successions lacking felsic volcanic rocks, such as the Tickalara Metamorphics and Biscay Formation, though it is possible that rapid rates of sedimentation in these units might have inhibited massive sulfide accumulation.

The Ni–Cu–Co and PGE mineral systems associated with the emplacement of 1857–1823 Ma mafic–ultramafic intrusions in the Halls Creek Orogen have commonly been interpreted in the context of subduction, arc formation and collision (e.g. Lindsay et al., 2016; Occhipinti et al., 2016, 2017; Kohanpour et al., 2018; Mole et al., 2018). In the model proposed in this study, this magmatism is considered to be a result of a prolonged intraplate extension, with emplacement of the Ni–Cu–Co-mineralized Sally Malay intrusion at c. 1842 Ma during Savannah Event rifting and emplacement of the c. 1823 Ma Copernicus intrusion as part of rift inversion during the Halls Creek Orogeny. Cu–Ni mineralization in the Ruins Dolerite was also associated with intraplate extension, but represents a distinct older phase of magmatism, though potentially emplaced in a similar geodynamic setting to the 1857–1842 Ma mafic–ultramafic rocks in the eastern part of the province.

Orogenic gold mineralization occurs in all three zones in the southern Halls Creek Orogen, with numerous occurrences forming a northeasterly trending belt in the Eastern Zone, 7–12 km east of the faulted contact with the Central Zone (Hassan, 2000). In the Central Zone, significant mineralization occurs at the Nicolson's deposit in the Koongie Park Formation. The present spatial distribution of occurrences may be influenced by differences in the degree of exhumation, with greenschist facies rocks of the Eastern Zone and southern Central Zone preserving

mineralization, whereas higher grade metamorphic rocks exhumed from greater depths in the central and northern parts of the orogen have few occurrences. Mineralization was driven by deformation of the Halls Creek Orogeny (Kohanpour et al., 2019b), which is here interpreted to have been focused on a juvenile rift developed on a boundary between Archean basement domains. The large amount of mafic and ultramafic material in the lower crust may have provided a source for gold, which was transported to higher crustal levels along interpreted steep lithospheric-scale structures (e.g. Shaw et al., 2000; Kohanpour et al., 2018). Alternatively, gold might have been sourced from low-degree partial melting of a metasomatized mantle source during the Halls Creek Orogeny, facilitated by an elevated heat flow developed during earlier rifting. As discussed above, the timing, distribution and driver of mantle metasomatism is largely unconstrained, and can be accommodated in both intraplate and collisional models.

Many of the diamondiferous lamproite and kimberlite intrusions in the Kimberley region are situated around the structurally reworked margins of the Kimberley Basin (Fig. 10), which formed a relatively stable domain from c. 1800 Ma (Hassan, 2000, 2004; Jaques and Milligan, 2004; Hutchison, 2018). The basement to the Kimberley Basin has previously been interpreted as a rigid Archean craton that collided with the proto-North Australian Craton during the Halls Creek Orogeny (e.g. Tyler et al., 1995, 2012; Griffin et al., 2000a; Lindsay et al., 2016). In the intraplate model presented here, the Archean crust beneath the Kimberley Basin comprised a para-autochthonous basement component of the proto-North Australian Craton and may have been reworked by the same Paleoproterozoic processes that produced the Paperbark Supersuite magmatic rocks exposed along the uplifted basin margins. If this is the case, it is possible that the rigid character of this domain only developed after emplacement of these voluminous igneous rocks. Nevertheless, the major crustal structures that controlled lamproite and kimberlite emplacement were probably controlled to some degree by basement heterogeneities, which may reflect a largely unknown history of Archean terrane assembly.

## Conclusions

U–Pb dating and Lu–Hf isotopes of detrital zircons from metasedimentary rocks of the Lamboo Province demonstrate marked similarities in units deposited prior to the 1837–1808 Ma Halls Creek Orogeny, an event previously interpreted to reflect collision of an exotic terrane with the proto-North Australian Craton. The oldest metasedimentary rocks contain a range of Neoproterozoic to Paleoproterozoic age components that may reflect the ages of local basement rocks. After 1870–1865 Ma, the metasedimentary successions in all three zones show remarkably uniform detrital zircon age spectra, with a dominant 1875–1860 Ma age component and a minor c. 2500 Ma component, and have similarly restricted ranges of Lu–Hf isotope values. The depositional ages and provenance signatures of these rocks are comparable with units of similar age elsewhere in the North Australian Craton. This suggests that the Western and Central Zones are not exotic with respect to the North Australian Craton and implies that differences between the three zones reflect spatial differences in intraplate tectonism during the evolution of the province.

The geochemical and isotopic characteristics of 1875–1840 Ma bimodal intrusive and extrusive igneous rocks in the Halls Creek Orogen are consistent with emplacement in a dominantly extensional setting, possibly an intraplate rift or back-arc developed inboard of a plate margin to the north of the Lamboo Province. Transient shortening during the c. 1865 Ma Hooper Orogeny punctuated this extensional regime, and was possibly a result of distal plate margin interactions. Bimodal magmatism, sedimentation and high-*T*, low-*P* metamorphism focused in the Central Zone between 1857 and 1840 Ma is interpreted to reflect partitioning of extension into a northeasterly trending intraplate rift. Intraplate reworking of this hot rift during the Halls Creek Orogeny produced a range of sodic to potassic granitic rocks, reflecting variable contributions of juvenile mafic–ultramafic underplate and Archean crust of intermediate composition.

## References

- Adlakha, V, Patel, RC and Lal, N 2013, Exhumation and mechanisms: a review of exhumation studies in the Himalaya: *Journal of the Geological Society of India*, v. 81, p. 481–502.
- Ahmad, M and Hollis, JA 2013, Chapter 5: Pine Creek Orogen, *in* *Geology and mineral resources of the Northern Territory compiled by M Ahmad and TJ Munson*: Northern Territory Geological Survey, Special Publication 5, p. 5:1–5:133.
- Ahmad, M, Hollis, JA and Glass, LM 2013, Chapter 4: Archaean, *in* *Geology and mineral resources of the Northern Territory compiled by M Ahmad and TJ Munson*: Northern Territory Geological Survey, Special Publication 5, p. 4:1–4:9.
- Aitken, ARA, Occhipinti, SA, Lindsay, MD, Joly, A, Howard, HM, Johnson, SP, Hollis, JA, Spaggiari, CV, Tyler, IM, McCuaig, TC and Dentith, MC 2018, The tectonics and mineral systems of Proterozoic Western Australia: relationships with supercontinents and global secular change: *Geoscience Frontiers*, v. 9, no. 2, p. 295–316.
- Aitken, ARA, Salmon, M and Kennett, B 2013, Australia's Moho: A test of the usefulness of gravity modelling for the determination of Moho depth: *Tectonophysics*, v. 609, p. 468–479.
- Alessio, KL, Hand, M, Kelsey, DE, Williams, MA, Morrissey, LJ and Barovich, K 2018, Conservation of deep crustal heat production: *Geology*, v. 46, p. 335–338.
- Bagas, L, Anderson, JAC and Bierlein, FP 2009, Palaeoproterozoic evolution of the Killi Killi Formation and orogenic mineralization in Granites–Tanami Orogen, Western Australia: *Ore Geology Reviews*, v. 35, p. 47–67.
- Bagas, L, Bierlein, FP, English, L, Anderson, J, Maidment, D and Huston, DL 2008, An example of a Paleoproterozoic back-arc basin: petrology and geochemistry of the ca. 1864 Ma Stubbins Formation as an aid towards an improved understanding of the Tanami Orogen, Western Australia: *Precambrian Research*, v. 166, no. 1–4, p. 168–184.
- Bagas, L, Boucher, R, Li, B, Miller, J, Hill, P, Depauw, G, Pascoe, J and Eggers, B 2014, Paleoproterozoic stratigraphy and gold mineralisation in the Granites–Tanami Orogen, North Australian Craton: *Australian Journal of Earth Sciences*, v. 61, p. 89–111.
- Barham, M, Kirkland, CL and Danišik, M 2019, Assessing volcanic origins within detrital zircon populations – A case study from the Mesozoic non-volcanic margin of southern Australia: *Geoscience Frontiers*, v. 10, p. 1371–1381.
- Barham, M, Kirkland, CL, Reynolds, S, O'Leary, MJ, Evans, NJ, Allen, H, Haines, PW, Hocking, RM, McDonald, BJ, Belousova, E and Goodall, J 2016, The answers are blowin' in the wind: Ultra-distal ashfall zircons, indicators of Cretaceous super-eruptions in eastern Gondwana: *Geology*, v. 44, p. 643–646.
- Barnes, SJ, Williams, M, Smithies, RH, Hanski, E and Lowrey, J 2021, Trace element contents of mantle-derived magmas through time: *Journal of Petrology*, v. 62, p. 1–38.
- Bennett, R and Gellatly, DC 1970, Rb–Sr age determinations of some rocks from the West Kimberley Region, Western Australia: Bureau of Mineral Resources, Geology and Geophysics, Record 1970/20, 27p.
- Betts, PG, Armit, RJ, Stewart, J, Aitken, ARA, Ailleres, L, Donchak, P, Hutton, L, Withnall, I and Giles, D 2016, Australia and Nuna: Geological Society of London Special Publication, v. 424 (Supercontinent cycles through Earth history), p. 47–81, doi:10.1144/SP424.2.
- Betts, PG, Giles, D, Lister, GS and Frick R 2002, Evolution of the Australian lithosphere: *Australian Journal of Earth Sciences*, v. 49, p. 661–695.
- Blake, DH and Hoatson, DM 1993, Granite, gabbro, and migmatite field relationships in the Proterozoic Lamboo Complex of the East Kimberley region: AGSO *Journal of Australian Geology and Geophysics*, v. 14, p. 319–330.
- Blake, DH, Tyler, IM, Griffin, TJ, Sheppard, S, Thorne, AM and Warren, RG 1999, Geology of the Halls Creek 1:100 000 Sheet area (4461), Western Australia: Australian Geological Survey Organisation, Explanatory Notes, 36p.
- Blake, DH, Tyler, IM and Warren, RG 2000, Gordon Downs, Western Australia – 1:250 000 Geological Series (2nd edition): Australian Geological Survey Organisation, Explanatory Notes SE/52-10, 58p.
- Bodorkos, S, Beyer, EE, Edgoose, CJ, Whelan, JA, Webb, G, Vandenberg, LC and Hallett, L 2013, Summary of results. Joint NTGS–GA geochronology project: central and eastern Arunta Region, January 2008 – June 2011: Northern Territory Geological Survey, Record 2013-003, 74p.
- Bodorkos, S, Cawood, PA and Oliver, NHS 2000a, Timing and duration of synmagmatic deformation in the Mabel Downs Tonalite, northern Australia: *Journal of Structural Geology*, v. 22, p. 1181–1198.
- Bodorkos, S, Cawood, PA, Oliver, NHS and Nemchin, AA 2000b, Rapidity of orogenesis in the Paleoproterozoic Halls Creek Orogen, northern Australia: evidence from SHRIMP zircon data, CL zircon images, and mixture modeling studies: *American Journal of Science*, v. 300, no. 1, p. 60–82.
- Bodorkos, S, Oliver, NHS and Cawood, PA 1999, Thermal evolution of the central Halls Creek Orogen, northern Australia: *Australian Journal of Earth Sciences*, v. 46, p. 453–465.
- Bodorkos, S and Reddy, SM 2004, Proterozoic cooling and exhumation of the northern central Halls Creek Orogen, Western Australia: constraints from a reconnaissance <sup>40</sup>Ar/<sup>39</sup>Ar study: *Australian Journal of Earth Sciences*, v. 51, no. 4, p. 561–609.
- Bodorkos, S, Sandiford, M, Oliver, NHS and Cawood, P 2002, High-*T*, low-*P* metamorphism in the Palaeoproterozoic Halls Creek Orogen, northern Australia: the middle crustal response to a mantle-related transient thermal pulse: *Journal of Metamorphic Geology*, v. 20, p. 217–237.
- Boudreau, AE and Hoatson, DM 2004, Halogen variations in the Paleoproterozoic layered mafic–ultramafic intrusions of East Kimberley, Western Australia: implications for platinum group element mineralization: *Economic Geology*, v. 99, no. 5, p. 1015–1026.
- Bouvier, A, Vervoort, JD and Patchett, PJ 2008, The Lu–Hf and Sm–Nd isotopic composition of CHUR: Constraints from unequilibrated chondrites and implications for the bulk composition of terrestrial planets: *Earth and Planetary Science Letters*, v. 273, p. 48–57.
- Boxer, GL, Jaques, AL and Rayner, MJ 2017, Argyle (AK1) diamond deposit, *in* *Australian ore deposits edited by GN Phillips*: Australasian Institute of Mining and Metallurgy, Melbourne, Monograph 32, p. 527–532.
- Braun, J, McQueen, H and Etheridge, M 1991, A fresh look at the Late Palaeozoic tectonic history of western-central Australia: *Exploration Geophysics*, v. 22, p. 49–54.
- Brett, JW 2018, 80 m radiometric merged grids of Western Australia 2018 version 1: Geological Survey of Western Australia, <www.dmp.wa.gov.au/geophysics>.

- Brett, JW 2019, 400 m Bouguer gravity merged grid of Western Australia 2019 version 1: Geological Survey of Western Australia, <www.dmp.wa.gov.au/geophysics>.
- Budd, AR, Wyborn, LAI and Bastrakova, IV 2001, The metallogenic potential of Australian Proterozoic granites: Geoscience Australia, Record 2001/12, 152p.
- Buxton Resources Ltd 2018, West Kimberley exploration update: Report to Australian Securities Exchange, 15 May 2018, 10p.
- Carson, CJ 2013, The Victoria and Birrindudu Basins, Victoria River region, Northern Territory, Australia: a SHRIMP U–Pb detrital zircon and Sm–Nd study: Australian Journal of Earth Sciences, v. 60, p. 175–196, doi:10.1080/08120099.2013.772920.
- Carson, CJ, Claoué-Long, J, Stern, R, Close, DF, Scrimgeour, IR and Glass, LM 2009, Summary of results. Joint NTGS–GA geochronology project: Central and eastern Arunta Region and Pine Creek Orogen, July 2006 – May 2007 (CD): Northern Territory Geological Survey, Record 2009-001.
- Carson, CJ, Hollis, JA, Glass, LM, Close, DF, Whelan, JA and Wygralak, A 2011, Summary of results. Joint NTGS–GA geochronology project: Pine Creek Orogen, eastern Arunta Region, Murphy Inlier and Amadeus Basin, July 2007 – June 2009: Northern Territory Geological Survey, Record 2010-004, 84p.
- Carson, CJ, Worden, KE, Scrimgeour, IR and Stern, RA 2008, The Palaeoproterozoic evolution of the Litchfield Province, western Pine Creek Orogen, northern Australia: Insight from SHRIMP U–Pb zircon and in situ monazite geochronology: Precambrian Research, v. 166, p. 145–167.
- Carter, LC, Williamson, BJ, Tapster, SR, Costa, C, Grime, GW and Rollinson, GK 2021, Crystal mush dykes as conduits for mineralising fluids in the Yerington porphyry copper district, Nevada: Communications, Earth and Environment, v. 2, 59.
- Castillo, PR 2012, Adakite petrogenesis: Lithos, v. 134–135, p. 304–316.
- Cawood, PA and Korsch, RJ 2008, Assembling Australia: Proterozoic building of a continent: Precambrian Research, v. 166, no. 1–4, p. 1–38.
- Claoué-Long, JC, Edgoose, C and Worden, K 2008, A correlation of Aileron Province stratigraphy in central Australia: Precambrian Research, v. 166, no. 1–4, p. 230–245.
- Coats, RP and Preiss, WV 1980, Stratigraphic and geochronological reinterpretation of late Proterozoic glaciogenic sequences in the Kimberley region, Western Australia: Precambrian Research, v. 13, p. 181–208.
- Compston, DM 1995, Time constraints on the evolution of the Tennant Creek Block, northern Australia: Precambrian Research, v. 71, p. 107–129.
- Crispe, AJ, Vandenberg, LC and Scrimgeour, IR 2007, Geological framework of the Archean and Paleoproterozoic Tanami Region, Northern Territory: Mineralium Deposita, v. 42, p. 3–26.
- Cross, A, Claoué-Long, JC, Scrimgeour, IR, Ahmad, M and Kruse, PD 2005a, Summary of results, Joint NTGS–GA geochronology project: Rum Jungle, basement to southern Georgina Basin and eastern Arunta Region 2001–2003: Northern Territory Geological Survey, Record 2005-006, 42p.
- Cross, A, Claoué-Long, JC, Scrimgeour, IR, Close, DF and Edgoose, CJ 2005b, Summary of results. Joint NTGS–GA geochronology project: southern Arunta Region: Northern Territory Geological Survey, Record 2004-003, 61p.
- Cross, AJ and Crispe, AJ 2007, SHRIMP U–Pb analyses of detrital zircon: a window to understanding the Paleoproterozoic development of the Tanami Region, northern Australia: Mineralium Deposita, v. 42, p. 27–50.
- DeBievre, P and Taylor, PDP 1993, Table of the isotopic composition of the elements: International Journal of Mass Spectrometry and Ion Processes, v. 123, p. 149.
- de Vries, ST, Pryer, LL and Fry, N 2008, Evolution of the Neoarchaeon and Proterozoic basins of Australia: Precambrian Research, v. 166, p. 39–53.
- Dilles, JH 1987, Petrology of the Yerington Batholith, Nevada; evidence for evolution of porphyry copper ore fluids: Economic Geology, v. 82, p. 1750–1789.
- Donnellan, N 2013, Chapter 9: Warramunga Province, in Geology and mineral resources of the Northern Territory compiled by M Ahmad and TJ Munson: Northern Territory Geological Survey, Special Publication 5, p. 9:1–9:61.
- Dow, DB and Gemuts, I 1967, Dixon Range, Western Australia – 1:250 000 Geological Series: Bureau of Mineral Resources, Australia, Explanatory Notes SE/52-6, 15p.
- Dow, DB and Gemuts, I 1969, Geology of the Kimberley region, Western Australia: the East Kimberley: Geological Survey of Western Australia, Bulletin 120, 135p.
- Dow, DB, Gemuts, I, Plumb, KA and Dunnet, D 1964, The Geology of the Ord River region, Western Australia: Australian Bureau of Mineral Resources, Geology and Geophysics, Record 1964/104, 164p.
- Downes, PJ, Dunkley, DJ, Fletcher, IR, McNaughton, NJ, Rasmussen, B, Jaques, AL, Verrall, M and Sweetapple, MT 2016, Zirconolite, zircon and monazite-(Ce) U–Th–Pb age constraints on the emplacement, deformation and alteration history of the Cummins Range Carbonatite Complex, Kimberley region, Western Australia: Mineralogy and Petrology, v. 110, no. 2, p. 199–222.
- Etheridge, MA, Rutland, RWR and Wyborn, LA 1987, Orogenesis and tectonic process in the early to middle Proterozoic of northern Australia, in Proterozoic lithospheric evolution edited by A Kröner: American Geophysical Union, Washington, DC, p. 131–147.
- Fielding, IOH, Korhonen, FJ, Romano, SS, Evans, NJ and Roberts, MP 2020a, The last gasp of King Leopold: new insights into the evolution of the west Kimberley, in GSWA 2020 extended abstracts: advancing the prospectivity of Western Australia: Geological Survey of Western Australia, Record 2020/2, p. 1–3.
- Fielding, IOH, Wingate, MTD, Fisher, CM, Maidment, DW and Phillips, C 2022, 218321: pelitic gneiss, Winnama Yard; Geochronology Record 1873: Geological Survey of Western Australia, 5p.
- Fielding, IOH, Wingate, MTD, Lu, Y and Hollis, JA 2020b, 212317: pelitic migmatite, Mount Joseph; Geochronology Record 1624: Geological Survey of Western Australia, 8p.
- Fielding, IOH, Wingate, MTD, Lu, Y, Korhonen, FJ and Hollis, JA 2019a, 210664: pelitic schist, Lennard River; Geochronology Record 1617: Geological Survey of Western Australia, 5p.
- Fielding, IOH, Wingate, MTD, Lu, Y, Korhonen, FJ and Hollis, JA 2019b, 210670: pelitic schist, Lennard River; Geochronology Record 1618: Geological Survey of Western Australia, 8p.
- Fielding, IOH, Wingate, MTD, Lu, Y, Korhonen, FJ and Hollis, JA 2019c, 210671: pelitic schist, Lennard River; Geochronology Record 1619: Geological Survey of Western Australia, 6p.
- Fielding, IOH, Wingate, MTD, Lu, Y, Korhonen, FJ and Hollis, JA 2019d, 212305: pelitic migmatite, Mount Joseph; Geochronology Record 1620: Geological Survey of Western Australia, 6p.
- Fielding, IOH, Wingate, MTD, Lu, Y, Korhonen, FJ and Hollis, JA 2019e, 212315: pelitic migmatite, Mount Joseph; Geochronology Record 1622: Geological Survey of Western Australia, 7p.
- Fielding, IOH, Wingate, MTD, Lu, Y, Korhonen, FJ and Hollis, JA 2020c, 212315: pelitic migmatite, Mount Joseph; Geochronology Record 1712: Geological Survey of Western Australia, 8p.
- Franklin, JM, Gibson, HL, Jonasson, IR and Galley, AG 2005, Volcanogenic massive sulphide deposits, in Economic Geology one hundredth anniversary volume edited by JW Hedenquist, JFH Thompson, RJ Goldfarb and JP Richards: The Economic Geology Publishing Company, p. 523–560.
- Fraser, GL, Huston, DL, Gibson, GM, Neumann, NL, Maidment, D, Kositcin, N, Skirrow, RG, Jaireth, S, Lyons, P, Carson, C, Cutten, H and Lambeck, A 2007, Geodynamic and metallogenic evolution of Proterozoic Australia from 1870–1550 Ma: a discussion: Geoscience Australia, Geoscience Australia Record 2007/16, 76p.



- Frogtech Geoscience 2017, Canning Basin SEEBASE study and GIS data package: Geological Survey of Western Australia, Report 182, 297p.
- Garzanti, E 2017, The maturity myth in sedimentology and provenance analysis: *Journal of Sedimentary Research*, v. 87, p. 353–365.
- Gellatly, DC, Derrick, GM and Plumb, KA 1975, The Geology of the Landsdowne 1:250 000 sheet area, Western Australia: Bureau of Mineral Resources, Geology and Geophysics, Report 152, 100p.
- Gellatly, DC, Sofoulis, J, Derrick, GM and Morgan, CM 1974, The older Precambrian geology of the Lennard River 1:250 000 sheet area SE51-8, Western Australia: Bureau of Mineral Resources, Geology and Geophysics, Report 153, 152p.
- Gemuts, I 1971, Metamorphic and igneous rocks of the Lamboo Complex, east Kimberley region, Western Australia: Bureau of Mineral Resources, Geology and Geophysics, Bulletin 107, 71p.
- Geological Survey of Western Australia 2022, GSWA geochronology, digital data layer: Geological Survey of Western Australia, viewed 23 May 2022, <www.dmp.wa.gov.au/geoview>.
- Glass, LM, Ahmad, M and Munson, TJ 2013, Chapter 30: Kalkarindji Province, in *Geology and mineral resources of the Northern Territory compiled by M Ahmad and TJ Munson*: Northern Territory Geological Survey, Special Publication 5, p. 30:1–30:17.
- Glass, LM and Phillips, D 2006, The Kalkarindji continental flood basalt province: a new Cambrian large igneous province in Australia with possible links to faunal extinctions: *Geology*, v. 34, no. 6, p. 461–464, doi:10.1130/G22122.1.
- Goleby, BR, Huston, DL, Lyons, P, Vandenberg, L, Bagas, L, Davies, BM, Jones, LEA, Gebre-Mariam, M, Johnson, W, Smith, T and English, L 2009, The Tanami deep seismic reflection experiment: an insight into gold mineralization and Paleoproterozoic collision in the North Australian Craton: *Tectonophysics*, v. 472, no. 1–4, p. 169–182.
- Griffin, TJ and Myers, JS 1988, A Proterozoic terrane boundary in the King Leopold Orogen, Western Australia: *Australian Journal of Earth Sciences*, v. 35, p. 131–132.
- Griffin, TJ, Page, RW, Sheppard, S and Tyler, IM 2000a, Tectonic implications of Palaeoproterozoic post-collisional, high-K felsic igneous rocks from the Kimberley region of northwestern Australia: *Precambrian Research*, v. 101, p. 1–23.
- Griffin, TJ and Tyler, IM 1992, Geology of the southern Halls Creek Orogen – a summary of field work in 1992: Geological Survey of Western Australia, Record 1992/17, 28p.
- Griffin, TJ and Tyler, IM 1994, Angelo, WA Sheet 4361: Geological Survey of Western Australia, 1:100 000 Geological Series.
- Griffin, TJ, Tyler, IM, Orth, K and Sheppard, S 1998, Geology of the Angelo 1:100 000 sheet: Geological Survey of Western Australia, 1:100 000 Geological Series Explanatory Notes, 27p.
- Griffin, TJ, Tyler, IM and Playford, PE 1993, Explanatory notes on the Lennard River 1:250 000 geological sheet SE/51-8, Western Australia (3rd edition): Geological Survey of Western Australia, Record 1992/5, 85p.
- Griffin, TJ, Tyler, IM and Playford, PE 1994, Lennard River, Western Australia (3rd edition): Geological Survey of Western Australia, 1:250 000 Geological Series Explanatory Notes, 56p.
- Griffin, WL, Pearson, NJ, Belousova, E, Jackson, SE, Achterbergh, E, O'Reilly, SY and Shee, SR 2000b, The Hf isotope composition of cratonic mantle: LAM-MC-ICPMS analysis of zircon megacrysts in kimberlites: *Geochimica et Cosmochimica Acta*, v. 64, p. 133–147.
- Griffin, WL, Wang, X, Jackson, SE, Pearson, NJ, O'Reilly, SY, Xu, XS and Zhou, XM 2002, Zircon chemistry and magma mixing, SE China: in-situ analysis of Hf isotopes, Tonglu and Pingtan igneous complexes: *Lithos*, v. 61, p. 237–269.
- Gunn, PJ and Meixner, AJ 1998, The nature of the basement to the Kimberley Block, northwestern Australia: *Exploration Geophysics*, v. 29, p. 506–511.
- Hancock, SL 1991, Tectonic development of the Lower Proterozoic basement in the Kimberley district of northwestern Western Australia: The University of Adelaide, Adelaide, South Australia, PhD thesis (unpublished).
- Hancock, SL and Rutland, RWR 1984, Tectonics of an early Proterozoic geosuture: the Halls Creek Orogenic Sub-province, northern Australia: *Journal of Geodynamics*, v. 1, p. 387–432.
- Hanley, LM and Wingate, MTD 2000, SHRIMP zircon age for an Early Cambrian dolerite dyke: an intrusive phase of the Antrim Plateau Volcanics of northern Australia: *Australian Journal of Earth Sciences*, v. 47, p. 1029–1040.
- Harms, JE 1959, The geology of the Kimberley Division, Western Australia, and of an adjacent area of the Northern Territory: The University of Adelaide, Adelaide, South Australia, MSc thesis (unpublished), 229p.
- Harris, LB, Koyi, HA and Fossen, H 2002, Mechanisms for folding of high-grade rocks in extensional tectonic settings: *Earth Science Reviews*, v. 59, p. 163–210.
- Hassan, LY 2000, Mineral occurrences and exploration potential of the east Kimberley: Geological Survey of Western Australia, Report 74, 83p.
- Hassan, LY 2004, Mineral occurrences and exploration potential of the west Kimberley: Geological Survey of Western Australia, Report 88, 88p.
- Hexagon Resources 2019, Revised McIntosh mineral resource estimate and additional updates – amended: Report to Australian Securities Exchange, 05 April 2019.
- Hoatson, DM 2000a, Geological setting, petrography and geochemistry of the mafic-ultramafic intrusions, in *Geology and economic potential of the Palaeoproterozoic layered mafic-ultramafic intrusions in the East Kimberley, Western Australia edited by DM Hoatson and DH Blake*: Australian Geological Survey Organisation, Canberra, Bulletin 246, p. 99–162.
- Hoatson, DM 2000b, Introduction, in *Geology and economic potential of the Palaeoproterozoic layered mafic-ultramafic intrusions in the East Kimberley, Western Australia edited by DM Hoatson and DH Blake*: Australian Geological Survey Organisation, Canberra, Bulletin 246, p. 1–12.
- Hoatson, DM 2000c, Mineralisation and economic potential of the mafic-ultramafic intrusions, in *Geology and economic potential of the Palaeoproterozoic layered mafic-ultramafic intrusions in the East Kimberley, Western Australia edited by DM Hoatson and DH Blake*: Australian Geological Survey Organisation, Canberra, Bulletin 246, p. 278–311.
- Hollis, JA, Beyer, EE, Whelan, JA, Kemp, AIS, Scherstén, A and Greig, A 2010, Summary of results. NTGS laser U–Pb and Hf geochronology project: Pine Creek Orogen, Murphy Inlier, McArthur Basin and Arunta Region: Northern Territory Geological Survey, Record 2010-001, 150p.
- Hollis, JA, Carson, CJ and Glass, LM 2009a, SHRIMP U–Pb zircon geochronological evidence for Neoproterozoic basement in western Arnhem Land, northern Australia: *Precambrian Research*, v. 174, no. 3–4, p. 364–380.
- Hollis, JA, Carson, CJ, Glass, LM, Kositcin, N, Scherstén, A, Worden, KE, Armstrong, RA, Yaxley, GM, Kemp, AIS and EIMF 2014a, Detrital zircon U–Pb–Hf and O isotope character of the Cahill Formation and Nourlangie Schist, Pine Creek Orogen: implications for the tectonic correlation and evolution of the North Australian Craton: *Precambrian Research*, v. 246, p. 35–53.
- Hollis, JA, Kemp, AIS, Tyler, IM, Kirkland, CL, Wingate, MTD, Phillips, C, Sheppard, S, Belousova, E and Greau, Y 2014b, Basin formation by orogenic collapse: zircon U–Pb and Lu–Hf isotope evidence from the Kimberley and Speewah Groups, northern Australia: Geological Survey of Western Australia, Report 137, 46p.
- Hollis, JA, Kirkland, CL, Spaggiari, CV, Tyler, IM, Haines, PW, Wingate, MTD, Belousova, EA and Murphy, RC 2013, Zircon U–Pb–Hf isotope evidence for links between the Warumpi and Aileron Provinces, west Arunta region: Geological Survey of Western Australia, Record 2013/9, 30p.

- Hollis, JA, Scherstén, A, Glass, LM and Carson, CJ 2009b, Stratigraphic and tectonic evolution of the Nimbuwah Domain: a separate terrane to the rest of the Pine Creek Orogen?, in Annual Exploration Geoscience Seminar (AGES) 2009, Record of Abstracts: Northern Territory Geological Survey; Annual Exploration Geoscience Seminar (AGES) 2009, Alice Springs, March 2009; NTGS Record 2009-002, p. 21–26.
- Hollis, JA, Tyler, IM and Kirkland, CL 2015, Geology of the Kimberley Craton, Halls Creek and King Leopold Orogens, in GSWA Kimberley workshop 2014: extended abstracts: Geological Survey of Western Australia; GSWA Kimberley workshop 2014, Perth, 21 November 2014; Record 2015/6, p. 1–5.
- Howard, KE, Hand, M, Barovich, KM, Reid, A, Wade, BP and Belousova, EA 2009, Detrital zircon ages: Improving interpretation via Nd and Hf isotopic data: *Chemical Geology*, v. 262, p. 277–292.
- Huston, DL, Blewett, RS and Champion, DC 2012, Australia through time: a summary of its tectonic and metallogenic evolution: *Episodes*, v. 35, no. 1, p. 23–43.
- Huston, DL, Vandenberg, L, Wygralak, AS, Mernagh, TP, Bagas, L, Crispe, A, Lambeck, A, Cross, A, Fraser, G, Williams, N, Worden, K, Meixner, T, Goleby, B, Jones, L, Lyons, P and Maidment, D 2007, Lode-gold mineralization in the Tanami region, northern Australia: *Mineralium Deposita*, v. 42, p. 175–204.
- Hutchison, MT 2018, Diamond exploration and prospectivity of Western Australia: Geological Survey of Western Australia, Report 179, 70p.
- Huyghe, P, Bernet, M, Galy, A, Naylor, M, Cruz, J, Gyawali, BR, Gemignani, L and Mugnier, J-L 2020, Rapid exhumation since at least 13 Ma in the Himalaya recorded by detrital apatite fission-track dating of Bengal fan (IODP Expedition 354) and modern Himalayan river sediments: *Earth and Planetary Science Letters*, v. 534, 116078.
- Iaccheri, LM and Bagas, L 2020, Zircon provenances provide paleogeographic constraints on models reconstructing the Paleoproterozoic Columbia Supercontinent: *Gondwana Research*, v. 82, p. 254–266.
- Iaccheri, LM, Kemp, AIS and EIMF 2018, Detrital zircon age, oxygen and hafnium isotope systematics record rigid continents after 2.5 Ga: *Gondwana Research*, v. 57, p. 90–118.
- Jaques, AL and Milligan, PR 2004, Patterns and controls on the distribution of diamondiferous intrusions in Australia: *Lithos*, v. 77, p. 783–802.
- Jaques, AL, Lugué, A, Smith, CB, Pearson, DG, Yaxley, GM and Kobussen, AF 2018, Nature of the mantle beneath the Argyle AK1 lamproite pipe: constraints from mantle xenoliths, diamonds, and lamproite geochemistry: *Society of Economic Geologists, Special Publication*, v. 20, p. 119–143.
- Johnson, SP 2013, The birth of supercontinents and the Proterozoic assembly of Western Australia: Geological Survey of Western Australia, 78p.
- Jones, S 2011, Proterozoic deformation in the east Pilbara Craton and tectonic setting of fault-hosted manganese at the Woodie Woodie mine: *Australian Journal of Earth Sciences*, v. 58, p. 639–673.
- Jourdan, F, Hodges, K, Sell, B, Schaltegger, U, Wingate, MTD, Evins, LZ, Söderlund, U, Haines, PW, Phillips, D and Blenkinsop, T 2014, High-precision dating of the Kalkarindji large igneous province, Australia, and synchrony with the Early–Middle Cambrian (Stage 4–5) extinction: *Geology*, v. 42, no. 6, p. 543–546, doi:10.1130/G35434.1.
- Kemp, AIS, Sheppard, S, Tyler, IM and Bodorkos, S 2015, Constraints on Paleoproterozoic crust–mantle evolution from the Hf, Nd and O isotope record of igneous rocks in the Lamboo Province of the Halls Creek and King Leopold Orogens, in GSWA Kimberley workshop 2014: extended abstracts: Geological Survey of Western Australia; GSWA Kimberley workshop 2014, Perth, Western Australia, 21 November 2014; Record 2015/6, p. 18–19.
- Kennett, BLN, Chopping, R and Blewett, R 2018, The Australian continent: a geophysical synthesis: ANU Press and Geoscience Australia, Canberra, 133p.
- Kirkland, CL, Wingate, MTD, Hollis, J and Phillips, C 2014, 206154: pelitic migmatite, Paperbark Bore; Geochronology Record 1204: Geological Survey of Western Australia, 6p.
- Kirkland, CL, Wingate, MTD, Tyler, IM, Hollis, J and Bodorkos, S 2013, 206102: sandstone, Richenda River; Geochronology Record 1135: Geological Survey of Western Australia, 5p.
- Kohanpour, F, Gorczyk, W, Lindsay, MD and Occhipinti, S 2017, Examining tectonic scenarios using geodynamic numerical modelling: Halls Creek Orogen, Australia: *Gondwana Research*, v. 46, p. 95–113.
- Kohanpour, F, Kirkland, CL, Gorczyk, W, Occhipinti, S, Lindsay, MD, Mole, D and Le Vaillant, M 2019a, Hf isotopic fingerprinting of geodynamic settings: Integrating isotopes and numerical models: *Gondwana Research*, v. 73, p. 190–199.
- Kohanpour, F, Lindsay, M, Occhipinti, S and Gorczyk, W 2018, Structural controls on proterozoic nickel and gold mineral systems identified from geodynamic modelling and geophysical interpretation, east Kimberley, Western Australia: *Ore Geology Reviews*, v. 95, p. 552–568.
- Kohanpour, F, Occhipinti, S, Lindsay, M and Gorczyk, W 2019b, Tectonic controls on nickel and gold mineral systems, Halls Creek Orogen, Western Australia in SGTSG and SGSEG 2019 abstracts: Biennial meeting of the Specialist Group for Tectonics and Structural Geology and the Specialist Group in Solid Earth Geophysics, Convergence on the Coast, 18–22 November 2019, Port Lincoln, South Australia, Report Book 2019/00019: Department for Energy and Mining, South Australia, Adelaide, p. 90.
- Korhonen, FJ, Romano, SS, Fielding, IOH, Kelsey, DE and Hollis, JA 2022, 212305.2: andalusite–sillimanite pelitic migmatite, Mount Joseph; Metamorphic History Record 13: Geological Survey of Western Australia, 9p.
- Kositcin N, Beyer EE, Whelan JA, Close DF, Hallett L and Dunkley DJ 2013a, Summary of results. Joint NTGS–GA geochronology project: Arunta Region, Ngalia Basin, Tanami Region and Murphy Province, July 2011–June 2012: Northern Territory Geological Survey, Record 2013-004, 31p.
- Kositcin, N, Carson, CJ, Hollis, JA, Glass, LM, Close, DF, Whelan, JA, Webb, G and Donnellan, N 2013b, Joint NTGS – GA geochronology project: Arunta Region, Davenport Province and Pine Creek Orogen, July 2009 – June 2011: Northern Territory Geological Survey, Record 2012-008, 49p.
- Kositcin, N, Kraus, S and Whelan, JA 2015, Summary of results. Joint NTGS–GA SHRIMP geochronology project: Arnhem Province, July 2014 – June 2015: Northern Territory Geological Survey, Record 2015-010, 28p.
- Kositcin, N, Whelan JA, Reno, BL, Kraus, S and Beyer, EE 2018, Summary of results. Joint NTGS–GA geochronology project: Arnhem Province, July 2014 – June 2016: Northern Territory Geological Survey, Record 2017-008, 37p.
- Li, B, Bagas, L, Gallardo LA, Said, N, Diwu, C and McCuaig, TC 2013, Back-arc and post-collisional volcanism in the Palaeoproterozoic Granites–Tanami Orogen, Australia: *Precambrian Research*, v. 224, p. 570–587.
- Liebmann, J, Kirkland, CL, Korhonen, FJ, Kelsey, DE, Rankenburg, K, Duuring, P and Quentin de Gromard, R 2022, In situ biotite and apatite Rb–Sr geochronology of metasedimentary and meta-igneous rocks in Western Australia: Geological Survey of Western Australia, Record 2022/6, 33p.
- Lindsay, MD, Occhipinti, S, Aitken, ARA, Metelka, V, Hollis, J and Tyler, I 2016, Proterozoic accretionary tectonics in the east Kimberley region, Australia: *Precambrian Research*, v. 278, p. 265–282.
- Lu, Y, Fielding, IOH and Wingate, MTD 2020a, Introduction to geochronology information 2020: Geological Survey of Western Australia, 8p.
- Lu, Y, Wingate, MTD and Griffin, TJ 2017a, 95464: biotite metagranodiorite, King Creek; Geochronology Record 1385: Geological Survey of Western Australia, 4p.
- Lu, Y, Wingate, MTD and Hollis, JA 2017b, 212335: metagabbro, Clara Hill; Geochronology Record 1390: Geological Survey of Western Australia, 4p.

- Lu, Y, Wingate, MTD, Hollis, JA, Maidment, DW and Phillips, C 2017c, 212327: pelitic schist, Mondooma Creek; Geochronology Record 1465: Geological Survey of Western Australia, 6p.
- Lu, Y, Wingate, MTD, Hollis, JA, Maidment, DW and Phillips, C 2017d, 215562: metasandstone, Neville Gorge; Geochronology Record 1467: Geological Survey of Western Australia, 7p.
- Lu, Y, Wingate, MTD, Kirkland, CL and Griffin, TJ 2017e, 95416: biotite monzogranite, Mount Disaster; Geochronology Record 1382: Geological Survey of Western Australia, 3p.
- Lu, Y, Wingate, MTD, Kirkland, CL and Griffin, TJ 2017f, 95449: hornblende–biotite monzogranite, King Creek; Geochronology Record 1383: Geological Survey of Western Australia, 3p.
- Lu, Y, Wingate, MTD, Kirkland, CL and Griffin, TJ 2017g, 95459: biotite monzogranite, Swift Creek; Geochronology Record 1384: Geological Survey of Western Australia, 3p.
- Lu, Y, Wingate, MTD, Kirkland, CL, Maidment, DW, Phillips, C and Hollis, JA 2016a, 206106: pelitic migmatite, Sydney Harbour Yard; Geochronology Record 1340: Geological Survey of Western Australia, 6p.
- Lu, Y, Wingate, MTD, Kirkland, CL, Maidment, DW, Phillips, C and Hollis, JA 2016b, 206128: pelitic schist, Panton mine; Geochronology Record 1341: Geological Survey of Western Australia, 6p.
- Lu, Y, Wingate, MTD, Kirkland, CL, Maidment, DW, Phillips, C and Hollis, JA 2016c, 206131: migmatitic pelitic gneiss, Six Mile Bore; Geochronology Record 1342: Geological Survey of Western Australia, 5p.
- Lu, Y, Wingate, MTD, Kirkland, CL, Maidment, DW, Phillips, C and Hollis, JA 2016d, 206155: porphyritic dacite, Idamere Yard; Geochronology Record 1343: Geological Survey of Western Australia, 4p.
- Lu, Y, Wingate, MTD, Kirkland, CL, Maidment, DW, Phillips, C and Hollis, JA 2016e, 206173: psammitic schist, Lissadell Road; Geochronology Record 1346: Geological Survey of Western Australia, 5p.
- Lu, Y, Wingate, MTD, Kirkland, CL, Maidment, DW, Phillips, C and Hollis, JA 2016f, 212344: pelitic schist, Napier Creek; Geochronology Record 1348: Geological Survey of Western Australia, 6p.
- Lu, Y, Wingate, MTD and Maidment, DW 2020b, 218313: metamonzogranite, Bow River homestead; Geochronology Record 1650: Geological Survey of Western Australia, 4p.
- Lu, Y, Wingate, MTD and Maidment, DW 2020c, 218350: biotite–hornblende metatonalite, Alice Downs homestead; Geochronology Record 1651: Geological Survey of Western Australia, 4p.
- Lu, Y, Wingate, MTD and Maidment, DW 2020d, 226523: biotite–muscovite granodiorite gneiss, Rose Bore; Geochronology Record 1652: Geological Survey of Western Australia, 4p.
- Lu, Y, Wingate, MTD, Maidment, DW and Phillips, C 2017h, 218305: metasiltstone, O'Donnell Brook; Geochronology Record 1468: Geological Survey of Western Australia, 7p.
- Lu, Y, Wingate, MTD, Maidment, DW and Phillips, C 2017i, 218315: psammitic gneiss, Stock Route Bore; Geochronology Record 1469: Geological Survey of Western Australia, 7p.
- Lu, Y, Wingate, MTD, Maidment, DW and Phillips, C 2017j, 218321: pelitic gneiss, Winnama Yard; Geochronology Record 1470: Geological Survey of Western Australia, 7p.
- Lu, Y, Wingate, MTD, Maidment, DW and Phillips, C 2018a, 218310: metasandstone, Bow River; Geochronology Record 1543: Geological Survey of Western Australia, 6p.
- Lu, Y, Wingate, MTD, Maidment, DW and Phillips, C 2018b, 218318: muscovite–chlorite schist, Palms Yard; Geochronology Record 1544: Geological Survey of Western Australia, 7p.
- Lu, Y, Wingate, MTD, Maidment, DW and Phillips, C 2018c, 218330: lithic metasandstone, Ragged Range; Geochronology Record 1545: Geological Survey of Western Australia, 6p.
- Lu, Y, Wingate, MTD, Maidment, DW and Phillips, C 2018d, 218333: psammitic gneiss, Two Mile Yard; Geochronology Record 1546: Geological Survey of Western Australia, 6p.
- Lu, Y, Wingate, MTD, Maidment, DW and Sheppard, S 2020e, 124442: biotite–hornblende syenogranite, Turkey Nest Dam; Geochronology Record 1695: Geological Survey of Western Australia, 4p.
- Lu, Y, Wingate, MTD, Phillips, C and Maidment, DW 2018e, 216661: lithic sandstone, Sophie Downs homestead; Geochronology Record 1510: Geological Survey of Western Australia, 7p.
- Lu, Y, Wingate, MTD, Phillips, C and Maidment, DW 2020f, 218355: biotite–hornblende metatonalite, Winnama Yard; Geochronology Record 1699: Geological Survey of Western Australia, 4p.
- Maidment, DW, Hand, M and Williams, IS 2006, A time frame for protracted multiphase metamorphism, magmatism and deformation in the exhumed core of the Alice Springs Orogen, Harts Range, central Australia, *in* ASEG Extended Abstracts 2006, v. 1, p. 1–4.
- Maidment, DW, Hand, M and Williams, IS 2013a, High-grade metamorphism of sedimentary rocks during Palaeozoic rift basin formation in central Australia: Gondwana Research, v. 24, p. 856–885.
- Maidment, DW, Huston, DL, Donnellan, N and Lambeck, A 2013b, Constraints on the timing of the Tennant Event and associated Au–Cu–Bi mineralization in the Tennant Region, Northern Territory: Precambrian Research, v. 237, p. 51–63.
- Maidment, DW, Wingate, MTD, Claoué-Long, JC, Bodorkos, S, Huston, D, Whelan, JA, Lambeck, A and Lu, Y 2020, Geochronology of metasedimentary and granitic rocks in the Granites–Tanami Orogen: 1885–1790 Ma geodynamic evolution: Geological Survey of Western Australia, Report 196, 50p.
- Martin, H, Smithies, RH, Rapp, R, Moya, J-F and Champion, DC 2005, An overview of adakite, tonalite–trondhjemite–granodiorite (TTG) and sanukitoid: relationships and some implications for crustal evolution: Lithos, v. 79, p. 1–24.
- Mole, DR, Barnes, SJ, Le Vaillant, M, Martin, LAJ and Hicks, J 2018, Timing, geochemistry and tectonic setting of Ni–Cu sulfide-associated intrusions of the Halls Creek Orogen, Western Australia: Lithos, v. 314–315, p. 425–446.
- Morin-Ka, S, Beardsmore, T, Hancock, EA, Rasmussen, B, Dunkley, DJ, Zi, J, Muhling, JR, Wilson, R and Chapman, J 2016, Alteration and age of the Browns Range heavy rare earth deposits, *in* GSWA 2016 extended abstracts: promoting the prospectivity of Western Australia: Geological Survey of Western Australia, Record 2016/2, p. 21–25.
- Mory, AJ 1990, Ord Basin, *in* Geology and mineral resources of Western Australia: Geological Survey of Western Australia, Memoir 3, p. 415–425.
- Mory, AJ and Beere, GM 1985, Palaeozoic stratigraphy of the Ord Basin, Western Australia and Northern Territory, *in* Professional papers for 1983: Geological Survey of Western Australia, Report 14, p. 36–45.
- Moya, J-F 2009, High Sr/Y and La/Yb ratios: the meaning of the “adakitic signature”: Lithos, v. 112, p. 556–574.
- Murphy, JB 2007, Igneous rock associations 8. Arc magmatism II: geochemical and isotopic characteristics: Geoscience Canada, v. 34, p. 7–36.
- Myers, JS, Shaw, RD and Tyler, IM 1996, Tectonic evolution of Proterozoic Australia: Tectonics, v. 15, p. 1431–1446.
- Najman, Y, Jenks, D, Godin, L, Boudagher-Fadel, M, Millar, I, Garzanti, E, Horstwood, M and Bracciali, L 2017, The Tethyan Himalayan detrital record shows that India–Asia terminal collision occurred by 54 Ma in the Western Himalaya: Earth and Planetary Science Letters, v. 459, p. 301–310.
- Occhipinti, S, Lindsay, M, Tyler, I and Aitken, A 2017, Geology and metallogeny of the Kimberley Province, *in* Australian Ore Deposits edited by GN Phillips: The Australasian Institute of Mining and Metallurgy, Melbourne, Monograph 32, p. 429–434.
- Occhipinti, SA, Metelka, V, Lindsay, MD, Hollis, JA, Aitken, ARA, Tyler, IM, Miller, JM and McCuaig, TC 2016, Multicommodity mineral systems analysis highlighting minerals prospectivity in the Halls Creek Orogen: Ore Geology Reviews, v. 72, no. P1, p. 86–113.



- Ogasawara, M 1988, Geochemistry of the Early Proterozoic granitoids in the Halls Creek orogenic subprovince, northern Australia: *Precambrian Research*, v. 40–41, p. 469–486.
- Olierook, HKH, Agangi, A, Plavska, D, Reddy, SM, Yao, W, Clark, C, Occhipinti, SA and Kylander-Clark, ARC 2019, Neoproterozoic hydrothermal activity in the West Australian Craton related to Rodinia assembly or breakup?: *Gondwana Research*, v. 68, p. 1–12.
- Oliver, NHS and Barr, TD 1997, The geometry and evolution of magma pathways through migmatites of the Halls Creek Orogen, Western Australia: *Mineralogical Magazine*, v. 61, p. 3–14.
- Oliver, NHS, Bodorkos, S, Nemchin, AA, Kinny, PD and Watt, GR 1999, Relationships between zircon U–Pb SHRIMP ages and leucosome type in migmatites of the Halls Creek Orogen, Western Australia: *Journal of Petrology*, v. 40, no. 10, p. 1553–1575.
- Orth, K 1997, Notes on the geology of the Koongie Park Formation southwest of Halls Creek, Western Australia: AGSO Record, v. 1997/25, 18p.
- Orth, K 2002, Setting of the Palaeoproterozoic Koongie Park Formation and carbonate-associated base metal mineralisation, at Koongie Park, Northwestern Australia: University of Tasmania, Hobart, Tasmania, PhD thesis (unpublished), 460p.
- Page, R 1996a, Sample ID 93526025, Tickalara Metamorphics: Geoscience Australia geochronology database, viewed 9 May 2018, <<http://www.ga.gov.au/geochron-sapub-web/geochronology/shrimp/search.htm>>.
- Page, R 1996b, Sample ID 93526034, Tickalara Metamorphics: Geoscience Australia geochronology database, viewed 9 May 2018, <<http://www.ga.gov.au/geochron-sapub-web/geochronology/shrimp/search.htm>>.
- Page, RW, Blake, DH, Sun, S-S, Tyler, IM, Griffin, TJ and Thorne, AM 1994, New geological and geochronological constraints on volcanogenic massive sulphide prospectivity near Halls Creek (WA): AGSO Research Newsletter, v. 20, p. 5–7.
- Page, RW, Griffin, TJ, Tyler, IM and Sheppard, S 2001, Geochronological constraints on tectonic models for Australian Palaeoproterozoic high-K granites: *Journal of the Geological Society*, v. 158, p. 535–545.
- Page, RW and Hancock, SL 1988, Geochronology of a rapid 1.85–1.86 Ga tectonic transition: Halls Creek orogen, northern Australia: *Precambrian Research*, v. 40, p. 447–467.
- Page, RW and Hoatson, DM 2000, Geochronology of the mafic–ultramafic intrusions, in *Geology and economic potential of the Palaeoproterozoic layered mafic–ultramafic intrusions in the East Kimberley, Western Australia* edited by DM Hoatson and DH Blake: Australian Geological Survey Organisation, Bulletin 246, p. 163–172.
- Page, RW and Sun, S-S 1994, Evolution of the Kimberley Region, W.A. and adjacent Proterozoic inliers – new geochronological constraints, in *Geoscience Australia – 1994 and Beyond: Geological Society of Australia; 12th Australian Geological Convention, Perth, Western Australia, 26–30 September 1994; Abstracts*, v. 37, p. 332–333.
- Page, RW, Sun, S-S and Blake, DH 1995, Geochronology of an exposed late Archean basement terrane in The Granites–Tanami Region: AGSO Research Newsletter 22, p. 19–20.
- Payne, JL, Hand, M, Barovich, KM, Reid, A and Evans, DAD 2009, Correlations and reconstruction models for the 2500–1500 Ma evolution of the Mawson Continent: Geological Society, London, Special Publications, v. 323, p. 319–355.
- Pearce, JA 2008, Geochemical fingerprinting of oceanic basalts with applications to ophiolite classification and the search for Archean oceanic crust: *Lithos*, v. 100, p. 14–48.
- Pearson, NJ, Griffin, WL and O'Reilly, SY 2008, Mass fractionation correction in laser ablation multiple-collector ICP-MS: implications for overlap corrections and precise and accurate in situ isotope ratio measurement, in *Laser ablation ICP-MS in the earth sciences: current practices and outstanding issues* edited by P Sylvester: Mineralogical Association of Canada, Short Course 40, p. 93–116.
- Phillips, C 2019, Kimberley basins – results of detrital zircon geochronology: Geological Survey of Western Australia Open Day 2019, poster 20190231.
- Phillips, C, Maidment, D and de Souza Kovacs, N 2018, Lansdowne, WA Sheet SE 52-5 (2nd edition): Geological Survey of Western Australia, 1:250 000 Geological Series.
- Phillips, C, Maidment, DW and Lu, Y 2017, Revised tectono-stratigraphy of the Kimberley Basin, northern Western Australia, in *GSWA 2017 Extended abstracts: promoting the prospectivity of Western Australia: Geological Survey of Western Australia, Record 2017/2*, p. 33–37.
- Phillips, C, Orth, K, Hollis, JA, Kirkland, CL, Bodorkos, S, Kemp, AIS, Wingate, MTD, Lu, Y, Iaccheri, L and Page, RW 2016, Geology of the Eastern Zone of the Lamboo Province, Halls Creek Orogen, Western Australia: Geological Survey of Western Australia, Report 164, 57p.
- Pidgeon, RT, Smith, CB and Fanning, CM 1989, Kimberlite and lamproite emplacement ages in Western Australia, in *Kimberlites and related rocks: their composition, occurrence, origin and emplacement* edited by J Ross: Geological Society of Australia, Special Publication 14, p. 369–381.
- Plumb, KA 1981, Late Proterozoic (Adelaidian) tillites of the Kimberley – Victoria River region, Western Australia and Northern Territory, in *Earth's pre-Pleistocene glacial record* edited by MJ Hambrey and WB Harland: Cambridge University Press, Cambridge, UK, p. 528–530.
- Plumb, KA and Gemuts, I 1976, Precambrian geology of the Kimberley Region, Western Australia, in *25th International Geological Congress (Sydney, August 1976) Excursion Guide 44C: Geological Society of Australia*; p. 6–10.
- Ramsay, RR, Eves, AE, Denyszyn, SW, Wingate, MTD, Fiorentini, M, Gwalani, LG and Rogers, KA 2019, Geology and geochronology of the Paleoproterozoic Hart Dolerite, Western Australia: *Precambrian Research*, v. 335, 105482.
- Ramsay, RR, Eves, A, Wingate, MTD, Fiorentini, ML, Batt, G, Rogers, K, Gwalani, LG and Martin, S 2017, Detrital zircon geochronology of the Speewah Group, Kimberley region, Western Australia: evidence for intracratonic development of the Paleoproterozoic Speewah Basin: *Australian Journal of Earth Sciences*, v. 64, p. 419–434.
- Reno, BL, Whelan, JA, Kraus, S, Thompson, JM and Meffre, S 2017, Summary of results, NTGS laser ablation ICP-MS in situ monazite geochronology project: Arnhem Province, Gove and Blue Mud Bay 1:250 000 map sheets: Northern Territory Geological Survey, Record 2017-007, 35p.
- Richards, JP 2011, High Sr/Y arc magmas and porphyry Cu ± Mo ± Au deposits: just add water: *Economic Geology*, v. 106, p. 1075–1081.
- Richards, JP and Kerrich, R 2007, Special paper: adakite-like rocks: their diverse origins and questionable role in metallogenesis: *Economic Geology*, v. 102, no. 4, p. 537–575.
- Ruddock, I 2003, Mineral occurrences and exploration potential of the north Kimberley: Geological Survey of Western Australia, Report 85, 58p.
- Rutland, RWR 1973, Tectonic evolution of the continental crust of Australia: implications of continental drift to the earth sciences, in *Continental Evolution (volume 2): Academic Press, London, UK*, p. 1011–1033.
- Sanders, TS 1999, Mineralization of the Halls Creek Orogen, east Kimberley region, Western Australia: Geological Survey of Western Australia, Report 66, 44p.
- Sayona Mining Ltd, 2015, Robust anomalies defined in the Corkwood geophysical survey: Report to Australian Securities Exchange, 21 October 2015.
- Schmid, S, Davis, J and Evans, NJ 2021, Geochemical classification of Palaeoproterozoic oceanic volcanic front and backarc basin remnants of the Granites–Tanami Orogen, Australia: *Precambrian Research*, v. 364, 106362.
- Scrimgeour, IR 2013, Chapter 12: Aileron Province, in *Geology and mineral resources of the Northern Territory* compiled by M Ahmad and TJ Munson: Northern Territory Geological Survey, Special Publication 5, p. 12:1–12:74.

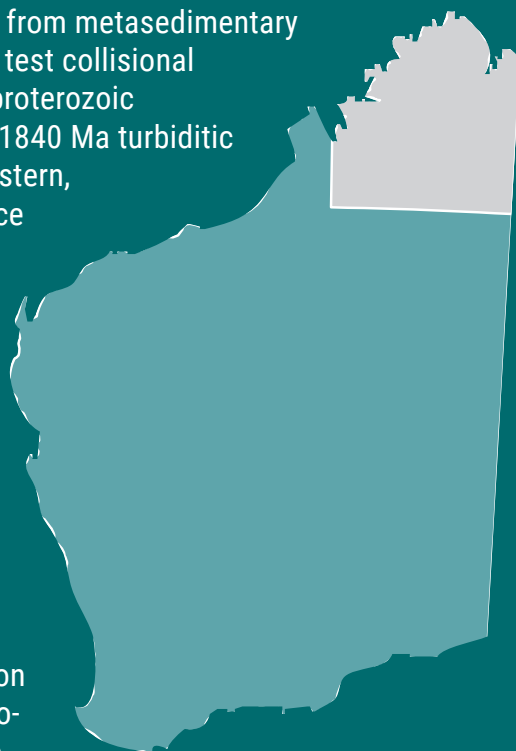
- Shaw, RD, Meixner, A and Murray, A 2000, Regional geophysical setting and tectonic implications of the mafic-ultramafic intrusions, *in* *Geology and economic potential of the Palaeoproterozoic layered mafic-ultramafic intrusions in the East Kimberley, Western Australia* edited by DM Hoatson and DH Blake: Australian Geological Survey Organisation, Canberra, Australian Capital Territory, p. 63–98.
- Shaw, RD, Tyler, IM, Griffin, TJ and Webb, A 1992, New K–Ar constraints on the onset of subsidence in the Canning Basin, Western Australia: *BMR Journal of Australian Geology and Geophysics*, v. 13, p. 31–35.
- Sheppard, S 1996, Mafic–felsic magma mingling in the Bow River batholith of the Halls Creek Orogen: *Geological Survey of Western Australia, 1995–96 Annual Review*, p. 56–59.
- Sheppard, S, Griffin, TJ and Tyler, IM 1995, Geochemistry of felsic igneous rocks from the southern Halls Creek Orogen: *Geological Survey of Western Australia, Record 1995/4*, 81p.
- Sheppard, S, Griffin, TJ and Tyler, IM 1997a, The tectonic setting of granites in the Halls Creek and King Leopold Orogens, northwest Australia: *Australian Geological Survey Organisation, Record 1997/44*, p. 107–109.
- Sheppard, S, Griffin, TJ, Tyler, IM and Page, RW 2001, High- and low-K granites and adakites at a Palaeoproterozoic plate boundary in northwestern Australia: *Journal of the Geological Society*, v. 158, p. 547–560.
- Sheppard, S, Page, RW, Griffin, TJ, Rasmussen, B, Fletcher, IR, Tyler, IM, Kirkland, CL, Wingate, MTD, Hollis, J and Thorne, AM 2012, Geochronological and isotopic constraints on the tectonic setting of the c. 1800 Ma Hart Dolerite and the Kimberley and Speewah Basins, northern Western Australia: *Geological Survey of Western Australia, Record 2012/7*, 28p.
- Sheppard, S, Thorne, AM and Tyler, IM 1997b, Bow, WA Sheet 4564: *Geological Survey of Western Australia, 1:100 000 Geological Series*.
- Sheppard, S, Thorne, AM and Tyler, IM 1999a, *Geology of the Bow 1:100 000 sheet: Geological Survey of Western Australia, 1:100 000 Geological Series Explanatory Notes*, 36p.
- Sheppard, S, Tyler, IM, Griffin, TJ and Taylor, RW 1999b, Palaeoproterozoic subduction-related and passive-margin basalts in the Halls Creek Orogen, northwest Australia: *Australian Journal of Earth Sciences*, v. 46, p. 679–690.
- Sheppard, S, Tyler, IM and Hoatson, DM 1997c, *Geology of the Mount Remarkable 1:100 000 sheet: Geological Survey of Western Australia, 1:100 000 Geological Series Explanatory Notes*, 27p.
- Silva, D, Piazzolo, S, Daczko, N, Houseman, G, Raimondo, T and Evans, L 2018, Intracontinental orogeny enhanced by far-field extension and local weak crust: *Tectonics*, v. 37, p. 4421–4443.
- Smith, JB 2001, Summary of results. Joint NTGS–AGSO age determination program 1999–2001: *Northern Territory Geological Survey, Record 2001-007*, 53p.
- Söderlund, U, Patchett, PJ, Vervoort, JD and Isachsen, CE 2004, The  $^{176}\text{Lu}$  decay constant determined by Lu–Hf and U–Pb isotope systematics of Precambrian mafic intrusions: *Earth and Planetary Science Letters*, v. 219, p. 311–324.
- Spratt, J, Dentith, MC, Evans, S, Aitken, ARA, Lindsay, M, Hollis, JA, Tyler, IM, Joly, A and Shragge, J 2014, A magnetotelluric survey across the Kimberley Craton, northern Western Australia: *Geological Survey of Western Australia, Report 136*, 92p.
- Sproule, RA, Lambert, DD and Hoatson, DM 2002, Decoupling of the Sm–Nd and Re–Os isotopic systems in sulphide-saturated magmas in the Halls Creek Orogen, Western Australia: *Journal of Petrology*, v. 43, no. 2, p. 375–402.
- Stacey, JS and Kramers, JD 1975, Approximation of terrestrial lead isotope evolution by a two-stage model: *Earth and Planetary Science Letters*, v. 26, p. 207–221.
- Stachel, T, Harris, JW, Hunt, L, Muehlenbachs, K, Kobussen, AF and Edinburgh Ion Micro-Probe Facility (EIMF) 2018, Argyle diamonds: how subduction along the Kimberley Craton edge generated the world's biggest diamond deposit: *Society of Economic Geologists, Special Publication*, v. 20, p. 145–167.
- Stern, RA, Bodorkos, S, Kamo, SL, Hickman, AH and Corfu, F 2009, Measurement of SIMS instrumental mass fractionation of Pb isotopes during zircon dating: *Geostandards and Geoanalytical Research*, v. 33, p. 145–168.
- Sun, S-S and Hoatson, DM 2000, Trace-element geochemical and Nd isotopic study of the mafic–intrusions: implications for their petrogenesis and tectonic environment, *in* *Geology and economic potential of the Palaeoproterozoic layered mafic-ultramafic intrusions in the East Kimberley, Western Australia* edited by DM Hoatson and DH Blake: Australian Geological Survey Organisation, Canberra, Australian Capital Territory, *Bulletin* 246, p. 163–172.
- Sun, S-S, Wallace, DA, Hoatson, DM, Glikson, AY and Keays, RR 1991, Use of geochemistry as a guide to platinum group element potential of mafic–ultramafic rocks: examples from the west Pilbara Block and Halls Creek Mobile Zone, Western Australia: *Precambrian Research*, v. 50, p. 1–35.
- Taylor, WR, Esslemont, G and Sun, S-S 1995, *Geology of the volcanic-hosted Brockman rare-metals deposit, Halls Creek Mobile Zone, northwest Australia. II. Geochemistry and petrogenesis of the Brockman volcanics: Mineralogy and Petrology*, v. 52, no. 3–4, p. 231–255.
- Thorne, AM, Sheppard, S and Tyler, IM 1998, Lissadell, WA Sheet SE 52-2 (2nd edition): *Geological Survey of Western Australia, 1:250 000 Geological Series*.
- Thorne, AM, Sheppard, S and Tyler, IM 1999, Lissadell, Western Australia (2nd edition): *Geological Survey of Western Australia, 1:250 000 Geological Series Explanatory Notes*, 68p.
- Thorne, AM and Tyler, IM 1996, Mesoproterozoic and Phanerozoic sedimentary basins in the northern Halls Creek Orogen: constraints on the timing of strike-slip movement on the Halls Creek Fault system, *in* *Geological Survey of Western Australia Annual Review 1995–96: Geological Survey of Western Australia*, p. 156–168.
- Thornett, JR 1986, *Evolution of a high-grade metamorphic terrain in the Proterozoic Halls Creek mobile zone, Western Australia: The University of Western Australia, Perth, PhD thesis (unpublished)*, 350p.
- Tucker, NM, Hand, M and Payne JL 2015, A rift-related origin for medium-pressure, high-temperature metamorphism: *Earth and Planetary Science Letters*, v. 421, p. 75–88.
- Tyler, IM 2004, *Geology of the Dixon 1:100 000 sheet: Geological Survey of Western Australia, 1:100 000 Geological Series Explanatory Notes*, 30p.
- Tyler, IM and Griffin, TJ 1990, Structural development of the King Leopold Orogen, Kimberley region, Western Australia: *Journal of Structural Geology*, v. 12, p. 703–714.
- Tyler, IM, Griffin, TJ, Page, RW and Shaw, RD 1995, Are there terranes within the Lamboo Complex of the Halls Creek Orogen?, *in* *Geological Survey of Western Australia Annual Review 1993–94: Geological Survey of Western Australia*, p. 37–46.
- Tyler, IM, Griffin, TJ and Sheppard, S 1998, *Geology of the Dockrell 1:100 000 sheet: Geological Survey of Western Australia, 1:100 000 Geological Series Explanatory Notes*, 24p.
- Tyler, IM, Griffin, TJ, Sheppard, S, Blake, DH and Warren, RG 1997a, McIntosh, WA Sheet 4462: *Geological Survey of Western Australia, 1:100 000 Geological Series*.
- Tyler, IM, Hocking, RM and Haines, PW 2012, *Geological evolution of the Kimberley region of Western Australia: Episodes*, v. 35, p. 298–306.
- Tyler, IM, Page, RW and Griffin, TJ 1999, Depositional age and provenance of the Marboo Formation from SHRIMP U–Pb zircon geochronology: Implications for the early Palaeoproterozoic tectonic evolution of the Kimberley region, Western Australia: *Precambrian Research*, v. 95, no. 3, p. 225–243.

- Tyler, IM, Sheppard, S, Pirajno, F and Griffin, TJ 2006, Hart–Carson LIP, Kimberley region, northern Western Australia: Large Igneous Provinces Commission, viewed 10 February 2014, <<http://www.largeigneousprovinces.org/06aug>>.
- Tyler, IM, Thorne, AM, Hoatson, DM and Blake, DH 1997b, Turkey Creek, WA Sheet 4563: Geological Survey of Western Australia, 1:100 000 Geological Series.
- Ware, BD, Jourdan, F, Merle, R, Chiaradia, M and Hodges, K 2018, The Kalkarindji Large Igneous Province, Australia: Petrogenesis of the oldest and most compositionally homogeneous province of the Phanerozoic: *Journal of Petrology*, v. 59, p. 636–666.
- Warren, RG 1994, Role of early extensional faults in the Grants Patch district, east Kimberley, Western Australia: Geological Society of Australia, Abstracts, v. 37, 12th Australian Geological Convention, Perth, September 1994, p. 453–454.
- Warren, RG 1997, Reconnaissance geological mapping in Dixon, SE McIntosh and northernmost Halls Creek 1:100 000 Sheet areas, East Kimberley, WA, 1992–3: Australian Geological Survey Organisation, Record 1997/026.
- Wei, X, Feng, YG and Zhao, JX 2014, Plume–lithosphere interaction in the generation of the Tarim large igneous province, NW China: geochronological and geochemical constraints: *American Journal of Sciences*, v. 314, p. 314–356.
- Whelan, JA, Reno, BL, Weisheit, A, Kraus, S, Kositsin, N, Woodhead, JD, Maas, R and Armstrong, RA 2017, The geological evolution of the Arnhem Province: implications for craton-scale correlations, in *Annual Geoscience Exploration Seminar (AGES) Proceedings: Northern Territory Geological Survey; AGES 2017, Alice Springs, Northern Territory*, 28 March 2017, p. 68–73.
- Whelan, JA, Woodhead, JD and Cliff, J 2014, Zircon LA-ICP-MS Hf and SIMS O isotopic data for granitic gneiss of the Billabong Complex, Tanami Region: Northern Territory Geological Survey, Record 2014-002, 8p.
- Wingate, MTD and Evans, DAD 2003, Palaeomagnetic constraints on the Proterozoic tectonic evolution of Australia: Geological Society, London, Special Publications, v. 206, p. 77–91.
- Wingate, MTD, Kirkland, CL, Griffin, TJ and Sheppard, S 2011, 95406: porphyritic microgranite, Wotjulum Mission; Geochronology Record 973: Geological Survey of Western Australia, 4p.
- Wingate, MTD, Kirkland, CL, Hollis, JA and Phillips, C 2015, 206184: metasandstone, Palm Springs; Geochronology Record 1243: Geological Survey of Western Australia, 6p.
- Worden, KE, Carson, CJ, Close, DF, Donnellan, N and Scrimgeour, IR 2008, Summary of results. Joint NTGS–GA geochronology project: Tanami Region, Arunta Region, Pine Creek Orogen, and Halls Creek Orogen correlatives, January 2005 – March 2007: Northern Territory Geological Survey, Record 2008-003, 180p.
- Worden, KE, Claoué-Long, JC and Scrimgeour, IR 2006a, Summary of results. Joint NTGS–GA geochronology project: Pine Creek Orogen, Tanami Region, Arunta Region and Amadeus Basin, July–December 2004: Northern Territory Geological Survey, Record 2006-006, 63p.
- Worden, KE, Claoué-Long, JC, Scrimgeour, IR and Doyle, N 2006b, Summary of results, Joint NTGS–GA geochronology project: Pine Creek Orogen and Arunta Region, January–June 2004: Northern Territory Geological Survey, Record 2006-005, 39p.
- Worden, KE, Claoué-Long, JC, Scrimgeour, IR and Lally, JH 2004, Summary of results. Joint NTGS–GA geochronology project: August – December 2003: Northern Territory Geological Survey, Record 2004-004 (digital publication on CD).
- Wyborn, LAI 1998, Petrology, geochemistry and origin of a major Australian 1880–1840 Ma felsic volcano-plutonic suite: a model for intracontinental felsic magma generation: *Precambrian Research*, v. 40–41, p. 37–60.
- Wyborn, LAI and Blake, DH 2000, Comments on relationships of mafic and felsic magmatism, in *Geology and economic potential of the Palaeoproterozoic layered mafic–ultramafic intrusions in the east Kimberley, Western Australia* edited by DM Hoatson and DH Blake: Australian Geological Survey Organisation, Canberra, Australian Capital Territory, Bulletin 246, p. 220–225.
- Wyborn, LAI, Page, RW and Parker, AJ 1987, Geochemical and geochronological signatures in Australian Proterozoic igneous rocks, in *Geochemistry and mineralization of Proterozoic volcanic suites* edited by TC Pharaoh, RD Beckinsale and D Rickard: Geological Society, London, Special Publications, v. 33, p. 377–394.
- Wynne, P 2016, Australian National Gravity Database onshore complete Bouguer anomaly grid: Geoscience Australia, July 2016.
- Yang, Q, Jenkins, SF, Lerner, GA, Li, W, Suzuki, T, McLean, D, Derkachev, AN, Utkin, IV, Wei, H, Xu, J and Pan, B 2021, The Millennium Eruption of Changbaishan Tianchi Volcano is VEI 6, not 7: *Bulletin of Volcanology*, v. 84, article 74.



GEOCHRONOLOGY OF METASEDIMENTARY AND IGNEOUS  
ROCKS IN THE LAMBOO PROVINCE, KIMBERLEY REGION:  
REASSESSING COLLISIONAL GEODYNAMIC MODELSDW Maidment, Y Lu, C Phillips, FJ Korhonen, IOH Fielding, MTD Wingate,  
CL Kirkland, R Murphy, R Tilhac, M Poujol and J Zhao

U–Pb and Lu–Hf isotope data for detrital zircons from metasedimentary rocks of the Lamboo Province have been used to test collisional and intraplate geodynamic models for the Paleoproterozoic development of the Kimberley region. The 1870–1840 Ma turbiditic metasedimentary rocks deposited across the Western, Central and Eastern Zones of the Lamboo Province have remarkably consistent detrital zircon age signatures, with a dominant 1875–1860 Ma age component and a subsidiary c. 2500 Ma age component. These age components have similar Lu–Hf isotope values across all three zones, consistent with a common source for the sedimentary protoliths. The close similarities in provenance suggest that all three zones of the Lamboo Province developed in a continental intraplate setting prior to the 1837–1808 Ma Halls Creek Orogeny, which has previously been considered to represent a collision between an exotic Kimberley Craton and the proto-North Australian Craton. Comparable provenance signatures of coeval metasedimentary rocks across the broader North Australian Craton suggest that assembly of the main craton elements was complete prior to c. 1885 Ma.



Further details of geoscience products are available from:

First Floor Counter  
Department of Mines, Industry Regulation and Safety  
100 Plain Street  
EAST PERTH WESTERN AUSTRALIA 6004  
Phone: +61 8 9222 3459 Email: [publications@dmirs.wa.gov.au](mailto:publications@dmirs.wa.gov.au)  
[www.dmirs.wa.gov.au/GSWApublications](http://www.dmirs.wa.gov.au/GSWApublications)